Robert Schütky

Density Matrix Approach for Trapped Bose-Einstein Condensates

Doctoral Thesis

to be awarded the degree of
Doctor rerum naturalium (Dr. rer. nat.)
at the University of Graz

submitted by

Robert Schütky

at the Institute of Physics

Supervisor: Ao. Univ.-Prof. Mag. Dr. Ulrich Hohenester

Graz, 2016

Abstract / Kurzzusammenfassung

Density Matrix Approach for Trapped Bose-Einstein Condensates

This thesis is concerned with the simulation of Bose-Einstein condensates (BEC) trapped on atom chips.
Their dynamics can be described by the many-body Schrödinger equation, but analytic solutions are rare exceptions and approximations and numerical methods are generally indispensable. For weakly interacting systems, a mean field theory like the Gross-Pitaevskii equation gives a good approximation. In a double-well potential two modes or even more have to be used to correctly describe the dynamics of the splitting process. The powerful multi-configuration time-dependent Hartree for bosons approach with a time-adaptive optimized basis set reaches its limits in form of computational time and memory even for a few modes on typical workstations because of the exponential growth of the Hilbert space.
To take into account four and more modes we investigate the density matrix formalism which formulates equations of motion (EoM) for the reduced density matrices using the Von Neumann equation for quantum many-particle systems. It allows for a numerically exact treatment as well as for approximations necessary in the hierarchy of EoM, where the time evolution of a first-order quantity is coupled to a second-order quantity, the time evolution of a second-order quantity to a third-order quantity and so on.
The key point of the applied approximation scheme is the fact that every expectation value (EV) can uniquely be represented as a sum of products of correlation functions (CFs) and vice versa, and higher order CFs can systematically be neglected.
We apply this formalism to a simple example of an adiabatic deformation of a harmonic potential trapping a BEC into a double well potential.
The density matrix formalism experiences difficulties already in this case. For a two mode system they can be overcome by explicitly keeping the trace of the 3-particle reduced density matrix constant. For more than two modes instabilities arise in the EoM of the density matrix formalism that prevent its application.

Dichtematrixformalismus für eingesperrte Bose-Einstein-Kondensate

Diese Arbeit befasst sich mit der Simulation von Bose-Einstein-Kondensaten (BEK) auf Atom Chips.
Ihre Dynamik kann durch die Vielteilchen-Schrödinger-Gleichung beschrieben werden, allerdings sind analytischen Lösungen Ausnahmen und Näherungsverfahren und numerische Methoden sind unerlässlich. Für schwach wechselwirkende Systeme ist eine mittlere Feld-Näherung, wie die Gross-Pitaevskii Gleichung eine gute Näherung. In einem Doppelmuldenpotential müssen zwei oder mehr Moden berücksichtigt werden um den Splitting-Prozess korrekt zu beschreiben. Der leistungsfähige *multi-configuration time-dependent Hartree for bosons* Zugang mit einer Zeit-adaptiven Basis stößt schon bei wenigen Moden wegen des exponentiellen Wachstums des Hilbert-Raums an seine Grenzen in Bezug auf Rechen- und Speicherkapazität.
Um vier und mehr Moden berücksichtigen zu können, untersuchen wir den Dichtematrixformalismus, der die Bewegungsgleichungen für reduzierte Dichtematrizen quantenmechanischer Vielteilchen - Systeme mit Hilfe der Von Neumann Gleichung formuliert. Er erlaubt sowohl eine numerisch exakte Behandlung als auch Näherungen bei der sich entfaltenden Hierarchie der Bewegungsgleichungen bei der Größen immer von Größen nächsthöherer Ordnung abhängen.
Der entscheidende Punkt des verwendeten Näherungsverfahrens ist die Tatsache, dass sich jeder Erwartungswert (EW) als Summe von Produkten von Korrelationsfunktionen (KF) und vice versa darstellen lässt und so KFen systematisch vernachlässigt werden können.
Wir wenden diesen Formalismus auf die adiabatische Verformung eines harmonischen Potentials in ein Doppelmuldenpotential an, in dem sich ein BEK befindet.
Der Dichtematrixformalismus versagt bereits dabei, was zumindest für ein zwei Moden System durch explizites Konstanthalten der 3 Teilchen reduzierten Dichtematrix behoben werden kann. Für mehr als zwei Moden treten Instabilitäten in den Bewegungsgleichungen des Dichtematrixformalismus auf, die seine Anwendbarkeit verhindern.

Contents

Contents iii

1. Introduction 1

1.1. Structure of this Thesis 4

1.2. Bose-Einstein Condensates 6

1.2.1. Basic Principles 8

1.2.2. Historical Overview - The Path to Bose-Einstein Condensation 11

1.2.3. Current Research and Applications 14

1.2.4. BECs in lower Dimensions 15

1.2.5. Theories for Bose-Einstein Condensates 16

2. Quantum Interferometry 21

2.1. Introduction to Interferometry 21

2.2. Atom Chips 23

2.3. Interferometry with BECs 28

2.4. Quantum Enhanced Metrology - Squeezed States 33

2.4.1. Enhanced Phase Sensitivity by Squeezed States 33

2.4.2. Creation of Squeezed States 38

2.4.3. Standard Quantum Limit 44

2.4.4. Exploiting Quantum Correlations 45

3. Description Schemes for BECs **49**

3.1. The Field Operator 50

3.2. The Many-Body Hamiltonian 52

3.3. The Time-Dependent Variational Principle 55

3.4. The Many-Boson Wave Function 57

3.5. Reduced Density Matrices and their Eigenfunctions 61

3.6. Definition of Bose-Einstein Condensation and Fragmentation 67

3.7. Classification of Interacting Regimes of Trapped Bose-Gases 69

4. Quantum Dynamics of Identical Bosons **73**

4.1. Gross-Pitaevskii Equation 75

4.2. Two-Mode Model 77

4.3. Pseudospin States and Visualization on the Bloch Sphere 81

4.4. The MCTDHB Method 85

5. Density Matrix Formalism **95**

5.1. Definition of Correlation Functions 95

5.2. Approximation by Lower-Order Quantities 99

5.3. Equations of Motion (EoM) 103

6. BECs in a Double Well Potential **111**

6.1. Approximation of the 3PRDM for a BEC in a DWP 113

6.2. Approximated EoM for EVs for a BEC in a DWP 117

6.3. Approximated EoM for EVs for a BEC in a DWP Higher Order CFs . 124

6.4. Approximated EoM for EVs for a BEC in a DWP 'Constant Trace' . . 127

6.5. Comparison to Anglin & Vardi Approximation 131

6.6. Four Mode Model and Discussion 136

A. Appendix **139**

A.1. Approximation of 3-Point Functions for a BEC in a DWP 139

A.2. Mathematica Code for Approximating EVs 148

A.3. Mathematica Code for the Density Matrix Formalism 156

Bibliography **187**

List of Equations **205**

List of Figures **213**

1. Introduction

This thesis is concerned with Bose-Einstein condensates (BECs) and especially the simulation of its dynamical behavior when trapped in potentials, e.g. on atom chips, that can be varied over time.
When describing the dynamics of $N \gg 1$ interacting, identical, bosonic particles under the influence of external forces, the many-body wavefunction, $\Psi(\mathbf{r}_1, ..., \mathbf{r}_N; t)$, is the natural starting point. Knowing this function, the condensate's atoms and their dynamics can be described by the many-body Schrödinger equation. Unfortunately, analytic solutions of the Schrödinger equation are rare exceptions and approximations and numerical methods are generally indispensable.
For weakly interacting systems, a *mean field* theory like the Gross-Pitaevskii equation gives a good approximation.
When considering the groundstate of a BEC in a double-well potential with very high barrier, it becomes intuitively clear that we end up with a two-fold fragmented state and the assumption of a single mode (like in the case of the Gross-Pitaevskii equation) is therefore questionable in general. Hence at least a two-mode model has to be used for the description of the BEC in a double-well potential, which is a good approximation if we assume the two lowest states to be very closely spaced in energy and well separated from higher levels of the potential.
In order to correctly describe the dynamics of the splitting process of trapped BECs even more than two modes might be necessary as further excitations arise. The quality of the results then depends crucially on the chosen basis set.
The use of a time-adaptive optimized basis set like in the multi-configuration time-dependent Hartree for bosons approach, MCTDHB(M), where M specifies the number of time-dependent orbitals used to construct the many-body states, proposes a cure to this problem. Nevertheless, even in the case of M-fold fragmentation, M orbitals might not be enough and more orbitals might be needed as also some small,

but finite eigenvalues (quantum depletion) can be of importance. Hence also the MCTDHB(M) method reaches its limits in form of computational time and memory even for single digit values of M on typical workstations because of the exponential growth of the Hilbert space.
In order to overcome these limitations and especially to take into account four and more modes in our simulations to better describe excitations of the BEC, in this thesis we investigate the density matrix formalism introduced in chapter 5 to the splitting process of a BEC in a double well trap, and compare our results with solutions from different approximations.
The density matrix formalism is a method to formulate equations of motion for quantum many-particle systems that allows for a numerically exact treatment as well as for approximations necessary in large systems. The method generalizes the cluster expansion technique by using expectation values instead of correlation functions which not only makes the equations more transparent but also considerably reduces the amount of algebraic effort to derive the equations.
The key point of the approximation scheme used is the fact that every expectation value (EV) of operators can uniquely be represented as a sum of products of correlation functions (CFs) (and vice versa). It is further possible to introduce a truncation operator that applied to any function of CFs (EVs), sets all CFs (EVs) of order larger than N equal zero. This concept of representing a quantity by a sum of products of another quantity, together with truncation operators can be exploited for approximation schemes.
In this thesis we will set up equations for the time evolution of EVs of the matrix elements of the x-particle reduced density matrices, (xPRDM), $x \in \{1, 2, 3, ...\}$, for the splitting process of a BEC in a double well trap using the Ehrenfest equation of motion (EoM). This leads to a hierarchy of EoM, where the time evolution of a first-order quantity is coupled to a second-order quantity, the time evolution of a second-order quantity to a third-order quantity and so on. This hierarchy is naturally truncated for systems containing n particles as EVs of normal ordered $n+1$ particle operators vanish. As the number of particles in typical experiments with BECs on atom chips is in the order of 1000, the unfolding hierarchy of differential equations has to be truncated at an earlier stage.
If the neglect of CFs of a certain order is appropriate, the representation change to

express an EV of operators as a sum of products of CFs, followed by the application of the truncation operator for CFs and one more representation change to re-express CFs as a sum of products of EVs, can be used to derive a closed set of differential equations describing the time evolution of EVs of the matrix elements of the reduced x-particle density matrices.

In the appendix we briefly present and describe the computer algebra code that was used to calculate the approximations of expectation vales (EVs) as a sum of products of lower-order EVs, see appendix A.2, as well as the code for the density matrix formalism applied to the two mode model where correlation functions (CFs) of order three and higher have been neglected, see appendix A.3. In the appendix of this thesis we restrict ourself to a special case to demonstrate the formalism and the computer algebra code in a clear way rather than in the most compact and rigorous form. The complete code used for the calculations is available for download, as detailed in the appendix.

Before actually employing the density matrix formalism for simulations that need more than two modes, we stick with a simple example of an adiabatic deformation of a harmonic potential trapping a BEC into a double well potential. As there are no further excitations the two mode model as well as the MCTDHB(2) lead to the same results.

As will be shown, unfortunately, the density matrix formalism experiences difficulties already in this simple case. At least in the case of a two mode system they can be overcome by explicitly keeping the trace of the x-particle reduced density matrix (xPRDM) constant. For more than two modes instabilities due to non-linearities arise in the equations of motion of the density matrix formalism that prevent its further applications.

1.1. Structure of this Thesis

This thesis is divided into seven chapters plus appendix. Especially the introductory chapters of this thesis follow the path of a handful of wonderful summaries of first theoretical predictions and descriptions as well as underlying experiments and historical background information found in [24, 54, 74, 135, 140].
Without further ado, we outline the basic principles and concepts needed to describe Bose-Einstein condensates (BECs), give a short historical overview and present current research and applications before coming to theories for BECs in chapter one.
Chapter two is dedicated to a famous application of BECs, namely quantum interferometry. We give a short introduction to interferometry after which we describe atom chips that are used to capture and manipulate BECs. We further present the concept of quantum enhanced metrology that can be used to beat the standard quantum limit in measurements.
The most fundamental concepts of the theory of ultracold bosons are reviewed starting with the many-body Hamiltonian and its different representations in chapter three. We next derive the Schrödinger equation from the time-dependent variational principle and discuss the representation and implications of a many-body wave function in a finite basis. We further introduce reduced density matrices and relate them to observables before reviewing criteria for Bose-Einstein condensation and classifying regimes of interacting bosons.
In chapter four we describe the standard numerical methods used in the description of the dynamics of BECs beginning with the time-dependent many-particle Schrödinger equation and a first approximation in form of the mean field theory Gross-Pitaevskii equation. Finally the multi-configuration time-dependent Hartree approach (MCTDH), one realization of the use of a time-adaptive optimized basis set, is outlined.
Chapter five is devoted to the density matrix formalism. We start with the definition of correlation functions and show how expectation values can be represented as correlation functions and vice versa. We further introduce approximation schemes by neglecting higher order correlation functions and use them to get a closed set of equations from the Heisenberg equation of motion.
Finally we apply this new formalism to the splitting process of a BEC in a double well

trap and compare our results with solutions from different approximations in chapter six, where we also discuss the four mode model in our approximation scheme.

1.2. Bose-Einstein Condensates

A Bose-Einstein condensation is a phase transition for a gas of bosons that takes place at very low temperatures (that is, in the range of 10^{-7} K) where nearly all bosons occupy the ground state, see Fig. 1.1. In their ground state, non-interacting bosons - in contrast to fermions that obey the Pauli exclusion principle - all occupy the energetically lowest single-particle state and form a so called Bose-Einstein condensate (BEC) [42]. What makes BECs, themselves being objects of macroscopic size - typically in the range of μm, Fig. 1.2 - so fascinating is their peculiarity to show behavior typically associated with wave properties of quantum objects like interference, Fig. 1.3 [84]. Hence BECs are a prime candidate for the study of quantum mechanical properties on macroscopic length scales.

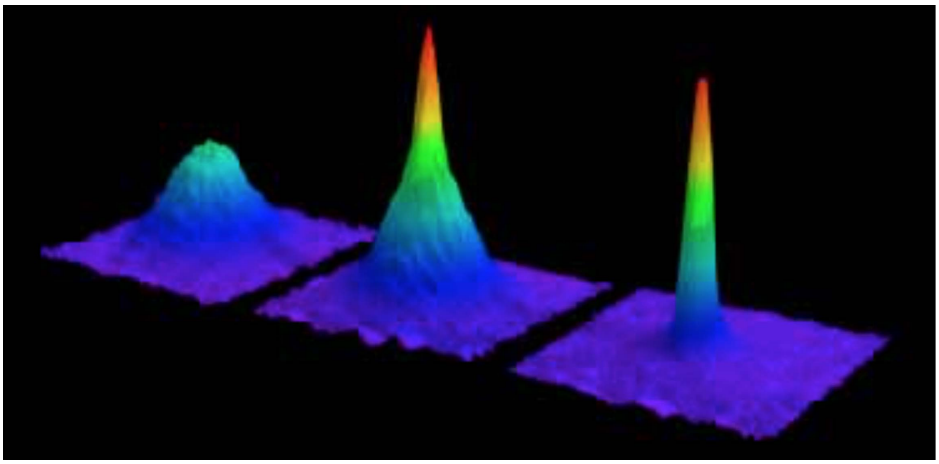

Figure 1.1.: Observation of an atomic cloud in Bose-Einstein condensation by using absorption imaging. Shown is absorption vs. two spatial dimensions. The left picture shows an expanding cloud of sodium atoms cooled to just above the transition temperature; middle: absorption image just after the condensate appeared; right: an almost pure condensate is left after further evaporative cooling. The total number of atoms at the phase transition is about 7×10^5, the temperature at the transition point is 2 μK [84].

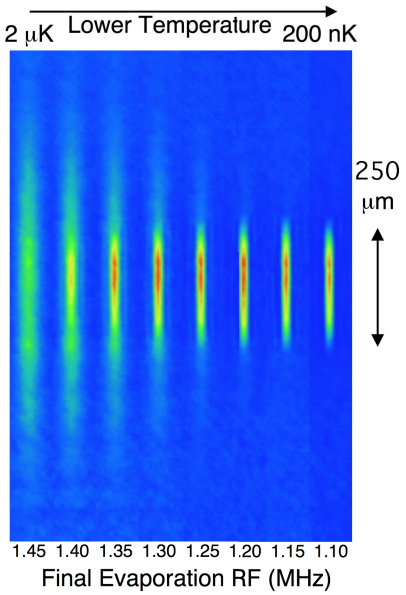

Figure 1.2.: Direct observation of the formation of a Bose-Einstein condensate (of sodium atoms) using dispersive light scattering (phase contrast images). The intensity of the scattered light shows the density of atoms. The left picture shows the cloud still slightly above the BEC transition temperature. When the temperature is lowered, a dense core forms in the center of the trap - the Bose condensate. Further cooling increases the condensate fraction to close to 100% [84].

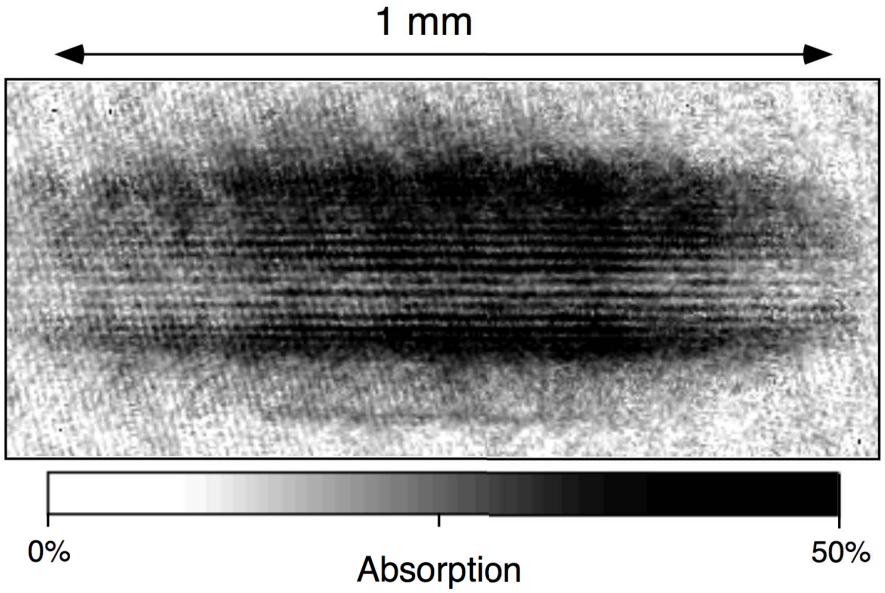

Figure 1.3.: Interference pattern of two expanding condensates (of sodium atoms) observed after 40 msec time of flight. The width of the absorption image is 1.1 mm. The interference fringes have a spacing of 15μm and show the long-range coherence of Bose-Einstein condensates [84].

1.2.1. Basic Principles

In a world that can be described by Einsteins theory of relativity, e.g. that physical laws do not change under Lorentz transformations and quantum mechanics, the spin-statistics theorem binds two particular kinds of combinatorial symmetry with two particular kinds of spin symmetry, namely bosons and fermions. The wave function describing a system of identical particles is either symmetric when swapping the positions of any two particles or antisymmetric. Particles whose wave function is symmetric under this position exchange are called bosons and posses integer spin. Particles with a wave function antisymmetric under exchange posses half-integer spin and are called fermions. The spin-statistics relation was formulated by Markus Fierz [44] in 1939 and more systematically rederived by Wolfgang Pauli [123]. In 1950 Julian Schwinger provided a more conceptual argument [148].
Examples for Fermions are elementary particles like electrons or quarks but also

composite particles such as the proton. Elementary particle bosons are the gauge bosons like the photon and the scalar Higgs boson, detected by CERN in 2012 [13,32]. Atoms with integer spin, such as ^{87}Rb, can be treated as (composite) bosons, as long as the average distance between two atoms is large compared to the size of the atoms, as the binding energy of the electron (a fermion) paired with the nucleus (a composite fermion) is much higher than the kinetic energy per atom at temperatures where the BEC of Rb is formed.
At room temperatures a gas of bosons has very similar properties to those of a gas of fermions as can easily be seen when comparing the expected number of particles N_i in an energy state i of the Fermi-Dirac statistic describing fermions with those of the Bose-Einstein statistic describing bosons.

Fermi-Dirac Distribution

$$N_i(\epsilon_i, \mu, T) = \frac{1}{e^{\frac{\epsilon_i - \mu}{k_B T}} + 1} \tag{1.1}$$

Bose-Einstein Distribution

$$N_i(\epsilon_i, \mu, T) = \frac{1}{e^{\frac{\epsilon_i - \mu}{k_B T}} - 1} \tag{1.2}$$

These occupancy functions converge in the limit

Occupancy Functions Limit

$$\frac{\epsilon_i - \mu}{k_B T} \gg 1 \quad \Rightarrow \quad N_i(\epsilon_i, \mu, T) = e^{-\frac{\epsilon_i - \mu}{k_B T}} \tag{1.3}$$

This demonstrates that a more rigorous description of the classical limit is 'small single-orbital occupancy' rather than simply high temperature, as is also shown in Fig. 1.4 comparing the two distributions above with the semiclassical Maxwell-Boltzmann statistics [83].

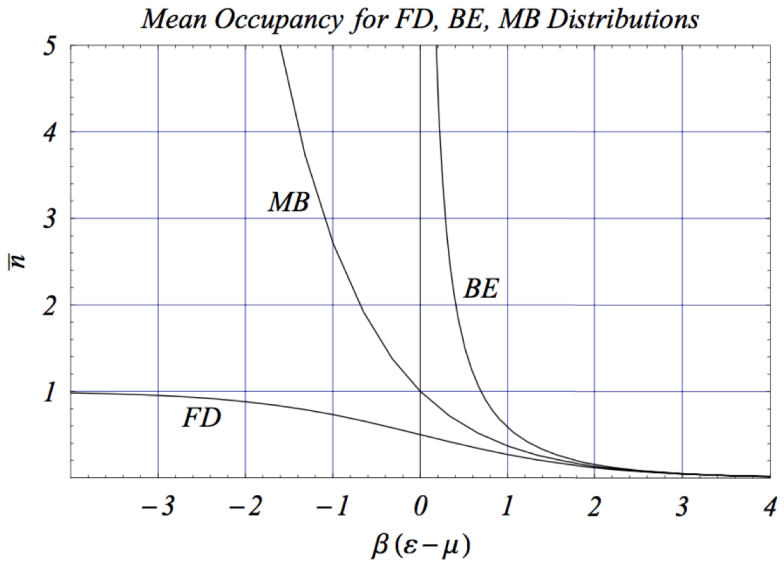

Figure 1.4.: Comparison of the mean occupancy in the Fermi-Dirac, Bose-Einstein und Maxwell-Boltzmann statistics. As can be seen all three distributions converge in the limit of 'small single-orbital occupancy' [83].

At low temperatures when the system approaches its ground state the fundamental difference between those two types of particles becomes apparent. While fermions obey the Pauli exclusion principle and are hence limited in their occupation number per state, a macroscopic number of bosons can occupy the ground state of the system and form a BEC. As all the atoms are in the exact same quantum state, they can be described by a single wave function and quantum effects like interference become important for a macroscopic object in the order of μm what makes BECs intriguing objects to study.

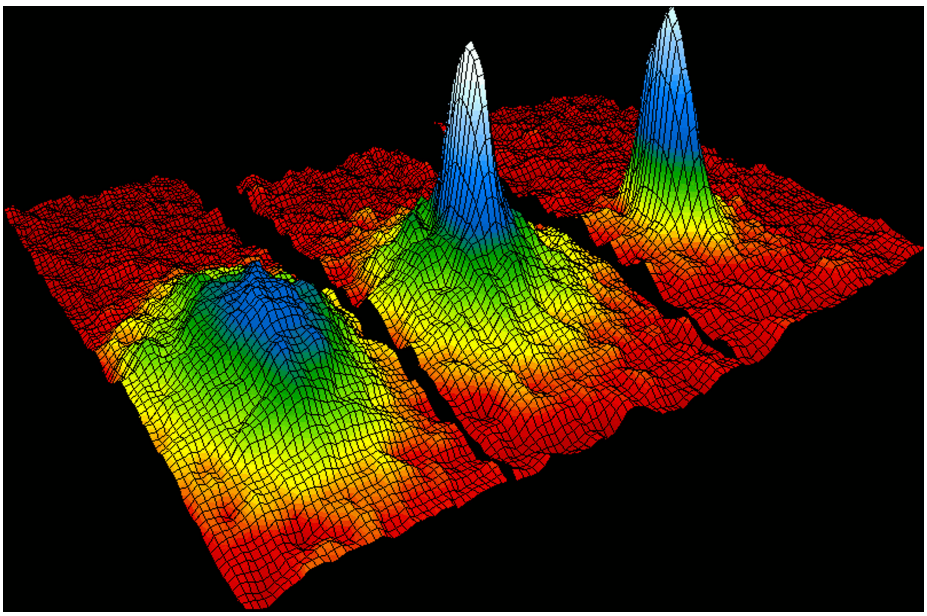

Figure 1.5.: Simulation of the momentum distribution of a boson gas undergoing a phase transition to a BEC. On the left, for higher temperatures many states are occupied. A phase transition occurs in the middle leaving only the ground state occupied for even lower temperatures (right) [34].

Although a BEC is typically defined as a bosonic gas in the ground state of the system, we call a gas consisting of bosons a BEC, if at least one state of the system is macroscopically occupied, i.e. in the order of the total number of atoms. We define it as a simple BEC if only one state that does not have to be the ground state is highly occupied and a fragmented BEC if more than one state possesses macroscopical occupation.

1.2.2. Historical Overview - The Path to Bose-Einstein Condensation

In the first half of the 20th century the theoretical concept of Bose-Einstein condensation was first proposed. The Indian physicist Satayendra N. Bose discovered that the thermal distribution of photons does not obey the Maxwell-Boltzmann statistics when investigating the statistics of photons [20]. Particles obeying the distribution function derived by Bose are nowadays known as bosons. The extension to a gas of

massive, noninteracting particles was carried out by Albert Einstein who realized that a large fraction of particles would occupy the state of lowest energy for sufficiently low temperatures [38, 39]. For temperatures at absolute zero all particles would even 'condense' into the state of lowest energy and all behave in the same manner. Hence the theoretical base for Bose-Einstein condensation was found and the search began. Following a suggestion by London in 1938 [99, 100] superfluid liquid ^4He was the first candidate for a physical system exhibiting Bose-Einstein condensation. However, as the particles in superfluid liquid ^4He exhibit strong interactions, in stark contrast to the noninteracting particles in Einstein's model, it was expected already back then that Bose-Einstein condensation would be strongly modified by these interactions, what is indeed the case. Modern experiments as well as theoretical results suggest that even at absolute zero temperature the fraction of condensed particles in superluid liquid ^4He is not larger than about 7% [28, 33, 125, 149].
Soon the search was extended to other systems, see Ref. [53] for an overview. With the developments of novel laser and magnetic based cooling techniques in the 1980s experimentalists were able to cool dilute gases of neutral atoms down to extremely low temperatures, see Refs. [29, 30, 131] for overviews of these techniques. In the year 1995, on June 5th, Eric Cornell and Carl Wiemann from the University of Colorado at Boulder NIST-JILA lab finally succeeded in producing the first BEC in a gas of rubidium atoms that was cooled down to 170nK. Main ingredients of their successful procedure were evaporative cooling in combination with an extremely good vacuum. Shortly thereafter Wolfgang Ketterle at MIT was successful in producing a BEC using Sodium. See Ref. [9, 22, 37, 111, 112] for the path that eventually proved to be successful. In 2001, 6 years after the first successful experimental realization of BECs, Wieman, Cornell and Ketterle received the Nobel Prize in Physics 'for the achievement of Bose-Einstein condensation in dilute gases of alkali atoms, and for early fundamental studies of the properties of the condensates' [85, 121].

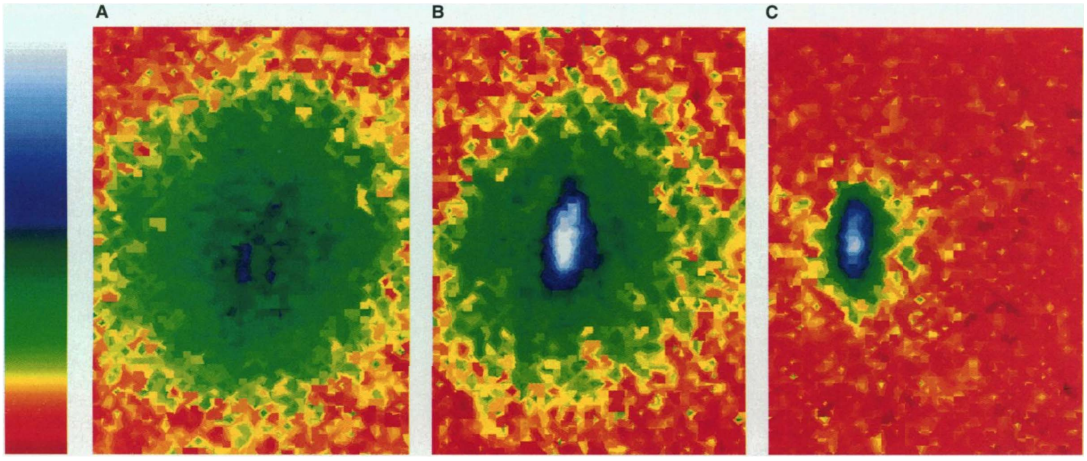

Figure 1.6.: False-color image of the velocity distribution of the cloud forming a BEC as published in Science in 1995 [9]. In (A) we see the gas just before the appearance of the condensate. In (B) just after the appearance of the condensate und in (C) after further evaporation. The condensate fraction in blue and white is elliptical, indicating a highly nonthermal distribution. In fact, it is an image of a single, macroscopically occupied quantum state. The field of view of each image is $200\mu m$ by $270\mu m$ [9].

Two major new developments in the years after 1995 accelerated the progress in the field of ultracold atoms. The possibility to tune the interaction strength between particles using Feshbach resonances was the first one [35, 73] making it possible to tune between weakly and strongly interacting BECs. The progress that was made in the shaping of the trap geometries was the second development enabling experiments with traps of arbitrary shape and several potential minima. Multi-well traps as well as whole lattices of wells are nowadays commonly used in experiments [19, 36, 89, 113]. Combining the developments of interaction-strength tuning and shaping of trap geometries it became possible to realize quasi two- and one-dimensional BECs by strongly confining the atoms in some of the spatial dimensions. A vast range of physical phenomena is hence accessible to ultracold gases like matter wave interference, tunneling, Josephson-like effects and strongly correlated bosons to name just a few. Further extension of the field has even lead to ultracold fermions and the formation of ultracold molecules. An overview of these developments can be found in Refs. [19, 36, 43, 50, 89, 113] [140].

1.2.3. Current Research and Applications

Using so-called atom chips BECs can nowadays conveniently be generated and controlled [46,47,66]. Atom chips are micro-fabricated chips with wires that use magnetic fields in order to trap and accurately control BECs enabling many interesting experiments and applications.
Quantum simulation is one of the interesting applications of BECs. In these simulations a BEC is used in order to simulate other physical systems, not only relevant in the field of solid state physics but also in astrophysics or the area of gravitational waves [23].
Another area of application of BECs is in the field of metrology and sensing. It is possible to realize matter wave interferometers relying on the wave-like nature of BECs. See Ref. [65,80,146] for the wide investigation of such interferometers. Many different kinds of interferometers can be realized, like Mach-Zehnder interferometers [17, 56], Michelson interferometers [164] or multimode interferometers [10]. There are several advantages of using matter waves instead of light waves like a finite rest mass leading to higher sensitivity to gravity and a shorter (de-Broglie) wavelength which helps to detect much smaller signals, making BECs a candidate for experiments that are not possible with conventional interferometry. The most prominent example were an interferometer with matter waves would excel a conventional light interferometer is the detection of gravity waves [40].
The search for dark matter is an other field which currently benefits from the application of BECs: Like demonstrated in [63] with the help of a matter wave interferometer it was possible to probe the gravitational field of a spherical mass by individual atoms helping to constrain certain parameters for a large class of dark energy theories.
BECs can also provide alternative approaches to known problems and experiments as shown in [138] where the value of the gravitational constant was measured in an entirely new way using BECs. This experiment could be carried out not only with high precession but can also help in the identification of systematic errors that occur when using macroscopic objects in conventional techniques.
Not mentioned yet was that matter wave interferometry beats light interferometry in accuracy not only because of the fact that matter waves posses a much shorter (de-Broglie) wavelength but also because it is possible to use non-classical states to improve the precision of an interferometer below the classical shot noise limit, as

shown in [161].
All this advancements might enable future matter wave interferometers to outperform conventional ones in terms of accuracy [74].

1.2.4. BECs in lower Dimensions

Bose-Einstein condensation is not possible in 1D and 2D for a homogenous system because the density of states does not approach 0 for low energies but should occur in atom traps because the confining potential modifies the density of states [15, 52]. Hence a 1D quasi BEC can be realized inside magnetic microtraps where the trap fields constrict the gas thereby changing the density of states so that Bose-Einstein condensation can occur.

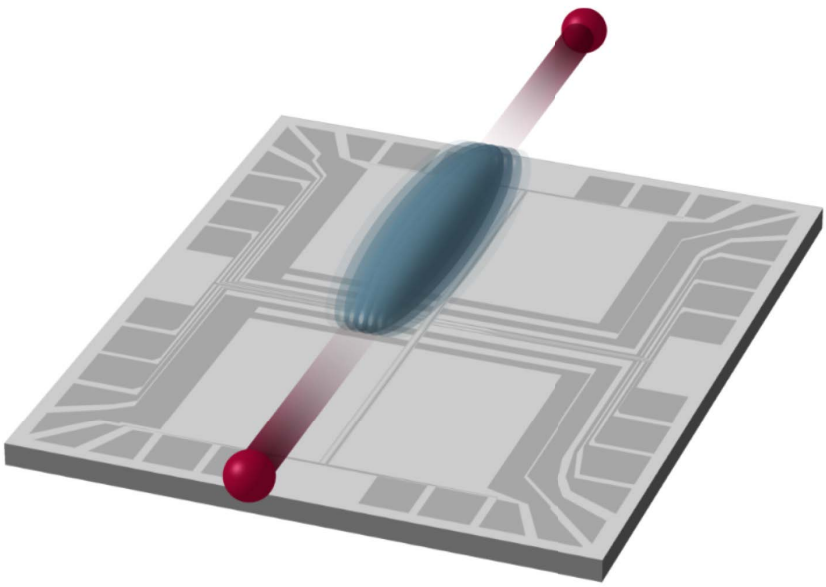

Figure 1.7.: Illustration (not drawn to scale) of a one dimensional Bose gas (blue) trapped on an atom chip with longitudinal emission of a quantum correlated pair of twin-beams (red) due to excitations of the BEC via fast transverse motion (shaking) [24].

For all simulations and most experiments reported on in thesis a quasi 1D BEC is

used – for brevity we will from now on always refer to this quasi 1D BEC simply as BEC. These BECs are constricted to a cigar like shape by the trap fields with possible excitations in longitudinal direction, a Bose Einstein condensation occurs only in the radial direction [52, 74, 97, 128].

1.2.5. Theories for Bose-Einstein Condensates

The Bose gas marks the beginning of the theory of Bose-Einstein condensates. We recommend standard textbooks on statistical mechanics like Ref. [42, 71] or alternatively [127] which contains a good chapter on the ideal Bose-gas for a more rigorous treatment.
The Bosonic occupation number for a single particle state with energy ϵ_i is given by

Bose-Einstein Distribution

$$N_i(\epsilon_i, \mu, T) = \frac{1}{e^{\frac{\epsilon_i - \mu}{k_B T}} - 1} = \frac{z e^{-\frac{\epsilon_i}{k_B T}}}{1 - z e^{-\frac{\epsilon_i}{k_B T}}} \tag{1.4}$$

with the chemical potential μ or equivalently the fugacity $z = e^{\frac{\mu}{k_B T}}$ which are implicitly determined by conservation of the particle number N:

Particle Number

$$N = \sum_{i=0}^{\infty} N_i(\epsilon_i, \mu, T). \tag{1.5}$$

The occupation numbers rise as the temperatures decrease and in order to keep N fixed, the chemical potential μ has to rise. Nevertheless the chemical potential μ can not exceed the lowest single-particle state ϵ_{min} as this would lead to negative

occupation numbers. At a sufficiently low temperature T, depending on the level structure ϵ_i, the occupation numbers may reach their limit where the excited states are said to be saturated.

Occupation Number Minimum

$$N_{min}(\epsilon_{min}, \mu, T) = \frac{1}{e^{\frac{\epsilon_{min}-\mu}{k_B T}} - 1} \tag{1.6}$$

In order to still keep the particle number fixed, the occupation of the absolute single-particle ground state has to become macroscopic, giving rise to the phenomenon of Bose-Einstein condensation (BEC).
As the particle number $N \to \infty$ and the system volume $V \to \infty$ both go to infinity in the thermodynamic limit, still keeping a constant density N/V the discrete level structure is smoothed out and the summation can be replaced by an integral. Due to the divergence at $\mu \to \epsilon_{min}$, one has to separate the ground state population N_0 as it is not properly accounted for in the continuous approximation:

Particle Number in Continuous Approximation

$$N - N_0 = \int_0^\infty D(\epsilon) N(\epsilon, \mu, T) d\epsilon, \tag{1.7}$$

where we have introduced the density of states $D(\epsilon)$, which depends on the confinement and the dimensionality of the system and typically has a power-law dependence [24].
While the ideal gas model already predicts the phenomenon of Bose-Einstein condensation for non-interacting bosons, it is too crude to describe current experiments as even in three dimensions many of the crucial properties of BEC are affected by interactions between the atoms. In fact, for realistic experimental parameters in low-dimensional systems, the role of interactions is even stronger. For an ideal gas

most of these quantum effects are completely absent. The trap geometry, number of particles and their interaction determine the shape and size of the condensate and variating only one of these parameters can have a huge effect on the properties of the condensate. Thus, in order to describe important features of trapped ultracold highly inhomogeneous, interacting Bose gases other more suitable approaches have to be derived.

An early example of the important role of interparticle interactions can already be found in [68] where an experiment with about 80.000 sodium atoms showed notable derivations in the density distribution of a factor of three to four from what can be calculated from the theory of a gas of noninteracting particles. It is therefore obvious that interactions in ultracold Bose gases must not be neglected in theoretical treatments, drastically complicating the theory of BECs but also leading to new exciting collective effects. As a matter of fact, when browsing through the literature on Bose-Einstein condensates, the largest part of the works address the behavior of interacting Bose gases near zero temperature. Hence, it is not statistical mechanics that governs the solution of the problems, but the theory of a quantum mechanical many boson systems.

In a quantum mechanical description the interacting many-body Schrödinger equation governs all properties of a Bose-Einstein condensate of dilute, atomic gases. As, even for just a few interacting particles, the many-body Schrödinger equation is very difficult to solve, approximations are usually indispensable.

The Gross-Pitaevskii theory, developed independently by Gross and Pitaevskii in 1961, is without question the most popular of these approximations [61, 133, 134]. Later in this thesis we will derive the Gross-Pitaevskii equation in chapter 4.1. As the only assumption on which the Gross-Pitaevskii theory rests, is the seemingly evident presumption that the quantum state is fully condensed at all times, it creates the impression to be a formidable general purpose theory for Bose-Einstein condensates with which it is possible to investigate inhomogeneous, interacting condensates in arbitrary trap geometries. Actually, in case the Bose-Einstein condensate remains fully condensed at all times, the Gross-Pitaevskii equation provides the same solution as the many-body Schrödinger equation.

Admittedly, the major drawback of the Gross-Pitaevskii theory is the assumption of a fully condensed state at all times as there is no way to justify this assumption

beforehand without going beyond Gross-Pitaevskii theory. The example of the superfluid liquid ^4He, as mentioned before, with only about 7% of all particles believed to be condensed, already proves that the basic assumption of a fully condensed state is not easily justifiable. In the case of a BEC captured in a double well potential, which we will discuss later, with a very high potential barrier between left and right well, it becomes intuitively clear that the assumption of a single condensed state can not be justified any more and the application of the Gross-Pitaevskii theory reaches its limits.

Another important aspect of trapped interacting Bose-Einstein condensates is the influence not only of the interaction strength but also of the geometry of the trap on the nature of the condensate. While the conceptually simplest condensates, the ones that can be described by the Gross-Pitaevskii theory, are fully condensed in one state, other types of condensates, so called fragmented condensates exist, where two or more single-particle quantum states are macroscopically occupied by atoms [53, 120]. Initially thought to be unphysical, it turned out that the opposite was the case, especially in double- and multi-well traps, where fragmented condensates appear already in the ground state, provided that the separating potential barrier is high enough. We will describe the concept of fragmentation later in more detail [1–3, 27, 114, 141, 150, 151, 157]. In the presence of long-range interparticle interactions, even for a single-well trap, the ground state can be fragmented as shown in [14].

The Bose-Hubbard model is, apart from the Gross-Pitaevskii theory, another very popular approximation for the theoretical description of trapped ultracold bosons [14, 45, 76, 77, 110]. Contrary to the Gross-Pitaevskii theory, the Bose-Hubbard model can be used for the description of fragmented condensates. The Bose-Hubbard model is a spatially discrete lattice model, thus very different from Gross-Pitaevskii theory and allows bosons to move through the lattice by hopping between neighboring lattice sites. However, it is not as generally applicable as the Gross-Pitaevskii theory as it makes explicit use of the trap potential which is assumed to be a lattice of potential wells.

While both of these models, the Gross-Pitaevskii theory and the Bose-Hubbard model are widely used to explain experiments, they give very little insight in the true physics which is governed by the many-body Schrödinger equation. A more so-

phisticated model called MCTDHB, which is the abbrivation for multiconfigurational time-dependent Hartree method for bosons is used in order to describe problems where both number and orbital dynamics are important [5, 152, 156]. This strictly variational many-body method allows for the solution of the time-dependent many-boson Schrödinger equation for large numbers of particles. With the MCTDHB method it is possible to obtain exact results from first principles for the dynamics of many-body BECs in arbitrary trap geometries. As can be seen on many examples in literature, [6, 7, 55, 57, 59, 139, 142, 143, 153–155, 158], even for very simple cases the Gross-Pitaevskii theory or the Bose-Hubbard model are not sufficient to describe the true physics of interacting many-boson systems [140].

2. Quantum Interferometry

Chapter two is dedicated to a famous application of BECs, namely quantum interferometry. We give a short introduction to interferometry after which we describe atom chips that are used to capture and manipulate BECs. We further present the concept of quantum enhanced metrology that can be used to beat the standard quantum limit in measurements.

2.1. Introduction to Interferometry

Interferometry is a technique, or rather a family of techniques, where the interference of waves, usually electromagnetic waves, is used for measurements. It exhibits extensive applications in a multitude of scientific fields like astronomy, fiber optics, engineering metrology, optical metrology, oceanography, seismology, spectroscopy (and its applications to chemistry), quantum mechanics, nuclear and particle physics, plasma physics, remote sensing, biomolecular interactions, surface profiling, microfluidics, mechanical stress/strain measurement, velocimetry, and optometry [67].
The basic principle behind interferometry is the principle of superposition. Two waves superimpose to form a resultant wave with some meaningful property like greater or lower amplitude that can be used for diagnostics. If two waves of the same frequency are combined, the resulting intensity pattern is determined by the phase difference between the two waves. For waves that are in phase we get constructive interference (greater amplitude) while waves that are out of phase will undergo destructive interference (lower amplitude) [163].
To illustrate how interferometry works we describe a conventional optical light interferometer (here a Mach-Zehnder interferometer). The Mach-Zehnder interferometer Fig. 2.1 uses a beam splitter to split an incoming laser beam. The two beams travel

different paths and a phase shift $\Delta\Phi$ is acquired by one of the beams. At a second beam splitter the two beams are recombined and the phase difference is transformed into a number difference detected at the output ports. It transforms a phase difference into a number difference. In order to accumulate this phase shift, the two paths of the laser beams have to differ in some way or the other. This may be a longer or differently orientated path or a placed sample that interacts with one of the laser beams [101, 169].

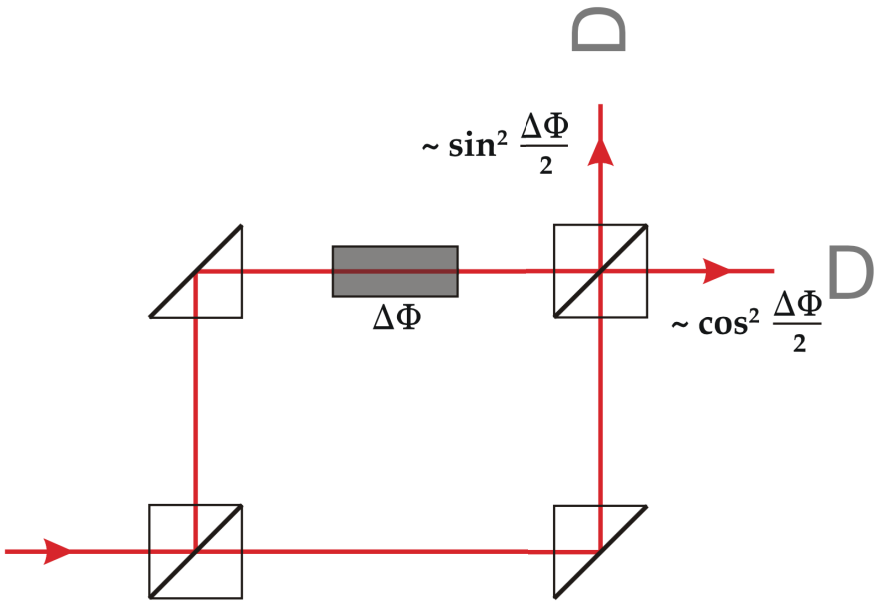

Figure 2.1.: A Mach-Zehnder interferometer uses a beam splitter to split an incoming laser beam. The two beams travel different paths and a phase shift $\Delta\Phi$ is acquired by one of the beams. At a second beam splitter the two beams are recombined and the phase difference is transformed into a number difference detected at the output ports. It transforms a phase difference into a number difference.

A Mach-Zehnder interferometer can also be realized with BECs as will be shown in the section 'Interferometry with BECs', chapter 2.3 [74, 130, 146].

2.2. Atom Chips

An overview over magnetic microtraps on atom chips, which are very versatile tools for manipulating and controlling BECs, is given in this section [48, 49].
The Zeeman Hamiltonian can be used to describe the magnetic trapping of neutral atoms in an external magnetic field **B**:

Zeeman Hamiltonian

$$H_Z = -\mu \cdot \mathbf{B} \tag{2.1}$$

with the atom's magnetic moment $\mu = -\frac{g_F \mu_B}{\hbar}\mathbf{S}$, where μ_B is the Bohr magneton, $\mathbf{S}$ the atom's spin due to hyperfine states and g_F is the corresponding Landé g-factor, whose sign distinguishes between atomic states that are aligned parallel or antiparallel to $\mathbf{B}$, respectively [136]. In an inhomogeneous magnetic field $\mathbf{B} = \mathbf{B}(\mathbf{r})$, atomic states that are aligned parallel to $\mathbf{B}$ prefer stronger fields, hence these atoms will tend to occupy locations with higher fields and are therefore called *strong field seakers*. Conversely, atomic states which are aligned anti parallel to $\mathbf{B}$ have higher energies in stronger fields, will tend to occupy locations with weaker fields and are therefore called *weak field seakers*. In Fig. 2.2 the basic mechanism of trapping is visualized. A wire carrying current I induces a magnetic field which loops around the wire. If we now apply a static magnetic field perpendicular to this wire, the two fields add up - and we find a potential minimum along a line parallel to the wire. A force is exerted on weak field seakers pushing the atoms into the minimum. This force is proportional to R^{-2}, the inverse square of the distance to the wire. A more complicated setup is needed for creating a 3D potential minimum, such as the the *Ioffe-Pritchard trap* [136], where 2D quadrupole fields are used.

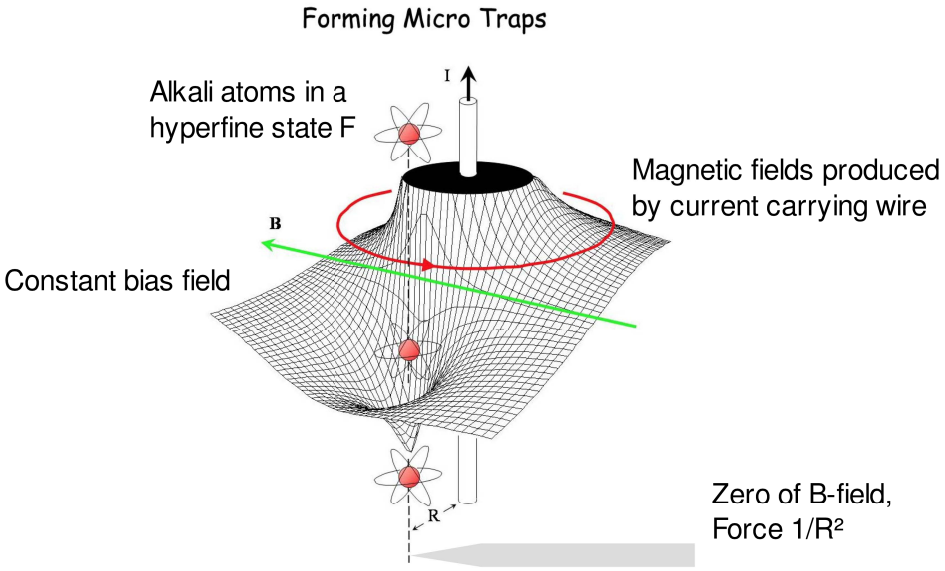

Figure 2.2.: Atoms in a magnetic trap. A current I carrying wire induces a magnetic field which loops around the wire (red circle). When applying a static magnetic field perpendicular to this wire (green arrow), the two fields add up - and a potential minimum along a line parallel to the wire is formed. On atoms which are aligned anti parallel to the resulting field **B** - so called weak field seakers, a force is exerted pushing the atoms into the minimum. This force is proportional to R^{-2}, the inverse square of the distance to the wire [54].

As the wires carrying the current can be micro-fabricated, these magnetic traps can easily be miniaturized, allowing very complex surface-mounted structures. This offers very appealing properties concerning heat dissipation through the substrate and a very robust setup, see Fig. 2.3 [145, 165].

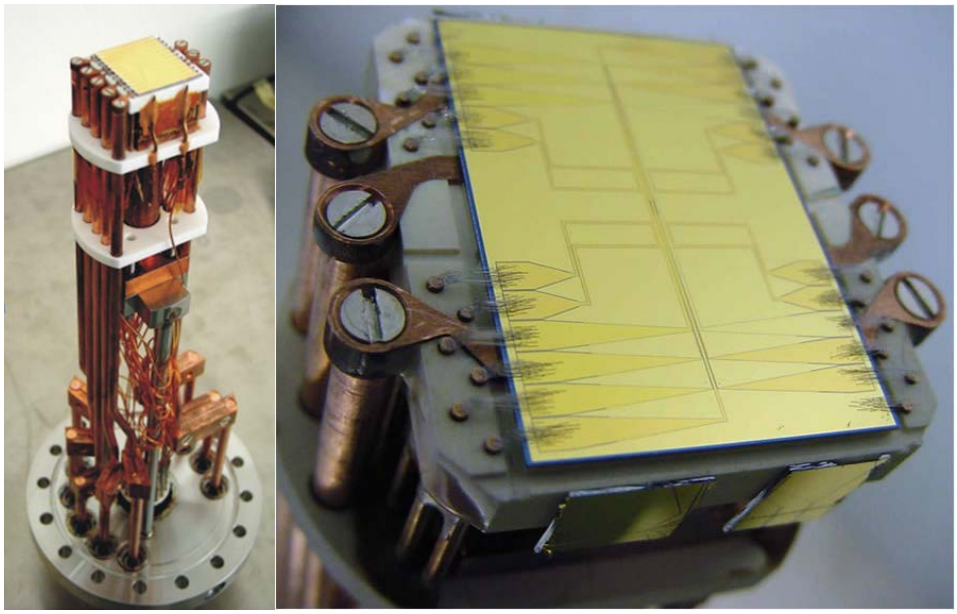

Figure 2.3.: Atom chip from the Schmiedmayer group [54].

Due to comparably high magnetic field gradients, tightly confining traps can be realized and Bose-Einstein condensation has been successfully achieved on atom chips [62,66,122,137]. Atom chips allow for a precise control of BECs hence providing a toolbox for experiments like coherent splitting and interference of condensates [146]. For these kind of experiments, *adiabatic dressed state potentials* that use time dependent magnetic radio frequency (rf) fields instead of static magnetic fields are best suited [92, 93]. This stems from the fact that splitting and merging relies on higher multipole components, even weaker than the quadrupole component of a simpel trap leading to atom losses due to weak confinement during the splitting process. This can be circumvented by the use of alternating currents. In order to realize a double well potential one can use a static magnetic field (here given in polar coordinates)

Static Magnetic Field

$$\mathbf{B}_S(\mathbf{r}) = G\rho[\cos\phi\mathbf{e}_x - \sin\phi\mathbf{e}_y] + B_I\mathbf{e}_z \tag{2.2}$$

with the gradient G of the quadrupole field and B_I being related to the inhomogeneous Ioffe field strength. The time dependent field is given by

Time Dependent Field

$$\mathbf{B}_O(\mathbf{r}, t) = B_{rf}\mathbf{e}_x \cos\omega t \tag{2.3}$$

Transforming the Zeeman Hamiltonian to a time-independent frame of reference and using a rotating wave approximation results in a time-independent Hamiltonian with adiabatic potentials (along x) as eigenvalues for different hyperfine sub levels m'_F

Adiabatic Potentials along x

$$V_\lambda(x) = m'_F g_F \mu_B \sqrt{\left[|\mathbf{B}_S(x)| - \frac{\hbar\omega}{g_F\mu_B}\right]^2 + \left[\frac{B_{rf}B_I}{2|\mathbf{B}_S(x)|}\right]^2} \tag{2.4}$$

For current experiments potentials have to be calculated beyond this approximation as can be found in [92].
In Fig. 2.4 and Fig. 2.5 typical experimental setups as well as the continuous transformation from a single into a double well potential are sketched. For convenience the control parameter λ with $B_{rf} = 0.5{+}0.3\lambda$ G is introduced which can be used to transform a single well potential into a double well potential for increasing λ. Throughout this thesis it is exactly this splitting scenario which will be investigated [54].

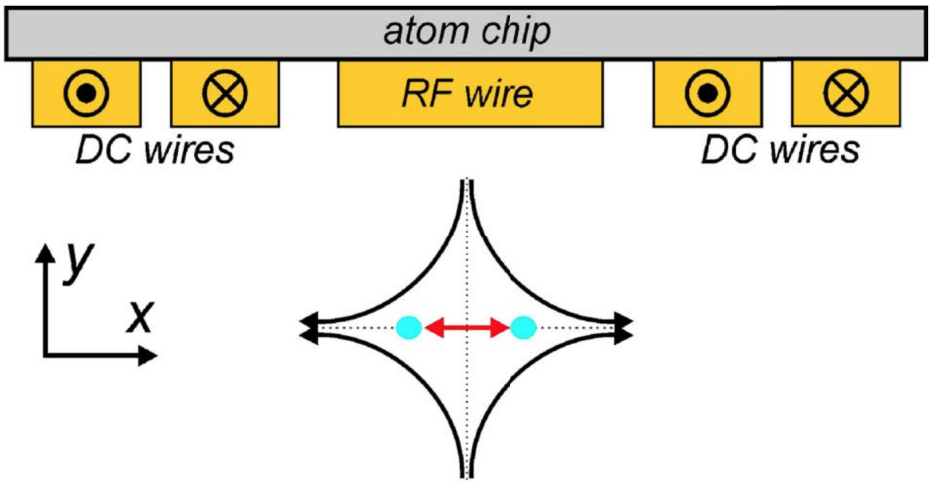

Figure 2.4.: Sketch of the experimental setup for adiabatic radio-frequency potentials with DC and AC wires mounted around the chip [54].

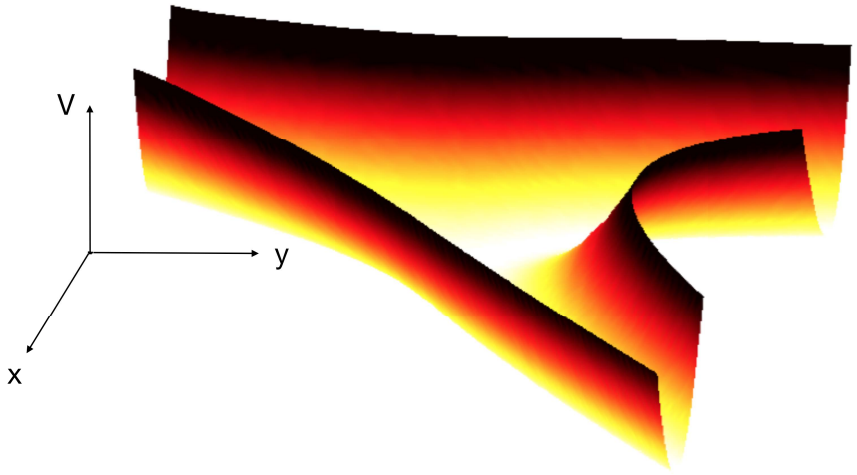

Figure 2.5.: Continuous transformation of a single well potential into a double well potential by changing the rf amplitude [54].

2.3. Interferometry with BECs

Interferometry with BECs or matter waves in general, is based on the same principles as light interferometry described before in the section 'Introduction to Interferometry', chapter 2.1. In the following we will shortly come back to atom chips introduced in the last section and describe how they can be used in order to perform interferometic experiments before describing the matter wave equivalent of a Mach-Zehnder interferometer as well as the so-called Time-of-flight (TOF) interferometer.

Before any kind of interferometric experiment can be performed, the BEC must first be created and prepared on an atom chip [46, 47, 66]. As mentioned in the last section and illustrated in Fig. 2.6 the BEC is trapped on the atom chip via magnetic fields induced by wires in an elongated cigar like shape.

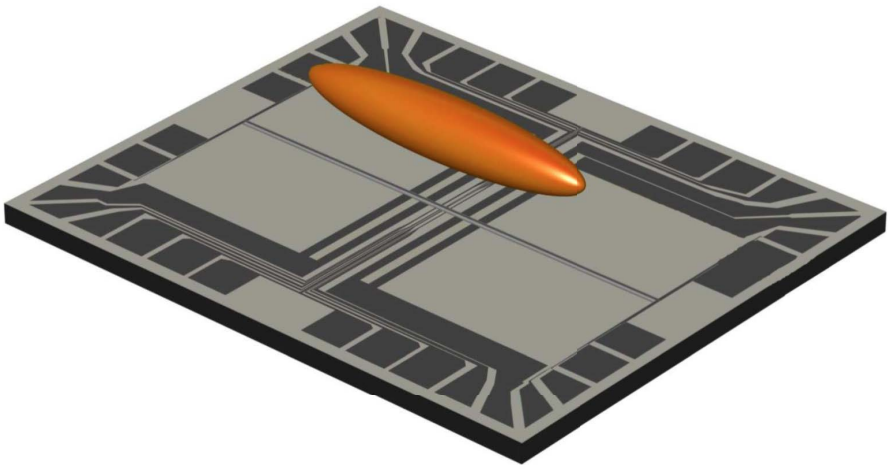

Figure 2.6.: The BEC is trapped on the atom chip via magnetic fields induced by wires in an elongated cigar like shape [74].

We reduce the problem to one dimension, using the high symmetry of the y-z-plane and ignoring the longitudinal extension of the ultra cold gas as only the radial direction is of interest to us because that is the direction where the 1D quasi BEC is formed. A possible wire-setup of an atom chip is shown in Fig 2.7. The BEC can be

trapped and controlled via a combination of B-fields in the x- and y-direction. As mentioned before, in order to produce a double well potential in this radially symmetric trap a radio frequency field is needed. Furthermore also in a single well trap anharmonicities and anisotropies can be induced with the help of this radio frequency field [25].

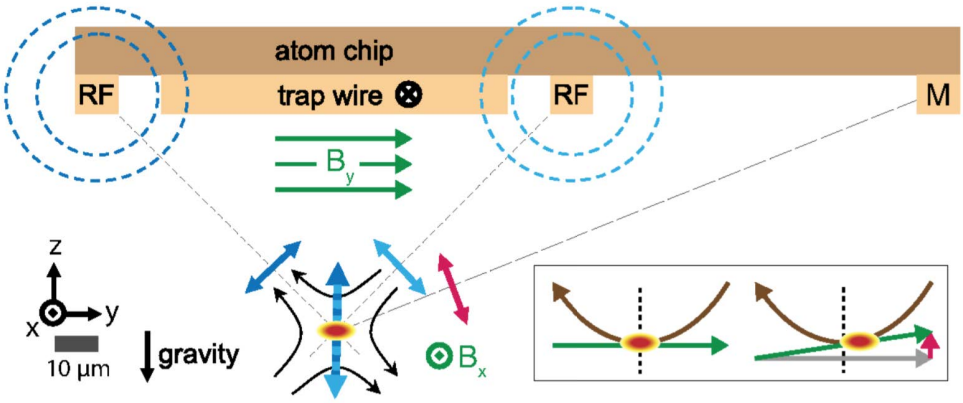

Figure 2.7.: The BEC can be trapped and controlled on a atom chip via a combination of B-fields in the x- and y-direction [25].

The first step in the optical Mach-Zehnder interferometer was the splitting of the laser beam. For a matter wave equivalent of this beam splitter the potential on the atom chip must be able to transform from a single well to a double well what can be realized by an addition of a radio frequency field with variable strength, leading to a Lesanovsky-type potential [69]. In Fig. 2.8 the harmonic potential (green) and the wave function of a BEC in the groundstate (blue) - picture on the left side - as well as the double well potential (green) and the wave function of a BEC in the groundstate (blue) - picture on the right side - are depicted. The x-axis characterizes the elongation in radial direction.

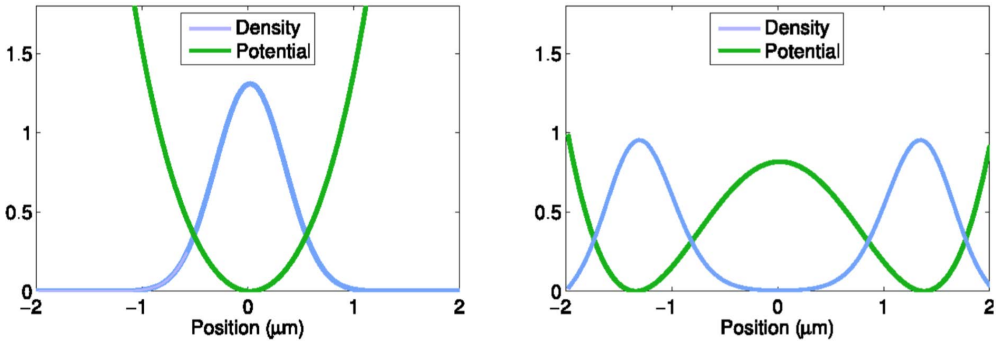

Figure 2.8.: Harmonic potential (green) and the wave function of a BEC in the groundstate (blue) - picture on the left side - for the radio-frequency parameter $\lambda = 0$ as well as the double well potential (green) and the wave function of a BEC in the groundstate (blue) - picture on the right side - for $\lambda = 1$ [74].

A demonstration of matter wave interferometry on an atom chip can be found in [17]. The main stages of the process are the same as in the case of the optical Mach-Zehnder interferometer:

- Preparation
- Beam/Condensate splitting
- Phase acquisition
- Recombination
- Readout

First of all a BEC has to be produced and trapped on an atom chip. In the next step a coherent splitting into two spatially separated waves takes place which in the case of matter waves can be simply done be transforming the trapping potential from a single well to a double well. One way to do this is to transform the potential very slowly in order to make an adiabatic transition to keep the BEC in the ground state at all time. Another way - the fast way - is with help of optimal control theory, see [54, 74] for an extended review of how optimal quantum control of trapped Bose-Einstein condensates works. After this splitting process the BEC's density has one maxima in the left well and one in the right well of the trapping potential.

Now one of the two BECs somehow accumulates a phase difference due to some interaction with an external potential. This can be done for example by tilting the potential.
In the next step, after the accumulation step, a recombination has to take place. In the optical case for a Mach-Zehnder interferometer this is again done by a half silvered mirror. For matter waves there are several approaches to convert the relative phase of the condensates into an atom number difference like the use of phase dependent heating [80], the use of a quarter of a Josephson oscillation [56, 129] or, like in [17], by abruptly decreasing the well distance and barrier height causing an acceleration of the condensates towards each other and separating the wells again afterwards for counting the atoms.
The final step is the readout stage where the wells first get separated even further on a short time scale, giving the atoms in different wells opposite momenta. When switching off the magnetic fields afterwards, the atoms fall down because of the gravitational field and can be counted by a fluorescence detector. The relative phase of the BECs and thus information about the occurred interaction can be retrieved form the atom number difference that is the final result of the experiment.
Fig. 2.9 shows the main steps of a matter wave Mach-Zehnder interferometer by sketching the potential and the BEC's wave function.

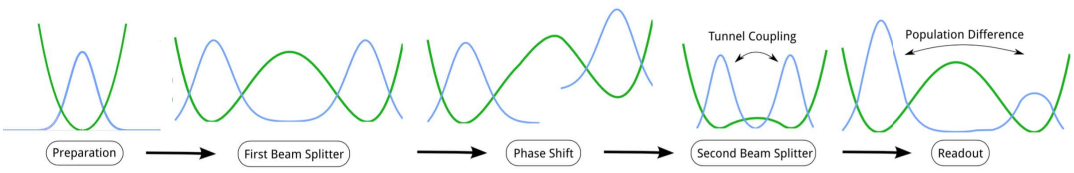

Figure 2.9.: Stages of a matter wave Mach-Zehnder interferometer [74]

The stages of a matter wave Mach-Zehnder interferometer can be summarized as follows:

- Preparation of a BEC in a double well potential
- 'Beam splitter' in form of an increase of the tunnel coupling
- Phase acquisition

- Recombination by a second 'beam splitter' in form of an increase of the tunnel coupling, transforming the phase information into a population difference
- Readout by atom counting

The time of flight (TOF) interferometer is a second important type of interferometer when working with matter waves. As there are no beam splitters like in the Mach-Zehnder interferomter, a slightly different principle is behind it. Like in the case of a Mach-Zehnder interferometer the BEC has to be prepared in a double well potential. One part of the BEC in one of the wells experiences a phase shift by some interaction, for example by tilting the trap potential. When the magnetic field is switched off, the BEC is released as it is no longer trapped by the potential. It falls down due to gravity, interferes and leaves a fringe pattern on the detector that can be observed and measured. Information about the interaction/phase shift can then be extracted from the interference pattern [74].
Fig. 2.10 shows the main steps of a matter wave time of flight interferometer by sketching the potential and the BEC's wave function.

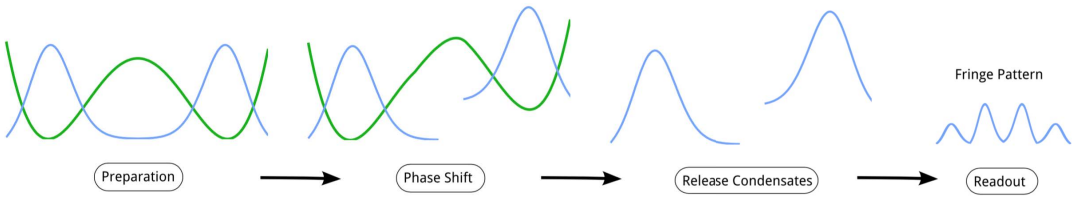

Figure 2.10.: Stages of a matter wave TOF interferometer [74]

The stages of a matter wave TOF interferometer can be summarized as follows:

- Preparation of a BEC in a double well potential
- Phase acquisition
- Release of the BEC
- BEC falls down due to gravity, interferes and leaves a fringe pattern on the detector that can be observed an measured.

2.4. Quantum Enhanced Metrology - Squeezed States

As mentioned already in the section of current research and applications of BECs, there are several advantages of using matter waves instead of light waves as matter waves have a finite rest mass and hence higher sensitivity to gravity. Another improvement when using matter waves instead of light waves is the short de-Broglie wavelength which helps to detect much smaller signals.
A maybe not so directly apparent advantage of matter wave interferometry over interferometry with classical light lies in the fact that one can also use non-classical states to increase the precision of measurements [161]. Note that non-classical light states also lead to sensitivity improvements as shown in [160].

2.4.1. Enhanced Phase Sensitivity by Squeezed States

When performing a measurement in an interferometer experiment, either the atom number in each well or the relative phase between the two wells is determined. Here the quantum uncertainties Δn and $\Delta\phi$ influence the precision of these measurements and are governed by Heisenberg's uncertainty relation [166]

Heisenberg's Uncertainty Relation

$$\Delta n \Delta\phi \gtrsim \frac{1}{2} \tag{2.5}$$

Note that the phase fluctuations $\Delta\phi$ may be arbitrarily large when measuring the atom number difference between the two wells as long as we still fulfill Heisenberg's uncertainty relation. This fact gives rise to the idea to decrease the uncertainty of either the number uncertainty Δn by increasing the phase uncertainty $\Delta\phi$ or vice versa.

In the case of a binomial state we get:

Binomial State Uncertainties

$$\Delta n = \frac{\sqrt{N}}{2} \quad \text{and} \quad \Delta\phi = \frac{1}{\sqrt{N}} \tag{2.6}$$

which fulfills Heisenberg's uncertainty relation and leads to the standard quantum shot noise limit [41]. As we are dealing with a two state system, with atoms in the left or the right well, we can use the Bloch sphere as a geometrical representation of the pure state space of a two-level quantum mechanical system [18]. A more detailed introduction into pseudospin states and visualization on the Bloch sphere can be found in chapter 4.3. In our case we use a Bloch sphere to represent states of a BEC in a double well potential. The poles represent states with all atoms in the left/right well, whereas states without number imbalance between the wells are depicted between the poles, hence are centered around the equator. The variance of the number imbalance Δn and the relative phase imbalance $\Delta\phi$ are also visible. States that differ from the binomial one by either having a smaller Δn and larger $\Delta\phi$ or vice versa are called squeezed states. Number squeezed states are states with lower number uncertainty than the binomial one, phase squeezed states are states with lower phase uncertainty than the binomial one.
There are several quantities that describe how much the shot noise can be lowered by squeezing. The first one is the so-called number squeezing ξ_n:

Number Squeezing ξ_n

$$\xi_n = \frac{2\Delta n}{\sqrt{N}} \tag{2.7}$$

As a binomial state has $\Delta n = \frac{\sqrt{N}}{2}$, its number squeezing is $\xi_n = 1$. For number squeezed states we find $\xi_n < 1$.

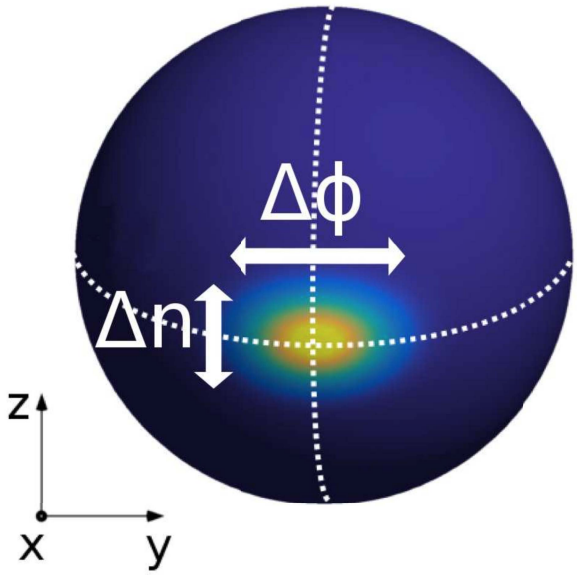

Figure 2.11.: We use a Bloch sphere to represent states of a BEC in a double well potential. The poles represent states with all atoms in the left/right well, whereas states without number imbalance between the wells are centered around the equator. The variance of the number imbalance Δn and the relative phase imbalance $\Delta\phi$ are also visible [74].

On the other hand, in the case of phase squeezed states, we define a similar quantity called phase squeezing ξ_ϕ as

Phase Squeezing ξ_ϕ

$$\xi_\phi = \Delta\phi\sqrt{N} \tag{2.8}$$

and find again $\xi_\phi = 1$ for a binomial state. An illustration of such squeezed states can be seen in Fig. 2.12 on the Bloch sphere.

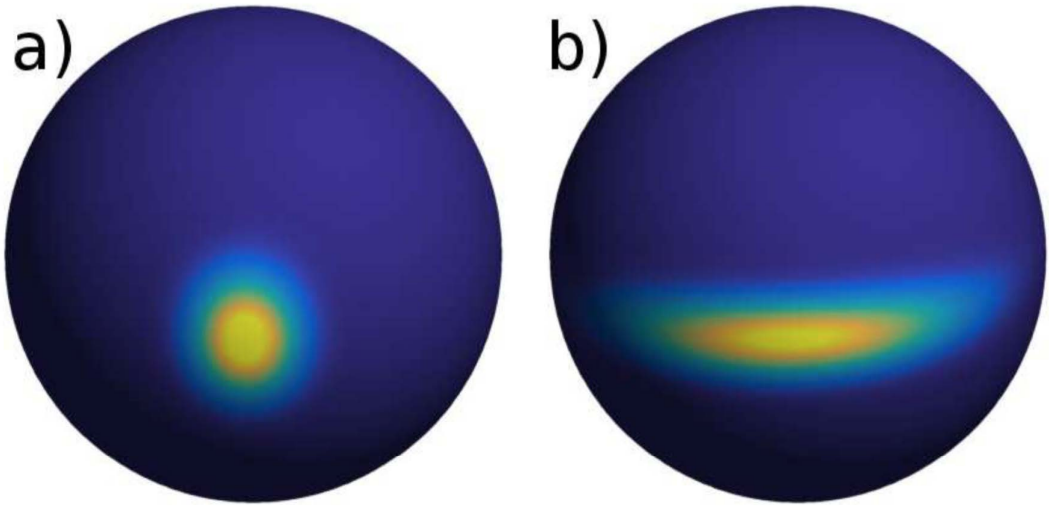

Figure 2.12.: Illustration of a phase squeezed state (a) and a number squeezed state (b) on a Bloch sphere [74].

While the number squeezing ξ_n and the phase squeezing ξ_ϕ describe the derivations from a binomial state quite well, their applicability for describing the quality of a state in regard to interferometry is very limited as the very important concept of coherence is completely neglected. As can easily be seen for the case of a Fock state, a state with a well defined number of atoms located either in the left or in the right well, not every number squeezed state improves precision. A system in a Fock state possesses a very high number squeezing, since the atoms do not tunnel from one well to the other. Nevertheless, because of the lack of coherence between these two totally separated BECs, interferometry would not be possible. It is therefore necessary to include coherence in these squeezing factors. This can be done with the use of the so-called coherence factor α [132, 166]:

Coherence Factor α

$$\alpha = \frac{1}{2}\sqrt{\langle \hat{J}_x \rangle^2 + \langle \hat{J}_y \rangle^2} = \langle \cos\phi \rangle \tag{2.9}$$

which is equal 1 for a coherent state and 0 for an incoherent state that is not suitable for interferometry. $\hat{J}_x = \frac{1}{2}(\hat{b}_L^\dagger \hat{b}_R + \hat{b}_R^\dagger \hat{b}_L)$ and $\hat{J}_y = \frac{i}{2}(\hat{b}_L^\dagger \hat{b}_R - \hat{b}_R^\dagger \hat{b}_L)$ are two of the three pseudospin operators that will be introduced in the next subsection 2.4.2 in Eq. (2.17) with the creation and annihilation operators in left-right basis. We thereby find the most important squeezing quantity when including this factor into to previously defined squeezing parameters, the so called useful or coherent spin squeezing factor ξ_S [166]

Spin Squeezing Factor ξ_S

$$\xi_S = \frac{\Delta n}{(\sqrt{N}/2)\alpha} = \frac{\xi_n}{\alpha} \tag{2.10}$$

From here on, unless specifically stated otherwise, we will always use the coherent spin squeezing factor and call a state with low numerical squeezing factor a 'highly squeezed' state.
We can now determine the precision improvement by the usage of a squeezed state instead of a binomial state when using the coherent spin squeezing ξ_S. For a binomial state we find for the spin squeezing factor ξ_S and the minimal phase error $\Delta\phi$:

Spin Squeezing Factor ξ_S and Phase Varriance $\Delta\phi$ for Binomial State

$$\xi_S = 1 \quad \text{and} \quad \Delta\phi = \frac{1}{\sqrt{N}} \tag{2.11}$$

while for the spin squeezed state we find a reduced error of $\xi_S/\sqrt{N}$ [60].
There is also another advantage of using squeezed states, namely the fact that number squeezed states are very robust against dephasing effects [80]. On the Bloch sphere this can be understood intuitively when considering the fact that dephasing effects, stemming from nonlinear interactions proportional to the square of $\hat{J}_z$ in the Hamiltonian Eq. (2.18), that curl the distribution around the x-axis are stronger near the poles of the Bloch sphere, see Fig. 2.13 and number squeezed states are located mainly near the equator, hence experiencing less of such effects [74].

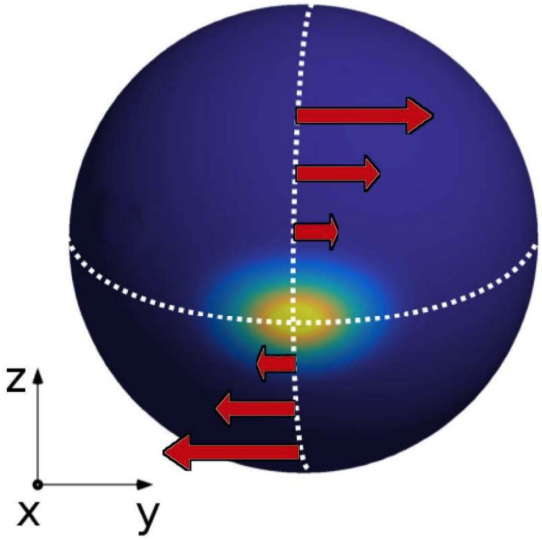

Figure 2.13.: Illustration of dephasing effects on the Bloch sphere. These dephasing effects that curl the distribution around the x-axis are stronger near the poles of the Bloch sphere than at the equator as they depend on the atom number imbalance which is is zero on the equator of the Bloch sphere and increases towards the poles [74].

2.4.2. Creation of Squeezed States

The most natural way to produce squeezed states is to simply split the trap containing the BEC quasi adiabatically from a single to a double well potential. Thereby the BEC becomes number squeezed as the tunneling between the two wells is reduced.

The main disadvantage of this procedure is that this process is relatively slow.
An alternative approach to produce squeezed states is the much faster so called two parameter optimization method [57–59]. Also in the two parameter optimization method the trap containing the BEC is transformed from a single to a double well potential but in a nonlinear fashion according to

Two Parameter Optimization Method

$$\Omega(t) = \Omega_0 \left(1 - \frac{\Omega_c}{\Omega_0}\right) \exp\left(\frac{-t}{t_c}\right) + \Omega_c \tag{2.12}$$

where Ω_0 is the tunnel coupling at $t = 0$, Ω_c the final tunnel coupling strength and t_c the time which can be optimized analytically to produce the best squeezing [79].
Parametric squeezing amplification is a more sophisticated way to produce squeezed states based on modulating the tunnel coupling at a certain resonance frequency to increase number or phase squeezing. To demonstrate the idea behind parametric amplification we decompose the field operator of the exact Hamiltonian into only two modes: a left-mode $\phi_L(\mathbf{r})$ and a right-mode $\phi_R(\mathbf{r})$

Decomposition of the Field Operator into a *Left-* and *Right-* Mode

$$\hat{\Psi}(\mathbf{r}) = \hat{b}_L \phi_L(\mathbf{r}) + \hat{b}_L \phi_R(\mathbf{r}) \tag{2.13}$$

Inserting this decomposition into the many-body Hamiltonian in 2nd quantized form leads to the following Hamiltonian in left-right (LR) -basis:

Two Mode Hamiltonian 2nd Quantized Form in LR-Basis

$$\hat{H} = -\frac{\Omega(t)}{2}(\hat{b}_L^\dagger \hat{b}_R + \hat{b}_L \hat{b}_R^\dagger) + \kappa(\hat{b}_L^\dagger \hat{b}_L^\dagger \hat{b}_L \hat{b}_L + \hat{b}_R^\dagger \hat{b}_R^\dagger \hat{b}_R \hat{b}_R) \tag{2.14}$$

The parameters are the *tunnel coupling*

Tunnel Coupling

$$\Omega = -\int dx \phi_L^*(x) \hat{h}(x) \phi_R(x) + h.c. \tag{2.15}$$

and the nonlinear interaction, or *charging energy*

Nonlinear Interaction / Charging Energy

$$\kappa = \frac{U_0}{2} \int dx |\phi_{L,R}(x)|^4 \tag{2.16}$$

with the interaction parameter $U_0 = \frac{4\pi\hbar^2 a_s}{m}$ containing the the s-wave scattering length a_s and the atom mass m. We can now use pseudospin operators in order to rewrite the many particle Hamiltonian even further. We treat the system as spin $N/2$-system as we deal with N atoms that are only allowed to live in two states. The operators are constructed from the creation and annihilation operators in LR-basis in the following way:

Pseudospin Operators

$$\hat{J}_x = \frac{1}{2}(\hat{b}_L^\dagger \hat{b}_R + \hat{b}_R^\dagger \hat{b}_L), \quad \hat{J}_y = \frac{i}{2}(\hat{b}_L^\dagger \hat{b}_R - \hat{b}_R^\dagger \hat{b}_L), \quad \hat{J}_z = \frac{1}{2}(\hat{b}_L^\dagger \hat{b}_L - \hat{b}_R^\dagger \hat{b}_R) \tag{2.17}$$

The action of $\hat{J}_x$ on a state is the exchange of one atom between the left and right well, whereas $\hat{J}_z$ measures atom number imbalances between left and right well. For the Hamiltonian we get

Hamiltonian with Pseudospin Operators

$$\hat{H} = -\Omega \hat{J}_x + 2\kappa \hat{J}_z^2. \tag{2.18}$$

We therefrom derive a model Hamiltonian with n corresponding to the particle imbalance $\langle \hat{J}_z \rangle$ and ϕ to the relative phase, $\langle \hat{J}_x \rangle$ [91, 105]

Model Hamiltonian with n and ϕ

$$\hat{H} = -\Omega \cos\phi + 2\kappa n^2 \tag{2.19}$$

This model Hamiltonian can, at least in the coupled regime where we expect very small ϕ, be further simplified by approximating $\cos\phi$ as $1 - \phi^2/2$ and neglecting higher orders of ϕ. We then arrive, finally, at the following, very familiar looking Hamiltonian

Simplified Model Hamiltonian with n and ϕ

$$\hat{H} = \frac{\Omega}{2}\phi^2 + 2\kappa n^2 \tag{2.20}$$

where we have neglected constant quantities that not depend on ϕ nor n as they do not contribute to the dynamics.
The here deducted Hamiltonian looks very similar to the Hamiltonian of a harmonic oscillator

Hamiltonian of Harmonic Oscillator

$$\hat{H} = \frac{p^2}{2m} + \frac{1}{2}m\omega^2 x^2 \tag{2.21}$$

with the momentum operator p, mass m, frequency ω and position operator x if we replace momentum and position operators by ϕ and n. We even find from the commutator relation of the spin operators that ϕ and n are canonically conjugated variables obeying

Commutator of ϕ and n

$$[\phi, n] = i \tag{2.22}$$

like momentum and position operator of the harmonic oscillator [105]. Hence we can formally treat a BEC like a harmonic oscillator with the identifications for mass $m = 1\Omega$ and the (Josephson-) frequency $\omega = 2\sqrt{\kappa\Omega}$. We can now use this similarity between a BEC in a double well potential and a harmonic oscillator with frequency ω_J in order to produce squeezed states.

There are two mechanisms that can be used to increase the amplitude of a harmonic oscillator. When thinking of a swing as a familiar mechanical picture of a harmonic oscillator, it is very easy to figure them out. One possible way to increase the amplitude is simply to push a child sitting on the swing. This corresponds to applying a force on the oscillator and thereby producing a driven oscillator. Unfortunately, for a BEC system, this process is not well suited. Like a child sitting on a swing with no one present to push the swing the only other way to increase the amplitude is by pumping on a swing. This is accomplished by a periodical change of the center of mass in the case of the swinging child and corresponds to a parametric amplification that happens when parameters of the oscillator like frequency change at twice the frequency of the oscillator.

The two main differences between the driven and the parametric amplified oscillator

are that in order to apply parametric amplification the modulation of a parameter must occur at twice the natural frequency of the system and secondly that a non-zero amplitude is necessary from the beginning. In the mechanical picture the first circumstance corresponds to the fact that you have to know *when* to pump the swing, whereas the latter corresponds to the fact that you can not start your swinging on the swing by pumping, but only by pushing off with your legs from the ground.
Parametric amplification is the method of choice when dealing with BECs where we change the frequency ω of the system periodically. This can be done very easily as the frequency ω and the tunneling energy Ω are directly related to each other and the tunneling energy can be tuned simply by the distance between the two wells. The necessary initial amplitude for parametric amplification can be achieved by inducing a breathing mode in the BEC via fast changes in the distance between the wells. The BEC thereby starts to rotate on the Bloch sphere around the x-axis, oscillating between a number to a phase squeezed state Fig. 2.14 [74].

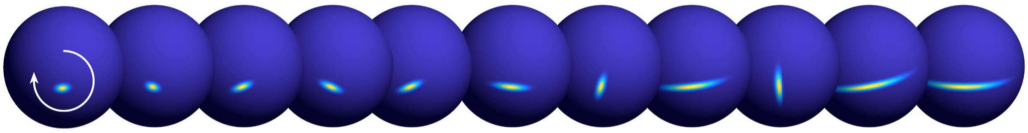

Figure 2.14.: Illustration of parametric squeezing amplification on a Bloch sphere. The BEC rotates on the Bloch sphere around the x-axis (left), oscillating between a number and a phase squeezed state as the squeezing increases over time [74].

As a side note we want to mention that there exists an important difference between the quantum mechanical and the classical, mechanical system as in the mechanical picture the values of some observables oscillate and are amplified, whereas in the quantum mechanical system, depending on the initial conditions, it are the fluctuations that are amplified, as the expectation values stay the same. See [75] for more details about parametric amplification.

2.4.3. Standard Quantum Limit

To better understand the importance of quantum effects when enhancing the sensitivity of our interferometer, lets exploit the standard quantum limit of phase sensitivity for uncorrelated particles and compare it to the case of correlated particles. We use the example of N two-level systems (TLS) with states $|0\rangle_i$ and $|1\rangle_i$ $(i = 1, ..., N)$ and demonstrate how quantum correlations can be used to beat the shot noise limit following [51].
The standard quantum limit describes the phase sensitivity of uncorrelated particles like the N-fold product state of a superposition of N two-level systems

N-fold product state of N two-level systems

$$|\Psi\rangle = \prod_{j=1}^{N} \frac{(|0\rangle_j + |1\rangle_j)}{\sqrt{2}} \tag{2.23}$$

As a consequence of the central limit theorem that can be applied when dealing with uncorrelated measurement results, the average of the variance of each particle gives the variance of the N-particle state.
For the population of the levels with particle j we measure x_j either 0 or 1 depending on whether a particle has been detected or not. Its mean value is given by

Mean Value N-fold Product State

$$\bar{x} = \frac{1}{N} \sum_{j=1}^{N} x_j \tag{2.24}$$

and the variance is

Variance N-fold Product State

$$var\left(\frac{1}{N}\sum_{j=1}^{N} x_j\right) = \sqrt{\frac{1}{N}\sum_{j=1}^{N}\Delta^2 x_j} = \frac{1}{\sqrt{N}} \tag{2.25}$$

where the last equality holds because of quantum projection noise. This means that the variance for $|0\rangle_j + |1\rangle_j$ is given by $\Delta x_j = 1$. Also in the case of coherent light, consisting of uncorrelated photons, a similar behavior can be found with the photons obeying Poissonian statistics, also known as shot noise [54].

2.4.4. Exploiting Quantum Correlations

Quantum mechanics can now help us to improve phase sensitivity and beat the $1/\sqrt{N}$ scaling when using N particles for the measurement. What we therefore need is a correlated N-particle state on the one hand and a collective or 'nonlocal' measurement on the other hand. Lets imagine a fictitious interferometer where a state of a two-level system experiences a phase shift and is then projected onto the input state $|\Psi_{IN}\rangle$

Projection of Output-State on Input-State

$$p(\theta) = |\langle\Psi_{IN}|\Psi_{OUT}(\theta)\rangle|^2 \tag{2.26}$$

for one atom input and output states are given by

Input-State and Output-State

$$|\Psi_{IN}\rangle = \frac{(|0\rangle + |1\rangle)}{\sqrt{2}}, \quad |\Psi_{OUT}\rangle = \frac{(|0\rangle + e^{i\theta}|1\rangle)}{\sqrt{2}} \tag{2.27}$$

and thus

Projection of Output-State on Input-State after Phase-Shift

$$p(\theta) = \cos^2\left(\frac{\theta}{2}\right) \tag{2.28}$$

Using error propagation for the determination of the phase sensitivity we find

Phase Sensitivity

$$\Delta\theta = \frac{\Delta p}{\left|\frac{\partial p(\theta)}{\partial \theta}\right|} \quad \text{and} \quad (\Delta p)^2 = p(\theta) - p(\theta)^2 \tag{2.29}$$

We hence find $\Delta\theta = 1$ or, carrying out N independent measurements, $\Delta\theta = 1/\sqrt{N}$. Now turning to entangled states

Entangled State

$$|\Psi_{IN}\rangle = \frac{\left(\prod_{j=1}^{N}|0\rangle_j + \prod_{j=1}^{N}|1\rangle_j\right)}{\sqrt{2}} \quad \rightarrow \quad \frac{\left(\prod_{j=1}^{N}|0\rangle_j + e^{iN\theta}\prod_{j=1}^{N}|1\rangle_j\right)}{\sqrt{2}} \tag{2.30}$$

we find for the measurement probability

Measurement Probability

$$p(\theta) = \cos^2\left(\frac{N\theta}{2}\right) \tag{2.31}$$

This leads with the definition of the phase sensitivity 2.29 to the so-called Heisenberg limited measurement

$$\Delta\theta = \frac{\Delta p}{\left|\frac{\partial p(\theta)}{\partial\theta}\right|} \quad \text{and} \quad (\Delta p)^2 = p(\theta) - p(\theta)^2$$

$$\frac{\partial p(\theta)}{\partial\theta} = -N\cos\left(\frac{N\theta}{2}\right)\sin\left(\frac{N\theta}{2}\right)$$

$$\Delta p = \sqrt{p(\theta) - p(\theta)^2}$$

$$= \sqrt{\cos^2\left(\frac{N\theta}{2}\right) - \cos^4\left(\frac{N\theta}{2}\right)}$$

$$= \cos\left(\frac{N\theta}{2}\right)\sqrt{1 - \cos^2\left(\frac{N\theta}{2}\right)}$$

$$= \cos\left(\frac{N\theta}{2}\right)\sin\left(\frac{N\theta}{2}\right)$$

$$\Delta\theta = \frac{\cos\left(\frac{N\theta}{2}\right)\sin\left(\frac{N\theta}{2}\right)}{\left|-N\cos\left(\frac{N\theta}{2}\right)\sin\left(\frac{N\theta}{2}\right)\right|} = \frac{1}{N}$$

Heisenberg Limited Measurement

$$\Delta\theta = \frac{1}{N} \tag{2.32}$$

The change rate of $p(\theta)$ with θ increases by N while the error Δp remains the same. This is a fundamental quantum limit [54].

3. Description Schemes for BECs

The most fundamental concepts of the theory of ultracold bosons are reviewed in this chapter, starting with the many-body Hamiltonian and its different representations. We next derive the Schrödinger equation from the time-dependent variational principle and discuss the representation and implications of a many-body wave function in a finite basis. We further introduce reduced density matrices and relate them to observables before reviewing criteria for Bose-Einstein condensation and classifying regimes of interacting bosons. Knowledge about the formalism of second quantization as treated e.g. in [147] is assumed.

3.1. The Field Operator

The bosonic (spinless) Schrödinger picture field operator $\hat{\Psi}(\mathbf{r})$ is the starting point of all theories and models used in this thesis and satisfies the usual bosonic commutation relations

Bosonic Commutation Relations

$$[\hat{\Psi}(\mathbf{r}), \hat{\Psi}^\dagger(\mathbf{r}')] = \delta(\mathbf{r} - \mathbf{r}'), \quad [\hat{\Psi}(\mathbf{r}), \hat{\Psi}(\mathbf{r}')] = 0. \tag{3.1}$$

$\hat{\Psi}(\mathbf{r})$ can be expanded in a complete set of orthonormal single-particle functions, which are called orbitals. We label this set of functions by $\{\phi_k\} = \{\phi_1, \phi_2, \phi_3, ...\}$. They are usually taken as a priori given, time-independent functions like plane waves or eigenfunctions of the harmonic oscillator. In the most general case, neither of these two properties need to be fulfilled: the set $\{\phi_k\}$ does not have to been known, nor must it be time-independent. We will from now on consider the general case of time-dependent orbitals $\{\phi_k(\mathbf{r}, t)\}$ that of course also includes the special case of time-independence where $\phi_k(\mathbf{r}, t) = \phi_k(\mathbf{r})$ and assume that the time-dependent orbitals form a complete orthonormal set at all times:

Orthonormality of Orbitals

$$\langle \phi_k | \phi_j \rangle = \delta_{kj} \tag{3.2}$$

We can use this complete orthonormal time dependent set $\{\phi_k(\mathbf{r}, t)\}$ to expand the time-independent field operator that then reads

Expansion of the Field Operator

$$\hat{\Psi}(\mathbf{r}) = \sum_{k=1}^{\infty} \hat{b}_k(t)\phi_k(\mathbf{r}, t) \tag{3.3}$$

where we have introduced the time-dependent annihilation and creation operators $\hat{b}_k(t)$ and $\hat{b}_k^\dagger(t)$ that obey the usual bosonic commutation relations

Bosonic Commutation Relations

$$[\hat{b}_k(t), \hat{b}_j^\dagger(t)] = \delta_{kj} \tag{3.4}$$

at any time.
Lastly, we find the closure relation when inserting the expansion of the field operator Eq. (3.3) into the first equation of the bosonic commutation relations Eq. (3.1) [140]

Closure Relation

$$\sum_{i=1}^{\infty} \phi_k(\mathbf{r}, t)\phi_k^*(\mathbf{r}', t) = \delta(\mathbf{r} - \mathbf{r}') \tag{3.5}$$

3.2. The Many-Body Hamiltonian

When describing the dynamics of $N \gg 1$ interacting, identical, bosonic particles under the influence of external forces, the many-body wavefunction, $\Psi(\mathbf{r}_1, ..., \mathbf{r}_N; t)$, is the natural starting point. Knowing this function, the condensate's atoms and their dynamics can be described by the many-body Schrödinger equation

Many-Body Schrödinger Equation

$$i\hbar \frac{\partial \Psi(\mathbf{r}_1, ..., \mathbf{r}_N; t)}{\partial t} = \hat{H}(t)\Psi(\mathbf{r}_1, ..., \mathbf{r}_N; t) \tag{3.6}$$

The Hamiltonian $\hat{H}(t)$ contains the single-particle Hamiltonian $\hat{h}(\mathbf{r}, t)$ with the atomic mass m and the external (confinement) potential $V_\lambda(\mathbf{r})$ as well as interaction potential $W(\mathbf{r}_i - \mathbf{r}_j)$ between the atoms.

Exact Hamiltonian

$$\hat{H}(\mathbf{r}_1, ..., \mathbf{r}_N; t) = \sum_{i=1}^{N} \hat{h}(\mathbf{r}_i, t) + \sum_{i<j} W(\mathbf{r}_i - \mathbf{r}_j) \tag{3.7a}$$

$$\hat{h}(\mathbf{r}_i, t) = -\frac{\hbar^2}{2m}\nabla_{\mathbf{r}}^2 + V_\lambda(\mathbf{r}) \tag{3.7b}$$

The real interaction potential between the atoms is rather complicated as it is strongly repulsive near the core before becoming attractive at intermediate distances. As the complicated part of the inter-atomic potential is rather short-ranged we can build a satisfactory theory by taking into account only its asymptotic region. In this low energy collision region, its properties can be described by a single interaction parameter, a_s, the s-wave scattering length. We can therefore use the simple contact

potential $U_0^{3D}\delta(\mathbf{r}-\mathbf{r}')$ with the correct a_s to describe low energy collision properties [36, 89].

Interaction Parameter of Contact Potential

$$U_0^{3D} = \frac{4\pi\hbar^2 a_s}{m} \tag{3.8}$$

In our case, for ^{87}Rb and very low temperatures, $a_s = 5.3\mathring{A}$ [54].
We rewrite the exact many-boson Hamiltonian in second quantized form

Exact Hamiltonian in 2nd Quantization

$$\hat{H}(t) = \int d\mathbf{r}\hat{\Psi}^\dagger(\mathbf{r})\hat{h}(\mathbf{r},t)\hat{\Psi}(\mathbf{r}) + \frac{1}{2}\int d\mathbf{r}\int d\mathbf{r}'\hat{\Psi}^\dagger(\mathbf{r})\hat{\Psi}^\dagger(\mathbf{r}')W(\mathbf{r}-\mathbf{r}')\hat{\Psi}(\mathbf{r})\hat{\Psi}(\mathbf{r}') \tag{3.9}$$

with the previously introduced bosonic creation and annihilation operators $\hat{\Psi}^\dagger(\mathbf{r})$ and $\hat{\Psi}(\mathbf{r})$, respectively.
Using the representation for the field operator given in Eq. (3.3) we find, by substitution into Eq. (3.9), the equivalent form of the exact Hamiltonian

Equivalent Exact Hamiltonian in 2nd Quantization

$$\hat{H} = \sum_{k,q}\hat{b}_k^\dagger(t)\hat{b}_q(t)h_{kq}(t) + \frac{1}{2}\sum_{k,s,l,q}\hat{b}_k^\dagger(t)\hat{b}_s^\dagger(t)\hat{b}_l(t)\hat{b}_q(t)W_{ksql}(t) \tag{3.10}$$

with the matrix elements of $h(\mathbf{r})$ and $W(\mathbf{r}-\mathbf{r}')$ given by

Matrix Elements for Exact Hamiltonian in 2nd Quantization

$$h_{kq}(t) = \int d\mathbf{r} \phi_k^*(\mathbf{r}, t) h(\mathbf{r}) \phi_q(\mathbf{r}, t) \tag{3.11a}$$

$$W_{ksql}(t) = \int d\mathbf{r} \int d\mathbf{r}' \phi_k^*(\mathbf{r}, t) \phi_s^*(\mathbf{r}', t) W(\mathbf{r} - \mathbf{r}') \phi_q(\mathbf{r}, t) \phi_l(\mathbf{r}', t) \tag{3.11b}$$

For a time-independent set of orbitals ϕ_k the matrix elements of Eq. (3.11) are also time-independent and need only be calculated once whereas they have to be evaluated at every time step of a computation in the case of a time-dependent set of orbitals. The evaluation time of these matrix elements in a calculation with a time-dependent set of orbitals can even become the limiting factor in a computational solution [54, 140].

3.3. The Time-Dependent Variational Principle

All physical laws of classical mechanics, optics, electrodynamics, general relativity, quantum mechanics and elementary particle physics can be derived from variational principles. In nearly any introductory textbook the variational principle in quantum mechanics can be found. We here introduce the time-dependent variational principle following [87] which will be needed later on when deriving equations of motion for a system of N identical bosons.
We start with the Langrangian

Langrangian

$$\mathcal{L}[\Psi(t), \Psi^*(t)] = \langle \Psi(t)|\hat{H} - i\frac{\partial}{\partial t}|\Psi(t)\rangle \tag{3.12}$$

with a wave function $\psi(t)$ normalized at all times

Normalized Wave Function

$$\langle \Psi(t)|\Psi(t)\rangle = 1. \tag{3.13}$$

We further define the nomenclature of the time derivative of Ψ as $\frac{\partial}{\partial t}\Psi(t) \equiv \dot{\Psi}$. The principle of least action (which, as a side note, is in practice just a principle of *stationary* action)

Principle of Least Action

$$\delta S = 0 \tag{3.14}$$

determines the equations of motion. Arbitrary variations of the action functional

Action Functional

$$S[\Psi, \Psi^*] = \int_{t_0}^{t_1} dt' \mathcal{L}[\Psi(t), \Psi^*(t)] \tag{3.15}$$

with respect to $\langle\Psi|$ and $|\Psi\rangle$ yield the Schrödinger equation and its hermitian conjugate if we assume a hermitian Hamiltonian $\hat{H}^\dagger = \hat{H}$

Schrödinger Equation

$$\hat{H}|\Psi\rangle = i|\dot{\Psi}\rangle \tag{3.16a}$$

$$\langle\Psi|\hat{H} = -i\langle\dot{\Psi}| \tag{3.16b}$$

In a real calculation for a many particle system, an *ansatz* has to be made for the wave function containing parameters. Hence, variations will be made with respect to these parameters and not the wave function, improving in accuracy as more and more parameters are included in the *ansatz* until convergence is reached [140].

3.4. The Many-Boson Wave Function

As already mentioned in the basic principles section 1.2.1 in the introduction, the wave function describing a system of identical particles is either symmetric (bosons) when swapping the positions of any two particles or antisymmetric (fermions). Hence a wave function of identical fermions can be expanded in a complete set of Slater determinants, whereas the wave function for a set of bosons can be expanded in a complete set of permanents. When distributing N bosons over M time-dependent orbitals $\{\phi_1, ..., \phi_M\}$ a total of $\binom{N+M-1}{N}$ permanents of the form

Permanents for N bosons in M orbitals

$$|n_1, n_2, ..., n_M; t\rangle = \frac{1}{\sqrt{n_1! n_2! ... n_M!}} \left(\hat{b}_1^\dagger(t)\right)^{n_1} \left(\hat{b}_2^\dagger(t)\right)^{n_2} ... \left(\hat{b}_M^\dagger(t)\right)^{n_M} |0\rangle \quad (3.17)$$

can be constructed. The occupations of the single orbitals can be collected in the vector $\vec{n}$

Occupation Number Vector $\vec{n}$

$$\vec{n} = (n_1, n_2, ..., n_M) \quad (3.18)$$

with the sum of the occupation numbers yielding the total number of particles N

Particle Number N

$$n_1 + n_2 + ... + n_M = N. \quad (3.19)$$

We can now use a linear combination of such time-dependent permanents to make the most general ansatz for the many-body wave function $|\Psi(t)\rangle$ of N identical bosons

Ansatz for Many-Body Bosonic Wave Function

$$|\Psi(t)\rangle = \sum_{\mathbf{n}} C_{\mathbf{n}}(t)|\mathbf{n};t\rangle \tag{3.20}$$

with the sum over all $\binom{N+M-1}{N}$ permanents. This ansatz is exact if M goes to infinity since the complete N-particle Hilbert space is spanned by the set of permanents $|\mathbf{n};t\rangle$. For real calculations where we are limited to a finite set of orbitals $\{\phi_1, ..., \phi_M\}$. This can of course only be an approximation and we get the finite size representations of the field operator $\hat{\Psi}_M$

Finite Size Representations of the Field Operator $\hat{\Psi}_M$

$$\hat{\Psi}_M(\mathbf{r};t) = \sum_{k=1}^{M} \hat{b}_k(t)\phi_k(\mathbf{r},t) \tag{3.21}$$

and the closure relation

Closure Relation for Finite Size Representations

$$\sum_{k=1}^{M} \phi_k(\mathbf{r},t)\phi_k^*(\mathbf{r}',t) = \delta_M(\mathbf{r}-\mathbf{r}';t) \tag{3.22}$$

which are both, in the most general case, time-dependent. As the field operator $\hat{\Psi}_M$ is just a finite size representation for finite M, so is $\delta_M(\mathbf{r}-\mathbf{r}';t)$ just a finite size approximation of a true delta function. Nevertheless, for any function lying in the finite dimensional Hilbert space spannend by a finite number of orbitals $\{\phi_1,\phi_2,...,\phi_M\}$ the finite size representations $\hat{\Psi}_M$ and δ_M act like their exact equivalents, Eq. (3.3) and Eq. (3.5). When working in the finite dimensional Hilbert space the finite size representation of the many-body Hamiltonian is obtained by substituting the respective finite M expansion for the field operator, Eq. (3.21), into the exact many-boson Hamiltonian in second quantized form Eq. (3.9).
Conventionally a time independent set of orbitals $\phi_1,\phi_2,...,\phi_M$ is used. It represents a special case of the more general time-dependent case. The formalism by means of a time-dependent base does not lead to any additional complications as far as quantities at a single time t are concerned. On contrary, this additional freedom (to choose a new set of base functions at every time step) can be a big advantage and is most effectively used, if the orbitals are determined by the time-dependent variational principle [87]. In the chapter about quantum dynamics of identical bosons we will introduce the multiconfigurational time-dependent Hartree for bosons method (MCTDHB), which is based on this principle. In the conventional case of time-independent orbitals $\phi_1,\phi_2,...,\phi_M$ only the coefficients $C_{\mathbf{n}}(t)$ in the ansatz wave function Eq. (3.20) are allowed to depend on time. Hence the finite size representations of the field operator $\hat{\Psi}_M$, Eq. (3.21), as well as the closure relation for finite size representations Eq. (3.22) constitute time-independent approximations of the exact field operator, Eq. (3.3), and the exact closure relation, Eq. (3.5). The ansatz Eq. (3.20) for a wave function as a sum of permanents, each multiplied with a time dependent coefficient, is the most general M-orbital many-boson ansatz possible. In literature there exist some common less general ansatz wave functions that can be divided into two categories. The ansatz is called

- mean-field ansatz, if only a single permanent is used
- many-body ansatz otherwise

Examples for the former one are the Gross-Pitaevskii model which we will discuss later or the MCTDHB method if only $M=1$ orbital is used. Examples for the latter are the MCTDHB method if more than one ($M>1$) orbitals are used or the Bose-

Hubbard model which, unlike the MCTDHB method, uses only time-independent orbitals [140].

3.5. Reduced Density Matrices and their Eigenfunctions

Next we introduce p-particle reduced density matrices and their eigenfunctions which can be used for the definition of a BEC and fragmentation, as well as for the description of its dynamics. For a given wave function $\Psi(\mathbf{r}_1, ..., \mathbf{r}_N; t)$ of N identical, spinless bosons, the pth order reduced density matrix (RDM) is defined as

p-Particle Reduced Densities

$$\rho^{(p)}(\mathbf{r}_1, ..., \mathbf{r}_p | \mathbf{r}'_1, ..., \mathbf{r}'_p; t) = \frac{N!}{(N-p)!} \int \Psi(\mathbf{r}_1, ..., \mathbf{r}_p, \mathbf{r}_{p+1}, ..., \mathbf{r}_N; t) \Psi^*(\mathbf{r}'_1, ..., \mathbf{r}'_p, \mathbf{r}_{p+1}, ..., \mathbf{r}_N; t) d\mathbf{r}_{p+1} ... d\mathbf{r}_N \tag{3.23}$$

where the wave function is assumed to be normalized, i.e. $\langle \Psi(t) | \Psi(t) \rangle = 1$.
Its diagonal $\rho^{(p)}(\mathbf{r}_1, ..., \mathbf{r}_p | \mathbf{r}_1, ..., \mathbf{r}_p; t)$ is simply $\frac{N!}{(N-p)!}$-times the p-particle probability distribution at time t.

Diagonal of p-Particle Reduced Densities

$$\rho^{(p)}(\mathbf{r}_1, ..., \mathbf{r}_p | \mathbf{r}_1, ..., \mathbf{r}_p; t) = \frac{N!}{(N-p)!} \int \Psi(\mathbf{r}_1, ..., \mathbf{r}_p, \mathbf{r}_{p+1}, ..., \mathbf{r}_N; t) \Psi^*(\mathbf{r}_1, ..., \mathbf{r}_p, \mathbf{r}_{p+1}, ..., \mathbf{r}_N; t) d\mathbf{r}_{p+1} ... d\mathbf{r}_N \tag{3.24}$$

Using field operators satisfying the usual bosonic commutation relations

Bosonic Commutation Relations

$$[\hat{\Psi}(\mathbf{r}), \hat{\Psi}^\dagger(\mathbf{r}')] = \delta(\mathbf{r} - \mathbf{r}'), \quad [\hat{\Psi}(\mathbf{r}), \hat{\Psi}(\mathbf{r}')] = 0, \tag{3.25}$$

the p-particle reduced densities can equivalently be expressed through

p-Particle Reduced Densities

$$\rho^{(p)}(\mathbf{r}_1, ..., \mathbf{r}_p | \mathbf{r}'_1, ..., \mathbf{r}'_p; t) = \langle \Psi(t) | \hat{\Psi}^\dagger(\mathbf{r}'_1) ... \hat{\Psi}^\dagger(\mathbf{r}'_p) \hat{\Psi}(\mathbf{r}_p) ... \hat{\Psi}(\mathbf{r}_1) | \Psi(t) \rangle \tag{3.26}$$

Using the ith eigenvalue, $n_i^{(p)}(t)$, of the pth order RDM and the corresponding eigenfunction $\alpha_i^{(p)}(\mathbf{r}'_1, ..., \mathbf{r}_p, t)$, leads to the following representation of the pth order RDM $\rho^{(p)}$:

***p*th order RDM $\rho^{(p)}$**

$$\rho^{(p)}(\mathbf{r}_1, ..., \mathbf{r}_p | \mathbf{r}'_1, ..., \mathbf{r}'_p; t) = \sum_i n_i^p(t) \alpha_i^{(p)}(\mathbf{r}_1, ..., \mathbf{r}_p, t) \alpha_i^{(p)^*}(\mathbf{r}'_1, ..., \mathbf{r}'_p, t) \tag{3.27}$$

where the eigenfunctions are called *natural p functions* and the eigenvalues are known as *natural occupations*. In the case $p = 1$ and $p = 2$, the eigenfunctions are known as *natural orbitals* and *natural geminals*, respectively.
The eigenvalues $n_i^p(t)$ can be ordered decreasingly for every p, such that $n_1^p(t)$ denotes the largest eigenvalue of the pth order RDM.
From the normalization of the many-body wave function, the definition of the p-particle reduced density matrix Eq. (3.23) and the decomposition of the density matrix with its eigenvalues and eigenfunctions Eq. (3.27) follows the restriction on the eigenvalues of the pth order RDM.

Restriction on Density Matrix Eigenvalues

$$\sum_i n_i^{(p)}(t) = \frac{N!}{(N-p)!} \tag{3.28}$$

The largest eigenvalue $n_i^{(p)}(t)$ is hence bounded from above by [21, 31] and from Eq. (3.27) follows the restriction on the eigenvalues of the pth order RDM.

Largest Eigenvalue of Density Matrix

$$n_i^{(p)}(t) \leq \frac{N!}{(N-p)!} \tag{3.29}$$

See [124] and [144] for lower bounds on $n_i^{(p)}(t)$ and relations between different orders of RDMs.
RDMs of first and second order are of special interest for us as generally, many-body quantum systems interact via two-body interaction potentials and the expectation value of any two-body operator can be expressed by an integral involving only the second-order RDM. We therefore summarize important properties of RDMs of first and second order.
For the one-body RDM we get:

1-Particle Reduced Density

$$\rho^{(1)}(\mathbf{r}_1|\mathbf{r}_1';t) = N \int \Psi(\mathbf{r}_1, \mathbf{r}_2, ..., \mathbf{r}_N; t)\Psi^*(\mathbf{r}_1', \mathbf{r}_2, ..., \mathbf{r}_N; t)d\mathbf{r}_2 d\mathbf{r}_3 ... d\mathbf{r}_N \tag{3.30}$$

or, using bosonic field operators $\hat{\Psi}(\mathbf{r})$

1-Particle Reduced Density

$$\rho^{(1)}(\mathbf{r}_1|\mathbf{r}_1';t) = \langle\Psi(t)|\hat{\Psi}^\dagger(\mathbf{r}_1')\hat{\Psi}(\mathbf{r}_1)|\Psi(t)\rangle \tag{3.31}$$

With the help of the orbitals ϕ and the bosonic annihilation and creation operators $\hat{b}_k(t)$ and $\hat{b}_k^\dagger(t)$ we further get

1-Particle Reduced Density

$$\rho^{(1)}(\mathbf{r}_1|\mathbf{r}_1';t) = \sum_{k,q}\rho_{kq}(t)\phi_k^*(\mathbf{r}_1,t)\phi_q(\mathbf{r}_1',t) \tag{3.32}$$

where the one-body density matrix elements are defined as [151]

One-Body Density Matrix Elements

$$\rho_{kq}(t) = \langle\Psi|\hat{b}_k^\dagger\hat{b}_q|\Psi\rangle \tag{3.33}$$

For the two-body RDM we get:

2-Particle Reduced Density

$$\rho^{(2)}(\mathbf{r}_1,\mathbf{r}_2|\mathbf{r}_1',\mathbf{r}_2';t) = N(N-1)\int\Psi(\mathbf{r}_1,\mathbf{r}_2,...,\mathbf{r}_N;t)\Psi^*(\mathbf{r}_1',\mathbf{r}_2',...,\mathbf{r}_N;t)d\mathbf{r}_3d\mathbf{r}_4...d\mathbf{r}_N \tag{3.34}$$

or, using bosonic field operators $\hat{\Psi}(\mathbf{r})$

2-Particle Reduced Density

$$\rho^{(2)}(\mathbf{r}_1, \mathbf{r}_2|\mathbf{r}_1', \mathbf{r}_2'; t) = \langle \Psi(t)|\hat{\Psi}^\dagger(\mathbf{r}_1')\hat{\Psi}^\dagger(\mathbf{r}_2')\hat{\Psi}(\mathbf{r}_2)\hat{\Psi}(\mathbf{r}_1)|\Psi(t)\rangle \tag{3.35}$$

With the help of the orbitals ϕ and the bosonic annihilation and creation operators $\hat{b}_k(t)$ and $\hat{b}_k^\dagger(t)$ we further get

2-Particle Reduced Density

$$\rho^{(2)}(\mathbf{r}_1, \mathbf{r}_2|\mathbf{r}_1', \mathbf{r}_2'; t) = \sum_{k,s,l,q} \rho_{kslq}(t)\phi_k^*(\mathbf{r}_1, t)\phi_s^*(\mathbf{r}_2, t)\phi_l(\mathbf{r}_2', t)\phi_q(\mathbf{r}_1', t) \tag{3.36}$$

where the two-body density matrix elements are defined as [151]

Two-Body Density Matrix Elements

$$\rho_{kslq}(t) = \langle \Psi|\hat{b}_k^\dagger \hat{b}_s^\dagger \hat{b}_l \hat{b}_q|\Psi\rangle \tag{3.37}$$

For the largest eigenvalue of the pth order RDM Eq. (3.29) we find the upper bounds for the 1-particle RDM and the 2-particle RDM [140]

Largest Eigenvalue of 1st and 2nd order RDM

$$n_1^{(1)}(t) \leq N \tag{3.38a}$$

$$n_1^{(2)}(t) \leq N(N-1) \tag{3.38b}$$

3.6. Definition of Bose-Einstein Condensation and Fragmentation

As mentioned before, the natural orbitals and their natural occupations $n_i^{(1)}$ can also be used to define Bose-Einstein-condensation and fragmentation in interacting systems. If the largest eigenvalue (natural occupation) of the first-order RDM (natural orbital) is of the order of the number of particles in the system, a system of identical bosons is said to be condensed [126].

Condensed Bosons System Condition

$$n_1^{(1)} = \mathcal{O}(N) \tag{3.39}$$

The big advantage of this definition of Bose-Einstein condensation is motivated by the fact that it is also well defined for interacting systems of a finite number of particles. For the special case of all particles occupying the same orbital, the system is said to be *fully condensed*.

Fully Condensed Bosons System Condition

$$n_1^{(1)} = N \tag{3.40}$$

Such a state is maximally coherent and satisfies

Eigenvalue of 1st and 2nd order RDM for Max. Coherence

$$n_1^{(1)}(t) = N \tag{3.41a}$$

$$n_1^{(2)}(t) = N(N-1) \tag{3.41b}$$

If there is more than one eigenvalue of a natural orbital of the order of the number of particles, the condensate is said to be *fragmented* [53, 120].

Fragmented Bosons System Condition

$$n_1^{(1)}, n_2^{(1)}, ... = \mathcal{O}(N) \tag{3.42}$$

In this case the *fragmentation* of a condensate is defined as the sum over all $n_i^{(1)}$ for $i \geq 2$. Contrary to the believe that fragmented BECs were unphysical, it turned out that in trapped BECs already the ground state exhibits fragmentation [1–3, 14, 27, 53, 114, 120, 141, 150, 151, 157].
The intermediate case of only one orbital being populated macroscopically and several orbitals being populated by only a small number of particles is usually referred to as condensate *depletion* [140]. A useful measure is provided by

Depleted Condensate Condition

$$\frac{n_1^{(1)}}{N} > 95\% \tag{3.43}$$

3.7. Classification of Interacting Regimes of Trapped Bose-Gases

In this section we present the classification scheme of trapped interacting Bose-gases in the one-dimensional case according to [96] and [97]. As we are only considering the one-dimensional case, we can set $\mathbf{r} \to x$. We further assume the interparticle interaction potential to be given by

1D Interaction Potential

$$W(x - x') = \lambda_0 \delta(x - x') \tag{3.44}$$

For a stationary state the mean density $\bar{n}$ is defined as [96, 97]

Mean Density

$$\bar{n} = \frac{1}{N} \int \rho(x; 0) dx \tag{3.45}$$

For a 1D homogeneous system of length L we find for the line density

1D Homogeneous System Density

$$\bar{n} = \frac{N}{L} \tag{3.46}$$

Following [95] we introduce the so called *Lieb-Liniger parameter*

Lieb-Liniger Parameter

$$\gamma = \frac{\lambda_0}{\bar{n}} \tag{3.47}$$

which was first introduced in the exact treatment of a homogeneous Bose gas on a ring. There the parameter range $0 \leq \gamma \leq 2$ is known as the weak coupling limit. In this limit the ground state energy can be well approximated by perturbation theory [95]. In this thesis also when treating inhomogeneous systems, we will call γ the Lieb-Liniger parameter since the definition of $\bar{n}$ in Eq. (3.45) is generally applicable.
The classification scheme of trapped interacting Bose-gases in the one-dimensional case according to [96] and [97] is

Classification Scheme of Trapped Interacting Bose-Gases

- $\gamma \ll N^{-2}$: the ideal gas regime
- $\gamma \approx N^{-2}$: the 1D Gross-Pitaevskii regime
- $N^{-2} \ll \gamma \ll 1$: the 1D Thomas-Fermi regime
- $\gamma \approx 1$: the Lieb-Liniger regime
- $\gamma \gg 1$: the Girardeau-Tonks regime

The motivation for this classification lies in the rigorous mathematical results for the ground states of trapped condensates in the limit $N \to \infty$ at constant $N\lambda_0$ where an asymptotically homogeneous trapping potential was assumed. A potential is called asymptotically homogeneous if $V(ax) = a^s V(x)$ for $s > 0$ in the limit $x \to \infty$.
The regimes with $\gamma \ll 1$ belong to the limit of weak interactions whereas those with $\gamma > 1$ are governed by strong interactions and are termed 'true' 1D regimes.

We want to emphasize again that the classification scheme above stems from rigorous mathematical results obtained in the limit of an infinite number of particles. In real experiments as well as in the systems considered in this thesis, the number of particles is finite and this naming convention may or may not be appropriate. As is shown for example in [140], the two most popular theories of the field, Gross-Pitaevskii theory, and the Bose-Hubbard model, even deep within the regime where they are expected to be valid can fail to describe the dynamics of a bosonic Josephson junction. We therefore want to point out again that the classification scheme above can be misleading when a finite number of particles is considered [140].

4. Quantum Dynamics of Identical Bosons

In this chapter we describe the standard numerical methods used in the description of the dynamics of BECs. The time-dependent many-particle Schrödinger equation governs the dynamics of non-relativistic many-body quantum systems [88, 159]. Analytic solutions of the Schrödinger equation are rare exceptions and approximations and numerical methods are generally indispensable.

In the direct diagonalization approach the Hamiltonian is diagonalized in some time-independent basis set and the solution of the Schrödinger equation is obtained at some time from the eigenvectors and energy eigenvalues thereby obtained. Unfortunately this approach is limited to systems of small size and weak interaction strength. Furthermore, the quality of the results depends crucially on the chosen basis set.

The use of a time-adaptive optimized basis set proposes a cure to this problem [64, 81, 102]. The multiconfiguration time-dependent Hartree approach (MCTDH), is one realization of the use of a time-adaptive optimized basis set which has been successfully applied to multi-dimensional dynamical systems consisting of distinguishable particles [16, 72, 103, 107, 118, 162, 167]. Even though also small systems of indistinguishable particles can be investigated using MCTDH [98, 104, 170–175], for systems of a large number of identical particles it is important to exploit the symmetry of the many-body wave function under particle exchange.

The first implementation of the symmetry of the many-body wave function under particle exchange was done for identical fermions leading to the fermionic version of MCTDH, namely MCTDHF [82, 117, 168]. MCTDHF can be adopted for the study of correlation effects in few-electron systems [26, 86, 119].

Of great interest for us in context of this thesis is the bosonic version of MCTDH, called MCTDHB [5, 152]. What makes the bosonic case particularly interesting is

the fact that bosons, unlike fermions, are subject to the Bose-Einstein statistic and hence a very large number of bosons can reside in a relatively small number of orbitals. With the help of MCTDHB it became possible to quantitatively investigate the true many-body dynamics of a large number of bosons:

- dynamics of condensates in double-wells [5]
- correlations and coherence of trapped condensates [141]
- buildup of coherence between two initially independent subsystems [7]
- optimal control of number squeezing and atom interferometry [55, 57, 59]
- quantum dynamics of a bosonic Josephson junction [139, 143]

As shown in [4] and [8] the fermionic and bosonic methods can be united in a common framework and also be extended to mixtures of identical particles with particle conversion [140].

4.1. Gross-Pitaevskii Equation

For weakly interacting systems, a *mean field* theory gives a good approximation. In the case of a gas of condensed atoms it is valid if on average there is less than one atom in the volume given by the s-wave scattering length a_s, i.e. $na_s^3 \ll 1$, with the atomic density n [36]. In order to derive the Gross-Pitaevskii equation, we first rewrite the exact many-boson Hamiltonian in second quantized form

Exact Hamiltonian in 2nd Quantization

$$\hat{H}(t) = \int \left[\hat{\Psi}^\dagger(\mathbf{r}) \hat{h}(\mathbf{r}, t) \hat{\Psi}(\mathbf{r}) + \frac{U_0^{3D}}{2} \hat{\Psi}^\dagger(\mathbf{r}) \hat{\Psi}^\dagger(\mathbf{r}) \hat{\Psi}(\mathbf{r}) \hat{\Psi}(\mathbf{r}) \right] d\mathbf{r} \tag{4.1}$$

with the previously introduced bosonic creation and annihilation operators $\hat{\Psi}^\dagger(\mathbf{r})$ and $\hat{\Psi}(\mathbf{r})$, respectively. The field operators equation of motion reads

Field Operator Equation of Motion

$$i\hbar \frac{\partial}{\partial t} \hat{\Psi}(\mathbf{r}, t) = [\hat{\Psi}, \hat{H}] = \left[\hat{h}(\mathbf{r}, t) + \frac{U_0^{3D}}{2} \hat{\Psi}^\dagger(\mathbf{r}, t) \hat{\Psi}(\mathbf{r}, t) \right] \hat{\Psi}(\mathbf{r}, t) \tag{4.2}$$

The wave function $\hat{\Psi}(\mathbf{r}, t)$ can be decomposed in a condensate and a non-condensate fraction, or depletion, according to Bogoliubov [116].

Condensate - Depletion Decomposition

$$\hat{\Psi}(\mathbf{r}, t) = \Phi(\mathbf{r}, t) \hat{b} + \hat{\Psi}'(\mathbf{r}, t) \tag{4.3}$$

with $\Phi(\mathbf{r},t) = \langle\hat{\Psi}(\mathbf{r},t)\rangle$, defined as the expectation value of the field operator in a reservoir of atoms, and $\hat{b}$ and $\hat{b}^\dagger$ annihilating (creating) a condensate atom. As we deal with a mainly condensed state, we can consider $\hat{\Psi}'(\mathbf{r},t)$ to be only a small perturbation and hence write the condensate density as $n_0(\mathbf{r}) = |\Phi(\mathbf{r},t)|^2$. In the regime of s-wave scattering we can make the replacement $\Psi(\mathbf{r},t) \to \Phi(\mathbf{r},t)$ in the equation of motion for the field operator $\hat{\Psi}(\mathbf{r},t)$ as a good approximation, thereby obtaining the time-dependent *Gross-Pitaevskii* (GP) equation

Time-Dependent Gross-Pitaevskii Equation

$$i\hbar\dot{\Phi}(\mathbf{r},t) = \left(\hat{h}(\mathbf{r},t) + U_0^{3D}(N-1)|\Phi(\mathbf{r},t)|^2\right)\Phi(\mathbf{r},t) \tag{4.4}$$

It contains the contact potential U_0^{3D} proportional to the density $n_0(\mathbf{r})$ and reduces in the limit $U_0^{3D} \to 0$ to the one-body Schrödinger equation. The time-independet GP-equation can be obtained by making the ansatz $\Phi(\mathbf{r},t) = \phi(\mathbf{r})exp(-i\mu t/\hbar)$:

Time-Independent Gross-Pitaevskii Equation

$$\left(\hat{h}(\mathbf{r},t) + U_0^{3D}(N-1)|\phi(\mathbf{r},t)|^2\right)\phi(\mathbf{r},t) = \mu\phi(\mathbf{r}) \tag{4.5}$$

with the chemical potential μ, corresponding to the energy per particle. For repulsive interactions ($U_0^{3D} > 0$), the contact potential leads to a broadening of the ground state wave function compared to the non-interacting case [54].

4.2. Two-Mode Model

When considering the groundstate of a double-well potential with very high barrier, it becomes intuitively clear that we end up with a two-fold fragmented state and the assumption of a single mode (like in the case of the Gross-Pitaevskii equation) is therefore questionable in general. We hence use a two-mode model for the description of the BEC in a double-well, which is a good approximation if we assume the two lowest states to be very closely spaced in energy and well separated from higher levels of the potential [78,109]. In this case we can decompose the field operator into a *left-* and *right-* mode:

Decomposition of the Field Operator into a *Left-* and *Right-* Mode

$$\hat{\Psi}(\mathbf{r}) = \hat{b}_L\phi_L(\mathbf{r}) + \hat{b}_R\phi_R(\mathbf{r}) \tag{4.6}$$

Inserting this decomposition into the many-body Hamiltonian in 2nd quantized form leads to the following Hamiltonian in LR-basis:

Two Mode Hamiltonian 2nd Quantized Form in LR-Basis

$$\hat{H} = -\frac{\Omega(t)}{2}(\hat{b}_L^\dagger a_R + \hat{b}_L\hat{b}_R^\dagger) + \kappa(\hat{b}_L^\dagger\hat{b}_L^\dagger\hat{b}_L\hat{b}_L + \hat{b}_R^\dagger\hat{b}_R^\dagger\hat{b}_R\hat{b}_R) \tag{4.7}$$

where terms not contributing to the dynamics of the system (terms proportional to the total particle number $\hat{N} = \hat{b}_L^\dagger\hat{b}_L + \hat{b}_R^\dagger\hat{b}_R$) have been neglected. We use the relative atom number k between left and right well to label the basis states as $|k\rangle \equiv |N/2+k\rangle_L|N/2-k\rangle_R$. The wave function can be expanded using this basis states $|\Psi(t)\rangle = \sum_{k=-N/2}^{k=N/2} C_k|k\rangle$ with the coefficients C_k forming the state vector $\mathbf{C}$. The term proportional the $\Omega(t)$ accounts for hopping of the atoms between the two wells,

the term proportional to κ penalizes atom number imbalances. The corresponding parameters are the *tunnel coupling*

Tunnel Coupling

$$\Omega = -\int dx \phi_L^*(x)\hat{h}(x)\phi_R(x) + h.c. \tag{4.8}$$

and the nonlinear interaction, or *charging enegry*

Nonlinear Interaction / Charging Energy

$$\kappa = \frac{U_0}{2}\int dx |\phi_{L,R}(x)|^4 \tag{4.9}$$

The specific shape of the two orbitals $\phi_L(x)$ and $\phi_R(x)$ is not specified further, instead we use the generic parameter Ω to characterize the splitting and a constant κ (typically taken to be $\kappa = \frac{U_0}{2}$) for the nonlinear interaction [59].
Our next objective is to analyze the ground state and number fluctuations of our double well trap. We start with two limiting (extreme) cases. Supposing totally dominating atom-atom interactions ($\kappa \gg \Omega$), the Hamiltonian describing our system basically reduces to

Hamiltonian $\kappa \gg \Omega$

$$\hat{H} = \kappa(\hat{b}_L^\dagger \hat{b}_L^\dagger \hat{b}_L \hat{b}_L + \hat{b}_R^\dagger \hat{b}_R^\dagger \hat{b}_R \hat{b}_R) \tag{4.10}$$

and the states $k \equiv |N/2+k\rangle_L |N/2-k\rangle_R$ are the eigenstates in this limit. For $k = 0$ we get the groundstate $|N/2\rangle_L |N/2\rangle_R$ with atoms split evenly between the wells, since

interactions penalize atom number fluctuations. There are obviously no fluctuations in atom number between the sides of the trap and we end up with a totally 2-fold fragmented BEC - a simple product state.
In the other extreme case, $\Omega \gg \kappa$, we have an unsplit trap and therefore tunneling dominates over the nonlinear interactions. In this case the Hamiltonian reduces to

Hamiltonian $\Omega \gg \kappa$

$$\hat{H} = \frac{\Omega(t)}{2}(\hat{b}_e^\dagger b_e - \hat{b}_g^\dagger \hat{b}_g) \tag{4.11}$$

which we rewrote in gerade-ungerade basis with the orbitals

Gerade-Ungerade Basis

$$\phi_{g,e} = \frac{(\phi_L \pm \phi_R)}{\sqrt{2}} \tag{4.12}$$

where $\hat{b}_g$ ($\hat{b}_g^\dagger$) and $\hat{b}_e$ ($\hat{b}_e^\dagger$) are the corresponding annihilation (creation) operators. The ground state in this case is simply the one with all N atoms in the state g, as raising another atom to the excited state always costs the energy $\delta = \Omega/2$.

We can easily rewrite this state in LR-basis

$\Omega \gg \kappa$ Groundstate

$$|\Psi_0\rangle = \frac{1}{\sqrt{N!}}(\hat{b}_g^\dagger)^N|0\rangle = \frac{1}{\sqrt{N!}}\left(\frac{\hat{b}_L^\dagger + \hat{b}_R^\dagger}{\sqrt{2}}\right)^N|0\rangle = \frac{1}{2^{N/2}}\sum_{k=-N/2}^{N/2}\sqrt{\binom{N}{N/2+k}}|k\rangle \tag{4.13}$$

and find the atom number statistics to be binomial in the LR-basis with number fluctuations $\Delta n = \sqrt{N}/2$. Hence, in both extreme cases, the ground state has an equal number of atoms in each well - the difference lies in the coherence between the wells, showing up in the atom number fluctuations between the sides of the trap. The states between these two extreme cases are referred to as *number squeezed* states, since $\Delta n < \sqrt{N}/2$ and are shown in the following figure 4.1 [54, 90].

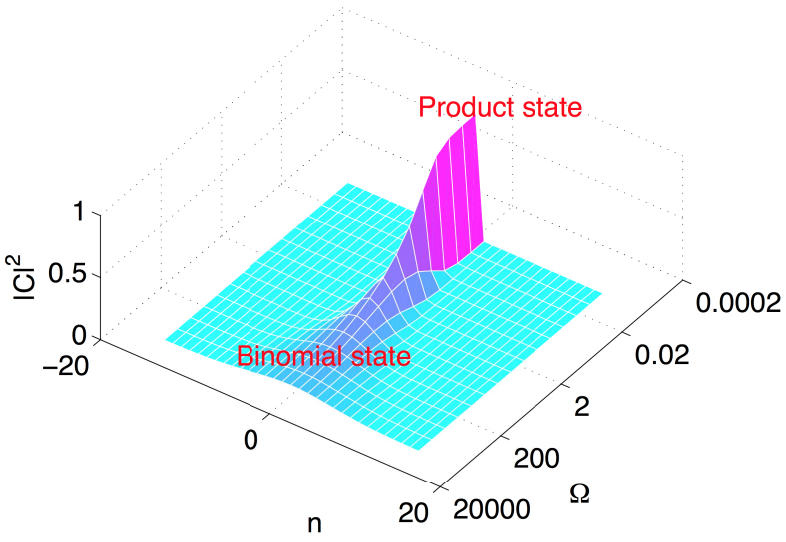

Figure 4.1.: Two-mode probability distribution $|\mathbf{C}|^2$ as a function of relative atom number n and the tunnel coupling Ω [54].

4.3. Pseudospin States and Visualization on the Bloch Sphere

The use of pseudospin operators is very comfortable in order to rewrite the many particle Hamiltonian as well as for visualization of states [109]. We treat the system as spin $N/2$-system as we deal with N atoms that are only allowed to live in two orbitals. The operators are constructed from the creation and annihilation operators in LR-basis in the following way:

Pseudospin Operators

$$\hat{J}_x = \frac{1}{2}(\hat{b}_L^\dagger \hat{b}_R + \hat{b}_R^\dagger \hat{b}_L), \quad \hat{J}_y = \frac{i}{2}(\hat{b}_L^\dagger \hat{b}_R - \hat{b}_R^\dagger \hat{b}_L), \quad \hat{J}_z = \frac{1}{2}(\hat{b}_L^\dagger \hat{b}_L - \hat{b}_R^\dagger \hat{b}_R) \tag{4.14}$$

The action of $\hat{J}_x$ on a state is the exchange of one atom between the left and right well, whereas $\hat{J}_z$ measures atom number imbalances between left and right well. For the Hamiltonian we get

Hamiltonian with Pseudospin Operators

$$\hat{H} = -\Omega(t)\hat{J}_x + 2\kappa \hat{J}_z^2. \tag{4.15}$$

Using a Fourier transformation of the atom number vector $\mathbf{C}$, a phase representation can be obtained [105]:

Phase Representation

$$\Phi(\phi) = \frac{1}{\sqrt{2\pi}} \sum_{k=-N/2}^{N/2} C_k e^{ik\phi}, \tag{4.16}$$

with $\langle\phi|k\rangle = e^{ik\phi}$, the phase eigenstates. The number operator $\hat{J}_z$ and the phase operator $\hat{\phi}$ are conjugated variables to each other, fulfilling $[\hat{\phi}, \hat{J}_z] = i$.
The mean and variance of $\hat{\phi}$ from this continuous phase representation read

Mean and Variance of $\hat{\phi}$

$$\langle\hat{\phi}\rangle = \int_{-\pi}^{\pi} d\phi\ \phi|\Phi(\phi)|^2, \quad \Delta\phi^2 = \int_{-\pi}^{\pi} d\phi\ \phi^2|\Phi(\phi)|^2 - \langle\hat{\phi}\rangle^2. \tag{4.17}$$

In the case of mean phase being zero, i.e. $\langle\hat{\phi}\rangle = 0$, the phase width $\Delta\phi$ is proportional to ΔJ_y the width of $\hat{J}_y$.

The Bloch sphere [12] can be of great help when visualizing these pseudospin states. The idea behind is the following: *atomic coherent states* provide an over-complete basis for the states of the $N/2$-spin system. These states can be obtained by rotations of the state with all atoms in one well, i.e. $|-N/2\rangle$

Rotations of the State $|-N/2\rangle$

$$|\theta, \phi\rangle = R_{\theta,\phi}|-N/2\rangle \tag{4.18}$$

using the rotation matrix

Rotation Matrix

$$R_{\theta,\phi} = e^{-i\theta(\hat{J}_x \sin(\phi) - \hat{J}_y \cos(\phi))} \tag{4.19}$$

For a given state vector $|C\rangle$, the probability distribution can be obtained as

Probability Distribution for a Given State Vector $|\mathbf{C}\rangle$

$$C(\theta,\phi) = |\langle\theta,\phi|\mathbf{C}\rangle|^2 \tag{4.20}$$

To give an example, let us take a look how the probability distribution looks for a coherent state with zero phase:

Prob. Distribution for Coherent State Vector $|\mathbf{C}\rangle$ with Zero Phase

$$|\langle\pi/2,\phi|\pi/2,0\rangle|^2 = \left(\frac{3+\cos(\phi)}{4}\right)^N \tag{4.21}$$

This corresponds approximately to a Gaussian [54]. Also see Fig. 4.2 where we plot the distributions for a coherent (a) and a number squeezed state (b) [109].

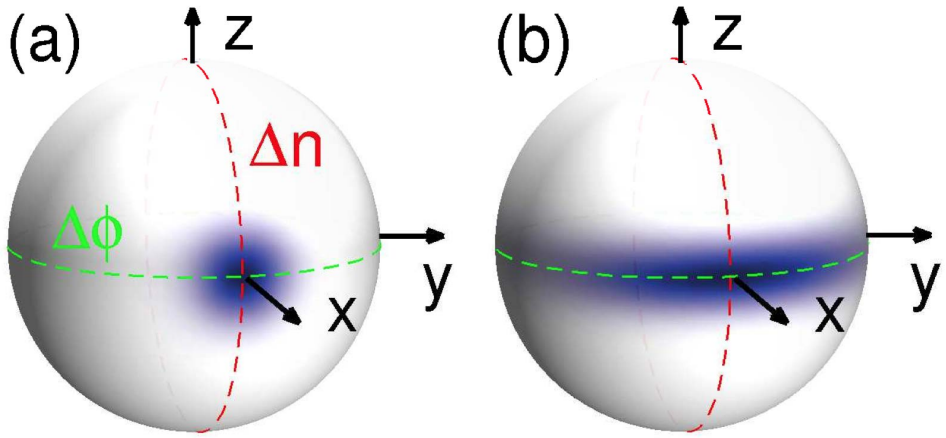

Figure 4.2.: Visualization of (a) a binomial, and (b) a number squeezed state on the Bloch Sphere with the number difference plotted on the z-axis and the phase on the equator. The width in z and y direction visualizes the number fluctuations Δn and phase fluctuations $\Delta\phi$, respectively [54].

4.4. The MCTDHB Method

For quasi adiabatic deformations of the trapping potential the generic two-mode model is a good approximation for weak interaction strength. In this case, Ω can approximately be determined as a function of the splitting parameter λ from the ground and excited states of the single-particle Schrödinger equation. Anyway, with the appearance of slight condensate oscillations this approximation does not work any more, as the generic two-mode model neglects the details about the orbitals ϕ_L and ϕ_R.

For many body systems a general variational framework has been developed in the Theoretical Chemistry group of L. S. Cederbaum in Heidelberg [108]. Notably, the *Multiconfigurational time-dependent Hartree* (MCTDH) method has been introduced in 1990 by H.-D. Meyer *et al.* [106]. In 2008 Alon *et al.* [6, 153] introduced the *Multiconfigurational time-dependent Hartree for bosons* (MCTDHB) method that takes explicitly into account the bosonic symmetry. A short introduction closely following [6, 153] into the MCTDHB method is give in this section.

The basement of MCTDHB is an ansatz for the field operator with time-dependent occupations (described by the annihilation operator $\hat{b}_k$) as well as time-dependent modes ϕ_k

MCTDHB Ansatz for the Field Operator

$$\hat{\Psi}(\mathbf{r}) = \sum_{k=1}^{M} \hat{b}_k(t)\phi_k(\mathbf{r}, t) \tag{4.22}$$

which is simply a general expansion of a state with no approximations for $M \to \infty$. As we are working with Bose-condensed systems which are M-fold *fragmented*, i.e. the one-body reduced density has M 'macroscopic' eigenvalues, M orbitals might be sufficient to capture the main physics of our system [125]. Remember that as long as only a single orbital is relevant, the GP equation might work well. Nevertheless, even in the case of M-fold fragmentation, M orbits might not be enough and more orbitals

might be needed as also some small, but finite eigenvalues (quantum depletion) can be of importance. Notwithstanding the effects of quantum depletion, bosonic systems exhibit a collective behavior of the particles, which can be used to reduce the basis of the state space enormously. As the computational effort grows exponentially with the number of modes M, cutting the sum in Eq. (4.22) for the MCTDHB field operator ansatz to finite M terms, is a very effective approximation.
A general state can be written as a superposition of symmetrized states, called *permanents*. We write a general permanent consisting of M different one-particle functions in the following way:

General Permanent of M One Particle Functions

$$|\mathbf{n};t\rangle = \frac{1}{\sqrt{n_1!n_2!...n_M!}} \left(\hat{b}_1^\dagger(t)\right)^{n_1} \left(\hat{b}_2^\dagger(t)\right)^{n_2} ... \left(\hat{b}_M^\dagger(t)\right)^{n_M} |0\rangle \tag{4.23}$$

with the vector $\mathbf{n} = (n_1, n_2, ..., n_M)$ describing the configuration. Hence, a general state is given as

General State

$$|\Psi(t)\rangle = \sum_{\mathbf{n}} C_{\mathbf{n}}(t)|\mathbf{n};t\rangle \tag{4.24}$$

We now have to determine a set of independent parameters, comprised of the coefficients $\{C_{\mathbf{n}}\}$ and orbitals $\{\phi_k(\mathbf{r},t)\}$. A variational calculus is used to find their time dependence.

Within Lagrange formalism we can formulate the action as

Action

$$S[\{C_{\mathbf{n}(t)}\},\{\phi_k(\mathbf{r},t)\}] = \int dt \left\{ \langle\Psi|\hat{H} - i\frac{\partial}{\partial t}|\Psi\rangle - \sum_{k,j=1}^{M} \mu_{kj}(t)[\langle\phi_k|\phi_j\rangle - \delta_{kj}] \right\} \tag{4.25}$$

and its variation, carried out with respect to the coefficients and orbitals, guarantees a minimization of the Schrödingers equation's expectation value as well as orthonormality of the orbitals.
The time-dependent Lagrange multipliers $\mu_{kj}(t)$ ensure that the time-dependent orbitals $\{\phi_k(\mathbf{r},t)\}$ remain orthonormal throughout the propagation. We require stationarity of the action with respect to its arguments $\{C_{\mathbf{n}}\}$ and $\{\phi_k(\mathbf{r},t)\}$. We first take expectation values and only subsequently perform the variation which somewhat simplifies the algebra.
Starting with the variation with respect to the orbitals, $\{\phi_k(\mathbf{r},t)\}$, it is helpful to express the expectation value of $\hat{H} - i\frac{\partial}{\partial t}$ in a form wich allows a direct functional differentiation with respect to $\phi_k(\mathbf{r},t)$. When acting on the orbitals, we write the expectation value of the operator as

Expectation Value of $\hat{H} - i\frac{\partial}{\partial t}$

$$\begin{aligned}\langle\Psi|\hat{H} - i\frac{\partial}{\partial t}|\Psi\rangle = &\sum_{k,q=1}^{M} \rho_{kq}\left[h_{kq} - \left(i\frac{\partial}{\partial t}\right)_{kq}\right] \\ &+ \frac{1}{2}\sum_{k,s,l,q=1}^{M} \rho_{kslq} W_{ksql} - i\sum_{\mathbf{n}} C^*_{\mathbf{n}}\frac{\partial C_{\mathbf{n}}}{\partial t}\end{aligned} \tag{4.26}$$

where the time-derivative $i\frac{\partial}{\partial t}$ is written as a one-body operator,

Time-Derivative $i\frac{\partial}{\partial t}$ as One-Body operator

$$i\frac{\partial}{\partial t} = \sum_{k,q} \hat{b}_k^\dagger \hat{b}_q \left(i\frac{\partial}{\partial t}\right)_{kq}, \quad \left(i\frac{\partial}{\partial t}\right)_{kq} = i\int \phi_k^*(\mathbf{r},t)\frac{\partial \phi_q(\mathbf{r},t)}{\partial t} d\mathbf{r} \tag{4.27}$$

The matrix elements h_{kq} and W_{ksql} are defined in Eq. (3.11) and the first and second order RDMs ρ_{kq} and ρ_{kslq} are introduced in 3.5. We collect the elements ρ_{kq} in a matrix $\boldsymbol{\rho}(t) = \rho_{kq}(t)$.
It is now straightforward to perform the variation of the action Eq. (4.25) with respect to the orbitals. Orthonormality of the functions $\{\phi_k(\mathbf{r},t)\}$ can be used to eliminate the Lagrange multipliers $\mu_{kj}(t)$ and leads to the following set of equations-of-motion for the time-dependent orbitals $\{\phi_j(\mathbf{r},t)\}$ with $j = 1, ..., M$:

Equations-of-Motion for the Time-Dependent Orbitals $\{\boldsymbol{\phi_j(\mathbf{r},t)}\}$

$$\begin{aligned} \hat{\mathbf{P}} i|\dot{\phi}_i\rangle &= \hat{\mathbf{P}}\left[\hat{h}|\phi_j\rangle + \sum_{k,s,l,q=1}^{M} \{\boldsymbol{\rho}(t)\}^{-1}_{jk}\rho_{kslq}\hat{W}_{sl}|\phi_q\rangle\right], \\ \hat{\mathbf{P}} &= 1 - \sum_{j'=1}^{M} |\phi_{j'}\rangle\langle\phi_{j'}| \end{aligned} \tag{4.28}$$

where we used $\dot{\phi}_j \equiv \frac{\partial \phi_j}{\partial t}$ and the time-dependent *local* potentials $\hat{W}_{sl}(\mathbf{r},t)$

Time-Dependent *Local* Potentials $\hat{\boldsymbol{W}}_{\boldsymbol{sl}}(\mathbf{r},\boldsymbol{t})$

$$\hat{W}_{sl}(\mathbf{r},t) = \int \phi_s^*(\mathbf{r}',t)\hat{W}(\mathbf{r}-\mathbf{r}')\phi_l(\mathbf{r}',t)d\mathbf{r}' \tag{4.29}$$

The elimination of the Lagrange multipliers $\mu_{kj}(t)$ has emerged as a projection operator $\hat{\mathbf{P}}$ onto the subspace orthogonal to that spanned by the orbitals.
Recalling that the many-body wave function Eq. (4.24) is invariant to unitary transformations of the orbitals, compensated by 'reverse' transformations of the coefficients, we can further simplify the equations-of-motion. We can perform a unitary transformation without introducing further constraints on the orbitals such that [107]

Conditions for Orthogonality Constraints

$$\langle \phi_k | \dot{\phi}_q \rangle = 0, \quad k, q = 1, ..., M \tag{4.30}$$

are satisfied at any time. If conditions Eq. (4.30) are satisfied at all times, the orbitals remain orthonormal functions at any time. The meaning of these conditions is that the temporal changes of the $\{\phi_k(\mathbf{r}, t)\}$ are always orthogonal to the $\{\phi_k(\mathbf{r}, t)\}$ themselves.
Hence we find the simplified equations-of-motion for the time-dependent orbitals $\{\phi_j(\mathbf{r}, t)\}$ with $j = 1, ..., M$:

Simplified EoM for the Time-Dependent Orbitals $\{\boldsymbol{\phi_j(\mathbf{r}, t)}\}$

$$\begin{aligned} i|\dot{\phi}_i\rangle &= \hat{\mathbf{P}} \left[\hat{h}|\phi_j\rangle + \sum_{k,s,l,q=1}^{M} \{\boldsymbol{\rho}(t)\}^{-1}_{jk} \rho_{kslq} \hat{W}_{sl} |\phi_q\rangle \right], \\ \hat{\mathbf{P}} &= 1 - \sum_{j'=1}^{M} |\phi_{j'}\rangle\langle\phi_{j'}| \end{aligned} \tag{4.31}$$

Next we have to perform the variation of Eq. (4.25) with respect to the coefficients $\{C_{\mathbf{n}}(t)\}$. We first express the expectation value in the action in a form which explicitly depends on the expansion coefficients

Expectation Value of $\hat{H} - i\frac{\partial}{\partial t}$ depending on $\{C_{\mathbf{n}}(t)\}$

$$\langle\Psi|\hat{H} - i\frac{\partial}{\partial t}|\Psi\rangle = \sum_{\mathbf{n}} C^*_{\mathbf{n}} \left[\sum_{\mathbf{n}'}\langle\mathbf{n};t|\hat{H} - i\frac{\partial}{\partial t}|\mathbf{n}';t\rangle C_{\mathbf{n}'} - i\frac{\partial C_{\mathbf{n}}}{\partial t}\right] \tag{4.32}$$

with

Expectation Value of $\hat{H} - i\frac{\partial}{\partial t}$

$$\mathcal{H}_{\mathbf{n}\mathbf{n}'}(t) = \langle n_1, n_2, ..., n_M; t|\hat{H} - i\frac{\partial}{\partial t}|n'_1, n'_2, ..., n'_M; t\rangle \tag{4.33}$$

we then find

Number Distribution

$$i\frac{\partial \mathbf{C}(t)}{\partial t} = \mathcal{H}(t)\mathbf{C}, \tag{4.34}$$

and the vector $\mathbf{C}(t)$ collecting the coefficients $C_{\mathbf{n}}(t)$. Making use of condition Eq. (4.30) we finally obtain the equations-of-motion for the propagation of the coefficients,

EoM for the Propagation of the Coefficients

$$i\frac{\partial \mathbf{C}(t)}{\partial t} = \mathbf{H}(t)\mathbf{C} \tag{4.35}$$

with

Expectation Value of $\hat{H}$

$$\mathcal{H}_{\mathbf{n}\mathbf{n}'}(t) = \langle n_1, n_2, ..., n_M; t|\hat{H}|n'_1, n'_2, ..., n'_M; t\rangle \tag{4.36}$$

The coupled equation sets Eq. (4.28) for the orbitals $\{\phi_j(\mathbf{r}, t)\}$ and Eq. (4.34) for the expansion coefficients $\{C_{\mathbf{n}}(t)\}$, or equivalently, Eq. (4.31) and Eq. (4.35) constitute the MCTDHB equations [6, 153].

We now prove that for $M = 1$ (only one orbital), variation of former action yields the GP equation.
For $M = 1$ the variation of S with respect to ϕ yields

Variation of S with Respect to ϕ for $M = 1$

$$i\frac{\partial}{\partial t}|\phi\rangle = \frac{\partial E[\phi]}{\partial \phi^*} \tag{4.37}$$

with the energy functional $E[\phi]$

Energy Functional

$$E[\phi] = \int dx \left[\frac{1}{2}|\nabla\phi|^2 + V_\lambda(x)|\phi|^2 + \frac{U_0^{3D}}{2}|\phi|^4\right] \tag{4.38}$$

We obtain the GP equation, which can be viewed as the one mode variational wave function. A product of single-particle wave functions yields the corresponding many-body wave function:

Many-Body Wave Function for Single Mode

$$\Psi(x_1, ..., x_N, t) = \prod_{i=1}^{N} \phi(x_i) \tag{4.39}$$

Time adaptive modes are in general very powerful, as they account for a lot of excitations. In comparison, in order to describe the same physics, a huge amount of time-independent modes would be necessary.

In the case of two modes ($M = 2$), we switch to gerade and ungerade orbitals Eq. (4.12):

Time Dependence of ϕ_g and ϕ_e

$$\begin{aligned} i\dot{\phi}_g &= \hat{\mathbf{P}}\left[\hat{h}\phi_g + (f_g^g|\phi_g|^2 + f_g^e|\phi_e|^2)\phi_g + \tilde{f}_g\phi_g^*\phi_e^2\right], \\ i\dot{\phi}_e &= \hat{\mathbf{P}}\left[\hat{h}\phi_e + (f_e^g|\phi_g|^2 + f_e^e|\phi_e|^2)\phi_e + \tilde{f}_e\phi_e^*\phi_e^2\right]. \end{aligned} \tag{4.40}$$

with the coefficients being given by the elements of the one- and two-particle reduced densities and k either g or e, and q the opposite.

Coefficients for $M = 2$

$$f_k^k = U_0\{\rho\}_{kk}^{-1}\rho_{kkkk}, \quad f_k^q = 2U_0\{\rho\}_{kk}^{-1}\rho_{kqkq}, \quad \tilde{f}_k = U_0\{\rho\}_{kk}^{-1}\rho_{kkqq} \tag{4.41}$$

Those orbitals are natural orbitals and the one-particle density is always diagonal since the orbitals have different parity. We also used the Projector $\hat{\mathbf{P}}$ to guarantee orthonormality of the orbitals.

Projector

$$\hat{\mathbf{P}} = 1 - |\phi_g\rangle\langle\phi_g| - |\phi_e\rangle\langle\phi_e| \tag{4.42}$$

For the number distribution we find

Number Distribution

$$i\frac{\partial \mathbf{C}(t)}{\partial t} = \mathcal{H}\mathbf{C}, \tag{4.43}$$

a very similar result to the two mode Hamiltonian in 2nd quantized form in LR-basis, except that more general matrix elements are involved:

Hamiltonian

$$\mathcal{H} = -\Omega\hat{J}_x + \frac{1}{2}\sum_{k,q,l,m}{}' \hat{b}_k^\dagger \hat{b}_q^\dagger \hat{b}_l \hat{b}_m W_{kqlm} \tag{4.44}$$

where the sum only runs over even combinations of indices. Using gerade and ungerade orbitals, we get $\hat{J}_x = \frac{1}{2}(\hat{b}_g^\dagger \hat{b}_g - \hat{b}_e^\dagger \hat{b}_e)$ and $\Omega = \langle\phi_e|\hat{h}|\phi_e\rangle - \langle\phi_g|\hat{h}|\phi_g\rangle$ and the two-particle matrix elements

Two-Particle Matrix Elements

$$W_{kqlm} = U_0 \int dx \phi_k^*(x)\phi_q^*(x)\phi_l(x)\phi_m(x) \tag{4.45}$$

A sketch of the method is given in Fig. 4.3 visualizing the self-consistent solution of the state vector $\mathbf{C}$ and the orbitals using the coupled equations for the time

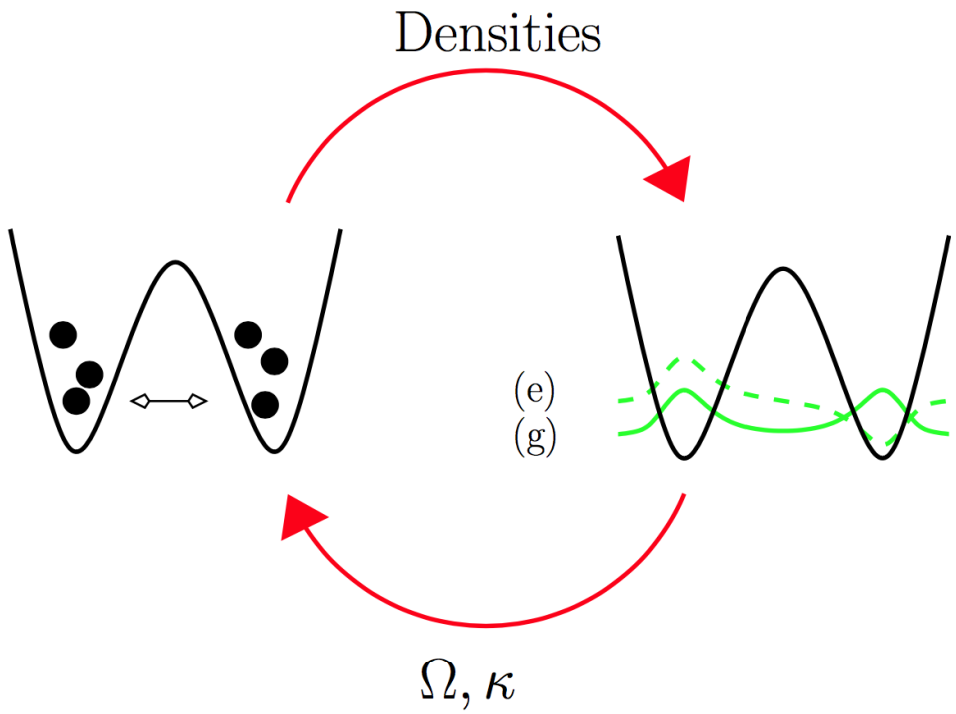

Figure 4.3.: Sketch of MCTDHB(2) in a double well potential. The two-mode Hamiltonian couples the gerade-ungerade orbitals by the densities and depends on the tunnel coupling Ω and the interactions κ. But vice versa the tunnel coupling Ω and the interactions κ again depend on the gerade-ungerade orbitals [54].

dependence of ϕ_g and ϕ_e and the number distribution.

Lets conclude this section with a short discussion of the MCTDHB groundstate. In the case of an unsplit trap, more than 99% of the atoms are in the groundstate ϕ_g and the GP-like nonlinearities f_k^k and f_k^q lead to a GP equation for ϕ_g with N atoms. The nonlinearity $\tilde{f}_e$ for ϕ_e is very large and we get a Bogoliubov like structure. If on the other hand we have a totally split trap, the orbitals $\phi_g \pm \phi_e$ resemble GP orbitals with $N/2$ atoms in each well [54].

5. Density Matrix Formalism

Chapter five is devoted to the density matrix formalism whose application to the splitting process of trapped BECs is motivated and demonstrated in chapter six.
We start with the definition of correlation functions and show how expectation values can be represented as correlation functions and vice versa. We further introduce approximation schemes by the neglect of higher order correlation functions and use them to get a closed set of equations from the Heisenberg equation of motion.

5.1. Definition of Correlation Functions

In this section we present a method to formulate equations of motion for quantum many-particle systems [94]. This approach allows for numerical exact treatment as well as for approximations that are necessary in large systems as the computational effort grows exponentially with the number of particles. The basic idea of this equation of motion (EoM) approach is the truncation of the unfolding hierarchy of differential equations at a certain level in order to end up with a closed system of differential equations. There are two ways to formulate these EoM, using correlation functions (CFs) on the one hand and expectation values (EVs) on the other hand.

We begin our discussion with the concept of CFs, where we use a formulation used by Leymann, Foerster and Wiersig [94] that will faciliate switching between a formulation in EVs or CFs. The key point is the fact that every EV $\langle b_1 b_2 ... b_k \rangle$ of operators b_i can uniquely be represented as a sum of products of CFs. In our mathematical framework we define a product of operators $b^I = b_1 b_2 ... b_k$ with a set of indices $I = \{1, 2, ..., k\}$. P labels a partition of the set I, i.e. a set family of disjoint nonempty

subsets J of I with $\bigcup_{J\in P} J = I$ and P_I is the set of all partitions of I. Next we introduce the factorization operator $\mathbf{F}$ that does not change the value of the complex number $\langle b^I \rangle$ but changes the representation of the EV. Using these definitions we can give a general definition of CFs $\delta(b^J)$:

Definition of CFs

$$\mathbf{F}\langle b^I \rangle = \delta(b^I) + \delta(b^I)_F = \sum_{P\in P_I} \prod_{J\in P} \delta(b^J) \tag{5.1}$$

with $\delta(b^I)_F$ the short notation for the sum of products of all possible factorizations of the operator EV $\langle b^I \rangle$ into CFs that only contain a smaller number of operators than the cardinality of I, $\#(I)$. We give the factorizations of the first EVs containing products up to three operators as example:

Factorization of up to Three Operators

$$\begin{aligned}
\mathbf{F}\langle b_1 \rangle &= \delta(b_1), \\
\mathbf{F}\langle b_1 b_2 \rangle &= \delta(b_1 b_2) + \delta(b_1)\delta(b_2), \\
\mathbf{F}\langle b_1 b_2 b_3 \rangle &= \delta(b_1 b_2 b_3) + \delta(b_1 b_2)\delta(b_3) + \delta(b_1 b_3)\delta(b_2) + \delta(b_2 b_3)\delta(b_1) \\
&\quad + \delta(b_1)\delta(b_2)\delta(b_3).
\end{aligned} \tag{5.2}$$

Defining $\mathbf{F}^{-1}$ as the inverse change of representation, $\mathbf{F}^{-1}\mathbf{F} = 1$ and applying it to the definition of CFs above, leads to an implicit definition of $\mathbf{F}^{-1}$

Implicit Definition of $\mathbf{F^{-1}}$

$$\mathbf{F}^{-1}\delta(b^I) = \langle b^I \rangle - \mathbf{F}^{-1}\delta(b^I)_F \tag{5.3}$$

When successively applying this definition to itself one arrives at the explicit definition of the inverse representation oprator

Explicit Definition of $\mathbf{F^{-1}}$

$$\mathbf{F}^{-1}\delta(b^I) = \sum_{P\in P_I} c_P \prod_{J\in P} \langle b^J \rangle \tag{5.4}$$

with $c_P = (-1)^{\#(P)-1}[\#(P)-1]!$. The CF is thereby entirely represented by EVs. The coefficients c_P are not equal to $+1$ as in the definition of $\mathbf{F}$ as can already be seen when explicitly writing out the first three 'refactorized' CFs

First Three 'Refactorized' CFs

$$\begin{aligned}
\mathbf{F}^{-1}\delta(b_1) &= \langle b_1 \rangle, \\
\mathbf{F}^{-1}\delta(b_1 b_2) &= \langle b_1 b_2 \rangle - \langle b_1 \rangle \langle b_2 \rangle, \\
\mathbf{F}^{-1}\delta(b_1 b_2 b_3) &= \langle b_1 b_2 b_3 \rangle - \langle b_1 b_2 \rangle \langle b_3 \rangle - \langle b_1 b_3 \rangle \langle b_2 \rangle \\
&\quad - \langle b_2 b_3 \rangle \langle b_1 \rangle + 2\langle b_1 \rangle \langle b_2 \rangle \langle b_3 \rangle.
\end{aligned} \tag{5.5}$$

By induction one can easily prove that every EV can unambiguously be represented by CFs and every CF can be represented by EVs as well. Note that a similar definition

can be introduced also for fermionic operators when taking care of the sign of $\delta(f^J)$ for every commutation of the operators.

5.2. Approximation by Lower-Order Quantities

Next we show how this concept of representation change by expressing a quantity by a sum of products of another quantity can be exploited for approximation schemes [94]. We introduce the notation $\bar{\delta}(N)$ as an abbreviation, for any function of CFs $\delta(b^I)$ up to order N, i.e. $\{O[\delta(b^I)] = \#(I) \leqslant N\}$. For example, the factorized EV of the product of three operators given before can be displayed in the following fashion:

Factorized EV of the Product of Three Operators

$$\mathbf{F}\langle b_1 b_2 b_3\rangle \equiv \delta(3) + 3\delta(2)\delta(1) + \delta(1)^3 \equiv \bar{\delta}(3) \tag{5.6}$$

The truncation operator $\Delta_{\delta(N)}$ is used to symbolize neglects of all CFs of order larger than N:

Truncation Operator CF

$$\Delta_{\delta(N)}\delta(N+1) = \bar{\delta}(N) \tag{5.7}$$

To give an example of its effect, we apply $\Delta_{\delta(2)}$ on the factorization of EVs containing products of three operators:

$\Delta_{\delta(2)}$ on $\mathbf{F}\langle b_1 b_2 b_3\rangle$

$$\Delta_{\delta(2)}[\delta(3) + 3\delta(2)\delta(1) + \delta(1)^3] = 3\delta(2)\delta(1) + \delta(1)^3 \equiv \bar{\delta}(2) \tag{5.8}$$

which leaves an expression that only contains CFs up to order two. Of course, the applicability of the neglect of higher order CFs of this kind depends on the system

under investigation.
We can also define an operator $\Delta_{\langle N \rangle}$ for the neglect of EVs of order larger than N, where we use the short notation $\langle N \rangle$ for any function of EVs containing N or less operators

Truncation Operator EV

$$\Delta_{\langle N \rangle} \langle N+1 \rangle = \langle N \rangle \tag{5.9}$$

Applying the truncation operator $\Delta_{\delta(N)}$ to CFs as well as the application of $\Delta_{\langle N \rangle}$ to EVs is trivial. However, one can also apply $\Delta_{\delta(N)}$ to EVs or $\Delta_{\langle N \rangle}$ to CFs as the representation of the quantities in EVs or CFs is independent from the applied approximation. We can therefore work with quantities formulated entirely in CFs and make an approximation by neglecting higher-order CFs as well as working with these same quantities formulated in EVs and still apply the same approximation. All we have to do is to use the factorization operator $\mathbf{F}$ to rewrite the EVs into CFs, set the highest order CF to zero (by application of $\Delta_{\delta(\#I-1)}$) an finally rewrite the remaining CFs as EVs with the help of $\mathbf{F}^{-1}$. The EV $\langle b^I \rangle$ can thereby be approximated by neglecting the highest order CF as a sum of products of lower-order EVs:

Approximation of EV as a Sum of Products of Lower-Order EVs

$$\mathbf{F}^{-1} \Delta_{\delta(\#I-1)} \mathbf{F} \langle b^I \rangle = - \sum_{P \in P_I \setminus I} c_P \prod_{J \in P} \langle b^J \rangle \tag{5.10}$$

This approximation scheme can be very useful when dealing with systems consisting of a large number of particles and many degrees of freedom.
As illustration, we apply the truncation operator $\Delta_{\delta(N)}$ to EVs of different products of operators:

$\boldsymbol{\Delta_{\delta(1)}\langle b_1 b_2\rangle}$

$$\mathbf{F}^{-1}\Delta_{\delta(1)}\mathbf{F}\langle b_1 b_2\rangle = \langle b_1\rangle\langle b_2\rangle \tag{5.11}$$

which is simply the mean-field approximation.

$\boldsymbol{\Delta_{\delta(1)}\langle b_1 b_2 b_3\rangle}$

$$\mathbf{F}^{-1}\Delta_{\delta(1)}\mathbf{F}\langle b_1 b_2 b_3\rangle = \langle b_1\rangle\langle b_2\rangle\langle b_3\rangle \tag{5.12}$$

The approximation $\Delta_{\delta(1)}\langle b_1 b_2 b_3\rangle$ is related to the second Born approximation, whereas the approximation $\Delta_{\delta(2)}\langle b_1 b_2 b_3\rangle$ reproduces the so-called Bogoliubov backreaction method [11].

$\boldsymbol{\Delta_{\delta(2)}\langle b_1 b_2 b_3\rangle}$

$$\begin{aligned}\mathbf{F}^{-1}\Delta_{\delta(2)}\mathbf{F}\langle b_1 b_2 b_3\rangle = {} & \langle b_1 b_2\rangle\langle b_3\rangle + \langle b_1 b_3\rangle\langle b_2\rangle + \langle b_2 b_3\rangle\langle b_1\rangle \\ & - 2\langle b_1\rangle\langle b_2\rangle\langle b_3\rangle\end{aligned} \tag{5.13}$$

Analogous approximations can also be formulated for the approximation of CFs by neglect of higher order EVs, when the truncation operator $\Delta_{\langle N\rangle}$ is applied to a CF:

Approximation of CF as a Sum of Products of Lower-Order CFs

$$\mathbf{F}^{-1}\Delta_{\langle N-1\rangle}\mathbf{F}^{-1}\delta(b^I) = -\sum_{P\in P_I}\prod_{J\in P}\delta(b^J) \tag{5.14}$$

Hence, we end up with two different approximations formulated in a very symmetric fashion. Nevertheless, they are quite the opposite of each other and can only be applied to totally contrary systems:
For systems with many degrees of freedom and negligible higher order CF, the corresponding EV is certainly not negligible,

$$\delta(b^I) = 0 \Rightarrow \langle b^I \rangle = \mathbf{F}^{-1} \delta(b^I)_F \tag{5.15}$$

and has to be approximated by products of lower-order EVs. If, on the other hand, a system has only a very limited number of particles and normal ordered EVs of a certain order vanish,

$$\langle b^I \rangle = 0 \Rightarrow \delta(b^I) = -\delta(b^I)_F \tag{5.16}$$

the corresponding CF has to be expressed by its factorization and can not be neglected.
We emphasize again that all considerations up to here are entirely formal and which of these approximations is applicable depends on the investigated physical system.

5.3. Equations of Motion (EoM)

As a preliminary example and to get insight into the scheme discussed in the previous section, we derive EoM for a given physical system and show how our previously described approximation schemes can be applied in order to get a closed set of differential equations. Following the description of Leymann, Foerster and Wiersig we derive EoM for an open quantum system [94].

The dynamics of an open quantum system is described by the von Neumann-Lindblad equation (vNL):

von Neumann-Lindblad Equation

$$\frac{\partial}{\partial t}\rho = -\frac{i}{\hbar}[H,\rho] + \sum_{\nu}\frac{\lambda_\nu}{2}(2L_\nu\rho L_\nu^\dagger - L_\nu^\dagger L_\nu\rho - \rho L_\nu^\dagger L_\nu) \tag{5.17}$$

where H is the Hamiltonian generating the internal dynamics of the system, ρ is the density operator and the Lindblad form describes the coupling to external baths with transition rates λ_ν and the collapse operators L_ν. Depending on the size of a system and the interaction part of the Hamiltonian H, an exact solution might not be feasible in many cases. Anyway, for many applications a solution of $\rho(t)$ might not be necessary and knowledge of the dynamics of some EVs $\langle A\rangle = \mathrm{tr}(A\rho)$ might be sufficient. The vNL equation can be used to derive generalized Ehrenfest equations of motion for the time evolution of any operator's EV $\langle A\rangle$,

Generalized Ehrenfest Equation of Motion

$$\begin{aligned}\frac{d}{dt}\langle A\rangle = \langle\mathcal{L}\rangle = \frac{i}{\hbar}\langle[H,A]\rangle \\ + \sum_{\nu}\frac{\lambda_\nu}{2}(2L_\nu A L_\nu^\dagger - L_\nu^\dagger L_\nu A - A L_\nu^\dagger L_\nu)\end{aligned} \tag{5.18}$$

where we introduced the superoperator $\mathcal{L}$ standing for the commutator with the Hamiltonian H and the application of the Lindblad form to the operator A. When describing the time evolution of the desired operator's EV $\langle A \rangle$, the interaction of the Hamiltonian H and the scattering terms in the Lindblad form lead to a hierarchy of EoM, where the time evolution of a first-order quantity is coupled to a second-order quantity, the time evolution of a second-order quantity to a third-order quantity and so on. Symbolically this can be written as

EV Hierarchy Without Truncation

$$\begin{aligned} \frac{d}{dt}\langle 1 \rangle &= \langle \mathcal{L}(1) \rangle = \langle 2 \rangle, \\ \frac{d}{dt}\langle 2 \rangle &= \langle \mathcal{L}(2) \rangle = \langle 3 \rangle, \\ &\vdots \end{aligned} \tag{5.19}$$

For systems containing n particles, normal ordered EVs of $n+1$ particles vanish:

$$\langle b^\dagger \dots b^\dagger \underbrace{b \dots b}_{n+1} \rangle = 0 \tag{5.20}$$

as $n+1$ times the action of the annihilation operator 'b' gives zero for particle states containing 'n' or less particles. This has the same effect as applying the truncation operator $\Delta_{\langle N \rangle}$ with $N = 2n$:

Application of $\boldsymbol{\Delta_{\langle 2n \rangle}}$

$$\langle 2n+1 \rangle \approx \Delta_{\langle 2n \rangle} \langle 2n+1 \rangle = \langle 2n \rangle \tag{5.21}$$

The application of the truncation operator $\Delta_{\langle N\rangle}$ on the Nth line of the hierarchy of equations coupling the EV's time derivation of nth-order to EVs of $n+1$ -order quantities leads to a finite system of linear differential equations:

EV Hierarchy Truncated by Neglecting EVs

$$\begin{aligned} \frac{d}{dt}\langle 1\rangle &= \langle \mathcal{L}(1)\rangle = \langle 2\rangle, \\ &\vdots \\ \frac{d}{dt}\langle N\rangle &= \langle \mathcal{L}(N)\rangle \approx \Delta_{\langle N\rangle}\langle N+1\rangle = \langle N\rangle \end{aligned} \tag{5.22}$$

This system of coupled linear EoM is visualized in Fig. 5.1.

Figure 5.1.: Illustration of an EV hierarchy with the black lines symbolizing the linear coupling between EVs of increasing order. The hierarchy is truncated by the application of the truncation operator $\Delta_{\langle N\rangle}$, i.e. setting the $(N+1)$ EV to zero [94].

In principle, if the considered system can be described by this method, it is also possible to find the solution by solving the vNL equation directly in the basis of configurations the finite number of particles occupy. Approaches of this kind are often called numerically exact methods.
For physical systems too large to be described by a finite Hilbert space, it is beneficial to use the so called cluster expansion method, where the EoM are derived for CFs and a closed set of differential equations is obtained by neglection of CFs of certain order. In order to derive the EoM for the CF $\delta(b^I)$, we first have to apply the Ehrenfest EoM to the corresponding EV. Next we have to factorize the resulting EVs into CF before

we lastly subtract the previously calculated derivatives of lower-order factorizations:

EoM for CFs

$$\frac{d}{dt}\delta(b^I) = \mathbf{F}\langle\mathcal{L}(b^I)\rangle - \frac{d}{dt}\delta(b^I)_F. \tag{5.23}$$

Like in the case for the EoM of EVs, the interaction part of the Hamiltonian H and the scattering terms in the Lindblad form give rise to an infinite hierarchy of equations coupling the CFs:

CF Hierarchy Without Truncation

$$\begin{aligned}
\frac{d}{dt}\delta(1) &= \mathbf{F}\langle\mathcal{L}(1)\rangle - \frac{d}{dt}\delta(1)_F = \bar{\delta}(2), \\
\frac{d}{dt}\delta(2) &= \mathbf{F}\langle\mathcal{L}(2)\rangle - \frac{d}{dt}\delta(2)_F = \bar{\delta}(3), \\
&\vdots
\end{aligned} \tag{5.24}$$

This infinite hierarchic system is equivalent to the previously obtained one for EVs and produces exactly the same results if they both were formulated up to infinite order and solved exactly.
If the system is large and has only weak interactions, the hierarchy of CFs can be truncated by neglecting CFs $\delta(b^I)$ of order $\#(I) > N$. This yields the same result as applying the truncation operator $\Delta_{\delta(N)}$ to the Nth line of the hierarchy of equations describing the time evolution of the CFs.

CF Hierarchy Truncated by Neglecting CFs

$$\begin{aligned}
\frac{d}{dt}\delta(1) &= \mathbf{F}\langle\mathcal{L}(1)\rangle - \frac{d}{dt}\delta(1)_F = \bar{\delta}(2), \\
&\vdots \\
\frac{d}{dt}\delta(N) &= \mathbf{F}\langle\mathcal{L}(N)\rangle - \frac{d}{dt}\delta(N)_F \\
&\approx \Delta_{\delta(N)}\mathbf{F}\langle\mathcal{L}(N)\rangle - \frac{d}{dt}\delta(N)_F = \bar{\delta}(N).
\end{aligned} \tag{5.25}$$

We visualize this hierarchic system in Fig. 5.2.

Figure 5.2.: Illustration of an CF hierarchy with the black lines symbolizing the linear coupling between CFs of increasing order. Compared to the EV hierarchy where we only had this linear coupling between the terms, for CFs we also get contributions from products of lower-order CF indicated by the blue merging lines on top. The hierarchy is truncated by the application of the truncation operator $\Delta_{\delta(N)}$, i.e. setting the $(N+1)$ CF to zero [94].

As we ended up with this system by application of a different truncation operator than in the case before for the EVs, these two systems are no longer equivalent to each other. Even more, the two hierarchic systems describe quite the opposite situations in the sense pointed out before, that the first system is a good approximation for vanishing higher-order EVs, whereas the second is useful for vanishing higher-order CFs.

Let us take a closer look at the hierarchies of EVs and of CFs and compare them to each other. The equations for the EVs are entirely linear since they originate from the linear Ehrenfest EoM and can be used for the description of the dynamics of a finite quantum system. On the other hand, the hierarchic equations system for CFs

is nonlinear for all orders larger than one which stems from the fact that in order to derive these equations, the EVs have to be factorized and the time derivative of the lower-order factorizations has to be subtracted. These operations are demanding and have to be performed for every single order in the hierarchy, but on the plus side, these equations can be used for the description of the dynamics of large systems with small correlations that would be too large to be described by the hierarchic set of equations for EVs.

As already shown before, the formulation of the EoM in EVs or CFs is independent from the used truncation scheme as one can also apply $\Delta_{\delta(N)}$ to EVs and $\Delta_{\langle N\rangle}$ to CFs. It follows that we can obtain a system of EoM formulated in EVs that is equivalent to the CF system if we apply the truncation operator $\Delta_{\delta(N)}$ on the Nth line of equations given in EVs.

EV Hierarchy Truncated by Neglecting CFs

$$\begin{aligned} \frac{d}{dt}\langle 1\rangle &= \langle \mathcal{L}(1)\rangle = \langle \mathcal{L}(2)\rangle, \\ &\vdots \\ \frac{d}{dt}\langle N\rangle &= \langle \mathcal{L}(N)\rangle \approx \mathbf{F}^{-1}\Delta_{\delta(N)}\mathbf{F}\langle N+1\rangle = \langle N\rangle. \end{aligned} \tag{5.26}$$

As we used the same truncation operator ($\Delta_{\delta(N)}$) here as in the case for the EoM formulated in CFs, the two systems of equations are equivalent and produce the same results. Note that these equations are almost linear, as nonlinearities only arise in the EoM where actual approximations are made. Hence we approximate an infinite system of linear equations by a finite set of nonlinear equations where only the approximations lead to nonlinearities. We show a visualization of these equations in Fig. 5.3.
The derivation of the hierarchy of equations of EVs with truncation by neglection of high-order CFs is much less demanding than that of the equivalent equations with CFs since an inductive scheme can be used to derive these equations and factorizations

Figure 5.3.: Illustration of an EV hierarchy truncated by neglecting CFs with the black lines symbolizing the linear coupling between EVs of increasing order. It is equivalent to the hierarchy illustrated for CFs (Fig. 5.2) though its structure is similar to the hierarchy for EVs (Fig. 5.1). Truncation is achieved by substituting the $N+1$th EV by products of lower-order EVs (indicated by the merging blue line entering the Nth EVs from the side mediated by the truncation operator) instead of setting the $(N+1)$th EV to zero. Hence we get an 'almost' straight line where only the last order couples nonlinearly to products of lower-order quantities [94].

that are required in $\mathbf{F}^{-1}\Delta_{\delta(N)}\langle N+1\rangle$ can be listed and all emerging EVs of order larger than N can be substituted according to such a list.
Just for completeness, we also give the system of equations equivalent to the equations of EVs with the truncaction operator $\Delta_{\langle N\rangle}$ entirely formulated in terms of CFs, illustrated in Fig. 5.4

CF Hierarchy Truncated by Neglecting EVs

$$\begin{aligned}
\frac{d}{dt}\delta(1) &= \mathbf{F}\langle\mathcal{L}(1)\rangle - \frac{d}{dt}\delta(1)_F = \bar{\delta}(2),\\
&\vdots\\
\frac{d}{dt}\delta(N) &= \mathbf{F}\langle\mathcal{L}(N)\rangle - \frac{d}{dt}\delta(N)_F\\
&\approx \mathbf{F}\Delta_{\langle N\rangle}\langle\mathcal{L}(N)\rangle - \frac{d}{dt}\delta(N)_F = \bar{\delta}(N).
\end{aligned} \tag{5.27}$$

We conclude this section by summarizing our findings regarding the setting up of EoM and its approximations. It is advantageous to formulate all EoM in terms of EVs and use the truncation operator in combination with the factorization operator $\mathbf{F}^{-1}\Delta_{\delta(N)}\mathbf{F}$ to neglect higher-order CFs, thereby making the factorizations only in the

Figure 5.4.: Illustration of an CF hierarchy truncated by neglecting EVs with the black lines symbolizing the linear coupling between CFs of increasing order and the blue merging lines on top indicating coupling to lower-order CFs. The truncation here is achieved by substituting the $N+1$th CF by products of lower-order CF instead of setting it zero. It is equivalent to the hierarchy illustrated in Fig. 5.1 but its structure is similar to the hierarchy of CF shown in Fig.5.2 [94].

highest-order EVs. We end up with EoM that are much simpler in structure than the equivalent ones in CFs. In addition the only occurring nonlinearities directly mark the effect of neglection of CFs [94].

6. BECs in a Double Well Potential

When describing the dynamics of $N \gg 1$ interacting, identical, bosonic particles under the influence of external forces, the many-body wavefunction, $\Psi(\mathbf{r}_1, ..., \mathbf{r}_N; t)$, is the natural starting point. Knowing this function, the condensate's atoms and their dynamics can be described by the many-body Schrödinger equation, see chapter 3.2. Unfortunately, analytic solutions of the Schrödinger equation are rare exceptions and approximations and numerical methods are generally indispensable.
For weakly interacting systems, a *mean field* theory like the Gross-Pitaevskii equation gives a good approximation, see chapter 4.1.
When considering the groundstate of a BEC in a double-well potential with very high barrier, it becomes intuitively clear that we end up with a two-fold fragmented state and the assumption of a single mode (like in the case of the Gross-Pitaevskii equation) is therefore questionable in general. Hence at least a two-mode model has to be used for the description of the BEC in a double-well potential, which is a good approximation if we assume the two lowest states to be very closely spaced in energy, see chapter 4.2.
In order to correctly describe the dynamics of the splitting process of trapped BECs even more than two modes might be necessary as further excitations arise. The quality of the results then depends crucially on the chosen basis set.
The use of a time-adaptive optimized basis set like in the MCTDHB(M) method, where M specifies the number of time-dependent orbitals used to construct the many-body states, proposes a cure to this problem, see chapter 4.4. Nevertheless, even in the case of M-fold fragmentation, M orbitals might not be enough and more orbitals might be needed as also some small, but finite eigenvalues (quantum depletion) can be of importance. Hence also the MCTDHB(M) method reaches its limits in form of computational time and memory even for single digit values of M on typical workstations, e.g. computations for $M = 4$ are hardly feasible.

In order to overcome these limitations and especially to take into account four and more modes in our simulations to better describe excitations of the BEC, we apply the density matrix formalism introduced in chapter 5 to the splitting process of a BEC in a double well trap and compare our results with solutions from different approximations. In the appendix we briefly present and describe the *Mathematica* code that was used to calculate the approximations of EVs as a sum of products of lower-order EVs, see appendix A.2, as well as the code for the density matrix formalism applied to the two mode model where CFs of order three and higher have been neglected, see appendix A.3. In the appendix of this thesis we restrict ourself to a special case to demonstrate the formalism and the *Mathematica* code in a clear way rather than in the most compact and rigorous form. The complete code used for the calculations can be downloaded here: `http://physik.uni-graz.at/~uxh/octbec/expectation_value_approximation.nb` and here: `http://physik.uni-graz.at/~uxh/octbec/density_matrix_formalism.nb`.

Before actually employing the density matrix formalism for simulations that need more than two modes, we stick with a simple example of an adiabatic deformation of a harmonic potential trapping a BEC into a double well potential. As there are no further excitations the two mode model as well as the MCTDHB(2) lead to the same results.

As will be shown, unfortunately, the density matrix formalism experiences difficulties already in this simple case. At least in the case of a two mode system they can be overcome by explicitly keeping the trace of the x-particle reduced density matrices, (xPRDM), constant. For more than two modes the nonlinearities lead to failure of the implemented scheme. Within this thesis unfortunately no satisfying solution to this problem could be found.

6.1. Approximation of the 3PRDM for a BEC in a DWP

Before actually deriving the EoM for our BEC in a double well potential described above, we will take a look at the accuracy of the approximation of elements of the three-particle reduced density matrix (3PRDM) by sums of products of lower-order quantities, i.e. products of elements of the one-particle reduced density matrix (1PRDM) and/or elements of the two-particle reduced density matrix (2PRDM). This is of interest for us, as we want to truncate the hierarchy of equations with the use of the truncation operator $\Delta_{\delta(3)}$, i.e. set all 3-particle correlations equal zero. As the 3PRDM for our two-level system possesses $8 \cdot 8 = 64$ elements, we will not verify the accuracy of the approximation for all elements, but only for those that will be of interest for the dynamics of the system. Of course, the knowledge of which matrix elements are 'important' is not given a priori but stems form the derivation of the equations of motion in the following section.
Using the guidance given in the previous section, we get the following approximations, where $b^\dagger_{g/e}$ and $b_{g/e}$ stand for the creation and annihilation operator, for particles in the ground (g) or excited (e) state respectively:

Approximation of 3PRDM with 3-Particle CF Equal Zero

$$
\begin{aligned}
\langle b_g^\dagger b_g^\dagger b_g^\dagger b_g b_e b_e\rangle &\approx \langle b_g^\dagger b_g^\dagger b_e b_e\rangle \cdot \langle b_g^\dagger b_g\rangle \\
\langle b_g^\dagger b_g^\dagger b_e^\dagger b_e b_e b_e\rangle &\approx \langle b_g^\dagger b_g^\dagger b_e b_e\rangle \cdot \langle b_e^\dagger b_e\rangle \\
\langle b_e^\dagger b_e^\dagger b_g^\dagger b_g b_g b_g\rangle &\approx \langle b_e^\dagger b_e^\dagger b_g b_g\rangle \cdot \langle b_g^\dagger b_g\rangle \\
\langle b_e^\dagger b_e^\dagger b_e^\dagger b_g b_g b_e\rangle &\approx \langle b_e^\dagger b_e^\dagger b_g b_g\rangle \cdot \langle b_e^\dagger b_e\rangle \\
\langle b_e^\dagger b_e^\dagger b_g^\dagger b_g b_e b_e\rangle &\approx \langle b_e^\dagger b_e^\dagger b_e b_e\rangle \cdot \langle b_g^\dagger b_g\rangle + \langle b_e^\dagger b_g^\dagger b_e b_g\rangle \cdot \langle b_e^\dagger b_e\rangle \\
&\quad - \langle b_g^\dagger b_g\rangle \cdot \langle b_e^\dagger b_e\rangle \cdot \langle b_e^\dagger b_e\rangle \\
\langle b_g^\dagger b_g^\dagger b_e^\dagger b_g b_g b_e\rangle &\approx \langle b_g^\dagger b_g^\dagger b_g b_g\rangle \cdot \langle b_e^\dagger b_e\rangle + \langle b_e^\dagger b_g^\dagger b_e b_g\rangle \cdot \langle b_g^\dagger b_g\rangle \\
&\quad - \langle b_g^\dagger b_g\rangle \cdot \langle b_g^\dagger b_g\rangle \cdot \langle b_e^\dagger b_e\rangle
\end{aligned}
\tag{6.1}
$$

We use the `fewmodepair` class of the Matlab OCTBEC Toolbox [70] in order to find exact solutions of our two-mode model for different states. We set the number of particles to $n = 100$, the nonlinearity parameter $\kappa = 1/100$ and the tunneling parameter $\Omega = 0.5$. We switch off the tunnel-coupling exponentially within different intervals ranging from 1ms to 100ms. This is accomplished within the software by changing the control parameter λ. Results for the different elements of the 3PRDM, Fig. 6.3, as well as an visualization of the states on the Bloch sphere, Fig. 6.2, and the atom number difference, Fig. 6.1, are given below. We emphasise that here we are just comparing elements of the 3PRDM (blue line) calculated within the two mode model with their approximations (red line) given by Eq. (6.1) also calculated within the two mode model.
As can clearly be seen in the following plots, when comparing the accuracy of the approximations with the density plots and the representation of the states on the Bloch sphere belonging to the same splitting process the approximations work quite well as long as the condensate is unsplit, and get worse as the condensates fragments. We start the comparison with plots of slow splitting processes where we end up with fragmented states and refer to the appendix A.1 for further comparisons.

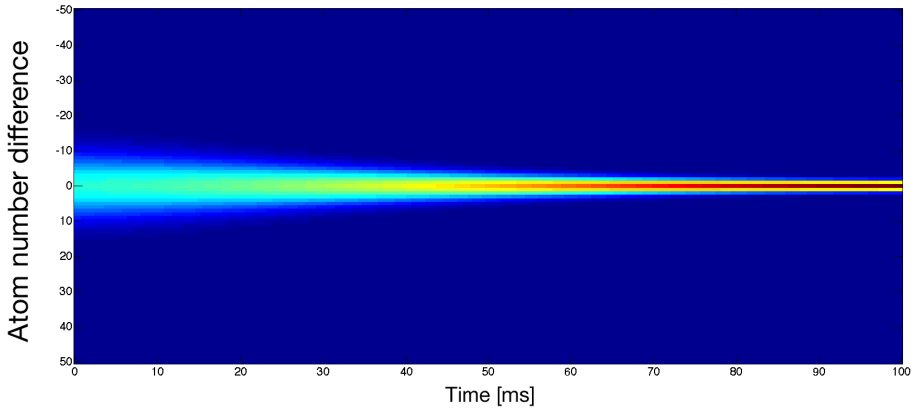

Figure 6.1.: Two mode model: density-plot of $n = 100$ particles and the nonlinearity parameter $\kappa = 1/100$ for a splitting process by switching off the tunnel-coupling exponentially starting with the tunneling parameter $\Omega = 0.5$ within a time span of 100ms.

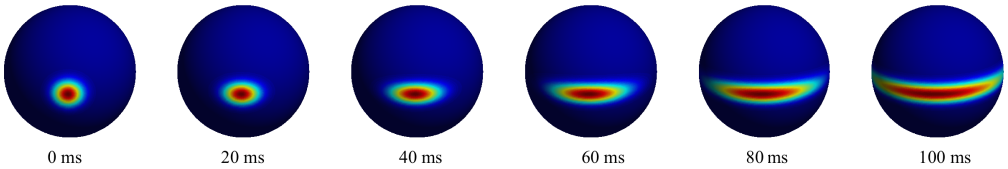

Figure 6.2.: Two mode model: illustration of the states on the Bloch sphere for $n = 100$ particles and the nonlinearity parameter $\kappa = 1/100$ for a splitting process by switching off the tunnel-coupling exponentially starting with the tunneling parameter $\Omega = 0.5$ within a time span of 100ms.

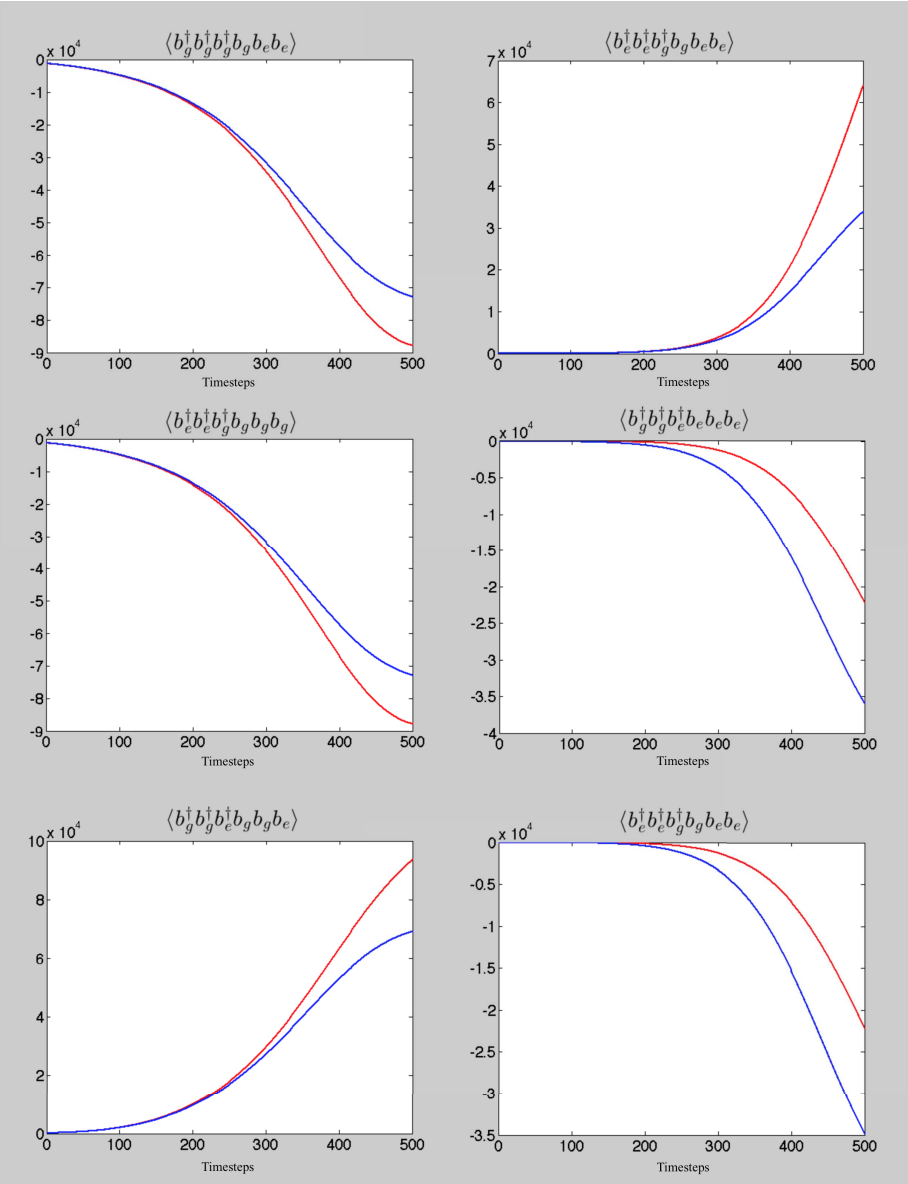

Figure 6.3.: Two mode model: comparison of elements of the 3PRDM (blue line) calculated within the two mode model with their approximations (red line) given by Eq. (6.1) also calculated within the two mode model for $n = 100$ particles and the nonlinearity parameter $\kappa = 1/100$ for a splitting process by switching off the tunnel-coupling exponentially starting with the tunneling parameter $\Omega = 0.5$ within a time span of 100ms (1 timestep $\equiv$ 0.2ms)

6.2. Approximated EoM for EVs for a BEC in a DWP

In this section we take the approximation from the last section in order to derive a closed set of differential equations for EVs describing the dynamics of our system. We begin with the two mode Hamiltonian in 2nd quantized form for the two mode model in gerade/ungerade(g/e) basis by simply rewriting the already before in LR-basis given Hamiltonian with orbitals $\phi_{g,e} = (\phi_L \pm \phi_R)/\sqrt{2}$, and $\hat{b}_g$ ($\hat{b}_g^\dagger$) and $\hat{b}_e$ ($\hat{b}_e^\dagger$) the corresponding annihilation (creation) operators. The gerade state can be identified as the ground state, whereas the ungerade state corresponds to the first excited state, hence the nomenclature 'e' for the ungerade state.

Two Mode Hamiltonian 2nd Quantized Form in GE-Basis

$$\hat{H} = -\frac{\Omega(t)}{2}(\hat{b}_e^\dagger b_e - \hat{b}_g \hat{b}_g^\dagger) + \frac{\kappa}{2}(\hat{b}_e^\dagger \hat{b}_e^\dagger \hat{b}_g \hat{b}_g + \hat{b}_g^\dagger \hat{b}_g^\dagger \hat{b}_e \hat{b}_e - \hat{b}_e^\dagger \hat{b}_e^\dagger \hat{b}_e \hat{b}_e - \hat{b}_g^\dagger \hat{b}_g^\dagger \hat{b}_g \hat{b}_g) \quad (6.2)$$

As the EVs of the 1PRDM's off-side diagonal are always zero in the g-e basis, not all EVs are relevant for the dynamics of our problem. Evaluating the commutators of the 1- and 2-PRDM elements leads to the following set of equations:

Commutators of the 1- and 2-PRDM Elements with H

$$
\begin{aligned}
\langle [b_g^\dagger b_g, H] \rangle &= \kappa(\langle b_g^\dagger b_g^\dagger b_e b_e \rangle - \langle b_e^\dagger b_e^\dagger b_g b_g \rangle) \\
\langle [b_e^\dagger b_e, H] \rangle &= -\kappa(\langle b_g^\dagger b_g^\dagger b_e b_e \rangle - \langle b_e^\dagger b_e^\dagger b_g b_g \rangle) \\
\langle [b_g^\dagger b_g^\dagger b_g b_g, H] \rangle &= \kappa(\langle b_g^\dagger b_g^\dagger b_e b_e \rangle - \langle b_e^\dagger b_e^\dagger b_g b_g \rangle) + 2\kappa(\langle b_g^\dagger b_g^\dagger b_g^\dagger b_g b_e b_e \rangle - \langle b_e^\dagger b_e^\dagger b_g^\dagger b_g b_g b_g \rangle) \\
\langle [b_g^\dagger b_g^\dagger b_e b_e, H] \rangle &= 2\delta \langle b_g^\dagger b_g^\dagger b_e b_e \rangle + \kappa(\langle b_g^\dagger b_g^\dagger b_g b_g \rangle - \langle b_e^\dagger b_e^\dagger b_e b_e \rangle) \\
&\quad + 2\kappa(\langle b_g^\dagger b_g^\dagger b_g^\dagger b_g b_e b_e \rangle + \langle b_g^\dagger b_g^\dagger b_e^\dagger b_e b_g b_g \rangle) \\
&\quad - 2\kappa(\langle b_g^\dagger b_g^\dagger b_e^\dagger b_e b_e b_e \rangle + \langle b_e^\dagger b_e^\dagger b_g^\dagger b_g b_e b_e \rangle) \\
\langle [b_g^\dagger b_e^\dagger b_g b_e, H] \rangle &= \kappa(\langle b_g^\dagger b_g^\dagger b_e^\dagger b_e b_e b_e \rangle + \langle b_g^\dagger b_e^\dagger b_e^\dagger b_g b_g b_g \rangle) \\
&\quad - \kappa(\langle b_e^\dagger b_e^\dagger b_e^\dagger b_g b_g b_e \rangle - \langle b_g^\dagger b_g^\dagger b_g^\dagger b_g b_e b_e \rangle) \\
\langle [b_e^\dagger b_e^\dagger b_g b_g, H] \rangle &= -2\delta \langle b_e^\dagger b_e^\dagger b_g b_g \rangle - \kappa(\langle b_g^\dagger b_g^\dagger b_g b_g \rangle - \langle b_e^\dagger b_e^\dagger b_e b_e \rangle) \\
&\quad + 2\kappa(\langle b_e^\dagger b_e^\dagger b_e^\dagger b_e b_g b_g \rangle + \langle b_e^\dagger b_e^\dagger b_g^\dagger b_g b_e b_e \rangle) \\
&\quad - 2\kappa(\langle b_e^\dagger b_e^\dagger b_g^\dagger b_g b_g b_g \rangle - \langle b_g^\dagger b_g^\dagger b_e^\dagger b_e b_g b_g \rangle) \\
\langle [b_e^\dagger b_g^\dagger b_e b_g, H] \rangle &= -\langle [b_g^\dagger b_e^\dagger b_g b_e, H] \rangle \\
\langle [b_e^\dagger b_e^\dagger b_e b_e, H] \rangle &= -\kappa(\langle b_g^\dagger b_g^\dagger b_e b_e \rangle - \langle b_e^\dagger b_e^\dagger b_g b_g \rangle) + 2\kappa(\langle b_e^\dagger b_e^\dagger b_e^\dagger b_e b_g b_g \rangle - \langle b_g^\dagger b_g^\dagger b_e^\dagger b_e b_e b_e \rangle)
\end{aligned}
\tag{6.3}
$$

Using these calculated commutators for the 1- and 2-PRDM elements with the Hamiltonian leads, together with the Ehrenfest EoM

Ehrenfest Equation of Motion

$$
\frac{d}{dt}\langle A \rangle = \frac{i}{\hbar}\langle [H, A] \rangle \tag{6.4}
$$

where from now on we set $\hbar = 1$ and the approximation of 3PRDM elements with

3-particle CF equal zero, to the following closed set of equations

EoM for EVs

$$
\begin{aligned}
\frac{d}{dt}\langle b_g^\dagger b_g\rangle &= i\kappa[\langle b_g^\dagger b_g^\dagger b_e b_e\rangle - \langle b_e^\dagger b_e^\dagger b_g b_g\rangle] \\
\frac{d}{dt}\langle b_e^\dagger b_e\rangle &= -i\kappa[\langle b_g^\dagger b_g^\dagger b_e b_e\rangle - \langle b_e^\dagger b_e^\dagger b_g b_g\rangle] \\
\frac{d}{dt}\langle b_g^\dagger b_g^\dagger b_g b_g\rangle &= i\kappa[(\langle b_g^\dagger b_g^\dagger b_e b_e\rangle - \langle b_e^\dagger b_e^\dagger b_g b_g\rangle) + 2\langle b_g^\dagger b_g\rangle(\langle b_g^\dagger b_g^\dagger b_e b_e\rangle - \langle b_e^\dagger b_e^\dagger b_g b_g\rangle)] \\
\frac{d}{dt}\langle b_g^\dagger b_g^\dagger b_e b_e\rangle &= i[2\delta\langle b_g^\dagger b_g^\dagger b_e b_e\rangle + \kappa(\langle b_g^\dagger b_g^\dagger b_g b_g\rangle - \langle b_e^\dagger b_e^\dagger b_e b_e\rangle) \\
&\quad + 2\kappa\{\langle b_e^\dagger b_e\rangle^2\langle b_g^\dagger b_g\rangle - \langle b_g^\dagger b_g\rangle^2\langle b_e^\dagger b_e\rangle \\
&\quad + \langle b_g^\dagger b_g\rangle(-\langle b_e^\dagger b_e^\dagger b_e b_e\rangle + \langle b_g^\dagger b_g^\dagger b_e b_e\rangle + \langle b_g^\dagger b_e^\dagger b_g b_e\rangle) \\
&\quad - \langle b_e^\dagger b_e\rangle(-\langle b_g^\dagger b_g^\dagger b_g b_g\rangle + \langle b_g^\dagger b_g^\dagger b_e b_e\rangle + \langle b_g^\dagger b_e^\dagger b_g b_e\rangle)\}] \\
\frac{d}{dt}\langle b_g^\dagger b_e^\dagger b_g b_e\rangle &= i\kappa[(\langle b_e^\dagger b_e^\dagger\rangle - \langle b_g^\dagger b_g^\dagger\rangle)(\langle b_g^\dagger b_g^\dagger b_e b_e\rangle - \langle b_e^\dagger b_e^\dagger b_g b_g\rangle) \\
\frac{d}{dt}\langle b_e^\dagger b_e^\dagger b_g b_g\rangle &= i[-2\delta\langle b_e^\dagger b_e^\dagger b_g b_g\rangle - \kappa(\langle b_g^\dagger b_g^\dagger b_g b_g\rangle - \langle b_e^\dagger b_e^\dagger b_e b_e\rangle) \\
&\quad + 2\kappa\{\langle b_g^\dagger b_g\rangle^2\langle b_e^\dagger b_e\rangle - \langle b_e^\dagger b_e\rangle^2\langle b_g^\dagger b_g\rangle \\
&\quad + \langle b_g^\dagger b_g\rangle(\langle b_e^\dagger b_e^\dagger b_e b_e\rangle - \langle b_e^\dagger b_e^\dagger b_g b_g\rangle - \langle b_g^\dagger b_e^\dagger b_g b_e\rangle) \\
&\quad + \langle b_e^\dagger b_e\rangle(-\langle b_g^\dagger b_g^\dagger b_g b_g\rangle + \langle b_e^\dagger b_e^\dagger b_g b_g\rangle + \langle b_g^\dagger b_e^\dagger b_g b_e\rangle)\}] \\
\frac{d}{dt}\langle b_e^\dagger b_g^\dagger b_e b_g\rangle &= -\frac{d}{dt}\langle b_g^\dagger b_e^\dagger b_g b_e\rangle \\
\frac{d}{dt}\langle b_e^\dagger b_e^\dagger b_e b_e\rangle &= i\kappa[(-\langle b_g^\dagger b_g^\dagger b_e b_e\rangle + \langle b_e^\dagger b_e^\dagger b_g b_g\rangle) + 2\langle b_e^\dagger b_e\rangle(\langle b_e^\dagger b_e^\dagger b_g b_g\rangle - \langle b_g^\dagger b_g^\dagger b_e b_e\rangle)]
\end{aligned}
\tag{6.5}
$$

We now solve this set of differential equations using initial values from the exact calculation by simply calculating the 1PRDM, Fig. 6.4, and 2PRDM, Fig. 6.5, and compare our results regarding the dynamics of the BEC in a double well potential with the exact calculation within our Matlab OCTBEC Toolbox. In the plots we show the exact results in blue and our approximation in red.

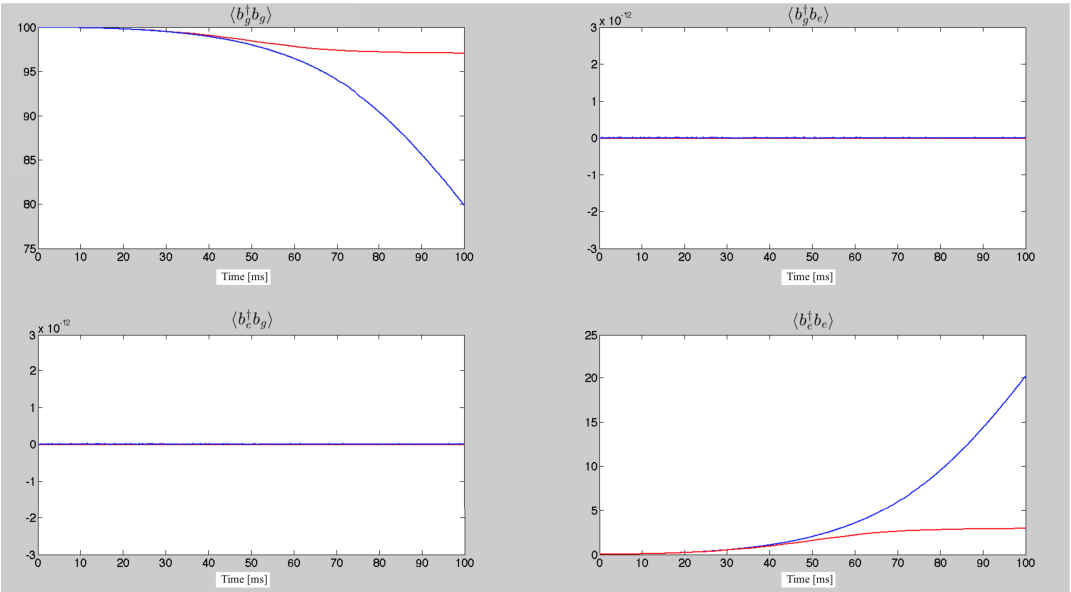

Figure 6.4.: Two mode model: expectation values of the reduced one particle density matrix for $n = 100$ particles and the nonlinearity parameter $\kappa = 1/100$ for a splitting process by switching off the tunnel-coupling exponentially starting with the tunneling parameter $\Omega = 0.5$ within a timespan of 100ms - exact results in blue, our approximation Eq. (6.1) in red.

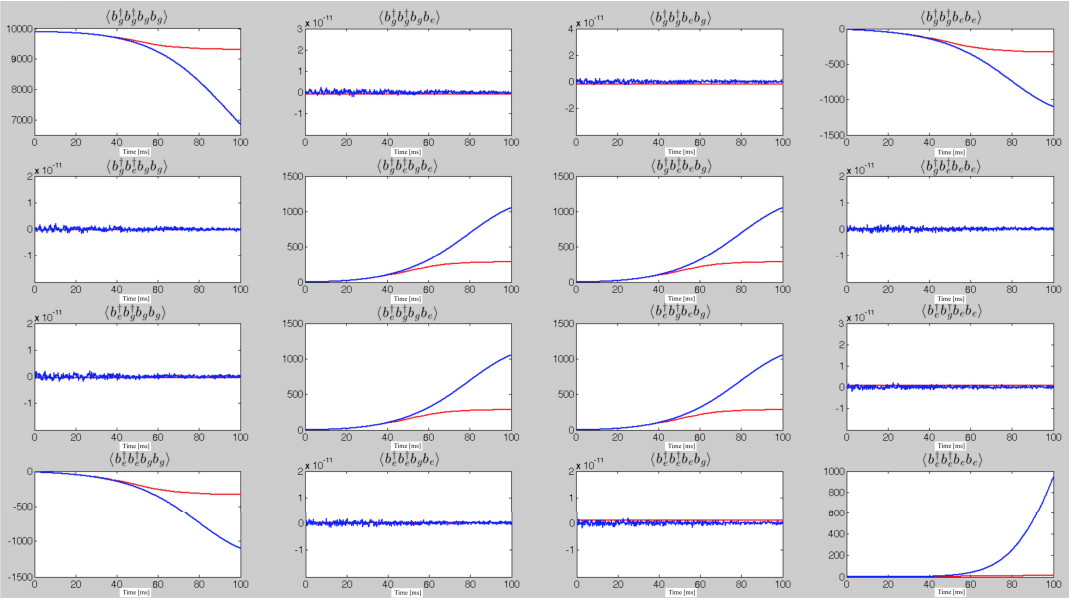

Figure 6.5.: Two mode model: expectation values of the reduced two particle density matrix for $n = 100$ particles and the nonlinearity parameter $\kappa = 1/100$ for a splitting process by switching off the tunnel-coupling exponentially starting with the tunneling parameter $\Omega = 0.5$ within a timespan of 100ms - exact results in blue, our approximation Eq. (6.1) in red.

As can be seen, the approximation is quite accurate as long as the condensate is in an unsplit - binomial state but gets quite worse as the condensate fragments more than 5%.

For completeness we also derive the EoM with the use of CFs. First we give the nomenclature used for CFs with which we want to formulate our problem. The 1 particle CF (which is simply the expectation value of the corresponding 1PRDM-element) will be called ρ_{ij} with $i, j \in \{g, e\}$, for the 2 particle CFs we will use Δ_{ijkl} with $i, j \in \{g, e\}$ accordingly. As the EVs (and therefore also the corresponding CFs) of the 1PRDM's off-side diagonal are always zero in the g-e basis, all relevant CFs for the dynamics of our problem are the following:

Defintion of CFs $\boldsymbol{\rho_{ij}}$ and $\boldsymbol{\Delta_{ijkl}}$

$$\begin{aligned}
\rho_{gg} &= \langle b_g^\dagger b_g \rangle \\
\rho_{ee} &= \langle b_e^\dagger b_e \rangle \\
\Delta_{gggg} &= \langle b_g^\dagger b_g^\dagger b_g b_g \rangle - \rho_{gg}\rho_{gg} \\
\Delta_{ggee} &= \langle b_g^\dagger b_g^\dagger b_e b_e \rangle \\
\Delta_{gege} &= \langle b_g^\dagger b_e^\dagger b_g b_e \rangle - \rho_{gg}\rho_{ee} \\
\Delta_{eegg} &= \langle b_e^\dagger b_e^\dagger b_g b_g \rangle \\
\Delta_{egeg} &= \langle b_e^\dagger b_g^\dagger g_e b_g \rangle - \rho_{gg}\rho_{ee} \\
\Delta_{eeee} &= \langle b_e^\dagger b_e^\dagger b_e b_e \rangle - \rho_{ee}\rho_{ee}
\end{aligned} \tag{6.6}$$

Evaluating the commutators of the 1- and 2-PRDM elements like in Eq. (6.3) and the approximation of 3PRDM with 3-particle CF equal zero leads together with the Ehrenfest EoM Eq. (6.4) to the following closed set of equations for correlation functions:

EoM for CFs

$$
\begin{aligned}
\dot{\rho}_{gg} &= i\kappa(\Delta_{gehe} - \Delta_{eegg}) \\
\dot{\rho}_{ee} &= i\kappa(\Delta_{eegg} - \Delta_{ggee}) \\
\dot{\Delta}_{gggg} &= i\kappa(\Delta_{eegg} - \Delta_{ggee}) \\
\dot{\Delta}_{gege} &= 0 \\
\dot{\Delta}_{ggee} &= i\,(2\delta\Delta_{ggee} + \kappa\,\{\Delta_{gggg} + 2\Delta_{gggg}\rho_{ee} - \Delta_{eeee}(1 + 2\rho_{gg}) \\
&\qquad -(\rho_{ee} - \rho_{gg})(4\Delta_{gege} + 2\Delta_{ggee} + \rho_{ee} + \rho_{gg} + 2\rho_{ee}\rho_{gg})\}) \\
\dot{\Delta}_{eegg} &= -\dot{\Delta}_{gehe} \\
\dot{\Delta}_{eeee} &= i\kappa(\Delta_{gehe} - \Delta_{eegg})
\end{aligned}
\tag{6.7}
$$

6.3. Approximated EoM for EVs for a BEC in a DWP Higher Order CFs

As we have seen in the last section, in the case of a Bose-Einstein condensate in a double well trap the truncation of the hierarchy of equations of motion given in expectation values by setting correlation functions of order three and higher equal zero leads to satisfactory approximations only for slightly fragmented condensates, but is not capable of describing the dynamics of the real splitting process.
On order to improve the approximation we can simply try to take into account higher order CFs in our calculations. The procedure resembles the one in the previous sections, it only gets lengthier as we have to calculate the time derivatives of more and more EVs and approximations for higher order CFs get longer. Nevertheless these calculations can be carried out straight-forwardly by setting up the reduced density matrices of higher orders, commutate their elements with the Hamiltonian Eq. (6.2) in order to get their time derivatives as given by the Ehrenfest equation of motion Eq. (6.4) and approximate higher order EVs by lower order quantities according to Eq. (5.10) by neglecting CFs of a certain order and higher.
We refrain from depicting these calculations and the analytical results explicitly but rather visualize our findings in the following two plots where we compare the exact two mode model solution for a splitting process of a BEC in a double well potential with approximations where CFs of a certain order and higher where set equal zero.
In Fig. 6.6 we plot the first millisecond of the groundstate population (expectation value $\langle b_g^\dagger b_g \rangle$ of the reduced one particle density matrix) for $n = 100$ particles and the nonlinearity parameter $\kappa = 1/100$ for a splitting process by switching off the tunnel-coupling exponentially starting with the tunneling parameter $\Omega = 0.5$ within a timespan of 100ms. As can clearly be seen, the approximations get better and better the more CFs we take into account.

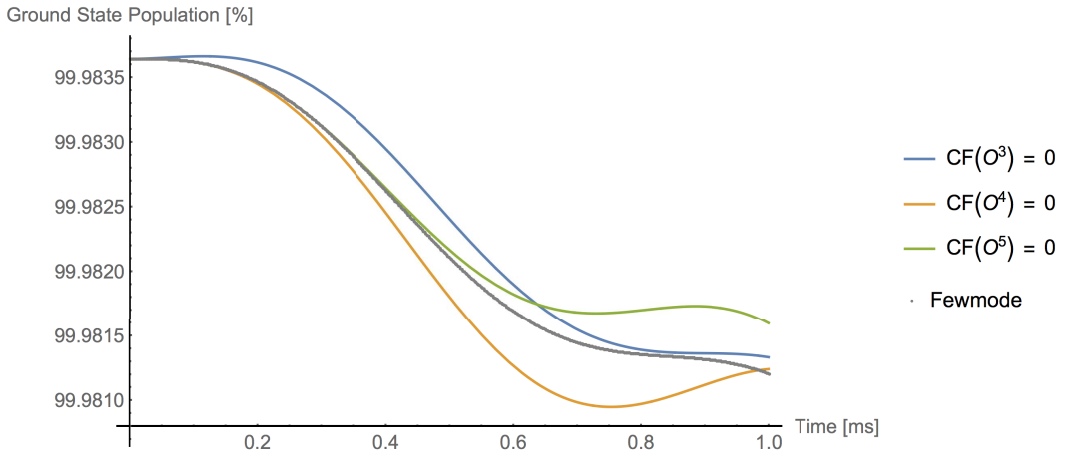

Figure 6.6.: Two mode model: groundstate population (expectation value $\langle b_g^\dagger b_g \rangle$ of the reduced one particle density matrix) for $n = 100$ particles and the nonlinearity parameter $\kappa = 1/100$ for a splitting process by switching off the tunnel-coupling exponentially starting with the tunneling parameter $\Omega = 0.5$ within a timespan of 100ms. Only the first ms is shown for comparison of different approximations by neglecting CFs of certain order and higher. The exact results for the two mode model as found in the numerical solution using our Matlab OCTBEC Toolbox [70] are plotted in grey.

Unfortunately simply taking more and more CFs into account is no feasible solution to this problem. On the one hand, the complexity of the equations as well as the number of CFs that have to be taken into account grows rapidly. In the case of a simple two mode model the number of reduced density matrix elements (the EVs in our equations of motion and hence also the CFs) grow like 4^n with n the order of the reduced density matrix. Even when taking symmetries into account the number of commutators that have to be evaluated grows rapidly when going to higher orders. Although this fact already reduces the benefits of this approach, it is not the critical point. Commutators and approximations for CFs have to be evaluated only once at the very beginning to set up the hierarchy of equations that describe the dynamics of our system. Once we have derived this closed set of equations varying parameters and solving it is straight forward and very fast. The main drawback stems from non-linearities that arise by the approximation of higher order EVs by neglecting CFs of certain order, chapter 5.3. This can already be seen when elongating the splitting

process from the plot above depicted for only 1ms to 13ms, Fig. 6.7. The 'better' the approximations, the more the solutions tend to oscillate and diverge.

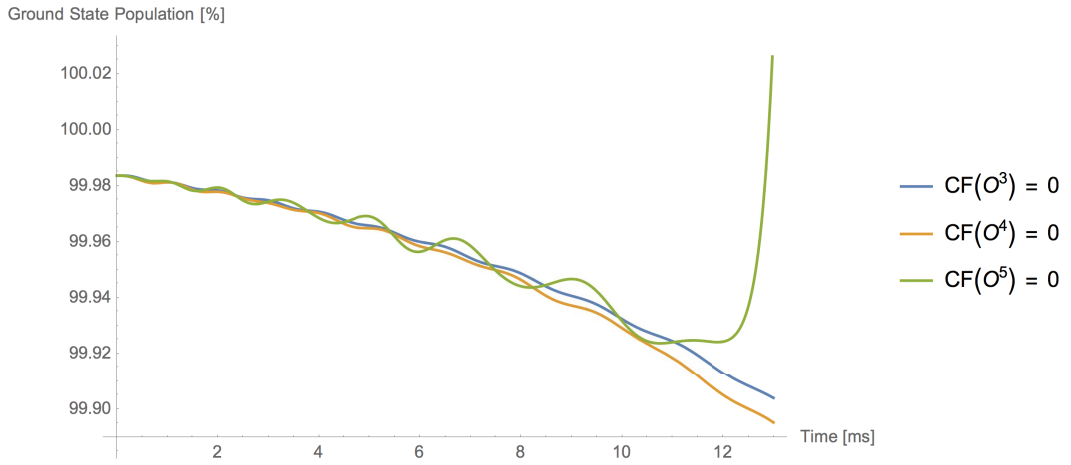

Figure 6.7.: Two mode model: groundstate population (expectation value $\langle b_g^\dagger b_g \rangle$ of the reduced one particle density matrix) for $n = 100$ particles and the nonlinearity parameter $\kappa = 1/100$ for a splitting process by switching off the tunnel-coupling exponentially starting with the tunneling parameter $\Omega = 0.5$ within a timespan of 100ms. Only the first 13ms is shown for comparison of different approximations by neglecting CFs of certain order and higher. The 'better' the approximations, the more non-linearities appear in our closed set of equations that lead to oscillations of the solutions and finally their divergence.

We thus conclude that the only feasible approximation is the one where we set CFs of order 3 and higher equal zero as taking into account any correlation functions of higher order leads to instabilities that make it impossible to solve the closed set of equations.

6.4. Approximated EoM for EVs for a BEC in a DWP 'Constant Trace'

In order to improve the approximation where we set CFs of order 3 and higher equal zero, we take a look at a certain quantity that should be conserved, also in the case of approximations, namely the trace of the xPRDM, $x \in \{1, 2, 3, ...\}$. This approach is motivated by the known importance of satisfying certain 'sum rules' in the approximate solution of dynamic equations.
The trace of the 1PRDM and 2PRDM are the particle number N and the number of ordered two particle combinations $N(N-1)$ respectively. Generally we find for the trace of the xPRDM:

Trace of the xPRDM

$$\mathrm{tr}(\hat{\rho}_x) = N(N-1)...(N-x) \tag{6.8}$$

Hence, for the trace of the 3PRDM we get

Trace of the 3PRDM

$$\begin{aligned}
\mathrm{tr}(\hat{\rho}_3) =& N(N-1)(N-2) \\
=& (\langle b_g^\dagger b_g\rangle + \langle b_e^\dagger b_e\rangle)(\langle b_g^\dagger b_g\rangle + \langle b_e^\dagger b_e\rangle - 1)(\langle b_g^\dagger b_g\rangle + \langle b_e^\dagger b_e\rangle - 2) \\
=& \langle b_g^\dagger b_g\rangle\langle b_g^\dagger b_g\rangle\langle b_g^\dagger b_g\rangle - 3\langle b_g^\dagger b_g\rangle\langle b_g^\dagger b_g\rangle + 2\langle b_g^\dagger b_g\rangle \\
&+ 3\langle b_g^\dagger b_g\rangle\langle b_g^\dagger b_g\rangle\langle b_e^\dagger b_e\rangle - 3\langle b_g^\dagger b_g\rangle\langle b_e^\dagger b_e\rangle \\
&+ 3\langle b_g^\dagger b_g\rangle\langle b_e^\dagger b_e\rangle\langle b_e^\dagger b_e\rangle - 3\langle b_g^\dagger b_g\rangle\langle b_e^\dagger b_e\rangle \\
&+ \langle b_e^\dagger b_e\rangle\langle b_e^\dagger b_e\rangle\langle b_e^\dagger b_e\rangle - 3\langle b_e^\dagger b_e\rangle\langle b_e^\dagger b_e\rangle + 2\langle b_e^\dagger b_e\rangle
\end{aligned} \tag{6.9}$$

where we used $N = \langle b_g^\dagger b_g\rangle + \langle b_e^\dagger b_e\rangle$.

Explicitly, the trace of the 3PRDM is given by

Explicit 3PRDM

$$\begin{aligned}\mathrm{tr}(\hat{\rho}_3) =&\langle b_g^\dagger b_g^\dagger b_g^\dagger b_g b_g b_g\rangle + \langle b_g^\dagger b_g^\dagger b_e^\dagger b_g b_g b_e\rangle + \langle b_g^\dagger b_e^\dagger b_g^\dagger b_g b_e b_g\rangle + \langle b_e^\dagger b_g^\dagger b_g^\dagger b_e b_g b_g\rangle +\\ &+ \langle b_g^\dagger b_e^\dagger b_e^\dagger b_g b_e b_e\rangle + \langle b_e^\dagger b_g^\dagger b_e^\dagger b_e b_g b_e\rangle + \langle b_e^\dagger b_e^\dagger b_g^\dagger b_e b_e b_g\rangle + \langle b_e^\dagger b_e^\dagger b_e^\dagger b_e b_e b_e\rangle\\ =&\langle b_g^\dagger b_g^\dagger b_g^\dagger b_g b_g b_g\rangle\\ &+ \langle b_g^\dagger b_g^\dagger b_e^\dagger b_g b_g b_e\rangle + \langle b_g^\dagger b_e^\dagger b_g^\dagger b_g b_e b_g\rangle + \langle b_e^\dagger b_g^\dagger b_g^\dagger b_e b_g b_g\rangle\\ &+ \langle b_g^\dagger b_e^\dagger b_e^\dagger b_g b_e b_e\rangle + \langle b_e^\dagger b_g^\dagger b_e^\dagger b_e b_g b_e\rangle + \langle b_e^\dagger b_e^\dagger b_g^\dagger b_e b_e b_g\rangle\\ &+ \langle b_e^\dagger b_e^\dagger b_e^\dagger b_e b_e b_e\rangle\end{aligned} \tag{6.10}$$

Comparing these 3PRDM elements from Eq. (6.10) with the 1PRDM elements found before in Eq. (6.9) and keeping in mind the commutator relations $[b_g, b_e] = 0$ and $[b_g^\dagger, b_e^\dagger] = 0$, we conjecture one possible approximation for the diagonal elements of the 3PRDM that keeps its trace constant:

3PRDM Diagonal Elements Approximation

$$\begin{aligned}\langle b_g^\dagger b_g^\dagger b_g^\dagger b_g b_g b_g\rangle \approx&\langle b_g^\dagger b_g\rangle\langle b_g^\dagger b_g\rangle\langle b_g^\dagger b_g\rangle - 3\langle b_g^\dagger b_g\rangle\langle b_g^\dagger b_g\rangle + 2\langle b_g^\dagger b_g\rangle\\ \langle b_g^\dagger b_g^\dagger b_e^\dagger b_g b_g b_e\rangle \approx&\langle b_g^\dagger b_g\rangle\langle b_g^\dagger b_g\rangle\langle b_e^\dagger b_e\rangle - \langle b_g^\dagger b_g\rangle\langle b_e^\dagger b_e\rangle\\ \langle b_e^\dagger b_e^\dagger b_g^\dagger b_e b_e b_g\rangle \approx&\langle b_g^\dagger b_g\rangle\langle b_e^\dagger b_e\rangle\langle b_e^\dagger b_e\rangle - \langle b_g^\dagger b_g\rangle\langle b_e^\dagger b_e\rangle\\ \langle b_e^\dagger b_e^\dagger b_e^\dagger b_e b_e b_e\rangle \approx&\langle b_e^\dagger b_e\rangle\langle b_e^\dagger b_e\rangle\langle b_e^\dagger b_e\rangle - 3\langle b_e^\dagger b_e\rangle\langle b_e^\dagger b_e\rangle + 2\langle b_e^\dagger b_e\rangle\end{aligned} \tag{6.11}$$

Approximating the remaining 3PRDM elements with 3-particle CF equal zero like before, the following closed set of equations is obtained that now guaranties conservation of the xPRDMs:

EoM for EVs

$$
\begin{aligned}
\frac{d}{dt}\langle b_g^\dagger b_g\rangle &= i\kappa[\langle b_g^\dagger b_g^\dagger b_e b_e\rangle - \langle b_e^\dagger b_e^\dagger b_g b_g\rangle] \\
\frac{d}{dt}\langle b_e^\dagger b_e\rangle &= -i\kappa[\langle b_g^\dagger b_g^\dagger b_e b_e\rangle - \langle b_e^\dagger b_e^\dagger b_g b_g\rangle] \\
\frac{d}{dt}\langle b_g^\dagger b_g^\dagger b_g b_g\rangle &= i\kappa[(\langle b_g^\dagger b_g^\dagger b_e b_e\rangle - \langle b_e^\dagger b_e^\dagger b_g b_g\rangle) + 2\langle b_g^\dagger b_g\rangle(\langle b_g^\dagger b_g^\dagger b_e b_e\rangle - \langle b_e^\dagger b_e^\dagger b_g b_g\rangle)] \\
\frac{d}{dt}\langle b_g^\dagger b_g^\dagger b_e b_e\rangle &= i[2\delta\langle b_g^\dagger b_g^\dagger b_e b_e\rangle + \kappa(\langle b_g^\dagger b_g^\dagger b_g b_g\rangle - \langle b_e^\dagger b_e^\dagger b_e b_e\rangle) \\
&\quad + 2\kappa\{-\langle b_e^\dagger b_e\rangle^2\langle b_g^\dagger b_g\rangle + \langle b_g^\dagger b_g\rangle^2\langle b_e^\dagger b_e\rangle \\
&\quad + \langle b_g^\dagger b_g\rangle\langle b_g^\dagger b_g^\dagger b_e b_e\rangle - \langle b_e^\dagger b_e\rangle(\langle b_g^\dagger b_g^\dagger b_e b_e\rangle\}] \\
\frac{d}{dt}\langle b_g^\dagger b_e^\dagger b_g b_e\rangle &= i\kappa[(\langle b_e^\dagger b_e^\dagger\rangle - \langle b_g^\dagger b_g^\dagger\rangle)(\langle b_g^\dagger b_g^\dagger b_e b_e\rangle - \langle b_e^\dagger b_e^\dagger b_g b_g\rangle) \\
\frac{d}{dt}\langle b_e^\dagger b_e^\dagger b_g b_g\rangle &= i[-2\delta\langle b_e^\dagger b_e^\dagger b_g b_g\rangle + \kappa(\langle b_e^\dagger b_e^\dagger b_e b_e\rangle - \langle b_g^\dagger b_g^\dagger b_g b_g\rangle) \\
&\quad + 2\kappa\{\langle b_e^\dagger b_e\rangle^2\langle b_g^\dagger b_g\rangle - \langle b_g^\dagger b_g\rangle^2\langle b_e^\dagger b_e\rangle \\
&\quad - \langle b_g^\dagger b_g\rangle\langle b_e^\dagger b_e^\dagger b_g b_g\rangle + \langle b_e^\dagger b_e\rangle(\langle b_e^\dagger b_e^\dagger b_g b_g\rangle\}] \\
\frac{d}{dt}\langle b_e^\dagger b_g^\dagger b_e b_g\rangle &= -\frac{d}{dt}\langle b_g^\dagger b_e^\dagger b_g b_e\rangle \\
\frac{d}{dt}\langle b_e^\dagger b_e^\dagger b_e b_e\rangle &= i\kappa[(-\langle b_g^\dagger b_g^\dagger b_e b_e\rangle + \langle b_e^\dagger b_e^\dagger b_g b_g\rangle) + 2\langle b_e^\dagger b_e\rangle(\langle b_e^\dagger b_e^\dagger b_g b_g\rangle - \langle b_g^\dagger b_g^\dagger b_e b_e\rangle)]
\end{aligned}
\tag{6.12}
$$

We now again solve this new differential equation system using initial values from the exact calculation by simply calculating the 1PRDM and 2PRDM and compare our results regarding the dynamics of the BEC in a double well potential with the exact calculation within our Matlab OCTBEC Toolbox. In the Fig. 6.8 we show the exact results of the groundstate population (expectation value $\langle b_g^\dagger b_g\rangle$ of the reduced one particle density matrix) for the same scenario as before, in grey, the approximation, where we set CFs of order 3 and higher equal zero in blue and our new approximation

where we set certain CFs of order 3 and higher equal zero but make a different approximation for the diagonal elements of the 3PRDM that keeps its trace constant, in orange.

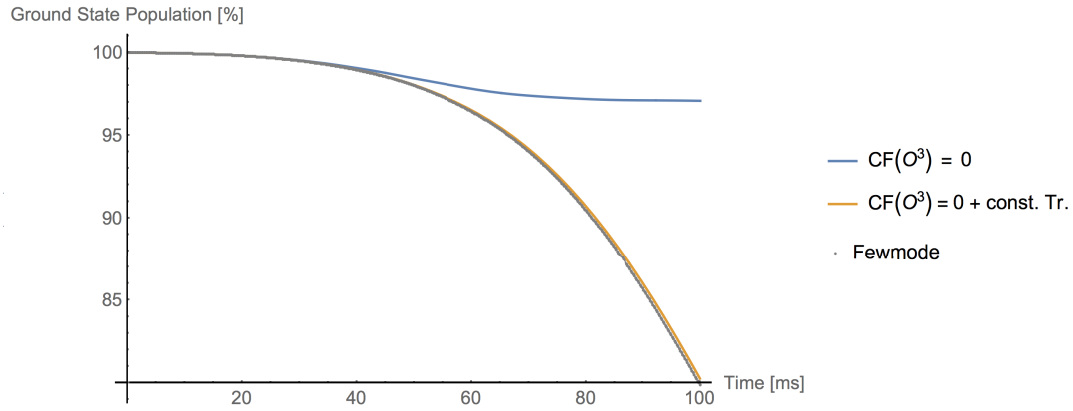

Figure 6.8.: Two mode model: groundstate population (expectation value $\langle b_g^\dagger b_g \rangle$ of the reduced one particle density matrix) for $n = 100$ particles and the nonlinearity parameter $\kappa = 1/100$ for a splitting process by switching off the tunnel-coupling exponentially starting with the tunneling parameter $\Omega = 0.5$ within a timespan of 100ms. We show a comparison of different approximations. The exact results of the two mode model are plotted in grey, the approximation where we set CFs of order 3 and higher equal zero in blue and our new approximation where we set certain CFs of order 3 and higher equal zero but make a different approximation for the diagonal elements of the 3PRDM that keeps its trace constant in orange. Clearly the conservation of the xPRDM trace has a huge impact on the accuracy of the approximation.

6.5. Comparison to Anglin & Vardi Approximation

In this section we want to compare the constant trace approximation from the last section to an approximation scheme from Anglin and Vardi [11] which is only suitable for systems with a *mildly fragmented condensate*.
Anglin and Vardi use the previously defined pseudo spin operators

Pseudospin Operators

$$\hat{J}_x = \frac{1}{2}(\hat{b}_L^\dagger \hat{b}_R + \hat{b}_R^\dagger \hat{b}_L), \quad \hat{J}_y = \frac{i}{2}(\hat{b}_L^\dagger \hat{b}_R - \hat{b}_R^\dagger \hat{b}_L), \quad \hat{J}_z = \frac{1}{2}(\hat{b}_L^\dagger \hat{b}_L - \hat{b}_R^\dagger \hat{b}_R) \tag{6.13}$$

to rewrite the Hamiltonian for the two mode model

Hamiltonian with Pseudospin Operators

$$\hat{H} = -\Omega(t)\hat{J}_x + 2\kappa \hat{J}_z^2. \tag{6.14}$$

where the action of $\hat{J}_x$ on a state is the exchange of one atom between the left and right well, whereas $\hat{J}_z$ measures atom number imbalances between left and right well.
From the Ehrenfest equations of motion

Ehrenfest Equation of Motion

$$\frac{d}{dt}\langle A\rangle = \langle \mathcal{L}\rangle = \frac{i}{\hbar}\langle [H, A]\rangle \tag{6.15}$$

we obtain, like before, the BBGKY hierarchy of equations of motion for the expectation-values of the pseudospin operators:

EoM for EVs

$$\begin{aligned}\frac{d}{dt}\langle\hat{J}_i\rangle &= f(\langle\hat{J}_{i'}\rangle, \langle\hat{J}_{i'}, \hat{J}_{j'}\rangle)\\ \frac{d}{dt}\langle\hat{J}_i\hat{J}_j\rangle &= f(\langle\hat{J}_{i'}, \hat{J}_{j'}\rangle, \langle\hat{J}_{i'}, \hat{J}_{j'}, \hat{J}_{k'}\rangle)\\ \frac{d}{dt}\langle\hat{J}_i\hat{J}_j\hat{J}_k\rangle &= f(\langle\hat{J}_{i'}, \hat{J}_{j'}, \hat{J}_{k'}\rangle, \langle\hat{J}_{i'}, \hat{J}_{j'}, \hat{J}_{k'}, \hat{J}_{l'}\rangle)\\ &\vdots\end{aligned} \tag{6.16}$$

where $i, j, k, ..., i', j', k', l', ... = x, y, z$.
To end up with a closed set of equations the following approximation is used

Approximation for Pseudospin Operators

$$\langle\hat{J}_i\hat{J}_j\hat{J}_k\rangle \approx \langle\hat{J}_i\hat{J}_j\rangle\langle\hat{J}_k\rangle + \langle\hat{J}_i\rangle\langle\hat{J}_j\hat{J}_k\rangle + \langle\hat{J}_i\hat{J}_k\rangle\langle\hat{J}_j\rangle - 2\langle\hat{J}_i\rangle\langle\hat{J}_j\rangle\langle\hat{J}_k\rangle \tag{6.17}$$

Together with the single-particle Bloch vector

Single-Particle Bloch Vector

$$\mathbf{s} = (s_x, s_y, s_z) \equiv \left(\frac{2\langle\hat{J}_x\rangle}{N}, \frac{2\langle\hat{J}_y\rangle}{N}, \frac{2\langle\hat{J}_z\rangle}{N}\right) \tag{6.18}$$

and corresponding second-order moments

Second-Order Moments

$$\Delta_{ij} = \frac{4}{N^2}(\langle \hat{L}_i \hat{L}_j + \hat{L}_j \hat{L}_i \rangle - 2\langle \hat{L}_i \rangle \langle \hat{L}_j \rangle) \tag{6.19}$$

where $i, j, k = x, y, z$, we obtain the following set of nine equations for the first- and second-order moments where we have defined $k \equiv 2N\kappa$:

Equations for the First- and Second-Order Moments

$$\begin{aligned}
\dot{s}_x &= -ks_z s_y - \frac{k}{2}\Delta_{yz} \\
\dot{s}_y &= \Omega s_z + ks_z s_x + \frac{k}{2}\Delta_{xz} \\
\dot{s}_x &= -\Omega s_y \\
\dot{\Delta}_{xz} &= -\Omega\Delta_{xy} - ks_z\Delta_{yz} - ks_y\Delta_{zz} \\
\dot{\Delta}_{yz} &= \Omega(\Delta_{zz} - \Delta_{yy}) + ks_z\Delta_{xz} + ks_x\Delta_{zz} \\
\dot{\Delta}_{xy} &= (\Omega + ks_x)\Delta_{xz} - ks_y\Delta_{yz} + ks_z(\Delta_{xx} - \Delta_{yy}) \\
\dot{\Delta}_{xx} &= -2ks_y\Delta_{xz} - 2ks_z\Delta_{xy} \\
\dot{\Delta}_{yy} &= 2(\Omega + ks_x)\Delta_{yz} + 2ks_z\Delta_{xy} \\
\dot{\Delta}_{zz} &= -2\Omega\Delta_{yz}
\end{aligned} \tag{6.20}$$

We again solve the differential equation system using initial values from the exact calculation by simply calculating the 1PRDM and 2PRDM and also compare our results regarding the dynamics of the BEC in a double well potential with the exact calculation within our Matlab OCTBEC Toolbox. In the plots we show the exact results in grey, our 'constant trace approximation' in orange and results form Anglin

and Vardi in blue. We start with a constant tunneling that does not change with time and find that both approximations deliver good results (notice the scale of the ordinate) even though Anglin and Vardi's approximation tends to stronger oscillations.

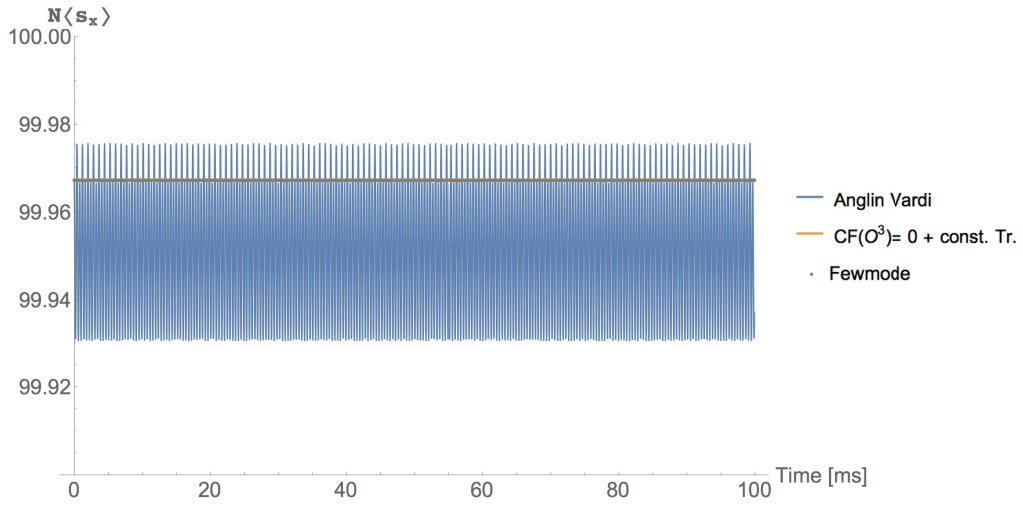

Figure 6.9.: Two mode model: expectation value $\langle \hat{s}_x \rangle$ times the number of particles N (proportional to the exchange of atoms between left and right well) for 100 particles and the nonlinearity parameter $\kappa = 1/100$ with the constant tunneling parameter $\Omega = 3$ within a timespan of 100ms. We show a comparison of different approximations. The exact results of the two mode model are plotted in grey, Anglin and Vardi's approximation in blue and our new approximation where we set certain CFs of order 3 and higher equal zero but make a different approximation for the diagonal elements of the 3PRDM that keeps its trace constant in orange. For constant tunneling that does not change with time we find that both approximations deliver good results (notice the scale of the ordinate) even though Anglin and Vardi's approximation tends to stronger oscillations.

But for a dynamical splitting process the two approximations lead to quite different results. While our 'constant trace' approximation is still in good agreement with the exact two-model calculation, Anglin and Vardi's approximation shows the right tendency but starts to oscillate at later times, thus being no longer suitable for an approximative description of the dynamic splitting process.

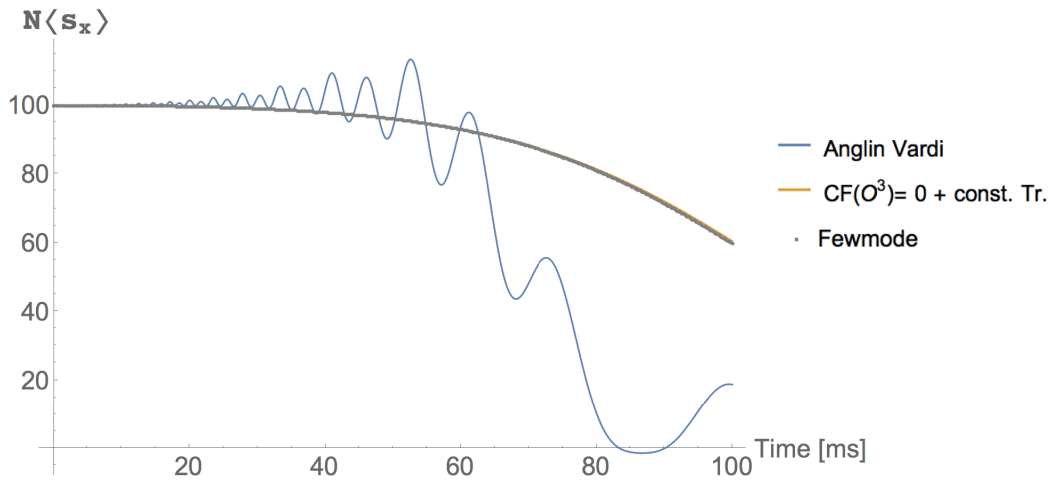

Figure 6.10.: Two mode model: expectation value $\langle \hat{s}_x \rangle$ times the number of particles N (proportional to the exchange of atoms between left and right well) for 100 particles and the nonlinearity parameter $\kappa = 1/100$ for a splitting process by switching off the tunnel-coupling exponentially starting with the tunneling parameter $\Omega = 3$ within a timespan of 100ms. We show a comparison of different approximations. The exact results of the two mode model are plotted in grey, Anglin and Vardi's approximation in blue and our new approximation where we set certain CFs of order 3 and higher equal zero but make a different approximation for the diagonal elements of the 3PRDM that keeps its trace constant in orange. Clearly the conservation of the xPRDM trace has a huge impact on the accuracy of the approximation as the two approximations lead to quite different results with our 'constant trace' approximation still in good agreement with the exact two-model calculation whereas Anglin and Vardi's approximation shows the right tendency but oscillates too much and can not be used any more for an approximative description of the dynamical splitting process.

6.6. Four Mode Model and Discussion

In the description of a splitting process of a BEC a four mode model is the natural next step as it can also account for higher excitations. As will be shown, unfortunately, already for $CF(O^3) = 0$ the derived system of differential equations can not be solved any more for longer time spans, even for a 'constant trace approximation', because of the former mentioned occurrence of instabilities that lead to oscillations. In order to demonstrate the power of the density matrix formalism for few particle systems, where it allows for a numerically exact treatment, we simulate the splitting process of a BEC consisting of only two atoms in a double well potential within a four mode model. The thereby derived hierarchy of EoM is naturally truncated as EVs of normal ordered 3 particle operators vanish. Nevertheless we can also apply our constant trace approximation where we set $CF(O^3) = 0$ for comparison. The obtained results for the ground state population are depicted in Fig. 6.11.

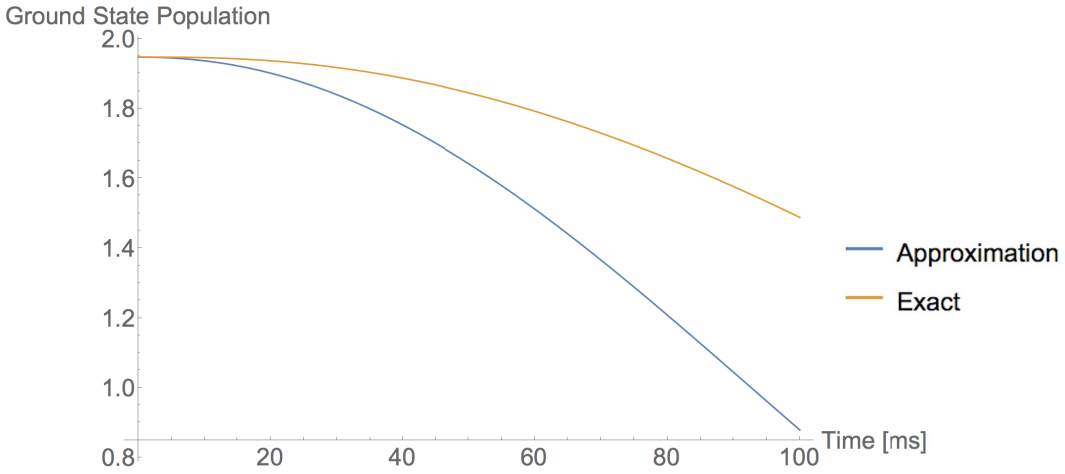

Figure 6.11.: Four mode model: goundstate population for $n = 2$ particles and the nonlinearity parameter $\kappa = 1/100$ for a splitting process by switching off the tunnel-coupling exponentially starting with the tunneling parameter $\lambda = 0.85$ within a timespan of 100ms. The approximation scheme does not yield a satisfying result for short time spans, e.g. low fragmentation. For more fragmented states this approximation scheme is clearly not applicable any more.

For this two particle system our approximation scheme does not yield a satisfying result for short time spans ($t < 20$ms) and hence hardly any fragmentation. For even more fragmented states this approximation scheme is clearly not applicable any more.
As is apparent from Fig. 6.12, where the same splitting process is plotted for 100 particles, former mentioned instabilities occur, leading to unphysical results and finally strong oscillations that make it impossible to solve the EoM system.

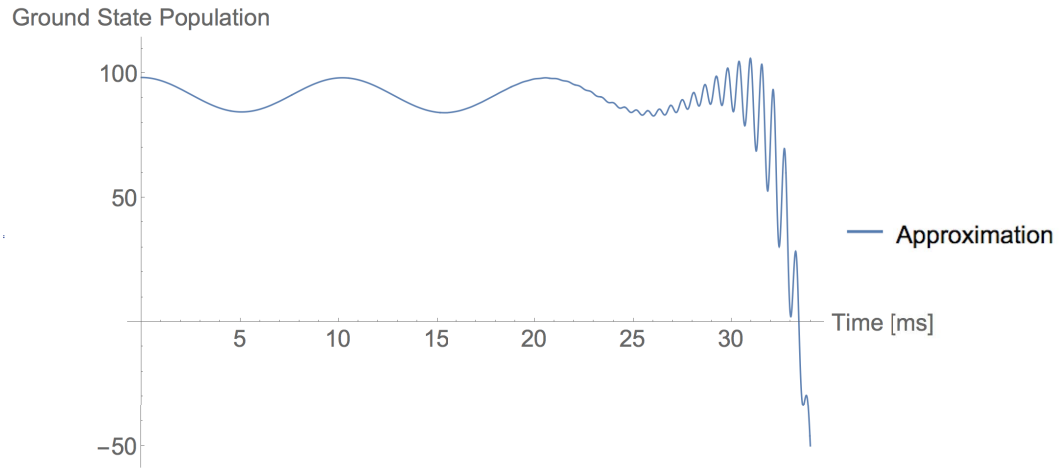

Figure 6.12.: Four mode model: goundstate population for $n = 100$ particles and the nonlinearity parameter $\kappa = 1/100$ for a splitting process by switching off the tunnel-coupling exponentially starting with the tunneling parameter $\lambda = 0.85$ within a timespan of 100ms. Only the first 33ms are shown as instabilities occur that lead to unphysical results and finally strong oscillations that make it impossible to solve the EoM system numerically.

We conclude that the density matrix formalism, as presented in this theses, is not able to properly describe the dynamics of moderately fragmented or excited condensates.

We have found that the constance of the xPRDM trace seems to play an important role in the dynamics, and hence special care has to be taken when making approximations. With the density matrix formalism presented in this thesis, using an explicit

conservation of the xPRDM trace, we have outlined a superior approximation scheme that can be applied not only for the case of BECs, like in this thesis, but in general. Nevertheless this approximation scheme has its own limitations founded in the occurrence of nonlinear terms which number grows with the number of EVs that are approximated. As has been shown this effectively limits its application already in a simple two mode model rather fast. If too many CFs are taken into account the system of differential equations can not be solved any more because of the occurrence of instabilities that lead to oscillations.
The density matrix formalism without approximations, e.g. in simulations with just a handful of particles, is very powerful and the code outlined in this thesis can be used to apply it to different problems for given many particle Hamiltonians. Nevertheless, the approximation scheme presented in this thesis in combination with the density matrix formalism is not capable of capturing the dynamics of moderately fragmented or excited condensates and is merely a perturbational approach.

A. Appendix

A.1. Approximation of 3-Point Functions for a BEC in a DWP

We use the `fewmodepair` class of the Matlab OCTBEC Toolbox [70] in order to find exact solutions of our two-mode model for different states. We set the number of particles to $n = 100$, the nonlinearity parameter $\kappa = 1/100$ and the tunneling parameter $\Omega = 0.5$. In order to end up with different states, we switch off the tunnel-coupling exponentially within different intervals ranging from 1ms to 100ms. This is accomplished within the software by changing the control parameter λ. Results for the different elements of the 3PRDM as well as an visualization of the states on the Bloch sphere and the atom number difference are given below. We emphasise that here we are just comparing elements of the 3PRDM (blue line) calculated within the two mode model with their approximations (red line) given by Eq. (6.1) also calculated within the two mode model.
As can clearly be seen in the following plots, when comparing the accuracy of the approximations with the density plots and the representation of the states on the Bloch sphere belonging to the same splitting process the approximations work quite well as long as the condensate is unsplit, and get worse as the condensates fragments.

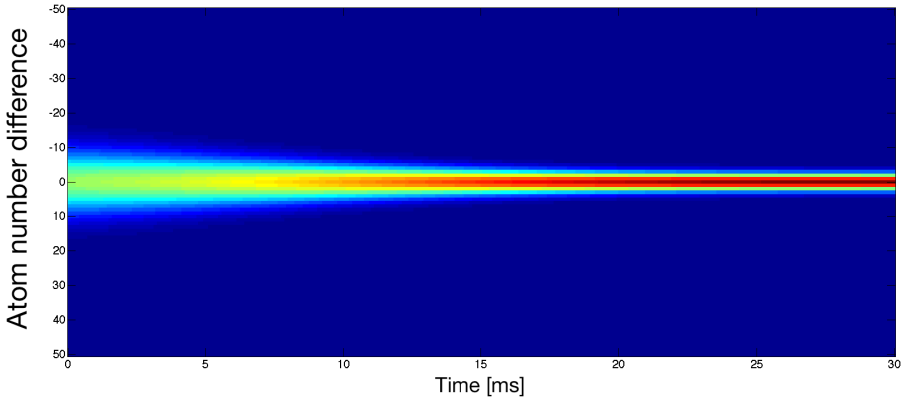

Figure A.1.: Two mode model: density-plot of $n = 100$ particles and the nonlinearity parameter $\kappa = 1/100$ for a splitting process by switching off the tunnel-coupling exponentially starting with the tunneling parameter $\Omega = 0.5$ within a time span of 30ms.

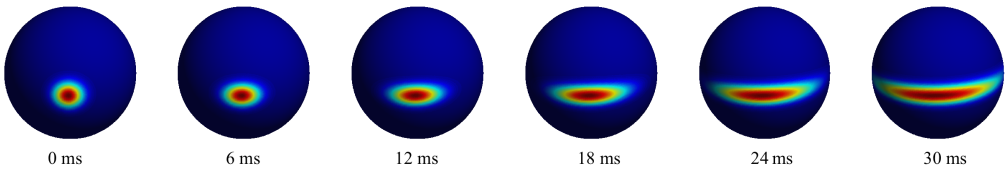

Figure A.2.: Two mode model: illustration of the states on the Bloch sphere for $n = 100$ particles and the nonlinearity parameter $\kappa = 1/100$ for a splitting process by switching off the tunnel-coupling exponentially starting with the tunneling parameter $\Omega = 0.5$ within a time span of 30ms.

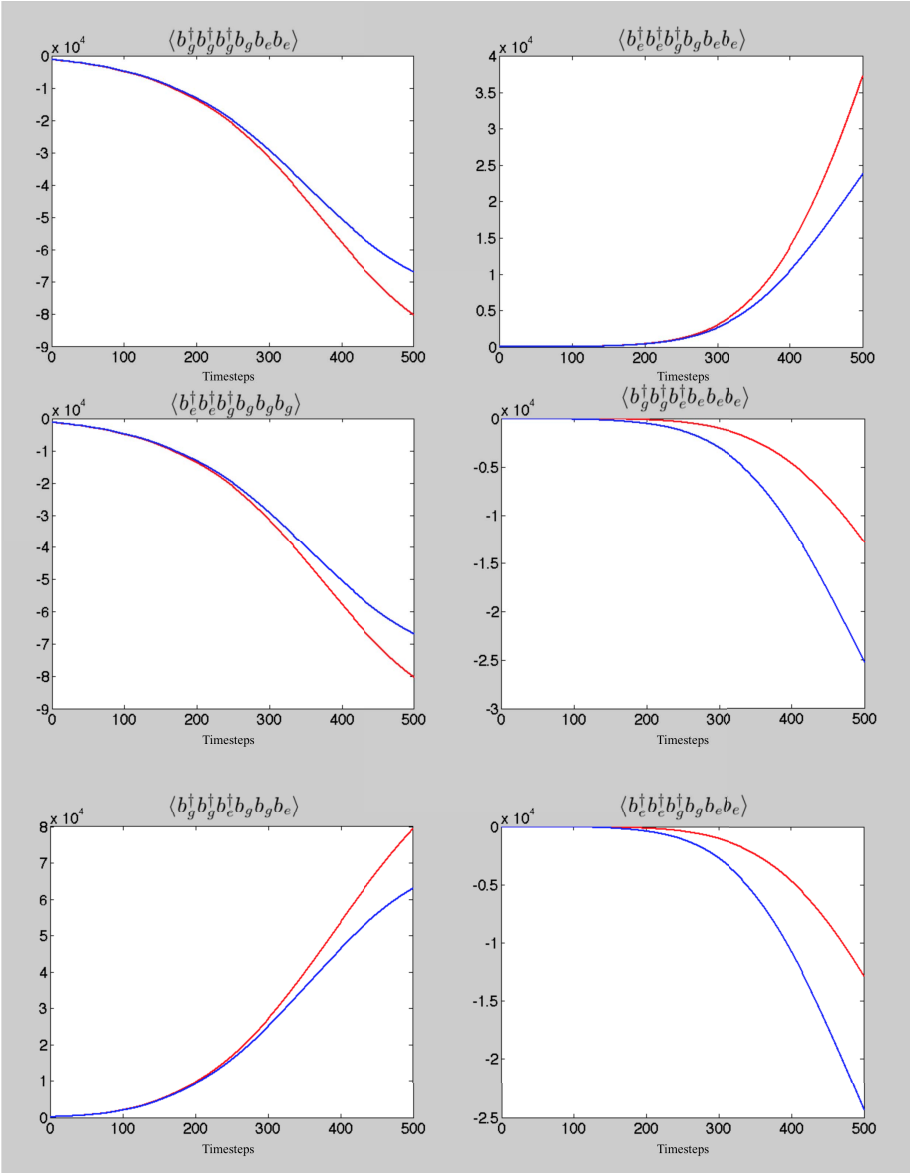

Figure A.3.: Two mode model: comparison of elements of the 3PRDM (blue line) calculated within the two mode model with their approximations (red line) given by Eq. (6.1) also calculated within the two mode model for $n = 100$ particles and the nonlinearity parameter $\kappa = 1/100$ for a splitting process by switching of the tunnel-coupling exponentially starting with the tunneling parameter $\Omega = 0.5$ within a time span of 30ms (1 timestep $\equiv$ 0.06ms).

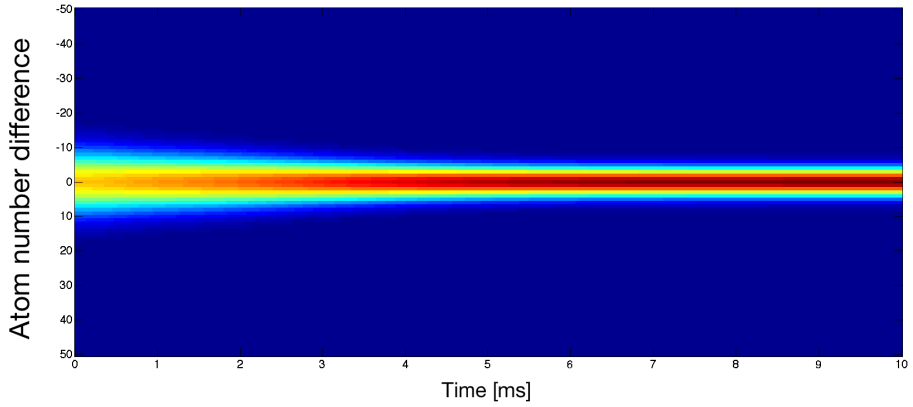

Figure A.4.: Same as Fig. A.1 but for a time span of 10ms.

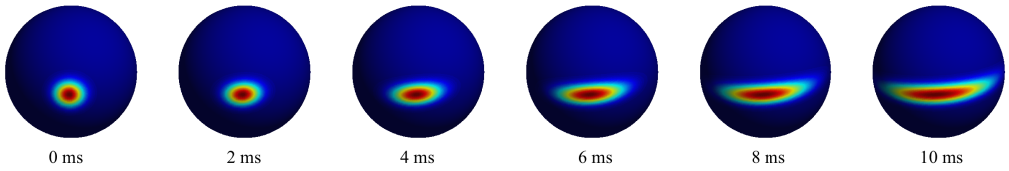

Figure A.5.: Same as Fig. A.2 but for a time span of 10ms.

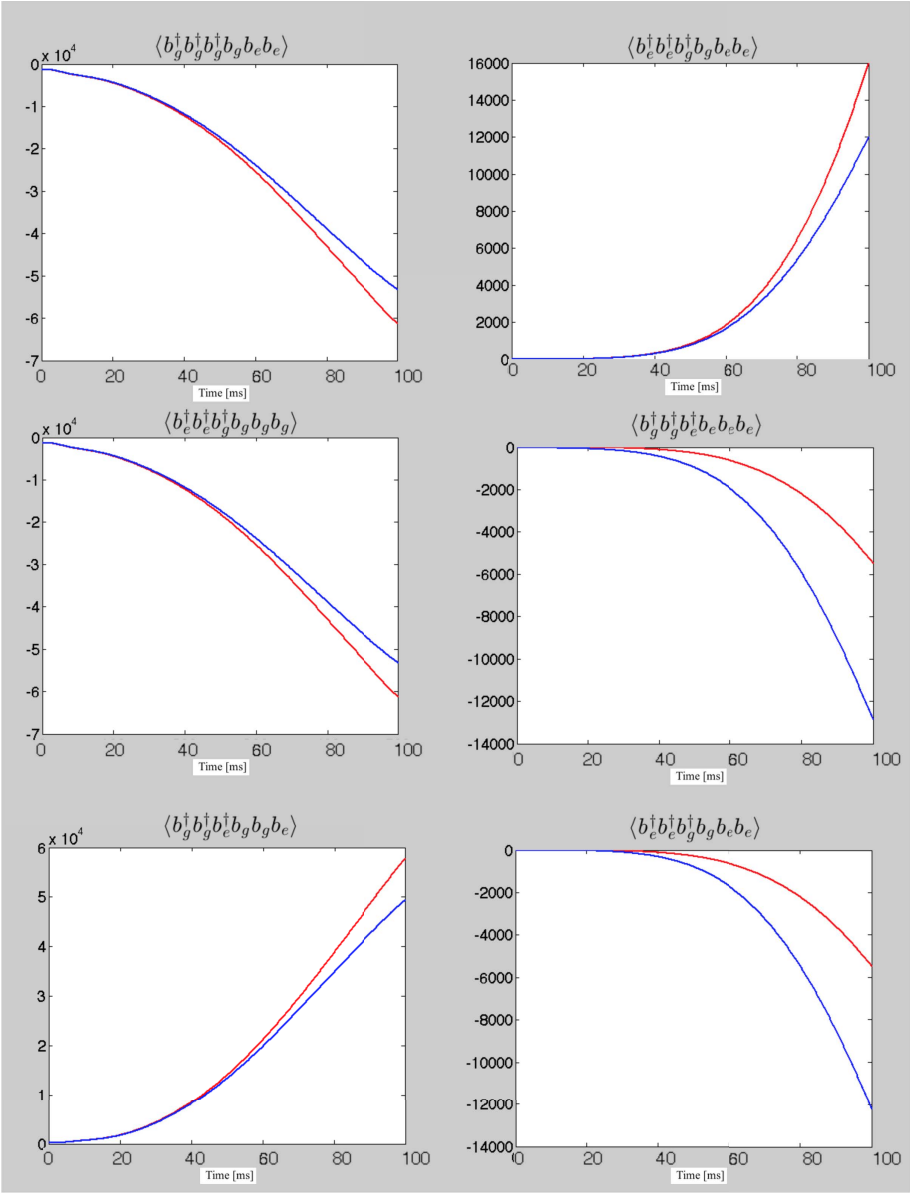

Figure A.6.: Same as Fig. A.3 but for a time span of 10ms (1 timestep ≡ 0.02ms).

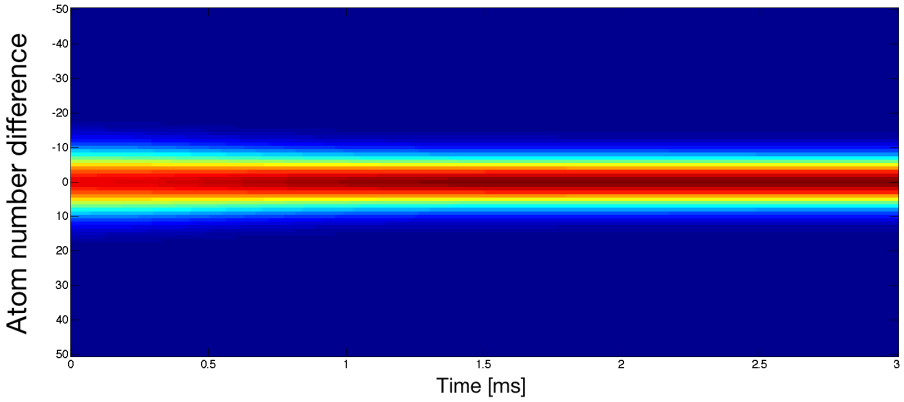

Figure A.7.: Same as Fig. A.1 but for a time span of 3ms.

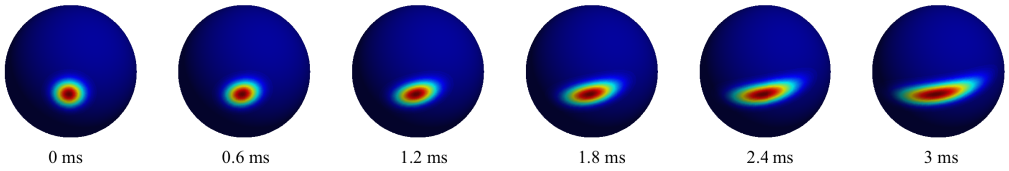

Figure A.8.: Same as Fig. A.2 but for a time span of 3ms.

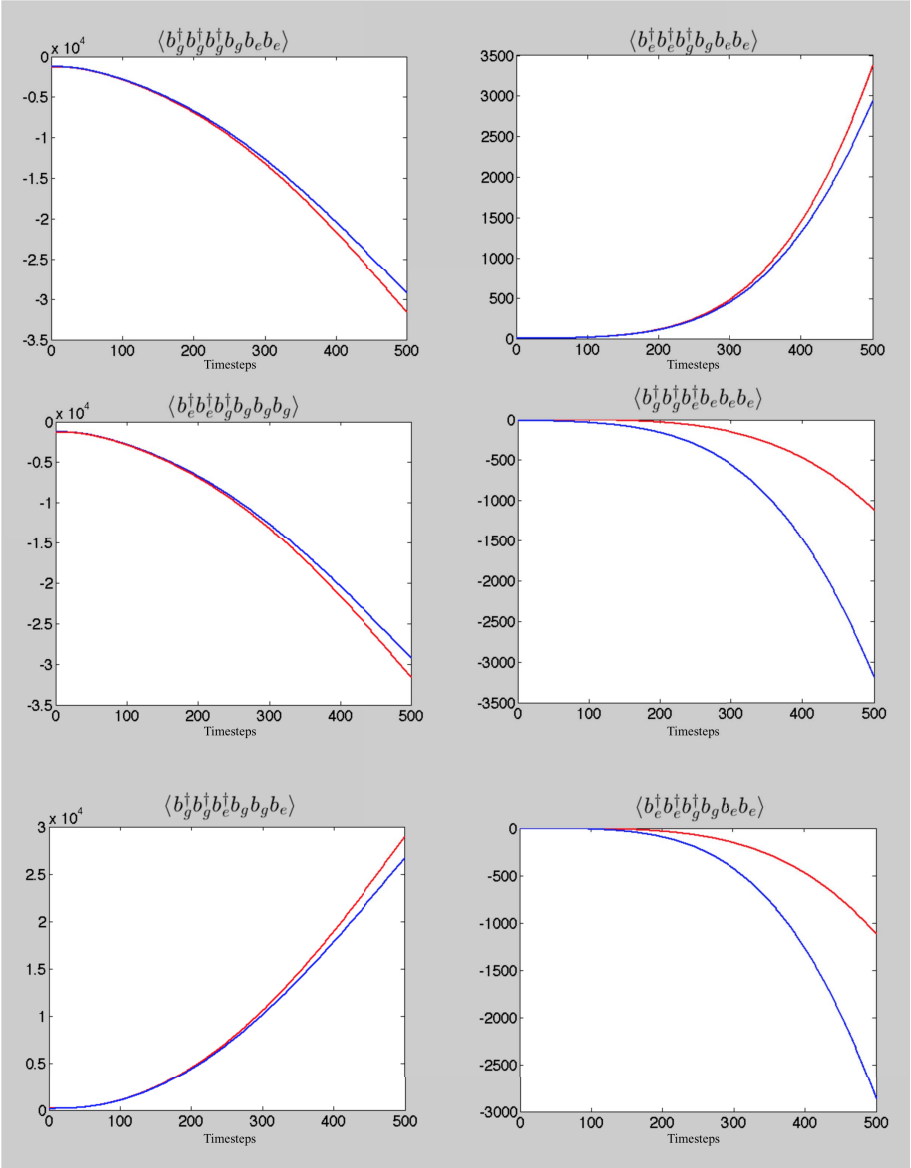

Figure A.9.: Same as Fig. A.3 but for a time span of 3ms (1 timestep $\equiv$ 0.006ms).

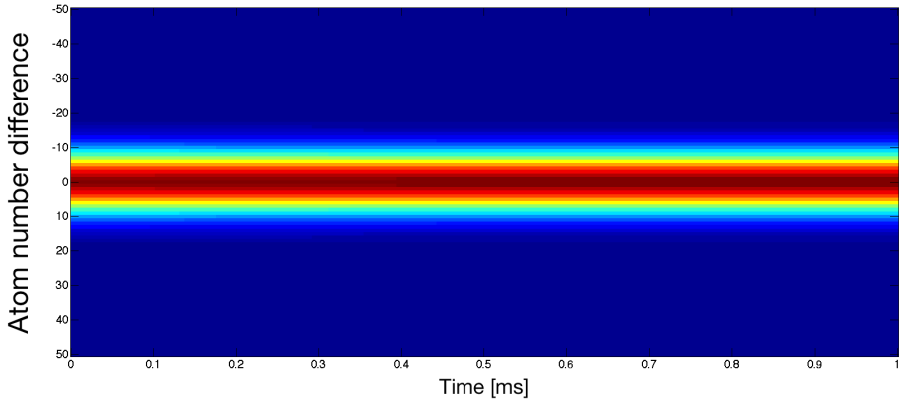

Figure A.10.: Same as Fig. A.1 but for a time span of 1ms.

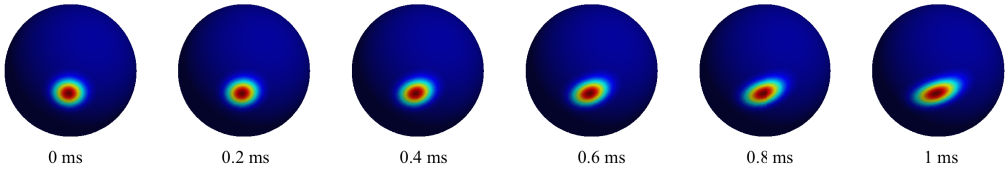

Figure A.11.: Same as Fig. A.2 but for a time span of 1ms.

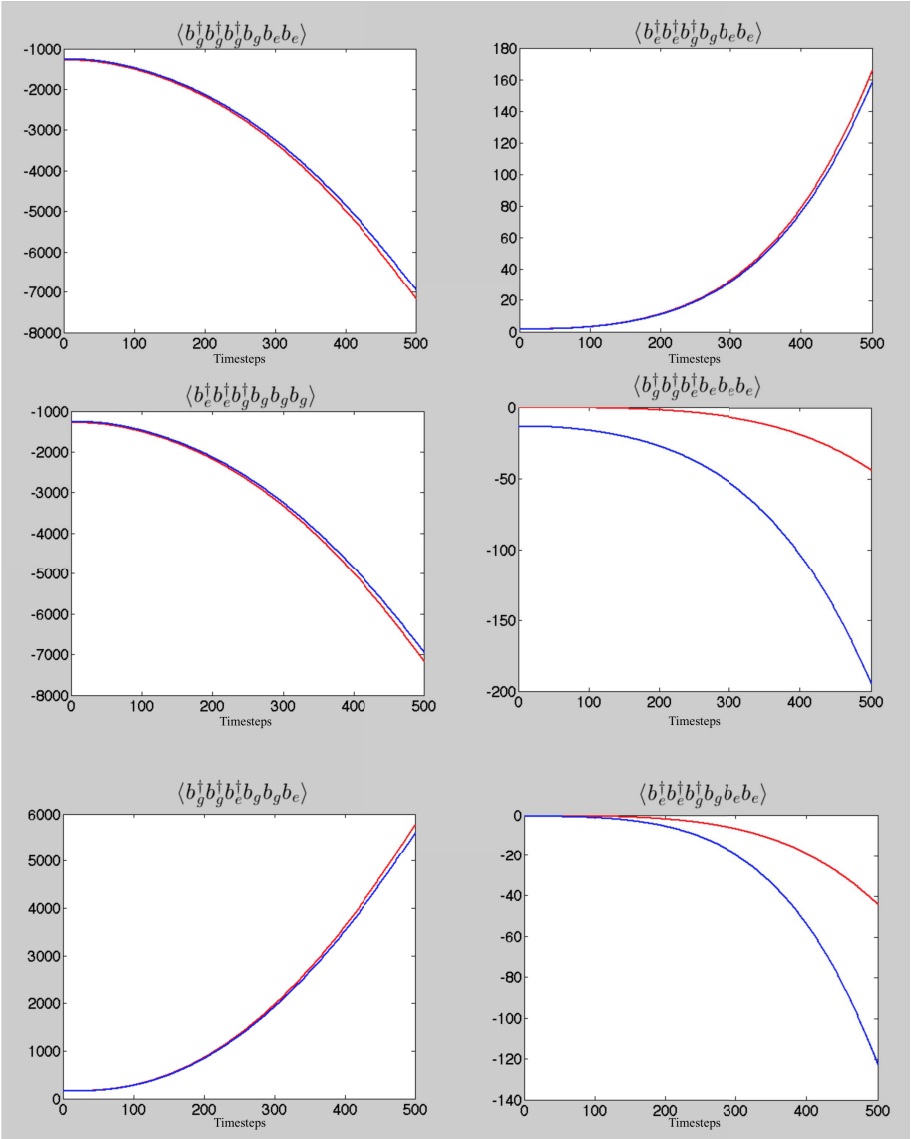

Figure A.12.: Same as Fig. A.3 but for a time span of 1ms (1 timestep $\equiv$ 0.002ms).

A.2. Mathematica Code for Approximating EVs

In this section we present some example *Mathematica* code[1] that was used to calculate the approximations of EVs as a sum of products of lower-order EVs. For better clarity it is not shown in the most general form but for the special case of setting CFs of order three and higher equal zero in a two mode model in gerade-ungerade basis. The main idea is to first represent all EVs of order three and lower as CFs and vice versa. In the sum of products of CFs describing EVs of order three we set CFs of order three equal zero and replace the remaining CFs of order two and lower by their representation as EVs.
We first have to load the *Combinatorica* package.

```
Needs["Combinatorica`"]
```

Next we define replacement rules for products of operators that will appear as single operators with subindices in our calculation and set quantities with vanishing expectation value equal zero.

```
rep1 = Flatten[Table[{b_{i} → 0}, {i, 1, 4}]];
rep2 = Flatten[Table[{b_{i,j} -> b_i · b_j}, {i, 1, 4}, {j, 1, 4}]];
rep3 = Flatten[Table[{b_{i,j,k} → 0}, {i, 1, 4}, {j, 1, 4}, {k, 1, 4}]];
rep4 = Flatten[Table[{b_{i,j,k,l} -> b_i · b_j · b_k · b_l}, {i, 1, 4}, {j, 1, 4},
    {k, 1, 4}, {l, 1, 4}]];
rep5 = Flatten[Table[{b_{i,j,k,l,m} → 0}, {i, 1, 4}, {j, 1, 4}, {k, 1, 4},
    {l, 1, 4}, {m, 1, 4}]];
rep6 = Flatten[Table[{b_{i,j,k,l,m,n} -> b_i · b_j · b_k · b_l · b_m · b_n}, {i, 1, 4},
    {j, 1, 4}, {k, 1, 4}, {l, 1, 4}, {m, 1, 4}, {n, 1, 4}]];
rep1to6 = Flatten[{rep1, rep2, rep3, rep4, rep5, rep6}];
```

The following replacement rule identifies the quantities in our combinatorics calculation with operators needed for our QM computation, namely the creation and annihilation operators for gerade (g) and ungerade (e) states.

[1] The *Mathematica* code can be downloaded at http://physik.uni-graz.at/~uxh/octbec/expectation_value_approximation.nb

```
rep1234toge = {b1 → (g)†, b2 → (e)†, b3 → g, b4 → e};
```

CFs of order one (written with double brackets) are expressed as EVs of order one (written with single brackets)

```
cf1toev = {⟨⟨g† · g⟩⟩ → ⟨g† · g⟩, ⟨⟨e† · e⟩⟩ → ⟨e† · e⟩};
```

Vanishing EVs are set equal zero

```
rules1pto0ev = {⟨e† · g⟩ → 0, ⟨g† · e⟩ → 0, ⟨e† · e†⟩ → 0, ⟨g† · g†⟩ → 0,
    ⟨e† · g†⟩ → 0, ⟨g† · e†⟩ → 0, ⟨e · e⟩ → 0, ⟨g · g⟩ → 0, ⟨e · g⟩ → 0, ⟨g · e⟩ → 0};
```

as well as vanishing CFs

```
rules1pto0cf = {⟨⟨e† · g⟩⟩ → 0, ⟨⟨g† · e⟩⟩ → 0, ⟨⟨e† · e†⟩⟩ → 0,
    ⟨⟨g† · g†⟩⟩ → 0, ⟨⟨e† · g†⟩⟩ → 0, ⟨⟨g† · e†⟩⟩ → 0, ⟨⟨e · e⟩⟩ → 0,
    ⟨⟨g · g⟩⟩ → 0, ⟨⟨e · g⟩⟩ → 0, ⟨⟨g · e⟩⟩ → 0};
```

We now express CFs of order two as sum of products of EVs of order two and lower

```
int2 = Flatten[Table[{i, j, l, m}, {i, 1, 2}, {j, 1, 2}, {l, 3, 4},
    {m, 3, 4}], 3]
```

```
{{1, 1, 3, 3}, {1, 1, 3, 4}, {1, 1, 4, 3}, {1, 1, 4, 4},
 {1, 2, 3, 3}, {1, 2, 3, 4}, {1, 2, 4, 3}, {1, 2, 4, 4},
 {2, 1, 3, 3}, {2, 1, 3, 4}, {2, 1, 4, 3}, {2, 1, 4, 4},
 {2, 2, 3, 3}, {2, 2, 3, 4}, {2, 2, 4, 3}, {2, 2, 4, 4}}
```

```
cf2toev =
 Table[pi = DeleteDuplicates[Map[Sort, SetPartitions[int2[[it4]]], 2]];
  ⟨⟨b_int2[[it4]]⟩⟩ →
    Sum[(-1)^(Length[pi[[j]]]-1) * (Length[pi[[j]]] - 1)! *
      Product[⟨bi⟩, {i, pi[[j]]}], {j, 1, Length[pi]}] //. repl1to6,
  {it4, 1, Length[int2]}]
```

$$\{\langle\langle b_1 \cdot b_1 \cdot b_3 \cdot b_3\rangle\rangle \to -\langle b_1 \cdot b_3\rangle^2 - \langle b_1 \cdot b_1\rangle\langle b_3 \cdot b_3\rangle + \langle b_1 \cdot b_1 \cdot b_3 \cdot b_3\rangle,$$
$$\langle\langle b_1 \cdot b_1 \cdot b_3 \cdot b_4\rangle\rangle \to -\langle b_1 \cdot b_3\rangle\langle b_1 \cdot b_4\rangle - \langle b_1 \cdot b_1\rangle\langle b_3 \cdot b_4\rangle + \langle b_1 \cdot b_1 \cdot b_3 \cdot b_4\rangle,$$
$$\langle\langle b_1 \cdot b_1 \cdot b_4 \cdot b_3\rangle\rangle \to -\langle b_1 \cdot b_3\rangle\langle b_1 \cdot b_4\rangle - \langle b_1 \cdot b_1\rangle\langle b_3 \cdot b_4\rangle + \langle b_1 \cdot b_1 \cdot b_3 \cdot b_4\rangle,$$
$$\langle\langle b_1 \cdot b_1 \cdot b_4 \cdot b_4\rangle\rangle \to -\langle b_1 \cdot b_4\rangle^2 - \langle b_1 \cdot b_1\rangle\langle b_4 \cdot b_4\rangle + \langle b_1 \cdot b_1 \cdot b_4 \cdot b_4\rangle,$$
$$\langle\langle b_1 \cdot b_2 \cdot b_3 \cdot b_3\rangle\rangle \to -\langle b_1 \cdot b_3\rangle\langle b_2 \cdot b_3\rangle - \langle b_1 \cdot b_2\rangle\langle b_3 \cdot b_3\rangle + \langle b_1 \cdot b_2 \cdot b_3 \cdot b_3\rangle,$$
$$\langle\langle b_1 \cdot b_2 \cdot b_3 \cdot b_4\rangle\rangle \to -\langle b_1 \cdot b_4\rangle\langle b_2 \cdot b_3\rangle - \langle b_1 \cdot b_3\rangle\langle b_2 \cdot b_4\rangle -$$
$$\langle b_1 \cdot b_2\rangle\langle b_3 \cdot b_4\rangle + \langle b_1 \cdot b_2 \cdot b_3 \cdot b_4\rangle, \langle\langle b_1 \cdot b_2 \cdot b_4 \cdot b_3\rangle\rangle \to$$
$$-\langle b_1 \cdot b_4\rangle\langle b_2 \cdot b_3\rangle - \langle b_1 \cdot b_3\rangle\langle b_2 \cdot b_4\rangle - \langle b_1 \cdot b_2\rangle\langle b_3 \cdot b_4\rangle + \langle b_1 \cdot b_2 \cdot b_3 \cdot b_4\rangle,$$
$$\langle\langle b_1 \cdot b_2 \cdot b_4 \cdot b_4\rangle\rangle \to -\langle b_1 \cdot b_4\rangle\langle b_2 \cdot b_4\rangle - \langle b_1 \cdot b_2\rangle\langle b_4 \cdot b_4\rangle + \langle b_1 \cdot b_2 \cdot b_4 \cdot b_4\rangle,$$
$$\langle\langle b_2 \cdot b_1 \cdot b_3 \cdot b_3\rangle\rangle \to -\langle b_1 \cdot b_3\rangle\langle b_2 \cdot b_3\rangle - \langle b_1 \cdot b_2\rangle\langle b_3 \cdot b_3\rangle + \langle b_1 \cdot b_2 \cdot b_3 \cdot b_3\rangle,$$
$$\langle\langle b_2 \cdot b_1 \cdot b_3 \cdot b_4\rangle\rangle \to -\langle b_1 \cdot b_4\rangle\langle b_2 \cdot b_3\rangle - \langle b_1 \cdot b_3\rangle\langle b_2 \cdot b_4\rangle -$$
$$\langle b_1 \cdot b_2\rangle\langle b_3 \cdot b_4\rangle + \langle b_1 \cdot b_2 \cdot b_3 \cdot b_4\rangle, \langle\langle b_2 \cdot b_1 \cdot b_4 \cdot b_3\rangle\rangle \to$$
$$-\langle b_1 \cdot b_4\rangle\langle b_2 \cdot b_3\rangle - \langle b_1 \cdot b_3\rangle\langle b_2 \cdot b_4\rangle - \langle b_1 \cdot b_2\rangle\langle b_3 \cdot b_4\rangle + \langle b_1 \cdot b_2 \cdot b_3 \cdot b_4\rangle,$$
$$\langle\langle b_2 \cdot b_1 \cdot b_4 \cdot b_4\rangle\rangle \to -\langle b_1 \cdot b_4\rangle\langle b_2 \cdot b_4\rangle - \langle b_1 \cdot b_2\rangle\langle b_4 \cdot b_4\rangle + \langle b_1 \cdot b_2 \cdot b_4 \cdot b_4\rangle,$$
$$\langle\langle b_2 \cdot b_2 \cdot b_3 \cdot b_3\rangle\rangle \to -\langle b_2 \cdot b_3\rangle^2 - \langle b_2 \cdot b_2\rangle\langle b_3 \cdot b_3\rangle + \langle b_2 \cdot b_2 \cdot b_3 \cdot b_3\rangle,$$
$$\langle\langle b_2 \cdot b_2 \cdot b_3 \cdot b_4\rangle\rangle \to -\langle b_2 \cdot b_3\rangle\langle b_2 \cdot b_4\rangle - \langle b_2 \cdot b_2\rangle\langle b_3 \cdot b_4\rangle + \langle b_2 \cdot b_2 \cdot b_3 \cdot b_4\rangle,$$
$$\langle\langle b_2 \cdot b_2 \cdot b_4 \cdot b_3\rangle\rangle \to -\langle b_2 \cdot b_3\rangle\langle b_2 \cdot b_4\rangle - \langle b_2 \cdot b_2\rangle\langle b_3 \cdot b_4\rangle + \langle b_2 \cdot b_2 \cdot b_3 \cdot b_4\rangle,$$
$$\langle\langle b_2 \cdot b_2 \cdot b_4 \cdot b_4\rangle\rangle \to -\langle b_2 \cdot b_4\rangle^2 - \langle b_2 \cdot b_2\rangle\langle b_4 \cdot b_4\rangle + \langle b_2 \cdot b_2 \cdot b_4 \cdot b_4\rangle\}$$

In the next step we use the previously defined replacement rule to identify the quantities in our combinatorics calculation with operators needed for our QM computation

```
cf2toev = cf2toev /. rep1234toge
```

$$\{\langle\langle g^\dagger\cdot g^\dagger\cdot g\cdot g\rangle\rangle \to -\langle g^\dagger\cdot g\rangle^2 - \langle g\cdot g\rangle\langle g^\dagger\cdot g^\dagger\rangle + \langle g^\dagger\cdot g^\dagger\cdot g\cdot g\rangle,$$
$$\langle\langle g^\dagger\cdot g^\dagger\cdot g\cdot e\rangle\rangle \to -\langle g^\dagger\cdot e\rangle\langle g^\dagger\cdot g\rangle - \langle g\cdot e\rangle\langle g^\dagger\cdot g^\dagger\rangle + \langle g^\dagger\cdot g^\dagger\cdot g\cdot e\rangle,$$
$$\langle\langle g^\dagger\cdot g^\dagger\cdot e\cdot g\rangle\rangle \to -\langle g^\dagger\cdot e\rangle\langle g^\dagger\cdot g\rangle - \langle g\cdot e\rangle\langle g^\dagger\cdot g^\dagger\rangle + \langle g^\dagger\cdot g^\dagger\cdot g\cdot e\rangle,$$
$$\langle\langle g^\dagger\cdot g^\dagger\cdot e\cdot e\rangle\rangle \to -\langle g^\dagger\cdot e\rangle^2 - \langle e\cdot e\rangle\langle g^\dagger\cdot g^\dagger\rangle + \langle g^\dagger\cdot g^\dagger\cdot e\cdot e\rangle,$$
$$\langle\langle g^\dagger\cdot e^\dagger\cdot g\cdot g\rangle\rangle \to -\langle e^\dagger\cdot g\rangle\langle g^\dagger\cdot g\rangle - \langle g\cdot g\rangle\langle g^\dagger\cdot e^\dagger\rangle + \langle g^\dagger\cdot e^\dagger\cdot g\cdot g\rangle,$$
$$\langle\langle g^\dagger\cdot e^\dagger\cdot g\cdot e\rangle\rangle \to -\langle e^\dagger\cdot g\rangle\langle g^\dagger\cdot e\rangle - \langle e^\dagger\cdot e\rangle\langle g^\dagger\cdot g\rangle -$$
$$\langle g\cdot e\rangle\langle g^\dagger\cdot e^\dagger\rangle + \langle g^\dagger\cdot e^\dagger\cdot g\cdot e\rangle, \langle\langle g^\dagger\cdot e^\dagger\cdot e\cdot g\rangle\rangle \to$$
$$-\langle e^\dagger\cdot g\rangle\langle g^\dagger\cdot e\rangle - \langle e^\dagger\cdot e\rangle\langle g^\dagger\cdot g\rangle - \langle g\cdot e\rangle\langle g^\dagger\cdot e^\dagger\rangle + \langle g^\dagger\cdot e^\dagger\cdot g\cdot e\rangle,$$
$$\langle\langle g^\dagger\cdot e^\dagger\cdot e\cdot e\rangle\rangle \to -\langle e^\dagger\cdot e\rangle\langle g^\dagger\cdot e\rangle - \langle e\cdot e\rangle\langle g^\dagger\cdot e^\dagger\rangle + \langle g^\dagger\cdot e^\dagger\cdot e\cdot e\rangle,$$
$$\langle\langle e^\dagger\cdot g^\dagger\cdot g\cdot g\rangle\rangle \to -\langle e^\dagger\cdot g\rangle\langle g^\dagger\cdot g\rangle - \langle g\cdot g\rangle\langle g^\dagger\cdot e^\dagger\rangle + \langle g^\dagger\cdot e^\dagger\cdot g\cdot g\rangle,$$
$$\langle\langle e^\dagger\cdot g^\dagger\cdot g\cdot e\rangle\rangle \to -\langle e^\dagger\cdot g\rangle\langle g^\dagger\cdot e\rangle - \langle e^\dagger\cdot e\rangle\langle g^\dagger\cdot g\rangle -$$
$$\langle g\cdot e\rangle\langle g^\dagger\cdot e^\dagger\rangle + \langle g^\dagger\cdot e^\dagger\cdot g\cdot e\rangle, \langle\langle e^\dagger\cdot g^\dagger\cdot e\cdot g\rangle\rangle \to$$
$$-\langle e^\dagger\cdot g\rangle\langle g^\dagger\cdot e\rangle - \langle e^\dagger\cdot e\rangle\langle g^\dagger\cdot g\rangle - \langle g\cdot e\rangle\langle g^\dagger\cdot e^\dagger\rangle + \langle g^\dagger\cdot e^\dagger\cdot g\cdot e\rangle,$$
$$\langle\langle e^\dagger\cdot g^\dagger\cdot e\cdot e\rangle\rangle \to -\langle e^\dagger\cdot e\rangle\langle g^\dagger\cdot e\rangle - \langle e\cdot e\rangle\langle g^\dagger\cdot e^\dagger\rangle + \langle g^\dagger\cdot e^\dagger\cdot e\cdot e\rangle,$$
$$\langle\langle e^\dagger\cdot e^\dagger\cdot g\cdot g\rangle\rangle \to -\langle e^\dagger\cdot g\rangle^2 - \langle g\cdot g\rangle\langle e^\dagger\cdot e^\dagger\rangle + \langle e^\dagger\cdot e^\dagger\cdot g\cdot g\rangle,$$
$$\langle\langle e^\dagger\cdot e^\dagger\cdot g\cdot e\rangle\rangle \to -\langle e^\dagger\cdot e\rangle\langle e^\dagger\cdot g\rangle - \langle g\cdot e\rangle\langle e^\dagger\cdot e^\dagger\rangle + \langle e^\dagger\cdot e^\dagger\cdot g\cdot e\rangle,$$
$$\langle\langle e^\dagger\cdot e^\dagger\cdot e\cdot g\rangle\rangle \to -\langle e^\dagger\cdot e\rangle\langle e^\dagger\cdot g\rangle - \langle g\cdot e\rangle\langle e^\dagger\cdot e^\dagger\rangle + \langle e^\dagger\cdot e^\dagger\cdot g\cdot e\rangle,$$
$$\langle\langle e^\dagger\cdot e^\dagger\cdot e\cdot e\rangle\rangle \to -\langle e^\dagger\cdot e\rangle^2 - \langle e\cdot e\rangle\langle e^\dagger\cdot e^\dagger\rangle + \langle e^\dagger\cdot e^\dagger\cdot e\cdot e\rangle\}$$

and set vanishing quantities equal zero

```
cf2toev = cf2toev /. rules1pto0ev
```

$$\{\langle\langle g^\dagger\cdot g^\dagger\cdot g\cdot g\rangle\rangle \to -\langle g^\dagger\cdot g\rangle^2 + \langle g^\dagger\cdot g^\dagger\cdot g\cdot g\rangle,$$
$$\langle\langle g^\dagger\cdot g^\dagger\cdot g\cdot e\rangle\rangle \to \langle g^\dagger\cdot g^\dagger\cdot g\cdot e\rangle, \langle\langle g^\dagger\cdot g^\dagger\cdot e\cdot g\rangle\rangle \to \langle g^\dagger\cdot g^\dagger\cdot g\cdot e\rangle,$$
$$\langle\langle g^\dagger\cdot g^\dagger\cdot e\cdot e\rangle\rangle \to \langle g^\dagger\cdot g^\dagger\cdot e\cdot e\rangle, \langle\langle g^\dagger\cdot e^\dagger\cdot g\cdot g\rangle\rangle \to \langle g^\dagger\cdot e^\dagger\cdot g\cdot g\rangle,$$
$$\langle\langle g^\dagger\cdot e^\dagger\cdot g\cdot e\rangle\rangle \to -\langle e^\dagger\cdot e\rangle\langle g^\dagger\cdot g\rangle + \langle g^\dagger\cdot e^\dagger\cdot g\cdot e\rangle,$$
$$\langle\langle g^\dagger\cdot e^\dagger\cdot e\cdot g\rangle\rangle \to -\langle e^\dagger\cdot e\rangle\langle g^\dagger\cdot g\rangle + \langle g^\dagger\cdot e^\dagger\cdot g\cdot e\rangle,$$
$$\langle\langle g^\dagger\cdot e^\dagger\cdot e\cdot e\rangle\rangle \to \langle g^\dagger\cdot e^\dagger\cdot e\cdot e\rangle, \langle\langle e^\dagger\cdot g^\dagger\cdot g\cdot g\rangle\rangle \to \langle g^\dagger\cdot e^\dagger\cdot g\cdot g\rangle,$$
$$\langle\langle e^\dagger\cdot g^\dagger\cdot g\cdot e\rangle\rangle \to -\langle e^\dagger\cdot e\rangle\langle g^\dagger\cdot g\rangle + \langle g^\dagger\cdot e^\dagger\cdot g\cdot e\rangle,$$
$$\langle\langle e^\dagger\cdot g^\dagger\cdot e\cdot g\rangle\rangle \to -\langle e^\dagger\cdot e\rangle\langle g^\dagger\cdot g\rangle + \langle g^\dagger\cdot e^\dagger\cdot g\cdot e\rangle,$$
$$\langle\langle e^\dagger\cdot g^\dagger\cdot e\cdot e\rangle\rangle \to \langle g^\dagger\cdot e^\dagger\cdot e\cdot e\rangle, \langle\langle e^\dagger\cdot e^\dagger\cdot g\cdot g\rangle\rangle \to \langle e^\dagger\cdot e^\dagger\cdot g\cdot g\rangle,$$
$$\langle\langle e^\dagger\cdot e^\dagger\cdot g\cdot e\rangle\rangle \to \langle e^\dagger\cdot e^\dagger\cdot g\cdot e\rangle, \langle\langle e^\dagger\cdot e^\dagger\cdot e\cdot g\rangle\rangle \to \langle e^\dagger\cdot e^\dagger\cdot g\cdot e\rangle,$$
$$\langle\langle e^\dagger\cdot e^\dagger\cdot e\cdot e\rangle\rangle \to -\langle e^\dagger\cdot e\rangle^2 + \langle e^\dagger\cdot e^\dagger\cdot e\cdot e\rangle\}$$

We now express EVs of order three as sum of products of CFs of order two and lower, neglecting CFs of order three (only a part of the lengthy output is shown)

```
int3 =
 DeleteCases[
  Flatten[
   Table[{i, j, k, l, m, n} *
     If[EvenQ[Count[{i, j, k, l, m, n}, 1] + Count[{i, j, k, l, m, n}, 3]],
      1, 0], {i, 1, 2}, {j, 1, 2}, {k, 1, 2}, {l, 3, 4}, {m, 3, 4},
    {n, 3, 4}], 5], {0, 0, 0, 0, 0, 0}]
```

```
{{1, 1, 1, 3, 3, 3}, {1, 1, 1, 3, 4, 4},
 {1, 1, 1, 4, 3, 4}, {1, 1, 1, 4, 4, 3}, {1, 1, 2, 3, 3, 4},
 {1, 1, 2, 3, 4, 3}, {1, 1, 2, 4, 3, 3}, {1, 1, 2, 4, 4, 4},
 {1, 2, 1, 3, 3, 4}, {1, 2, 1, 3, 4, 3}, {1, 2, 1, 4, 3, 3},
 {1, 2, 1, 4, 4, 4}, {1, 2, 2, 3, 3, 3}, {1, 2, 2, 3, 4, 4},
 {1, 2, 2, 4, 3, 4}, {1, 2, 2, 4, 4, 3}, {2, 1, 1, 3, 3, 4},
 {2, 1, 1, 3, 4, 3}, {2, 1, 1, 4, 3, 3}, {2, 1, 1, 4, 4, 4},
 {2, 1, 2, 3, 3, 3}, {2, 1, 2, 3, 4, 4}, {2, 1, 2, 4, 3, 4},
 {2, 1, 2, 4, 4, 3}, {2, 2, 1, 3, 3, 3}, {2, 2, 1, 3, 4, 4},
 {2, 2, 1, 4, 3, 4}, {2, 2, 1, 4, 4, 3}, {2, 2, 2, 3, 3, 4},
 {2, 2, 2, 3, 4, 3}, {2, 2, 2, 4, 3, 3}, {2, 2, 2, 4, 4, 4}}
```

```
ev3tocfex3 =
 Table[pi = DeleteDuplicates[Map[Sort, SetPartitions[int3[[it4]]], 2]];
  ⟨b_int3[[it4]]⟩ → Sum[Product[⟨⟨b_i⟩⟩, {i, pi[[j]]}], {j, 1, Length[pi]}] -
     (-1)^(Length[pi[[1]]]-1) * (Length[pi[[1]]] - 1)! *
      Product[⟨⟨b_i⟩⟩, {i, pi[[1]]}] //. repl to 6, {it4, 1, Length[int3]}]
```

```
{⟨b1 · b1 · b1 · b3 · b3 · b3⟩ → ⟨⟨b1 · b3⟩⟩^3 + ⟨⟨b1 · b1⟩⟩ ⟨⟨b1 · b3⟩⟩ ⟨⟨b3 · b3⟩⟩ +
   ⟨⟨b3 · b3⟩⟩ ⟨⟨b1 · b1 · b1 · b3⟩⟩ + ⟨⟨b1 · b3⟩⟩ ⟨⟨b1 · b1 · b3 · b3⟩⟩ +
   ⟨⟨b1 · b1⟩⟩ ⟨⟨b1 · b3 · b3 · b3⟩⟩, ⟨b1 · b1 · b1 · b3 · b4 · b4⟩ →
  ⟨⟨b1 · b3⟩⟩ ⟨⟨b1 · b4⟩⟩^2 + ⟨⟨b1 · b1⟩⟩ ⟨⟨b1 · b4⟩⟩ ⟨⟨b3 · b4⟩⟩ +
   ⟨⟨b1 · b1⟩⟩ ⟨⟨b1 · b3⟩⟩ ⟨⟨b4 · b4⟩⟩ + ⟨⟨b4 · b4⟩⟩ ⟨⟨b1 · b1 · b1 · b3⟩⟩ +
   ⟨⟨b3 · b4⟩⟩ ⟨⟨b1 · b1 · b1 · b4⟩⟩ + ⟨⟨b1 · b4⟩⟩ ⟨⟨b1 · b1 · b3 · b4⟩⟩ +
   ⟨⟨b1 · b3⟩⟩ ⟨⟨b1 · b1 · b4 · b4⟩⟩ + ⟨⟨b1 · b1⟩⟩ ⟨⟨b1 · b3 · b4 · b4⟩⟩,
 ⟨b1 · b1 · b1 · b4 · b3 · b4⟩ → ⟨⟨b1 · b3⟩⟩ ⟨⟨b1 · b4⟩⟩^2 +
   ⟨⟨b1 · b1⟩⟩ ⟨⟨b1 · b4⟩⟩ ⟨⟨b3 · b4⟩⟩ + ⟨⟨b1 · b1⟩⟩ ⟨⟨b1 · b3⟩⟩ ⟨⟨b4 · b4⟩⟩ +
   ⟨⟨b4 · b4⟩⟩ ⟨⟨b1 · b1 · b1 · b3⟩⟩ + ⟨⟨b3 · b4⟩⟩ ⟨⟨b1 · b1 · b1 · b4⟩⟩ +
   ⟨⟨b1 · b4⟩⟩ ⟨⟨b1 · b1 · b3 · b4⟩⟩ + ⟨⟨b1 · b3⟩⟩ ⟨⟨b1 · b1 · b4 · b4⟩⟩ +
   ⟨⟨b1 · b1⟩⟩ ⟨⟨b1 · b3 · b4 · b4⟩⟩, ⟨b1 · b1 · b1 · b4 · b4 · b3⟩ →
  ⟨⟨b1 · b3⟩⟩ ⟨⟨b1 · b4⟩⟩^2 + ⟨⟨b1 · b1⟩⟩ ⟨⟨b1 · b4⟩⟩ ⟨⟨b3 · b4⟩⟩ +
   ⟨⟨b1 · b1⟩⟩ ⟨⟨b1 · b3⟩⟩ ⟨⟨b4 · b4⟩⟩ + ⟨⟨b4 · b4⟩⟩ ⟨⟨b1 · b1 · b1 · b3⟩⟩ +
   ⟨⟨b3 · b4⟩⟩ ⟨⟨b1 · b1 · b1 · b4⟩⟩ + ⟨⟨b1 · b4⟩⟩ ⟨⟨b1 · b1 · b3 · b4⟩⟩ +
   ⟨⟨b1 · b3⟩⟩ ⟨⟨b1 · b1 · b4 · b4⟩⟩ + ⟨⟨b1 · b1⟩⟩ ⟨⟨b1 · b3 · b4 · b4⟩⟩,
 ⟨b1 · b1 · b2 · b3 · b3 · b4⟩ → ⟨⟨b1 · b3⟩⟩ ⟨⟨b1 · b4⟩⟩ ⟨⟨b2 · b3⟩⟩ +
   ⟨⟨b1 · b3⟩⟩^2 ⟨⟨b2 · b4⟩⟩ + ⟨⟨b1 · b2⟩⟩ ⟨⟨b1 · b4⟩⟩ ⟨⟨b3 · b3⟩⟩ +
   ⟨⟨b1 · b1⟩⟩ ⟨⟨b2 · b4⟩⟩ ⟨⟨b3 · b3⟩⟩ + ⟨⟨b1 · b2⟩⟩ ⟨⟨b1 · b3⟩⟩ ⟨⟨b3 · b4⟩⟩ +
   ⟨⟨b1 · b1⟩⟩ ⟨⟨b2 · b3⟩⟩ ⟨⟨b3 · b4⟩⟩ + ⟨⟨b3 · b4⟩⟩ ⟨⟨b1 · b1 · b2 · b3⟩⟩ +
   ⟨⟨b3 · b3⟩⟩ ⟨⟨b1 · b1 · b2 · b4⟩⟩ + ⟨⟨b2 · b4⟩⟩ ⟨⟨b1 · b1 · b3 · b3⟩⟩ +
   ⟨⟨b2 · b3⟩⟩ ⟨⟨b1 · b1 · b3 · b4⟩⟩ + ⟨⟨b1 · b4⟩⟩ ⟨⟨b1 · b2 · b3 · b3⟩⟩ +
   ⟨⟨b1 · b3⟩⟩ ⟨⟨b1 · b2 · b3 · b4⟩⟩ + ⟨⟨b1 · b2⟩⟩ ⟨⟨b1 · b3 · b3 · b4⟩⟩ +
   ⟨⟨b1 · b1⟩⟩ ⟨⟨b2 · b3 · b3 · b4⟩⟩, ⟨b1 · b1 · b2 · b3 · b4 · b3⟩ →
  ⟨⟨b1 · b3⟩⟩ ⟨⟨b1 · b4⟩⟩ ⟨⟨b2 · b3⟩⟩ + ⟨⟨b1 · b3⟩⟩^2 ⟨⟨b2 · b4⟩⟩ +
   ⟨⟨b1 · b2⟩⟩ ⟨⟨b1 · b4⟩⟩ ⟨⟨b3 · b3⟩⟩ + ⟨⟨b1 · b1⟩⟩ ⟨⟨b2 · b4⟩⟩ ⟨⟨b3 · b3⟩⟩ +
   ⟨⟨b1 · b2⟩⟩ ⟨⟨b1 · b3⟩⟩ ⟨⟨b3 · b4⟩⟩ + ⟨⟨b1 · b1⟩⟩ ⟨⟨b2 · b3⟩⟩ ⟨⟨b3 · b4⟩⟩ +
   ⟨⟨b3 · b4⟩⟩ ⟨⟨b1 · b1 · b2 · b3⟩⟩ + ⟨⟨b3 · b3⟩⟩ ⟨⟨b1 · b1 · b2 · b4⟩⟩ +
   ⟨⟨b2 · b4⟩⟩ ⟨⟨b1 · b1 · b3 · b3⟩⟩ + ⟨⟨b2 · b3⟩⟩ ⟨⟨b1 · b1 · b3 · b4⟩⟩ +
   ⟨⟨b1 · b4⟩⟩ ⟨⟨b1 · b2 · b3 · b3⟩⟩ + ⟨⟨b1 · b3⟩⟩ ⟨⟨b1 · b2 · b3 · b4⟩⟩ +
   ⟨⟨b1 · b2⟩⟩ ⟨⟨b1 · b3 · b3 · b4⟩⟩ + ⟨⟨b1 · b1⟩⟩ ⟨⟨b2 · b3 · b3 · b4⟩⟩,
 ⟨b1 · b1 · b2 · b4 · b3 · b3⟩ → ⟨⟨b1 · b3⟩⟩ ⟨⟨b1 · b4⟩⟩ ⟨⟨b2 · b3⟩⟩ +
   ⟨⟨b1 · b3⟩⟩^2 ⟨⟨b2 · b4⟩⟩ + ⟨⟨b1 · b2⟩⟩ ⟨⟨b1 · b4⟩⟩ ⟨⟨b3 · b3⟩⟩ +
   ⟨⟨b1 · b1⟩⟩ ⟨⟨b2 · b4⟩⟩ ⟨⟨b3 · b3⟩⟩ + ⟨⟨b1 · b2⟩⟩ ⟨⟨b1 · b3⟩⟩ ⟨⟨b3 · b4⟩⟩ +
   ⟨⟨b1 · b1⟩⟩ ⟨⟨b2 · b3⟩⟩ ⟨⟨b3 · b4⟩⟩ + ⟨⟨b3 · b4⟩⟩ ⟨⟨b1 · b1 · b2 · b3⟩⟩ +
   ⟨⟨b3 · b3⟩⟩ ⟨⟨b1 · b1 · b2 · b4⟩⟩ + ⟨⟨b2 · b4⟩⟩ ⟨⟨b1 · b1 · b3 · b3⟩⟩ +
   ⟨⟨b2 · b3⟩⟩ ⟨⟨b1 · b1 · b3 · b4⟩⟩ + ⟨⟨b1 · b4⟩⟩ ⟨⟨b1 · b2 · b3 · b3⟩⟩ +
   ⟨⟨b1 · b3⟩⟩ ⟨⟨b1 · b2 · b3 · b4⟩⟩ + ⟨⟨b1 · b2⟩⟩ ⟨⟨b1 · b3 · b3 · b4⟩⟩ +
   ⟨⟨b1 · b1⟩⟩ ⟨⟨b2 · b3 · b3 · b4⟩⟩, ⟨b1 · b1 · b2 · b4 · b4 · b4⟩ →
  ⟨⟨b1 · b4⟩⟩^2 ⟨⟨b2 · b4⟩⟩ + ⟨⟨b1 · b2⟩⟩ ⟨⟨b1 · b4⟩⟩ ⟨⟨b4 · b4⟩⟩ +
   ⟨⟨b1 · b1⟩⟩ ⟨⟨b2 · b4⟩⟩ ⟨⟨b4 · b4⟩⟩ + ⟨⟨b4 · b4⟩⟩ ⟨⟨b1 · b1 · b2 · b4⟩⟩ +
   ⟨⟨b2 · b4⟩⟩ ⟨⟨b1 · b1 · b4 · b4⟩⟩ + ⟨⟨b1 · b4⟩⟩ ⟨⟨b1 · b2 · b4 · b4⟩⟩ +
   ⟨⟨b1 · b2⟩⟩ ⟨⟨b1 · b4 · b4 · b4⟩⟩ + ⟨⟨b1 · b1⟩⟩ ⟨⟨b2 · b4 · b4 · b4⟩⟩,
```

Again vanishing EVs are set equal zero (only a part of the lengthy output is shown)

```
ev3tocfex3 = ev3tocfex3 /. rep1234toge /. rules1pto0cf
```

$$\{\langle\langle g^\dagger\cdot g^\dagger\cdot g^\dagger\cdot g\cdot g\cdot g\rangle\rangle \to \langle\langle g^\dagger\cdot g\rangle\rangle^3 + \langle\langle g^\dagger\cdot g\rangle\rangle\langle\langle g^\dagger\cdot g^\dagger\cdot g\cdot g\rangle\rangle,$$
$$\langle\langle g^\dagger\cdot g^\dagger\cdot g^\dagger\cdot g\cdot e\cdot e\rangle\rangle \to \langle\langle g^\dagger\cdot g\rangle\rangle\langle\langle g^\dagger\cdot g^\dagger\cdot e\cdot e\rangle\rangle,$$
$$\langle\langle g^\dagger\cdot g^\dagger\cdot g^\dagger\cdot e\cdot g\cdot e\rangle\rangle \to \langle\langle g^\dagger\cdot g\rangle\rangle\langle\langle g^\dagger\cdot g^\dagger\cdot e\cdot e\rangle\rangle,$$
$$\langle\langle g^\dagger\cdot g^\dagger\cdot g^\dagger\cdot e\cdot e\cdot g\rangle\rangle \to \langle\langle g^\dagger\cdot g\rangle\rangle\langle\langle g^\dagger\cdot g^\dagger\cdot e\cdot e\rangle\rangle, \langle\langle g^\dagger\cdot g^\dagger\cdot e^\dagger\cdot g\cdot g\cdot e\rangle\rangle \to$$
$$\langle\langle e^\dagger\cdot e\rangle\rangle\langle\langle g^\dagger\cdot g\rangle\rangle^2 + \langle\langle g^\dagger\cdot g\rangle\rangle\langle\langle g^\dagger\cdot e^\dagger\cdot g\cdot e\rangle\rangle + \langle\langle e^\dagger\cdot e\rangle\rangle\langle\langle g^\dagger\cdot g^\dagger\cdot g\cdot g\rangle\rangle,$$
$$\langle\langle g^\dagger\cdot g^\dagger\cdot e^\dagger\cdot g\cdot e\cdot g\rangle\rangle \to \langle\langle e^\dagger\cdot e\rangle\rangle\langle\langle g^\dagger\cdot g\rangle\rangle^2 + \langle\langle g^\dagger\cdot g\rangle\rangle\langle\langle g^\dagger\cdot e^\dagger\cdot g\cdot e\rangle\rangle +$$
$$\langle\langle e^\dagger\cdot e\rangle\rangle\langle\langle g^\dagger\cdot g^\dagger\cdot g\cdot g\rangle\rangle, \langle g^\dagger\cdot g^\dagger\cdot e^\dagger\cdot e\cdot g\cdot g\rangle \to$$
$$\langle\langle e^\dagger\cdot e\rangle\rangle\langle\langle g^\dagger\cdot g\rangle\rangle^2 + \langle\langle g^\dagger\cdot g\rangle\rangle\langle\langle g^\dagger\cdot e^\dagger\cdot g\cdot e\rangle\rangle + \langle\langle e^\dagger\cdot e\rangle\rangle\langle\langle g^\dagger\cdot g^\dagger\cdot g\cdot g\rangle\rangle,$$
$$\langle\langle g^\dagger\cdot g^\dagger\cdot e^\dagger\cdot e\cdot e\cdot e\rangle\rangle \to \langle\langle e^\dagger\cdot e\rangle\rangle\langle\langle g^\dagger\cdot g^\dagger\cdot e\cdot e\rangle\rangle, \langle g^\dagger\cdot e^\dagger\cdot g^\dagger\cdot g\cdot g\cdot e\rangle \to$$
$$\langle\langle e^\dagger\cdot e\rangle\rangle\langle\langle g^\dagger\cdot g\rangle\rangle^2 + \langle\langle g^\dagger\cdot g\rangle\rangle\langle\langle g^\dagger\cdot e^\dagger\cdot g\cdot e\rangle\rangle + \langle\langle e^\dagger\cdot e\rangle\rangle\langle\langle g^\dagger\cdot g^\dagger\cdot g\cdot g\rangle\rangle,$$
$$\langle\langle g^\dagger\cdot e^\dagger\cdot g^\dagger\cdot g\cdot e\cdot g\rangle\rangle \to \langle\langle e^\dagger\cdot e\rangle\rangle\langle\langle g^\dagger\cdot g\rangle\rangle^2 + \langle\langle g^\dagger\cdot g\rangle\rangle\langle\langle g^\dagger\cdot e^\dagger\cdot g\cdot e\rangle\rangle +$$
$$\langle\langle e^\dagger\cdot e\rangle\rangle\langle\langle g^\dagger\cdot g^\dagger\cdot g\cdot g\rangle\rangle, \langle g^\dagger\cdot e^\dagger\cdot g^\dagger\cdot e\cdot g\cdot g\rangle \to$$
$$\langle\langle e^\dagger\cdot e\rangle\rangle\langle\langle g^\dagger\cdot g\rangle\rangle^2 + \langle\langle g^\dagger\cdot g\rangle\rangle\langle\langle g^\dagger\cdot e^\dagger\cdot g\cdot e\rangle\rangle + \langle\langle e^\dagger\cdot e\rangle\rangle\langle\langle g^\dagger\cdot g^\dagger\cdot g\cdot g\rangle\rangle,$$
$$\langle\langle g^\dagger\cdot e^\dagger\cdot g^\dagger\cdot e\cdot e\cdot e\rangle\rangle \to \langle\langle e^\dagger\cdot e\rangle\rangle\langle\langle g^\dagger\cdot g^\dagger\cdot e\cdot e\rangle\rangle,$$
$$\langle\langle g^\dagger\cdot e^\dagger\cdot e^\dagger\cdot g\cdot g\cdot g\rangle\rangle \to \langle\langle g^\dagger\cdot g\rangle\rangle\langle\langle e^\dagger\cdot e^\dagger\cdot g\cdot g\rangle\rangle,$$
$$\langle\langle g^\dagger\cdot e^\dagger\cdot e^\dagger\cdot g\cdot e\cdot e\rangle\rangle \to \langle\langle e^\dagger\cdot e\rangle\rangle^2\langle\langle g^\dagger\cdot g\rangle\rangle + \langle\langle g^\dagger\cdot g\rangle\rangle\langle\langle e^\dagger\cdot e^\dagger\cdot e\cdot e\rangle\rangle +$$
$$\langle\langle e^\dagger\cdot e\rangle\rangle\langle\langle g^\dagger\cdot e^\dagger\cdot g\cdot e\rangle\rangle, \langle g^\dagger\cdot e^\dagger\cdot e^\dagger\cdot e\cdot g\cdot e\rangle \to$$
$$\langle\langle e^\dagger\cdot e\rangle\rangle^2\langle\langle g^\dagger\cdot g\rangle\rangle + \langle\langle g^\dagger\cdot g\rangle\rangle\langle\langle e^\dagger\cdot e^\dagger\cdot e\cdot e\rangle\rangle + \langle\langle e^\dagger\cdot e\rangle\rangle\langle\langle g^\dagger\cdot e^\dagger\cdot g\cdot e\rangle\rangle,$$
$$\langle\langle g^\dagger\cdot e^\dagger\cdot e^\dagger\cdot e\cdot g\cdot e\rangle\rangle \to \langle\langle e^\dagger\cdot e\rangle\rangle^2\langle\langle g^\dagger\cdot g\rangle\rangle + \langle\langle g^\dagger\cdot g\rangle\rangle\langle\langle e^\dagger\cdot e^\dagger\cdot e\cdot e\rangle\rangle +$$
$$\langle\langle e^\dagger\cdot e\rangle\rangle\langle\langle g^\dagger\cdot e^\dagger\cdot g\cdot e\rangle\rangle, \langle e^\dagger\cdot g^\dagger\cdot g^\dagger\cdot g\cdot g\cdot e\rangle \to$$
$$\langle\langle e^\dagger\cdot e\rangle\rangle\langle\langle g^\dagger\cdot g\rangle\rangle^2 + \langle\langle g^\dagger\cdot g\rangle\rangle\langle\langle g^\dagger\cdot e^\dagger\cdot g\cdot e\rangle\rangle + \langle\langle e^\dagger\cdot e\rangle\rangle\langle\langle g^\dagger\cdot g^\dagger\cdot g\cdot g\rangle\rangle,$$
$$\langle\langle e^\dagger\cdot g^\dagger\cdot g^\dagger\cdot g\cdot e\cdot g\rangle\rangle \to \langle\langle e^\dagger\cdot e\rangle\rangle\langle\langle g^\dagger\cdot g\rangle\rangle^2 + \langle\langle g^\dagger\cdot g\rangle\rangle\langle\langle g^\dagger\cdot e^\dagger\cdot g\cdot e\rangle\rangle +$$
$$\langle\langle e^\dagger\cdot e\rangle\rangle\langle\langle g^\dagger\cdot g^\dagger\cdot g\cdot g\rangle\rangle, \langle e^\dagger\cdot g^\dagger\cdot g^\dagger\cdot e\cdot g\cdot g\rangle \to$$
$$\langle\langle e^\dagger\cdot e\rangle\rangle\langle\langle g^\dagger\cdot g\rangle\rangle^2 + \langle\langle g^\dagger\cdot g\rangle\rangle\langle\langle g^\dagger\cdot e^\dagger\cdot g\cdot e\rangle\rangle + \langle\langle e^\dagger\cdot e\rangle\rangle\langle\langle g^\dagger\cdot g^\dagger\cdot g\cdot g\rangle\rangle,$$
$$\langle\langle e^\dagger\cdot g^\dagger\cdot g^\dagger\cdot e\cdot e\cdot e\rangle\rangle \to \langle\langle e^\dagger\cdot e\rangle\rangle\langle\langle g^\dagger\cdot g^\dagger\cdot e\cdot e\rangle\rangle,$$
$$\langle\langle e^\dagger\cdot g^\dagger\cdot e^\dagger\cdot g\cdot g\cdot g\rangle\rangle \to \langle\langle g^\dagger\cdot g\rangle\rangle\langle\langle e^\dagger\cdot e^\dagger\cdot g\cdot g\rangle\rangle, \langle e^\dagger\cdot g^\dagger\cdot e^\dagger\cdot g\cdot e\cdot e\rangle \to$$
$$\langle\langle e^\dagger\cdot e\rangle\rangle^2\langle\langle g^\dagger\cdot g\rangle\rangle + \langle\langle g^\dagger\cdot g\rangle\rangle\langle\langle e^\dagger\cdot e^\dagger\cdot e\cdot e\rangle\rangle + \langle\langle e^\dagger\cdot e\rangle\rangle\langle\langle g^\dagger\cdot e^\dagger\cdot g\cdot e\rangle\rangle,$$
$$\langle\langle e^\dagger\cdot g^\dagger\cdot e^\dagger\cdot e\cdot g\cdot e\rangle\rangle \to \langle\langle e^\dagger\cdot e\rangle\rangle^2\langle\langle g^\dagger\cdot g\rangle\rangle + \langle\langle g^\dagger\cdot g\rangle\rangle\langle\langle e^\dagger\cdot e^\dagger\cdot e\cdot e\rangle\rangle +$$
$$\langle\langle e^\dagger\cdot e\rangle\rangle\langle\langle g^\dagger\cdot e^\dagger\cdot g\cdot e\rangle\rangle, \langle e^\dagger\cdot g^\dagger\cdot e^\dagger\cdot e\cdot e\cdot g\rangle \to$$
$$\langle\langle e^\dagger\cdot e\rangle\rangle^2\langle\langle g^\dagger\cdot g\rangle\rangle + \langle\langle g^\dagger\cdot g\rangle\rangle\langle\langle e^\dagger\cdot e^\dagger\cdot e\cdot e\rangle\rangle + \langle\langle e^\dagger\cdot e\rangle\rangle\langle\langle g^\dagger\cdot e^\dagger\cdot g\cdot e\rangle\rangle,$$

and CFs of order one and two are expressed as sum of products of EVs of order two and lower (only a part of the lengthy output is shown)

```
ev3tocfex3 = Simplify[ev3tocfex3 /. cf1toev /. cf2toev]
```

$$\{\langle g^\dagger\cdot g^\dagger\cdot g^\dagger\cdot g\cdot g\cdot g\rangle \to \langle g^\dagger\cdot g\rangle\langle g^\dagger\cdot g^\dagger\cdot g\cdot g\rangle,$$
$$\langle g^\dagger\cdot g^\dagger\cdot g^\dagger\cdot g\cdot e\cdot e\rangle \to \langle g^\dagger\cdot g\rangle\langle g^\dagger\cdot g^\dagger\cdot e\cdot e\rangle,$$
$$\langle g^\dagger\cdot g^\dagger\cdot g^\dagger\cdot e\cdot g\cdot e\rangle \to \langle g^\dagger\cdot g\rangle\langle g^\dagger\cdot g^\dagger\cdot e\cdot e\rangle,$$
$$\langle g^\dagger\cdot g^\dagger\cdot g^\dagger\cdot e\cdot e\cdot g\rangle \to \langle g^\dagger\cdot g\rangle\langle g^\dagger\cdot g^\dagger\cdot e\cdot e\rangle,\ \langle g^\dagger\cdot g^\dagger\cdot e^\dagger\cdot g\cdot g\cdot e\rangle \to$$
$$\langle g^\dagger\cdot g\rangle\langle g^\dagger\cdot e^\dagger\cdot g\cdot e\rangle + \langle e^\dagger\cdot e\rangle\left(-\langle g^\dagger\cdot g\rangle^2 + \langle g^\dagger\cdot g^\dagger\cdot g\cdot g\rangle\right),$$
$$\langle g^\dagger\cdot g^\dagger\cdot e^\dagger\cdot g\cdot e\cdot g\rangle \to \langle g^\dagger\cdot g\rangle\langle g^\dagger\cdot e^\dagger\cdot g\cdot e\rangle +$$
$$\langle e^\dagger\cdot e\rangle\left(-\langle g^\dagger\cdot g\rangle^2 + \langle g^\dagger\cdot g^\dagger\cdot g\cdot g\rangle\right),\ \langle g^\dagger\cdot g^\dagger\cdot e^\dagger\cdot e\cdot g\cdot g\rangle \to$$
$$\langle g^\dagger\cdot g\rangle\langle g^\dagger\cdot e^\dagger\cdot g\cdot e\rangle + \langle e^\dagger\cdot e\rangle\left(-\langle g^\dagger\cdot g\rangle^2 + \langle g^\dagger\cdot g^\dagger\cdot g\cdot g\rangle\right),$$
$$\langle g^\dagger\cdot g^\dagger\cdot e^\dagger\cdot e\cdot e\cdot e\rangle \to \langle e^\dagger\cdot e\rangle\langle g^\dagger\cdot g^\dagger\cdot e\cdot e\rangle,\ \langle g^\dagger\cdot g^\dagger\cdot e^\dagger\cdot g\cdot e\cdot e\rangle \to$$
$$\langle g^\dagger\cdot g^\dagger\cdot e^\dagger\cdot e\cdot e\cdot e\rangle \to \langle e^\dagger\cdot e\rangle\langle g^\dagger\cdot g^\dagger\cdot e\cdot e\rangle,$$
$$\langle g^\dagger\cdot e^\dagger\cdot g^\dagger\cdot g\cdot e\cdot g\rangle \to \langle g^\dagger\cdot g\rangle\langle g^\dagger\cdot e^\dagger\cdot g\cdot e\rangle +$$
$$\langle e^\dagger\cdot e\rangle\left(-\langle g^\dagger\cdot g\rangle^2 + \langle g^\dagger\cdot g^\dagger\cdot g\cdot g\rangle\right),\ \langle g^\dagger\cdot e^\dagger\cdot g^\dagger\cdot e\cdot g\cdot g\rangle \to$$
$$\langle g^\dagger\cdot g\rangle\langle g^\dagger\cdot e^\dagger\cdot g\cdot e\rangle + \langle e^\dagger\cdot e\rangle\left(-\langle g^\dagger\cdot g\rangle^2 + \langle g^\dagger\cdot g^\dagger\cdot g\cdot g\rangle\right),$$
$$\langle g^\dagger\cdot e^\dagger\cdot g^\dagger\cdot e\cdot e\cdot e\rangle \to \langle e^\dagger\cdot e\rangle\langle g^\dagger\cdot g^\dagger\cdot e\cdot e\rangle,$$
$$\langle g^\dagger\cdot e^\dagger\cdot e^\dagger\cdot g\cdot g\cdot g\rangle \to \langle g^\dagger\cdot g\rangle\langle e^\dagger\cdot e^\dagger\cdot g\cdot g\rangle,\ \langle g^\dagger\cdot e^\dagger\cdot e^\dagger\cdot g\cdot e\cdot e\rangle \to$$
$$-\langle e^\dagger\cdot e\rangle^2\langle g^\dagger\cdot g\rangle + \langle g^\dagger\cdot g\rangle\langle e^\dagger\cdot e^\dagger\cdot e\cdot e\rangle + \langle e^\dagger\cdot e\rangle\langle g^\dagger\cdot e^\dagger\cdot g\cdot e\rangle,$$
$$\langle g^\dagger\cdot e^\dagger\cdot e^\dagger\cdot e\cdot g\cdot e\rangle \to -\langle e^\dagger\cdot e\rangle^2\langle g^\dagger\cdot g\rangle + \langle g^\dagger\cdot g\rangle\langle e^\dagger\cdot e^\dagger\cdot e\cdot e\rangle +$$
$$\langle e^\dagger\cdot e\rangle\langle g^\dagger\cdot e^\dagger\cdot g\cdot e\rangle,\ \langle g^\dagger\cdot e^\dagger\cdot e^\dagger\cdot e\cdot e\cdot g\rangle \to -\langle e^\dagger\cdot e\rangle^2\langle g^\dagger\cdot g\rangle +$$
$$\langle g^\dagger\cdot g\rangle\langle e^\dagger\cdot e^\dagger\cdot e\cdot e\rangle + \langle e^\dagger\cdot e\rangle\langle g^\dagger\cdot e^\dagger\cdot g\cdot e\rangle,\ \langle e^\dagger\cdot g^\dagger\cdot g^\dagger\cdot g\cdot g\cdot e\rangle \to$$
$$\langle g^\dagger\cdot g\rangle\langle g^\dagger\cdot e^\dagger\cdot g\cdot e\rangle + \langle e^\dagger\cdot e\rangle\left(-\langle g^\dagger\cdot g\rangle^2 + \langle g^\dagger\cdot g^\dagger\cdot g\cdot g\rangle\right),$$
$$\langle e^\dagger\cdot g^\dagger\cdot g^\dagger\cdot g\cdot e\cdot g\rangle \to \langle g^\dagger\cdot g\rangle\langle g^\dagger\cdot e^\dagger\cdot g\cdot e\rangle +$$
$$\langle e^\dagger\cdot e\rangle\left(-\langle g^\dagger\cdot g\rangle^2 + \langle g^\dagger\cdot g^\dagger\cdot g\cdot g\rangle\right),\ \langle e^\dagger\cdot g^\dagger\cdot g^\dagger\cdot e\cdot g\cdot g\rangle \to$$
$$\langle g^\dagger\cdot g\rangle\langle g^\dagger\cdot e^\dagger\cdot g\cdot e\rangle + \langle e^\dagger\cdot e\rangle\left(-\langle g^\dagger\cdot g\rangle^2 + \langle g^\dagger\cdot g^\dagger\cdot g\cdot g\rangle\right),$$
$$\langle e^\dagger\cdot g^\dagger\cdot g^\dagger\cdot e\cdot e\cdot e\rangle \to \langle e^\dagger\cdot e\rangle\langle g^\dagger\cdot g^\dagger\cdot e\cdot e\rangle,$$
$$\langle e^\dagger\cdot g^\dagger\cdot e^\dagger\cdot g\cdot g\cdot g\rangle \to \langle g^\dagger\cdot g\rangle\langle e^\dagger\cdot e^\dagger\cdot g\cdot g\rangle,\ \langle e^\dagger\cdot g^\dagger\cdot e^\dagger\cdot g\cdot e\cdot e\rangle \to$$
$$-\langle e^\dagger\cdot e\rangle^2\langle g^\dagger\cdot g\rangle + \langle g^\dagger\cdot g\rangle\langle e^\dagger\cdot e^\dagger\cdot e\cdot e\rangle + \langle e^\dagger\cdot e\rangle\langle g^\dagger\cdot e^\dagger\cdot g\cdot e\rangle,$$

A.3. Mathematica Code for the Density Matrix Formalism

Here we present some example *Mathematica* code[2] for the density matrix formalism applied to the two mode model where CFs of order three and higher have been neglected. We again restrict ourself to a special case to demonstrate the formalism and the *Mathematica* code in a clear way rather than in the most compact and rigorous form.
We first have to load the *Quantum QHD* package [115] which we use for the evaluation of the commutators occurring in the density matrix formalism.

```
Needs["Quantum`QHD`"]

ParallelNeeds["Quantum`QHD`"]
```

We further define a function for the expectation value

```
EV[A_] := ⟨A⟩
```

set our quantum objects (operators)

```
SetQuantumObject[e, g];
```

[2]The *Mathematica* code can be downloaded at http://physik.uni-graz.at/~uxh/octbec/density_matrix_formalism.nb

and enter their mutual commutator relations

```
⟦e, e⟧₋ = 0;
⟦(e)†, (e)†⟧₋ = 0;
⟦e, (e)†⟧₋ = 1;
⟦(e)†, e⟧₋ = -1;
⟦g, g⟧₋ = 0;
⟦(g)†, (g)†⟧₋ = 0;
⟦g, (g)†⟧₋ = 1;
⟦(g)†, g⟧₋ = -1;
⟦e, g⟧₋ = 0;
⟦e, (g)†⟧₋ = 0;
⟦g, e⟧₋ = 0;
⟦(g)†, e⟧₋ = 0;
⟦g, (e)†⟧₋ = 0;
⟦(e)†, g⟧₋ = 0;
⟦(e)†, (g)†⟧₋ = 0;
```

From our *Matlab* toolbox we import the initial values for the elements of the xPRDMs (only a part of the lengthy input is shown)

```
one =
  Flatten[{{{99.9836442786272`}, {3.606490106555782`*^-15},
     {3.9107172361552145`*^-15}, {0.016355721372899402`}}}];
two =
  Flatten[{{{9896.77869973996`}, {3.752553823233029`*^-13},
     {3.752553823233029`*^-13}, {-12.822221662538531`},
     {4.051758928369509`*^-13}, {1.602083844129944`},
     {1.602083844129944`}, {-2.09277040141842`*^-14},
     {4.051758928369509`*^-13}, {1.602083844129944`},
     {1.602083844129944`}, {-2.09277040141842`*^-14},
     {-12.822221662538519`}, {3.164309092529294`*^-14},
     {3.164309092529294`*^-14}, {0.017132571786893484`}}}];
three =
  Flatten[{{{969728.9849597921`}, {0.`}, {0.`}, {-1255.9715102372934`},
     {0.`}, {-1255.9715102372934`}, {-1255.9715102372934`},
     {0.`}, {0.`}, {155.32761472427188`}, {155.32761472427188`},
     {0.`}, {155.32761472427188`}, {0.`}, {0.`}, {-0.6062126914859702`},
     {0.`}, {155.32761472427188`}, {155.32761472427188`}, {0.`},
     {155.32761472427188`}, {0.`}, {0.`}, {-0.6062126914859702`},
     {-1255.9715102372936`}, {0.`}, {0.`}, {1.6766020004633213`},
     {0.`}, {1.6766020004633213`}, {1.6766020004633213`}, {0.`},
     {0.`}, {155.32761472427188`}, {155.32761472427188`}, {0.`},
     {155.32761472427188`}, {0.`}, {0.`}, {-0.6062126914859702`},
     {-1255.9715102372936`}, {0.`}, {0.`}, {1.6766020004633213`},
     {0.`}, {1.6766020004633213`}, {1.6766020004633213`}, {0.`},
     {-1255.9715102372936`}, {0.`}, {0.`}, {1.6766020004633213`},
     {0.`}, {1.6766020004633213`}, {1.6766020004633213`}, {0.`},
     {0.`}, {-0.6062126914859621`}, {-0.6062126914859621`},
     {0.`}, {-0.6062126914859621`}, {0.`}, {0.`},
     {0.002390034666290896`}}}];
```

and group them in a list (only a part of the lengthy output is shown)

```
inivallistmatlab = Flatten[{one, two, three, four, five, 3, 0.01}]
```

```
{99.9836, 3.60649×10^-15, 3.91072×10^-15, 0.0163557, 9896.78, 3.75255×10^-13,
 3.75255×10^-13, -12.8222, 4.05176×10^-13, 1.60208, 1.60208,
 -2.09277×10^-14, 4.05176×10^-13, 1.60208, 1.60208, -2.09277×10^-14,
 -12.8222, 3.16431×10^-14, 3.16431×10^-14, 0.0171326, 969 729., 0.,
 0., -1255.97, 0., -1255.97, -1255.97, 0., 0., 155.328, 155.328, 0.,
 155.328, 0., 0., -0.606213, 0., 155.328, 155.328, 0., 155.328, 0.,
 0., -0.606213, -1255.97, 0., 0., 1.6766, 0., 1.6766, 1.6766, 0.,
 0., 155.328, 155.328, 0., 155.328, 0., 0., -0.606213, -1255.97, 0.,
 0., 1.6766, 0., 1.6766, 1.6766, 0., -1255.97, 0., 0., 1.6766, 0.,
 1.6766, 1.6766, 0., 0., -0.606213, -0.606213, 0., -0.606213, 0., 0.,
 0.00239003, 9.40188×10^7, 0., 0., -121 771., 0., -121 771., -121 771., 0.,
 0., -121 771., -121 771., 0., -121 771., 0., 0., 475.215, 0., 14 904.4,
 14 904.4, 0., 14 904.4, 0., 0., -58.1502, 14 904.4, 0., 0., -58.1502,
 0., -58.1502, -58.1502, 0., 0., 14 904.4, 14 904.4, 0., 14 904.4, 0.,
 0., -58.1502, 14 904.4, 0., 0., -58.1502, 0., -58.1502, -58.1502, 0.,
 -121 771., 0., 0., 162.401, 0., 162.401, 162.401, 0., 0., 162.401,
 162.401, 0., 162.401, 0., 0., -0.652415, 0., 14 904.4, 14 904.4, 0.,
 14 904.4, 0., 0., -58.1502, 14 904.4, 0., 0., -58.1502, 0., -58.1502,
 -58.1502, 0., -121 771., 0., 0., 162.401, 0., 162.401, 162.401, 0.,
 0., 162.401, 162.401, 0., 162.401, 0., 0., -0.652415, -121 771., 0.,
 0., 162.401, 0., 162.401, 162.401, 0., 0., 162.401, 162.401, 0.,
 162.401, 0., 0., -0.652415, 0., -58.1502, -58.1502, 0., -58.1502,
 0., 0., 0.22914, -58.1502, 0., 0., 0.22914, 0., 0.22914, 0.22914, 0.,
 0., 14 904.4, 14 904.4, 0., 14 904.4, 0., 0., -58.1502, 14 904.4, 0.,
 0., -58.1502, 0., -58.1502, -58.1502, 0., -121 771., 0., 0., 162.401,
 0., 162.401, 162.401, 0., 0., 162.401, 162.401, 0., 162.401, 0.,
 0., -0.652415, -121 771., 0., 0., 162.401, 0., 162.401, 162.401, 0.,
 0., 162.401, 162.401, 0., 162.401, 0., 0., -0.652415, 0., -58.1502,
 -58.1502, 0., -58.1502, 0., 0., 0.22914, -58.1502, 0., 0., 0.22914,
 0., 0.22914, 0.22914, 0., -121 771., 0., 0., 162.401, 0., 162.401,
 162.401, 0., 0., 162.401, 162.401, 0., 162.401, 0., 0., -0.652415,
 0., -58.1502, -58.1502, 0., -58.1502, 0., 0., 0.22914, -58.1502, 0.,
 0., 0.22914, 0., 0.22914, 0.22914, 0., 0., -58.1502, -58.1502, 0.,
 -58.1502, 0., 0., 0.22914, -58.1502, 0., 0., 0.22914, 0., 0.22914,
```

we assign the initial values from this list to elements $\{y[1][0], y[2][0], ...\}$ containing the variables at time $t = 0$ of our system of equations of motion for the elements of the xPRDMs

```
inivallistmatlab =
 Flatten[Table[y[it8][0] = inivallistmatlab[[it8]],
   {it8, 1, Length[inivallistmatlab]}]]
```

$$\{y[1][0] = 99.9836,\ y[2][0] = 3.60649 \times 10^{-15},$$
$$y[3][0] = 3.91072 \times 10^{-15},\ y[4][0] = 0.0163557,\ y[5][0] = 9896.78,$$
$$y[6][0] = 3.75255 \times 10^{-13},\ y[7][0] = 3.75255 \times 10^{-13},\ y[8][0] = -12.8222,$$
$$y[9][0] = 4.05176 \times 10^{-13},\ y[10][0] = 1.60208,\ y[11][0] = 1.60208,$$
$$y[12][0] = -2.09277 \times 10^{-14},\ y[13][0] = 4.05176 \times 10^{-13},$$
$$y[14][0] = 1.60208,\ y[15][0] = 1.60208,\ y[16][0] = -2.09277 \times 10^{-14},$$
$$y[17][0] = -12.8222,\ y[18][0] = 3.16431 \times 10^{-14},\ \cdots 1331 \cdots,$$
$$y[1350][0] = 0.,\ y[1351][0] = 0.,\ y[1352][0] = -0.143372,$$
$$y[1353][0] = 0.,\ y[1354][0] = -0.143372,$$
$$y[1355][0] = -0.143372,\ y[1356][0] = 0.,\ y[1357][0] = 0.,$$
$$y[1358][0] = -0.143372,\ y[1359][0] = -0.143372,\ y[1360][0] = 0.,$$
$$y[1361][0] = -0.143372,\ y[1362][0] = 0.,\ y[1363][0] = 0.,$$
$$y[1364][0] = 0.000954621,\ y[1365][0] = 3,\ y[1366][0] = 0.01\}$$

large output | show less | show more | show all | set size limit...

Next we have to explicitly define the xPRDMs, in our case up to order three (only a part of the lengthy output is shown)

```
highestorder = 3;
```

```
rxpdm = Table[

  opscreation = {(g)†, (e)†};
opsannihilation = {g, e};

listcreation = {(g)†, (e)†};
  listannihilation = {g, e};

For[it = 1, it < itmax, it++,
    listcreation =
     Flatten[Table[listcreation[[i]] · opscreation[[j]],
       {i, 1, Length[listcreation]}, {j, 1, 2}]]]

listcreationnew = listcreation;

  listcreation = {(g)†, (e)†};

  For[it = 1, it < itmax, it++,
    listannihilation =
     Flatten[Table[listannihilation[[i]] · opsannihilation[[j]],
       {i, 1, Length[listannihilation]}, {j, 1, 2}]]]

listannihilationnew = listannihilation;

  listannihilation = {g, e};

  Table[CommutatorExpand[i · j, ReverseOrdering → True],
    {i, listcreationnew}, {j, listannihilationnew}] // MatrixForm,
  {itmax, 1, highestorder}]
```

$$\left\{\begin{pmatrix} g^\dagger \cdot g & g^\dagger \cdot e \\ e^\dagger \cdot g & e^\dagger \cdot e \end{pmatrix}, \begin{pmatrix} (g^\dagger)^2 \cdot g^2 & (g^\dagger)^2 \cdot g \cdot e & (g^\dagger)^2 \cdot g \cdot e & (g^\dagger)^2 \cdot e^2 \\ g^\dagger \cdot e^\dagger \cdot g^2 & g^\dagger \cdot e^\dagger \cdot g \cdot e & g^\dagger \cdot e^\dagger \cdot g \cdot e & g^\dagger \cdot e^\dagger \cdot e^2 \\ g^\dagger \cdot e^\dagger \cdot g^2 & g^\dagger \cdot e^\dagger \cdot g \cdot e & g^\dagger \cdot e^\dagger \cdot g \cdot e & g^\dagger \cdot e^\dagger \cdot e^2 \\ (e^\dagger)^2 \cdot g^2 & (e^\dagger)^2 \cdot g \cdot e & (e^\dagger)^2 \cdot g \cdot e & (e^\dagger)^2 \cdot e^2 \end{pmatrix}, \begin{pmatrix} (g^\dagger)^3 \cdot g^3 \\ (g^\dagger)^2 \cdot e^\dagger \cdot g^3 \\ (g^\dagger)^2 \cdot e^\dagger \cdot g^3 \\ g^\dagger \cdot (e^\dagger)^2 \cdot g^3 \\ (g^\dagger)^2 \cdot e^\dagger \cdot g^3 \\ g^\dagger \cdot (e^\dagger)^2 \cdot g^3 \\ g^\dagger \cdot (e^\dagger)^2 \cdot g^3 \\ (e^\dagger)^3 \cdot g^3 \end{pmatrix}$$

Vanishing EVs are set equal zero (only a part of the lengthy output is shown)

```
rxpdm = Table[

  opscreation = {(g)†, (e)†};
opsannihilation = {g, e};

listcreation = {(g)†, (e)†};
  listannihilation = {g, e};

For[it = 1, it < itmax, it++,
    listcreation =
     Flatten[Table[listcreation[[i]] · opscreation[[j]],
       {i, 1, Length[listcreation]}, {j, 1, 2}]]]

listcreationnew = listcreation;

  listcreation = {(g)†, (e)†};

  For[it = 1, it < itmax, it++,
    listannihilation =
     Flatten[Table[listannihilation[[i]] · opsannihilation[[j]],
       {i, 1, Length[listannihilation]}, {j, 1, 2}]]]

listannihilationnew = listannihilation;

  listannihilation = {g, e};

  Table[CommutatorExpand[i · j, ReverseOrdering → True] *
     If[EvenQ[Sum[n * Count[i · j, (g†)^n] + n * Count[i · j, g^n], {n, 1, 6}]],
      1, 0], {i, listcreationnew}, {j, listannihilationnew}] //
   MatrixForm, {itmax, 1, highestorder}]
```

$$\left\{\begin{pmatrix} g^{\dagger}\cdot g & 0 \\ 0 & e^{\dagger}\cdot e \end{pmatrix}, \begin{pmatrix} (g^{\dagger})^2\cdot g^2 & 0 & 0 & (g^{\dagger})^2\cdot e^2 \\ 0 & g^{\dagger}\cdot e^{\dagger}\cdot g\cdot e & g^{\dagger}\cdot e^{\dagger}\cdot g\cdot e & 0 \\ 0 & g^{\dagger}\cdot e^{\dagger}\cdot g\cdot e & g^{\dagger}\cdot e^{\dagger}\cdot g\cdot e & 0 \\ (e^{\dagger})^2\cdot g^2 & 0 & 0 & (e^{\dagger})^2\cdot e^2 \end{pmatrix}, \begin{pmatrix} (g^{\dagger})^3\cdot g^3 \\ 0 \\ 0 \\ g^{\dagger}\cdot (e^{\dagger})^2\cdot g^3 \\ 0 \\ g^{\dagger}\cdot (e^{\dagger})^2\cdot g^3 \\ g^{\dagger}\cdot (e^{\dagger})^2\cdot g^3 \\ 0 \end{pmatrix},$$

We take the EVs of all elements of the xPRDMs (only a part of the lengthy output is shown)

```
rxpdmevall = Table[

  opscreation = {(g)†, (e)†};
opsannihilation = {g, e};

listcreation = {(g)†, (e)†};
  listannihilation = {g, e};

For[it = 1, it < itmax, it++,
    listcreation =
     Flatten[Table[listcreation[[i]] · opscreation[[j]],
       {i, 1, Length[listcreation]}, {j, 1, 2}]]]

listcreationnew = listcreation;

  listcreation = {(g)†, (e)†};

  For[it = 1, it < itmax, it++,
    listannihilation =
     Flatten[Table[listannihilation[[i]] · opsannihilation[[j]],
       {i, 1, Length[listannihilation]}, {j, 1, 2}]]]

listannihilationnew = listannihilation;

  listannihilation = {g, e};

  Table[EV[CommutatorExpand[i · j, ReverseOrdering → True]],
    {i, listcreationnew}, {j, listannihilationnew}] // MatrixForm,
  {itmax, 1, highestorder}]
```

$$\left\{\begin{pmatrix} \langle g^\dagger \cdot g\rangle & \langle g^\dagger \cdot e\rangle \\ \langle e^\dagger \cdot g\rangle & \langle e^\dagger \cdot e\rangle \end{pmatrix},\right.$$

$$\begin{pmatrix} \langle (g^\dagger)^2 \cdot g^2\rangle & \langle (g^\dagger)^2 \cdot g \cdot e\rangle & \langle (g^\dagger)^2 \cdot g \cdot e\rangle & \langle (g^\dagger)^2 \cdot e^2\rangle \\ \langle g^\dagger \cdot e^\dagger \cdot g^2\rangle & \langle g^\dagger \cdot e^\dagger \cdot g \cdot e\rangle & \langle g^\dagger \cdot e^\dagger \cdot g \cdot e\rangle & \langle g^\dagger \cdot e^\dagger \cdot e^2\rangle \\ \langle g^\dagger \cdot e^\dagger \cdot g^2\rangle & \langle g^\dagger \cdot e^\dagger \cdot g \cdot e\rangle & \langle g^\dagger \cdot e^\dagger \cdot g \cdot e\rangle & \langle g^\dagger \cdot e^\dagger \cdot e^2\rangle \\ \langle (e^\dagger)^2 \cdot g^2\rangle & \langle (e^\dagger)^2 \cdot g \cdot e\rangle & \langle (e^\dagger)^2 \cdot g \cdot e\rangle & \langle (e^\dagger)^2 \cdot e^2\rangle \end{pmatrix},$$

$$\left.\begin{pmatrix} \langle (g^\dagger)^3 \cdot g^3\rangle \\ \langle (g^\dagger)^2 \cdot e^\dagger \cdot g^3\rangle \\ \langle (g^\dagger)^2 \cdot e^\dagger \cdot g^3\rangle \\ \langle g^\dagger \cdot (e^\dagger)^2 \cdot g^3\rangle \\ \langle (g^\dagger)^2 \cdot e^\dagger \cdot g^3\rangle \\ \langle g^\dagger \cdot (e^\dagger)^2 \cdot g^3\rangle \\ \langle g^\dagger \cdot (e^\dagger)^2 \cdot g^3\rangle \\ \langle (e^\dagger)^3 \cdot g^3\rangle \end{pmatrix}\right\}$$

and the EVs of non zero elements of the xPRDMs (only a part of the lengthy output is shown)

```
rxpdmev = Table[

  opscreation = {(g)†, (e)†};
opsannihilation = {g, e};

listcreation = {(g)†, (e)†};
  listannihilation = {g, e};

For[it = 1, it < itmax, it++,
    listcreation =
     Flatten[Table[listcreation[[i]] · opscreation[[j]],
       {i, 1, Length[listcreation]}, {j, 1, 2}]]]

listcreationnew = listcreation;

  listcreation = {(g)†, (e)†};

  For[it = 1, it < itmax, it++,
    listannihilation =
     Flatten[Table[listannihilation[[i]] · opsannihilation[[j]],
       {i, 1, Length[listannihilation]}, {j, 1, 2}]]]

listannihilationnew = listannihilation;

  listannihilation = {g, e};

  Table[EV[CommutatorExpand[i · j, ReverseOrdering → True]] *
     If[EvenQ[Sum[n * Count[i · j, (g†)^n] + n * Count[i · j, g^n], {n, 1, 6}]],
      1, 0], {i, listcreationnew}, {j, listannihilationnew}] //
   MatrixForm, {itmax, 1, highestorder}]
```

$$\left\{\begin{pmatrix} \langle g^\dagger \cdot g \rangle & 0 \\ 0 & \langle e^\dagger \cdot e \rangle \end{pmatrix},\right.$$

$$\begin{pmatrix} \langle (g^\dagger)^2 \cdot g^2 \rangle & 0 & 0 & \langle (g^\dagger)^2 \cdot e^2 \rangle \\ 0 & \langle g^\dagger \cdot e^\dagger \cdot g \cdot e \rangle & \langle g^\dagger \cdot e^\dagger \cdot g \cdot e \rangle & 0 \\ 0 & \langle g^\dagger \cdot e^\dagger \cdot g \cdot e \rangle & \langle g^\dagger \cdot e^\dagger \cdot g \cdot e \rangle & 0 \\ \langle (e^\dagger)^2 \cdot g^2 \rangle & 0 & 0 & \langle (e^\dagger)^2 \cdot e^2 \rangle \end{pmatrix},$$

$$\left.\begin{pmatrix} \langle (g^\dagger)^3 \cdot g^3 \rangle \\ 0 \\ 0 \\ \langle g^\dagger \cdot (e^\dagger)^2 \cdot g^3 \rangle \\ 0 \\ \langle g^\dagger \cdot (e^\dagger)^2 \cdot g^3 \rangle \\ \langle g^\dagger \cdot (e^\dagger)^2 \cdot g^3 \rangle \\ 0 \end{pmatrix}\right\}$$

We further define a list of the EVs of the 1PRDM and 2PRDM

```
rxpdmevshort = Table[

  opscreation = {(g)†, (e)†};
opsannihilation = {g, e};

listcreation = {(g)†, (e)†};
  listannihilation = {g, e};

For[it = 1, it < itmax, it++,
    listcreation =
     Flatten[Table[listcreation[[i]] · opscreation[[j]],
       {i, 1, Length[listcreation]}, {j, 1, 2}]]]

listcreationnew = listcreation;

  listcreation = {(g)†, (e)†};

  For[it = 1, it < itmax, it++,
    listannihilation =
     Flatten[Table[listannihilation[[i]] · opsannihilation[[j]],
       {i, 1, Length[listannihilation]}, {j, 1, 2}]]]

listannihilationnew = listannihilation;

  listannihilation = {g, e};

  Table[EV[CommutatorExpand[i · j, ReverseOrdering → True]],
    {i, listcreationnew}, {j, listannihilationnew}] // MatrixForm,
  {itmax, 1, highestorder - 1}]
```

$$\left\{\begin{pmatrix} \langle g^\dagger \cdot g\rangle & \langle g^\dagger \cdot e\rangle \\ \langle e^\dagger \cdot g\rangle & \langle e^\dagger \cdot e\rangle \end{pmatrix},\right.$$

$$\left.\begin{pmatrix} \langle (g^\dagger)^2 \cdot g^2\rangle & \langle (g^\dagger)^2 \cdot g \cdot e\rangle & \langle (g^\dagger)^2 \cdot g \cdot e\rangle & \langle (g^\dagger)^2 \cdot e^2\rangle \\ \langle g^\dagger \cdot e^\dagger \cdot g^2\rangle & \langle g^\dagger \cdot e^\dagger \cdot g \cdot e\rangle & \langle g^\dagger \cdot e^\dagger \cdot g \cdot e\rangle & \langle g^\dagger \cdot e^\dagger \cdot e^2\rangle \\ \langle g^\dagger \cdot e^\dagger \cdot g^2\rangle & \langle g^\dagger \cdot e^\dagger \cdot g \cdot e\rangle & \langle g^\dagger \cdot e^\dagger \cdot g \cdot e\rangle & \langle g^\dagger \cdot e^\dagger \cdot e^2\rangle \\ \langle (e^\dagger)^2 \cdot g^2\rangle & \langle (e^\dagger)^2 \cdot g \cdot e\rangle & \langle (e^\dagger)^2 \cdot g \cdot e\rangle & \langle (e^\dagger)^2 \cdot e^2\rangle \end{pmatrix}\right\}$$

```
rxpdmevshort = Table[

  opscreation = {(g)†, (e)†};
opsannihilation = {g, e};

listcreation = {(g)†, (e)†};
  listannihilation = {g, e};

For[it = 1, it < itmax, it++,
    listcreation =
     Flatten[Table[listcreation[[i]] · opscreation[[j]],
       {i, 1, Length[listcreation]}, {j, 1, 2}]]]

listcreationnew = listcreation;

  listcreation = {(g)†, (e)†};

  For[it = 1, it < itmax, it++,
    listannihilation =
     Flatten[Table[listannihilation[[i]] · opsannihilation[[j]],
       {i, 1, Length[listannihilation]}, {j, 1, 2}]]]

listannihilationnew = listannihilation;

  listannihilation = {g, e};

  Table[EV[CommutatorExpand[i · j, ReverseOrdering → True]] *
     If[EvenQ[Sum[n * Count[i · j, (g†)^n] + n * Count[i · j, g^n], {n, 1, 6}]],
      1, 0], {i, listcreationnew}, {j, listannihilationnew}] //
   MatrixForm, {itmax, 1, highestorder - 1}]
```

$$\left\{\begin{pmatrix} \langle g^\dagger \cdot g\rangle & 0 \\ 0 & \langle e^\dagger \cdot e\rangle \end{pmatrix},\right.$$

$$\left.\begin{pmatrix} \langle (g^\dagger)^2 \cdot g^2\rangle & 0 & 0 & \langle (g^\dagger)^2 \cdot e^2\rangle \\ 0 & \langle g^\dagger \cdot e^\dagger \cdot g \cdot e\rangle & \langle g^\dagger \cdot e^\dagger \cdot g \cdot e\rangle & 0 \\ 0 & \langle g^\dagger \cdot e^\dagger \cdot g \cdot e\rangle & \langle g^\dagger \cdot e^\dagger \cdot g \cdot e\rangle & 0 \\ \langle (e^\dagger)^2 \cdot g^2\rangle & 0 & 0 & \langle (e^\dagger)^2 \cdot e^2\rangle \end{pmatrix}\right\}$$

The two mode Hamiltonian containing the parameters δ and κ is entered

```
h = δ/2 * ((e)† · e - (g)† · g) +
    κ/2 * ((e)† · (e)† · g · g + (g)† · (g)† · e · e - (e)† · (e)† · e · e -
        (g)† · (g)† · g · g);
```

and the commutator with each element of the xPRDM is taken

```
rxpdmcom =
 ParallelTable[
  Table[Expand[CommutatorExpand[Expand[[[rxpdm[[it2, 1, i, j]], h]_],
      ReverseOrdering → True]], {i, 1, 2^it2}, {j, 1, 2^it2}] // MatrixForm,
  {it2, 1, highestorder}]
```

$$\left\{\begin{pmatrix} \kappa (g^\dagger)^2 \cdot e^2 - \kappa (e^\dagger)^2 \cdot g^2 & 0 \\ 0 & -\kappa (g^\dagger)^2 \cdot e^2 + \kappa (e^\dagger)^2 \cdot g^2 \end{pmatrix},\right.$$

$$\left.\begin{pmatrix} \\ \kappa (e^\dagger)^2 \cdot e^2 - 2\,\delta\, (e^\dagger)^2 \cdot g^2 - \end{pmatrix}\right.$$

```
rxpdmcomev =
 ParallelTable[
  Table[
    EV[Expand[CommutatorExpand[Expand[[[rxpdm[[it2, 1, i, j]], h]]-],
        ReverseOrdering → True]]], {i, 1, 2^it2}, {j, 1, 2^it2}] // MatrixForm,
  {it2, 1, 2}]
```

$$\left\{\begin{pmatrix} \kappa\left\langle \left(g^{\dagger}\right)^2\cdot e^2\right\rangle - \kappa\left\langle \left(e^{\dagger}\right)^2\cdot g^2\right\rangle & 0 \\ 0 & -\kappa\left\langle \left(g^{\dagger}\right)^2\cdot e^2\right\rangle + \kappa\left\langle \left(e^{\dagger}\right)^2\cdot g^2\right\rangle \end{pmatrix}, \begin{pmatrix} \\ \kappa\left\langle \left(e^{\dagger}\right)^2\cdot e^2\right\rangle - \end{pmatrix}\right.$$

```
rxpdmcom =
 ParallelTable[
  Table[
    EV[CommutatorExpand[
      Expand[CommutatorExpand[Expand[[[rxpdm[[it2, 1, i, j]], h]]-],
        ReverseOrdering → True]], ReverseOrdering → True]],
    {i, 1, 2^it2}, {j, 1, 2^it2}] // MatrixForm, {it2, 1, 3}]
```

$$\left\{\begin{pmatrix} \kappa\left\langle \left(g^{\dagger}\right)^2\cdot e^2\right\rangle - \kappa\left\langle \left(e^{\dagger}\right)^2\cdot g^2\right\rangle & 0 \\ 0 & -\kappa\left\langle \left(g^{\dagger}\right)^2\cdot e^2\right\rangle + \kappa\left\langle \left(e^{\dagger}\right)^2\cdot g^2\right\rangle \end{pmatrix}, \begin{pmatrix} \\ \kappa\left\langle \left(e^{\dagger}\right)^2\cdot e^2\right\rangle - \end{pmatrix}\right.$$

```
rxpdmcomev = Simplify[rxpdmcomev]
```

$$\left\{\begin{pmatrix} \kappa\left(\left\langle\left(g^{\dagger}\right)^2\cdot e^2\right\rangle-\left\langle\left(e^{\dagger}\right)^2\cdot g^2\right\rangle\right) & 0 \\ 0 & \kappa\left(-\left\langle\left(g^{\dagger}\right)^2\cdot e^2\right\rangle+\left\langle\left(e^{\dagger}\right)^2\cdot g^2\right\rangle\right)\end{pmatrix},\begin{pmatrix} \\ \kappa\left\langle\left(e^{\dagger}\right)^2\cdot e^2\right\rangle-\end{pmatrix}\right.$$

$$\text{rxpdmcomev} = \left\{\begin{pmatrix} \kappa\left(\left\langle\left(g^{\dagger}\right)^2\cdot e^2\right\rangle-\left\langle\left(e^{\dagger}\right)^2\cdot g^2\right\rangle\right) & 0 \\ 0 & \kappa\left(-\left\langle\left(g^{\dagger}\right)^2\cdot e^2\right\rangle+\left\langle\left(e^{\dagger}\right)^2\cdot g^2\right\rangle\right)\end{pmatrix},\right.$$

$$\begin{pmatrix} \kappa\left(\left\langle\left(g^{\dagger}\right)^2\cdot e^2\right\rangle-\left\langle\left(e^{\dagger}\right)^2\cdot g^2\right\rangle+2\left\langle\left(g^{\dagger}\right)^3\cdot g\cdot e^2\right\rangle- \\ 0 \\ 0 \\ \kappa\left\langle\left(e^{\dagger}\right)^2\cdot e^2\right\rangle-2\,\delta\left\langle\left(e^{\dagger}\right)^2\cdot g^2\right\rangle-\kappa\left(\left\langle\left(g^{\dagger}\right)^2\cdot g^2\right\rangle-2\left\langle\left(e^{\dagger}\right)^3\cdot g^2\cdot e\right\rangle+2\left\langle g^{\dagger}\cdot\left(e^{\dagger}\right)^2\right.\right.\end{pmatrix}$$

$$\begin{aligned}
&\left\{\left\{\left\{\kappa\left(\left\langle\left(g^{\dagger}\right)^2\cdot e^2\right\rangle-\left\langle\left(e^{\dagger}\right)^2\cdot g^2\right\rangle\right),\,0\right\},\,\left\{0,\,\kappa\left(-\left\langle\left(g^{\dagger}\right)^2\cdot e^2\right\rangle+\left\langle\left(e^{\dagger}\right)^2\cdot g^2\right\rangle\right)\right\}\right\},\\
&\left\{\left\{\kappa\left(\left\langle\left(g^{\dagger}\right)^2\cdot e^2\right\rangle-\left\langle\left(e^{\dagger}\right)^2\cdot g^2\right\rangle+2\left\langle\left(g^{\dagger}\right)^3\cdot g\cdot e^2\right\rangle-2\left\langle g^{\dagger}\cdot\left(e^{\dagger}\right)^2\cdot g^3\right\rangle\right),\,0,\,0,\right.\\
&\quad -\kappa\left\langle\left(e^{\dagger}\right)^2\cdot e^2\right\rangle+2\,\delta\left\langle\left(g^{\dagger}\right)^2\cdot e^2\right\rangle+\kappa\left(\left\langle\left(g^{\dagger}\right)^2\cdot g^2\right\rangle+2\left(\left\langle\left(g^{\dagger}\right)^3\cdot g\cdot e^2\right\rangle-\right.\right.\\
&\qquad\left.\left.\left\langle\left(g^{\dagger}\right)^2\cdot e^{\dagger}\cdot e^3\right\rangle+\left\langle\left(g^{\dagger}\right)^2\cdot e^{\dagger}\cdot g^2\cdot e\right\rangle-\left\langle g^{\dagger}\cdot\left(e^{\dagger}\right)^2\cdot g\cdot e^2\right\rangle\right)\right)\right\},\\
&\left\{0,\,\kappa\left(-\left\langle\left(e^{\dagger}\right)^3\cdot g^2\cdot e\right\rangle-\left\langle\left(g^{\dagger}\right)^3\cdot g\cdot e^2\right\rangle+\left\langle\left(g^{\dagger}\right)^2\cdot e^{\dagger}\cdot e^3\right\rangle+\left\langle g^{\dagger}\cdot\left(e^{\dagger}\right)^2\cdot g^3\right\rangle\right),\right.\\
&\quad\left.\kappa\left(-\left\langle\left(e^{\dagger}\right)^3\cdot g^2\cdot e\right\rangle-\left\langle\left(g^{\dagger}\right)^3\cdot g\cdot e^2\right\rangle+\left\langle\left(g^{\dagger}\right)^2\cdot e^{\dagger}\cdot e^3\right\rangle+\left\langle g^{\dagger}\cdot\left(e^{\dagger}\right)^2\cdot g^3\right\rangle\right),\,0\right\},\\
&\left\{0,\,\kappa\left(-\left\langle\left(e^{\dagger}\right)^3\cdot g^2\cdot e\right\rangle-\left\langle\left(g^{\dagger}\right)^3\cdot g\cdot e^2\right\rangle+\left\langle\left(g^{\dagger}\right)^2\cdot e^{\dagger}\cdot e^3\right\rangle+\left\langle g^{\dagger}\cdot\left(e^{\dagger}\right)^2\cdot g^3\right\rangle\right),\right.\\
&\quad\left.\kappa\left(-\left\langle\left(e^{\dagger}\right)^3\cdot g^2\cdot e\right\rangle-\left\langle\left(g^{\dagger}\right)^3\cdot g\cdot e^2\right\rangle+\left\langle\left(g^{\dagger}\right)^2\cdot e^{\dagger}\cdot e^3\right\rangle+\left\langle g^{\dagger}\cdot\left(e^{\dagger}\right)^2\cdot g^3\right\rangle\right),\,0\right\},\\
&\left\{\kappa\left\langle\left(e^{\dagger}\right)^2\cdot e^2\right\rangle-2\,\delta\left\langle\left(e^{\dagger}\right)^2\cdot g^2\right\rangle-\kappa\left(\left\langle\left(g^{\dagger}\right)^2\cdot g^2\right\rangle-2\left\langle\left(e^{\dagger}\right)^3\cdot g^2\cdot e\right\rangle+\right.\right.\\
&\qquad\left.2\left\langle g^{\dagger}\cdot\left(e^{\dagger}\right)^2\cdot g^3\right\rangle+2\left\langle\left(g^{\dagger}\right)^2\cdot e^{\dagger}\cdot g^2\cdot e\right\rangle-2\left\langle g^{\dagger}\cdot\left(e^{\dagger}\right)^2\cdot g\cdot e^2\right\rangle\right),\,0,\,0,\\
&\quad\left.\kappa\left(-\left\langle\left(g^{\dagger}\right)^2\cdot e^2\right\rangle+\left\langle\left(e^{\dagger}\right)^2\cdot g^2\right\rangle+2\left\langle\left(e^{\dagger}\right)^3\cdot g^2\cdot e\right\rangle-2\left\langle\left(g^{\dagger}\right)^2\cdot e^{\dagger}\cdot e^3\right\rangle\right)\right\}\right\}
\end{aligned}$$

The previously calculated approximations for EVs of order three are imported (only a part of the lengthy input is shown)

```
appcf3eq0inge = {⟨g† · g† · g† · g · g · g⟩ → ⟨g† · g⟩ ⟨g† · g† · g · g⟩,
  ⟨g† · g† · g† · g · e · e⟩ → ⟨g† · g⟩ ⟨g† · g† · e · e⟩,
  ⟨g† · g† · g† · e · g · e⟩ → ⟨g† · g⟩ ⟨g† · g† · e · e⟩,
  ⟨g† · g† · g† · e · e · g⟩ → ⟨g† · g⟩ ⟨g† · g† · e · e⟩,
  ⟨g† · g† · e† · g · g · e⟩ →
   ⟨g† · g⟩ ⟨g† · e† · g · e⟩ + ⟨e† · e⟩ (-⟨g† · g⟩^2 + ⟨g† · g† · g · g⟩),
  ⟨g† · g† · e† · g · e · g⟩ →
   ⟨g† · g⟩ ⟨g† · e† · g · e⟩ + ⟨e† · e⟩ (-⟨g† · g⟩^2 + ⟨g† · g† · g · g⟩),
  ⟨g† · g† · e† · e · g · g⟩ →
   ⟨g† · g⟩ ⟨g† · e† · g · e⟩ + ⟨e† · e⟩ (-⟨g† · g⟩^2 + ⟨g† · g† · g · g⟩),
  ⟨g† · g† · e† · e · e · e⟩ → ⟨e† · e⟩ ⟨g† · g† · e · e⟩,
  ⟨g† · e† · g† · g · g · e⟩ →
   ⟨g† · g⟩ ⟨g† · e† · g · e⟩ + ⟨e† · e⟩ (-⟨g† · g⟩^2 + ⟨g† · g† · g · g⟩),
  ⟨g† · e† · g† · g · e · g⟩ →
   ⟨g† · g⟩ ⟨g† · e† · g · e⟩ + ⟨e† · e⟩ (-⟨g† · g⟩^2 + ⟨g† · g† · g · g⟩),
  ⟨g† · e† · g† · e · g · g⟩ →
   ⟨g† · g⟩ ⟨g† · e† · g · e⟩ + ⟨e† · e⟩ (-⟨g† · g⟩^2 + ⟨g† · g† · g · g⟩),
  ⟨g† · e† · g† · e · e · e⟩ → ⟨e† · e⟩ ⟨g† · g† · e · e⟩,
  ⟨g† · e† · e† · g · g · g⟩ → ⟨g† · g⟩ ⟨e† · e† · g · g⟩,
  ⟨g† · e† · e† · g · e · e⟩ → -⟨e† · e⟩^2 ⟨g† · g⟩ + ⟨g† · g⟩ ⟨e† · e† · e · e⟩ +
    ⟨e† · e⟩ ⟨g† · e† · g · e⟩,
  ⟨g† · e† · e† · e · g · e⟩ → -⟨e† · e⟩^2 ⟨g† · g⟩ + ⟨g† · g⟩ ⟨e† · e† · e · e⟩ +
    ⟨e† · e⟩ ⟨g† · e† · g · e⟩,
  ⟨g† · e† · e† · e · e · g⟩ → -⟨e† · e⟩^2 ⟨g† · g⟩ + ⟨g† · g⟩ ⟨e† · e† · e · e⟩ +
    ⟨e† · e⟩ ⟨g† · e† · g · e⟩,
  ⟨e† · g† · g† · g · g · e⟩ →
   ⟨g† · g⟩ ⟨g† · e† · g · e⟩ + ⟨e† · e⟩ (-⟨g† · g⟩^2 + ⟨g† · g† · g · g⟩),
  ⟨e† · g† · g† · g · e · g⟩ →
   ⟨g† · g⟩ ⟨g† · e† · g · e⟩ + ⟨e† · e⟩ (-⟨g† · g⟩^2 + ⟨g† · g† · g · g⟩),
```

and applied to evaluated commutators between the Hamiltonian and the elements of the xPRDMs

```
rxpdmcomapprox = rxpdmcomev /. appcf3eq0inge
```

$$\{\{\{\kappa\left(\left\langle\left(g^{\dagger}\right)^{2}\cdot e^{2}\right\rangle-\left\langle\left(e^{\dagger}\right)^{2}\cdot g^{2}\right\rangle\right),\ 0\},\ \{0,\ \kappa\left(-\left\langle\left(g^{\dagger}\right)^{2}\cdot e^{2}\right\rangle+\left\langle\left(e^{\dagger}\right)^{2}\cdot g^{2}\right\rangle\right)\}\},$$
$$\{\{\kappa\left(\left\langle\left(g^{\dagger}\right)^{2}\cdot e^{2}\right\rangle+2\left\langle\left(g^{\dagger}\right)^{2}\cdot e^{2}\right\rangle\left\langle g^{\dagger}\cdot g\right\rangle-\left\langle\left(e^{\dagger}\right)^{2}\cdot g^{2}\right\rangle-2\left\langle g^{\dagger}\cdot g\right\rangle\left\langle\left(e^{\dagger}\right)^{2}\cdot g^{2}\right\rangle\right),$$
$$0,\ 0,\ -\kappa\left\langle\left(e^{\dagger}\right)^{2}\cdot e^{2}\right\rangle+2\,\delta\left\langle\left(g^{\dagger}\right)^{2}\cdot e^{2}\right\rangle+$$
$$\kappa\left(\left\langle\left(g^{\dagger}\right)^{2}\cdot g^{2}\right\rangle+2\left(-\left\langle e^{\dagger}\cdot e\right\rangle\left\langle\left(g^{\dagger}\right)^{2}\cdot e^{2}\right\rangle+\left\langle e^{\dagger}\cdot e\right\rangle^{2}\left\langle g^{\dagger}\cdot g\right\rangle-\left\langle\left(e^{\dagger}\right)^{2}\cdot e^{2}\right\rangle\right.\right.$$
$$\left\langle g^{\dagger}\cdot g\right\rangle+\left\langle\left(g^{\dagger}\right)^{2}\cdot e^{2}\right\rangle\left\langle g^{\dagger}\cdot g\right\rangle+\left\langle e^{\dagger}\cdot e\right\rangle\left(-\left\langle g^{\dagger}\cdot g\right\rangle^{2}+\left\langle\left(g^{\dagger}\right)^{2}\cdot g^{2}\right\rangle\right)-$$
$$\left.\left.\left\langle e^{\dagger}\cdot e\right\rangle\left\langle g^{\dagger}\cdot e^{\dagger}\cdot g\cdot e\right\rangle+\left\langle g^{\dagger}\cdot g\right\rangle\left\langle g^{\dagger}\cdot e^{\dagger}\cdot g\cdot e\right\rangle\right)\right)\},$$
$$\{0,\ \kappa\left(\left\langle e^{\dagger}\cdot e\right\rangle\left\langle\left(g^{\dagger}\right)^{2}\cdot e^{2}\right\rangle-\left\langle\left(g^{\dagger}\right)^{2}\cdot e^{2}\right\rangle\left\langle g^{\dagger}\cdot g\right\rangle-\left\langle e^{\dagger}\cdot e\right\rangle\left\langle\left(e^{\dagger}\right)^{2}\cdot g^{2}\right\rangle+\right.$$
$$\left.\left\langle g^{\dagger}\cdot g\right\rangle\left\langle\left(e^{\dagger}\right)^{2}\cdot g^{2}\right\rangle\right),$$
$$\kappa\left(\left\langle e^{\dagger}\cdot e\right\rangle\left\langle\left(g^{\dagger}\right)^{2}\cdot e^{2}\right\rangle-\left\langle\left(g^{\dagger}\right)^{2}\cdot e^{2}\right\rangle\left\langle g^{\dagger}\cdot g\right\rangle-\left\langle e^{\dagger}\cdot e\right\rangle\left\langle\left(e^{\dagger}\right)^{2}\cdot g^{2}\right\rangle+\right.$$
$$\left.\left\langle g^{\dagger}\cdot g\right\rangle\left\langle\left(e^{\dagger}\right)^{2}\cdot g^{2}\right\rangle\right),\ 0\},$$
$$\{0,\ \kappa\left(\left\langle e^{\dagger}\cdot e\right\rangle\left\langle\left(g^{\dagger}\right)^{2}\cdot e^{2}\right\rangle-\left\langle\left(g^{\dagger}\right)^{2}\cdot e^{2}\right\rangle\left\langle g^{\dagger}\cdot g\right\rangle-\right.$$
$$\left.\left\langle e^{\dagger}\cdot e\right\rangle\left\langle\left(e^{\dagger}\right)^{2}\cdot g^{2}\right\rangle+\left\langle g^{\dagger}\cdot g\right\rangle\left\langle\left(e^{\dagger}\right)^{2}\cdot g^{2}\right\rangle\right),$$
$$\kappa\left(\left\langle e^{\dagger}\cdot e\right\rangle\left\langle\left(g^{\dagger}\right)^{2}\cdot e^{2}\right\rangle-\left\langle\left(g^{\dagger}\right)^{2}\cdot e^{2}\right\rangle\left\langle g^{\dagger}\cdot g\right\rangle-\left\langle e^{\dagger}\cdot e\right\rangle\left\langle\left(e^{\dagger}\right)^{2}\cdot g^{2}\right\rangle+\right.$$
$$\left.\left\langle g^{\dagger}\cdot g\right\rangle\left\langle\left(e^{\dagger}\right)^{2}\cdot g^{2}\right\rangle\right),\ 0\},\ \{\kappa\left\langle\left(e^{\dagger}\right)^{2}\cdot e^{2}\right\rangle-2\,\delta\left\langle\left(e^{\dagger}\right)^{2}\cdot g^{2}\right\rangle-$$
$$\kappa\left(-2\left\langle e^{\dagger}\cdot e\right\rangle\left\langle\left(e^{\dagger}\right)^{2}\cdot g^{2}\right\rangle+2\left\langle g^{\dagger}\cdot g\right\rangle\left\langle\left(e^{\dagger}\right)^{2}\cdot g^{2}\right\rangle+\left\langle\left(g^{\dagger}\right)^{2}\cdot g^{2}\right\rangle-\right.$$
$$2\left(-\left\langle e^{\dagger}\cdot e\right\rangle^{2}\left\langle g^{\dagger}\cdot g\right\rangle+\left\langle\left(e^{\dagger}\right)^{2}\cdot e^{2}\right\rangle\left\langle g^{\dagger}\cdot g\right\rangle+\left\langle e^{\dagger}\cdot e\right\rangle\left\langle g^{\dagger}\cdot e^{\dagger}\cdot g\cdot e\right\rangle\right)+$$
$$\left.2\left(\left\langle e^{\dagger}\cdot e\right\rangle\left(-\left\langle g^{\dagger}\cdot g\right\rangle^{2}+\left\langle\left(g^{\dagger}\right)^{2}\cdot g^{2}\right\rangle\right)+\left\langle g^{\dagger}\cdot g\right\rangle\left\langle g^{\dagger}\cdot e^{\dagger}\cdot g\cdot e\right\rangle\right)\right),$$
$$0,\ 0,\ \kappa\left(-\left\langle\left(g^{\dagger}\right)^{2}\cdot e^{2}\right\rangle-2\left\langle e^{\dagger}\cdot e\right\rangle\left\langle\left(g^{\dagger}\right)^{2}\cdot e^{2}\right\rangle+\left\langle\left(e^{\dagger}\right)^{2}\cdot g^{2}\right\rangle+\right.$$
$$\left.2\left\langle e^{\dagger}\cdot e\right\rangle\left\langle\left(e^{\dagger}\right)^{2}\cdot g^{2}\right\rangle\right)\}\}\}$$

We check the list containing the EVs of the matrix elements of the 1PRDM and 2PRDM

```
rxpdmevlist =
 Flatten[Table[Flatten[rxpdmevall[[it3, 1]]],
   {it3, 1, Length[rxpdmevshort]}]]
```

$$\{\langle g^\dagger \cdot g\rangle, \langle g^\dagger \cdot e\rangle, \langle e^\dagger \cdot g\rangle, \langle e^\dagger \cdot e\rangle, \langle (g^\dagger)^2 \cdot g^2\rangle, \langle (g^\dagger)^2 \cdot g \cdot e\rangle,$$
$$\langle (g^\dagger)^2 \cdot g \cdot e\rangle, \langle (g^\dagger)^2 \cdot e^2\rangle, \langle g^\dagger \cdot e^\dagger \cdot g^2\rangle, \langle g^\dagger \cdot e^\dagger \cdot g \cdot e\rangle, \langle g^\dagger \cdot e^\dagger \cdot g \cdot e\rangle,$$
$$\langle g^\dagger \cdot e^\dagger \cdot e^2\rangle, \langle g^\dagger \cdot e^\dagger \cdot g^2\rangle, \langle g^\dagger \cdot e^\dagger \cdot g \cdot e\rangle, \langle g^\dagger \cdot e^\dagger \cdot g \cdot e\rangle,$$
$$\langle g^\dagger \cdot e^\dagger \cdot e^2\rangle, \langle (e^\dagger)^2 \cdot g^2\rangle, \langle (e^\dagger)^2 \cdot g \cdot e\rangle, \langle (e^\dagger)^2 \cdot g \cdot e\rangle, \langle (e^\dagger)^2 \cdot e^2\rangle\}$$

and assign functions to the parameters occurring in the two mode Hamiltonian

```
paramtoy = {δ → y[Length[rxpdmevlist] + 1][t],
   κ → y[Length[rxpdmevlist] + 2][t]}
```

$$\{\delta \to y[21][t], \kappa \to y[22][t]\}$$

as well as to the EVs of the matrix elements of the 1PRDM and 2PRDM

```
rulestoy =
 Flatten[
  {Table[rxpdmevlist[[it4]] →
     y[Flatten[Position[rxpdmevlist, rxpdmevlist[[it4]]]][[1]]][t],
    {it4, 1, Length[rxpdmevlist]}], paramtoy}]
```

$$\{\langle g^\dagger \cdot g\rangle \to y[1][t], \langle g^\dagger \cdot e\rangle \to y[2][t], \langle e^\dagger \cdot g\rangle \to y[3][t],$$
$$\langle e^\dagger \cdot e\rangle \to y[4][t], \langle (g^\dagger)^2 \cdot g^2\rangle \to y[5][t], \langle (g^\dagger)^2 \cdot g \cdot e\rangle \to y[6][t],$$
$$\langle (g^\dagger)^2 \cdot g \cdot e\rangle \to y[6][t], \langle (g^\dagger)^2 \cdot e^2\rangle \to y[8][t], \langle g^\dagger \cdot e^\dagger \cdot g^2\rangle \to y[9][t],$$
$$\langle g^\dagger \cdot e^\dagger \cdot g \cdot e\rangle \to y[10][t], \langle g^\dagger \cdot e^\dagger \cdot g \cdot e\rangle \to y[10][t],$$
$$\langle g^\dagger \cdot e^\dagger \cdot e^2\rangle \to y[12][t], \langle g^\dagger \cdot e^\dagger \cdot g^2\rangle \to y[9][t], \langle g^\dagger \cdot e^\dagger \cdot g \cdot e\rangle \to y[10][t],$$
$$\langle g^\dagger \cdot e^\dagger \cdot g \cdot e\rangle \to y[10][t], \langle g^\dagger \cdot e^\dagger \cdot e^2\rangle \to y[12][t], \langle (e^\dagger)^2 \cdot g^2\rangle \to y[17][t],$$
$$\langle (e^\dagger)^2 \cdot g \cdot e\rangle \to y[18][t], \langle (e^\dagger)^2 \cdot g \cdot e\rangle \to y[18][t],$$
$$\langle (e^\dagger)^2 \cdot e^2\rangle \to y[20][t], \delta \to y[21][t], \kappa \to y[22][t]\}$$

```
rxpdmcomapproxy = rxpdmcomapprox /. rulestoy
```

```
{{{(y[8][t] - y[17][t]) y[22][t], 0}, {0, (-y[8][t] + y[17][t]) y[22][t]}},
 {{(y[8][t] + 2 y[1][t] y[8][t] - y[17][t] - 2 y[1][t] y[17][t]) y[22][t],
    0, 0, 2 y[8][t] y[21][t] - y[20][t] y[22][t] +
     (y[5][t] + 2 (y[1][t] y[4][t]^2 + y[4][t] (-y[1][t]^2 + y[5][t]) +
           y[1][t] y[8][t] - y[4][t] y[8][t] + y[1][t] y[10][t] -
           y[4][t] y[10][t] - y[1][t] y[20][t])) y[22][t]},
  {0, (-y[1][t] y[8][t] + y[4][t] y[8][t] + y[1][t] y[17][t] -
      y[4][t] y[17][t]) y[22][t],
    (-y[1][t] y[8][t] + y[4][t] y[8][t] + y[1][t] y[17][t] -
      y[4][t] y[17][t]) y[22][t], 0},
  {0, (-y[1][t] y[8][t] + y[4][t] y[8][t] + y[1][t] y[17][t] -
      y[4][t] y[17][t]) y[22][t],
    (-y[1][t] y[8][t] + y[4][t] y[8][t] + y[1][t] y[17][t] -
      y[4][t] y[17][t]) y[22][t], 0},
  {-2 y[17][t] y[21][t] + y[20][t] y[22][t] -
     (y[5][t] + 2 (y[4][t] (-y[1][t]^2 + y[5][t]) + y[1][t] y[10][t]) +
        2 y[1][t] y[17][t] - 2 y[4][t] y[17][t] - 2 (-y[1][t] y[4][t]^2 +
           y[4][t] y[10][t] + y[1][t] y[20][t])) y[22][t], 0, 0,
    (-y[8][t] - 2 y[4][t] y[8][t] + y[17][t] + 2 y[4][t] y[17][t]) y[22][t]}}}
```

```
rxpdmcomapproxylist =
 Flatten[Table[Flatten[rxpdmcomapproxy[[it5]]],
   {it5, 1, Length[rxpdmcomapproxy]}]]
```

```
{(y[8][t] - y[17][t]) y[22][t], 0, 0, (-y[8][t] + y[17][t]) y[22][t],
 (y[8][t] + 2 y[1][t] y[8][t] - y[17][t] - 2 y[1][t] y[17][t]) y[22][t],
 0, 0, 2 y[8][t] y[21][t] - y[20][t] y[22][t] +
  (y[5][t] + 2 (y[1][t] y[4][t]^2 + y[4][t] (-y[1][t]^2 + y[5][t]) +
        y[1][t] y[8][t] - y[4][t] y[8][t] + y[1][t] y[10][t] -
        y[4][t] y[10][t] - y[1][t] y[20][t])) y[22][t], 0,
 (-y[1][t] y[8][t] + y[4][t] y[8][t] + y[1][t] y[17][t] - y[4][t] y[17][t])
  y[22][t],
 (-y[1][t] y[8][t] + y[4][t] y[8][t] + y[1][t] y[17][t] - y[4][t] y[17][t])
  y[22][t], 0, 0,
 (-y[1][t] y[8][t] + y[4][t] y[8][t] + y[1][t] y[17][t] - y[4][t] y[17][t])
  y[22][t],
 (-y[1][t] y[8][t] + y[4][t] y[8][t] + y[1][t] y[17][t] - y[4][t] y[17][t])
  y[22][t], 0, -2 y[17][t] y[21][t] + y[20][t] y[22][t] -
  (y[5][t] + 2 (y[4][t] (-y[1][t]^2 + y[5][t]) + y[1][t] y[10][t]) +
     2 y[1][t] y[17][t] - 2 y[4][t] y[17][t] -
     2 (-y[1][t] y[4][t]^2 + y[4][t] y[10][t] + y[1][t] y[20][t])) y[22][t],
 0, 0, (-y[8][t] - 2 y[4][t] y[8][t] + y[17][t] + 2 y[4][t] y[17][t])
  y[22][t]}
```

We set up the list of differential equations describing the time evolution of the EVs of the matrix elements of the 1PRDM and 2PRDM

```
deqlistexparameterexinival =
 Table[y[it6]'[t] == -i * rxpdmcomapproxylist[[it6]],
  {it6, 1, Length[rxpdmcomapproxylist]}]
```

```
{y[1]'[t] == -i (y[8][t] - y[17][t]) y[22][t], y[2]'[t] == 0,
 y[3]'[t] == 0, y[4]'[t] == -i (-y[8][t] + y[17][t]) y[22][t], y[5]'[t] ==
  -i (y[8][t] + 2 y[1][t] y[8][t] - y[17][t] - 2 y[1][t] y[17][t]) y[22][t],
 y[6]'[t] == 0, y[7]'[t] == 0,
 y[8]'[t] == -i (2 y[8][t] y[21][t] - y[20][t] y[22][t] +
      (y[5][t] + 2 (y[1][t] y[4][t]^2 + y[4][t] (-y[1][t]^2 + y[5][t]) +
            y[1][t] y[8][t] - y[4][t] y[8][t] + y[1][t] y[10][t] -
            y[4][t] y[10][t] - y[1][t] y[20][t])) y[22][t]),
 y[9]'[t] == 0, y[10]'[t] == -i (-y[1][t] y[8][t] + y[4][t] y[8][t] +
     y[1][t] y[17][t] - y[4][t] y[17][t]) y[22][t],
 y[11]'[t] == -i (-y[1][t] y[8][t] + y[4][t] y[8][t] +
     y[1][t] y[17][t] - y[4][t] y[17][t]) y[22][t],
 y[12]'[t] == 0, y[13]'[t] == 0, y[14]'[t] ==
  -i (-y[1][t] y[8][t] + y[4][t] y[8][t] +
     y[1][t] y[17][t] - y[4][t] y[17][t]) y[22][t],
 y[15]'[t] == -i (-y[1][t] y[8][t] + y[4][t] y[8][t] + y[1][t] y[17][t] -
     y[4][t] y[17][t]) y[22][t], y[16]'[t] == 0,
 y[17]'[t] == -i (-2 y[17][t] y[21][t] + y[20][t] y[22][t] -
      (y[5][t] + 2 (y[4][t] (-y[1][t]^2 + y[5][t]) + y[1][t] y[10][t]) +
         2 y[1][t] y[17][t] - 2 y[4][t] y[17][t] -
         2 (-y[1][t] y[4][t]^2 + y[4][t] y[10][t] + y[1][t] y[20][t]))
       y[22][t]), y[18]'[t] == 0, y[19]'[t] == 0, y[20]'[t] ==
  -i (-y[8][t] - 2 y[4][t] y[8][t] + y[17][t] + 2 y[4][t] y[17][t]) y[22][t]}
```

and enter the derivatives of the parameters occurring in the two mode Hamiltonian. In our case the parameter κ is constant whereas the tunnel-coupling δ between the two wells of the potential changes.

```
deqlistparameterexinival =
 {y[Length[rxpdmcomapproxylist] + 1]'[t] == 3 * Exp[-t / 10] / (-10),
  y[Length[rxpdmcomapproxylist] + 2]'[t] == 0}
```

$$\left\{y[21]'[t] == -\frac{3}{10}\, e^{-t/10},\ y[22]'[t] == 0\right\}$$

The two lists are combined

```
deqlistexinival =
 Flatten[{deqlistexparameterexinival, deqlistparameterexinival}]
```

$$
\begin{aligned}
&\{y[1]'[t] == -i\,(y[8][t] - y[17][t])\,y[22][t],\ y[2]'[t] == 0,\\
&y[3]'[t] == 0,\ y[4]'[t] == -i\,(-y[8][t] + y[17][t])\,y[22][t],\ y[5]'[t] ==\\
&\quad -i\,(y[8][t] + 2\,y[1][t]\,y[8][t] - y[17][t] - 2\,y[1][t]\,y[17][t])\,y[22][t],\\
&y[6]'[t] == 0,\ y[7]'[t] == 0,\\
&y[8]'[t] == -i\,\big(2\,y[8][t]\,y[21][t] - y[20][t]\,y[22][t] +\\
&\qquad \big(y[5][t] + 2\,\big(y[1][t]\,y[4][t]^2 + y[4][t]\,\big(-y[1][t]^2 + y[5][t]\big) +\\
&\qquad\quad y[1][t]\,y[8][t] - y[4][t]\,y[8][t] + y[1][t]\,y[10][t] -\\
&\qquad\quad y[4][t]\,y[10][t] - y[1][t]\,y[20][t]\big)\big)\,y[22][t]\big),\\
&y[9]'[t] == 0,\ y[10]'[t] == -i\,(-y[1][t]\,y[8][t] + y[4][t]\,y[8][t] +\\
&\qquad y[1][t]\,y[17][t] - y[4][t]\,y[17][t])\,y[22][t],\\
&y[11]'[t] == -i\,(-y[1][t]\,y[8][t] + y[4][t]\,y[8][t] +\\
&\qquad y[1][t]\,y[17][t] - y[4][t]\,y[17][t])\,y[22][t],\\
&y[12]'[t] == 0,\ y[13]'[t] == 0,\ y[14]'[t] ==\\
&\quad -i\,(-y[1][t]\,y[8][t] + y[4][t]\,y[8][t] +\\
&\qquad y[1][t]\,y[17][t] - y[4][t]\,y[17][t])\,y[22][t],\\
&y[15]'[t] == -i\,(-y[1][t]\,y[8][t] + y[4][t]\,y[8][t] + y[1][t]\,y[17][t] -\\
&\qquad y[4][t]\,y[17][t])\,y[22][t],\ y[16]'[t] == 0,\\
&y[17]'[t] == -i\,\big(-2\,y[17][t]\,y[21][t] + y[20][t]\,y[22][t] -\\
&\qquad \big(y[5][t] + 2\,\big(y[4][t]\,\big(-y[1][t]^2 + y[5][t]\big) + y[1][t]\,y[10][t]\big) +\\
&\qquad\quad 2\,y[1][t]\,y[17][t] - 2\,y[4][t]\,y[17][t] -\\
&\qquad\quad 2\,\big(-y[1][t]\,y[4][t]^2 + y[4][t]\,y[10][t] + y[1][t]\,y[20][t]\big)\big)\\
&\qquad y[22][t]\big),\ y[18]'[t] == 0,\ y[19]'[t] == 0,\ y[20]'[t] ==\\
&\quad -i\,(-y[8][t] - 2\,y[4][t]\,y[8][t] + y[17][t] + 2\,y[4][t]\,y[17][t])\,y[22][t],\\
&y[21]'[t] == -\frac{3}{10}\,e^{-t/10},\\
&y[22]'[t] == 0\}
\end{aligned}
$$

and a list of functions containing the matrix elements of the 1PRDM and 2PRDM as well as the functions describing the parameters is formed

```
funclist = Table[y[it7], {it7, 1, Length[rxpdmcomapproxylist] + 2}]
```

```
{y[1], y[2], y[3], y[4], y[5], y[6], y[7],
 y[8], y[9], y[10], y[11], y[12], y[13], y[14], y[15],
 y[16], y[17], y[18], y[19], y[20], y[21], y[22]}
```

The initial values of the matrix elements of the 1PRDM and 2PRDM as well as of the functions describing the parameters are imported

```
paraminival = {y[Length[rxpdmcomapproxylist] + 1][0] == 3 * Exp[-0 / 10],
   y[Length[rxpdmcomapproxylist] + 2][0] == 1/100}
```

$$\left\{y[21][0] == 3,\ y[22][0] == \frac{1}{100}\right\}$$

```
inivallistnew = Table[inivallistmatlab[[it8]], {it8, 1, 20}]
```

$$\begin{aligned}&\{y[1][0] == 99.9836,\ y[2][0] == 3.60649\times10^{-15},\ y[3][0] == 3.91072\times10^{-15},\\ &\ y[4][0] == 0.0163557,\ y[5][0] == 9896.78,\ y[6][0] == 3.75255\times10^{-13},\\ &\ y[7][0] == 3.75255\times10^{-13},\ y[8][0] == -12.8222,\ y[9][0] == 4.05176\times10^{-13},\\ &\ y[10][0] == 1.60208,\ y[11][0] == 1.60208,\ y[12][0] == -2.09277\times10^{-14},\\ &\ y[13][0] == 4.05176\times10^{-13},\ y[14][0] == 1.60208,\ y[15][0] == 1.60208,\\ &\ y[16][0] == -2.09277\times10^{-14},\ y[17][0] == -12.8222,\\ &\ y[18][0] == 3.16431\times10^{-14},\ y[19][0] == 3.16431\times10^{-14},\ y[20][0] == 0.0171326\}\end{aligned}$$

```
inivallist = Flatten[{inivallistnew, paraminival}]
```

$$\{y[1][0] = 99.9836,\ y[2][0] = 3.60649\times10^{-15},\ y[3][0] = 3.91072\times10^{-15},$$
$$y[4][0] = 0.0163557,\ y[5][0] = 9896.78,\ y[6][0] = 3.75255\times10^{-13},$$
$$y[7][0] = 3.75255\times10^{-13},\ y[8][0] = -12.8222,\ y[9][0] = 4.05176\times10^{-13},$$
$$y[10][0] = 1.60208,\ y[11][0] = 1.60208,\ y[12][0] = -2.09277\times10^{-14},$$
$$y[13][0] = 4.05176\times10^{-13},\ y[14][0] = 1.60208,\ y[15][0] = 1.60208,$$
$$y[16][0] = -2.09277\times10^{-14},\ y[17][0] = -12.8222,$$
$$y[18][0] = 3.16431\times10^{-14},\ y[19][0] = 3.16431\times10^{-14},$$
$$y[20][0] = 0.0171326,\ y[21][0] = 3,\ y[22][0] = \frac{1}{100}\}$$

and everything is now combined to one list

```
Flatten[{deqlistexinival, inivallist}]
```

$$
\begin{aligned}
&\{y[1]'[t] == -i\,(y[8][t] - y[17][t])\,y[22][t],\ y[2]'[t] == 0,\\
&y[3]'[t] == 0,\ y[4]'[t] == -i\,(-y[8][t] + y[17][t])\,y[22][t],\ y[5]'[t] ==\\
&\quad -i\,(y[8][t] + 2\,y[1][t]\,y[8][t] - y[17][t] - 2\,y[1][t]\,y[17][t])\,y[22][t],\\
&y[6]'[t] == 0,\ y[7]'[t] == 0,\\
&y[8]'[t] == -i\,\Big(2\,y[8][t]\,y[21][t] - y[20][t]\,y[22][t] +\\
&\qquad \big(y[5][t] + 2\,\big(y[1][t]\,y[4][t]^2 + y[4][t]\,\big(-y[1][t]^2 + y[5][t]\big) +\\
&\qquad\quad y[1][t]\,y[8][t] - y[4][t]\,y[8][t] + y[1][t]\,y[10][t] -\\
&\qquad\quad y[4][t]\,y[10][t] - y[1][t]\,y[20][t]\big)\big)\,y[22][t]\Big),\\
&y[9]'[t] == 0,\ y[10]'[t] == -i\,(-y[1][t]\,y[8][t] + y[4][t]\,y[8][t] +\\
&\qquad y[1][t]\,y[17][t] - y[4][t]\,y[17][t])\,y[22][t],\\
&y[11]'[t] == -i\,(-y[1][t]\,y[8][t] + y[4][t]\,y[8][t] +\\
&\qquad y[1][t]\,y[17][t] - y[4][t]\,y[17][t])\,y[22][t],\\
&y[12]'[t] == 0,\ y[13]'[t] == 0,\ y[14]'[t] ==\\
&\quad -i\,(-y[1][t]\,y[8][t] + y[4][t]\,y[8][t] +\\
&\qquad y[1][t]\,y[17][t] - y[4][t]\,y[17][t])\,y[22][t],\\
&y[15]'[t] == -i\,(-y[1][t]\,y[8][t] + y[4][t]\,y[8][t] + y[1][t]\,y[17][t] -\\
&\qquad y[4][t]\,y[17][t])\,y[22][t],\ y[16]'[t] == 0,\\
&y[17]'[t] == -i\,\Big(-2\,y[17][t]\,y[21][t] + y[20][t]\,y[22][t] -\\
&\qquad \big(y[5][t] + 2\,\big(y[4][t]\,\big(-y[1][t]^2 + y[5][t]\big) + y[1][t]\,y[10][t]\big) +\\
&\qquad\quad 2\,y[1][t]\,y[17][t] - 2\,y[4][t]\,y[17][t] -\\
&\qquad\quad 2\,\big(-y[1][t]\,y[4][t]^2 + y[4][t]\,y[10][t] + y[1][t]\,y[20][t]\big)\big)\\
&\qquad y[22][t]\Big),\ y[18]'[t] == 0,\ y[19]'[t] == 0,\ y[20]'[t] ==\\
&\quad -i\,(-y[8][t] - 2\,y[4][t]\,y[8][t] + y[17][t] + 2\,y[4][t]\,y[17][t])\,y[22][t],\\
&y[21]'[t] == -\frac{3}{10}\,e^{-t/10},\\
&y[22]'[t] == 0,\\
&y[1][0] == 99.9836,\\
&y[2][0] == 3.60649\times10^{-15},\\
&y[3][0] == 3.91072\times10^{-15},\\
&y[4][0] == 0.0163557,\\
&y[5][0] == 9896.78,\\
&y[6][0] == 3.75255\times10^{-13},\\
&y[7][0] == 3.75255\times10^{-13},\\
&y[8][0] == -12.8222,\\
&y[9][0] == 4.05176\times10^{-13},\\
&y[10][0] == 1.60208,\\
&y[11][0] == 1.60208,\\
&y[12][0] == -2.09277\times10^{-14},\\
&y[13][0] == 4.05176\times10^{-13},\\
&y[14][0] == 1.60208,\\
&y[15][0] == 1.60208,\\
&y[16][0] == -2.09277\times10^{-14},\\
&y[17][0] == -12.8222,\\
&y[18][0] == 3.16431\times10^{-14},\\
&y[19][0] == 3.16431\times10^{-14},\\
&y[20][0] == 0.0171326,\\
&y[21][0] == 3,\\
&y[22][0] == \frac{1}{100}\}
\end{aligned}
$$

We use the build in function 'NDSolve' to solve the system of differential equations for a time interval $[0, 100]$ (only a part of the lengthy output is shown)

```
sol2 = NDSolve[Flatten[{deqlistexinival, inivallist}], funclist,
  {t, 0, 100}]
```

```
{{y[1] → InterpolatingFunction[ Domain: {{0., 100.}}
                                Output: scalar ],
  y[2] → InterpolatingFunction[ Domain: {{0., 100.}}
                                Output: scalar ],
  y[3] → InterpolatingFunction[ Domain: {{0., 100.}}
                                Output: scalar ],
  y[4] → InterpolatingFunction[ Domain: {{0., 100.}}
                                Output: scalar ],
  y[5] → InterpolatingFunction[ Domain: {{0., 100.}}
                                Output: scalar ],
  y[6] → InterpolatingFunction[ Domain: {{0., 100.}}
                                Output: scalar ],
  y[7] → InterpolatingFunction[ Domain: {{0., 100.}}
                                Output: scalar ],
  y[8] → InterpolatingFunction[ Domain: {{0., 100.}}
                                Output: scalar ],
  y[9] → InterpolatingFunction[ Domain: {{0., 100.}}
                                Output: scalar ],
  y[10] → InterpolatingFunction[ Domain: {{0., 100.}}
                                 Output: scalar ],
```

and finally plot the time evolution of the matrix elements of the 1PRDM and 2PRDM (only a part of the lengthy output is shown)

```
Table[Plot[{Evaluate[Re[y[i][t] /. sol2]]}, {t, 0, 100}, PlotRange → All],
 {i, 1, 20}]
```

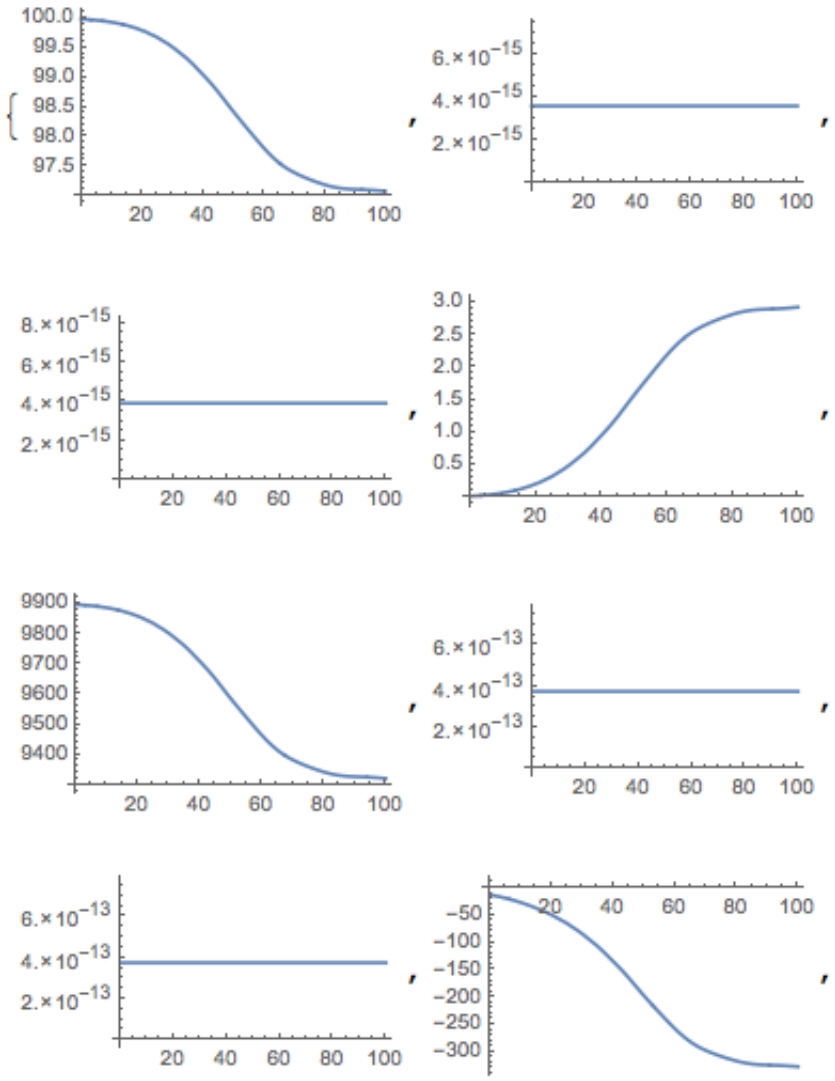

Bibliography

[1] OE Alon, AI Streltsov, and LS Cederbaum. Fragmentation of Bose-Einstein condensates in multi-well three-dimensional traps. *Physics Letters A*, 347(1):88–94, 2005.

[2] Ofir E Alon and Lorenz S Cederbaum. Pathway from condensation via fragmentation to fermionization of cold bosonic systems. *Physical Review Letters*, 95(14):140402, 2005.

[3] Ofir E Alon, Alexej I Streltsov, and Lorenz S Cederbaum. Zoo of quantum phases and excitations of cold bosonic atoms in optical lattices. *Physical Review Letters*, 95(3):030405, 2005.

[4] Ofir E Alon, Alexej I Streltsov, and Lorenz S Cederbaum. Unified view on multiconfigurational time propagation for systems consisting of identical particles. *The Journal of Chemical Physics*, 127(15):154103, 2007.

[5] Ofir E Alon, Alexej I Streltsov, and Lorenz S Cederbaum. Multiconfigurational time-dependent hartree method for bosons: Many-body dynamics of bosonic systems. *Physical Review A*, 77(3):033613, 2008.

[6] Ofir E. Alon, Alexej I. Streltsov, and Lorenz S. Cederbaum. Multiconfigurational time-dependent hartree method for bosons: Many-body dynamics of bosonic systems. *Phys. Rev. A*, 77:033613, Mar 2008.

[7] Ofir E Alon, Alexej I Streltsov, and Lorenz S Cederbaum. Build-up of coherence between initially-independent subsystems: The case of Bose-Einstein condensates. *Physics Letters A*, 373(3):301–304, 2009.

[8] Ofir E Alon, Alexej I Streltsov, and Lorenz S Cederbaum. Many-body theory for systems with particle conversion: Extending the multiconfigurational time-dependent hartree method. *Physical Review A*, 79(2):022503, 2009.

[9] Mike H Anderson, Jason R Ensher, Michael R Matthews, Carl E Wieman, and Eric A Cornell. Observation of Bose-Einstein condensation in a dilute atomic vapor. *Science*, 269(5221):198–201, 1995.

[10] Erika Andersson, Tommaso Calarco, Ron Folman, Mauritz Andersson, Björn Hessmo, and Jörg Schmiedmayer. Multimode interferometer for guided matter waves. *Physical Review Letters*, 88(10):100401, 2002.

[11] J. R. Anglin and A. Vardi. Dynamics of a two-mode Bose-Einstein condensate beyond mean-field theory. *Phys. Rev. A*, 64:013605, May 2001.

[12] F. T. Arecchi, Eric Courtens, Robert Gilmore, and Harry Thomas. Atomic coherent states in quantum optics. *Phys. Rev. A*, 6:2211–2237, Dec 1972.

[13] Wolfgang Nolting (auth.). *Grundkurs Theoretische Physik 7: Viel-Teilchen-Theorie*. Springer-Lehrbuch. Springer Berlin Heidelberg, 7., aktualisierte aufl. edition, 2009.

[14] Philipp Bader and Uwe R Fischer. Fragmented many-body ground states for scalar bosons in a single trap. *Physical Review Letters*, 103(6):060402, 2009.

[15] Vanderlei Bagnato and Daniel Kleppner. Bose-Einstein condensation in low-dimensional traps. *Physical Review A*, 44(11):7439, 1991.

[16] Michale H Beck, Andreas Jäckle, GA Worth, and H-D Meyer. The multiconfiguration time-dependent hartree (mctdh) method: a highly efficient algorithm for propagating wavepackets. *Physics reports*, 324(1):1–105, 2000.

[17] Tarik Berrada, Sandrine van Frank, Robert Bücker, Thorsten Schumm, J-F Schaff, and Jörg Schmiedmayer. Integrated mach-zehnder interferometer for Bose-Einstein condensates. *Nature Communications*, 4, 2013.

[18] F. Bloch. Nuclear induction. *Phys. Rev.*, 70:460–474, Oct 1946.

[19] Immanuel Bloch, Jean Dalibard, and Wilhelm Zwerger. Many-body physics with ultracold gases. *Reviews of Modern Physics*, 80(3):885, 2008.

[20] SN Bose. Planck'sches strahlgesetz und lichtquant hypothese. *Z. Phys*, 26(27):181–184, 1924.

[21] Bastiaan J Braams, Jerome K Percus, and Zhengji Zhao. The t1 and t2 representability conditions. *Reduced-Density-Matrix Mechanics: With Application to Many-Electron Atoms and Molecules, Volume 134*, pages 93–101, 2007.

[22] Cl C Bradley, CA Sackett, JJ Tollett, and Randall G Hulet. Evidence of Bose-Einstein condensation in an atomic gas with attractive interactions. *Physical Review Letters*, 75(9):1687, 1995.

[23] Tupac Bravo, Carlos Sabín, and Ivette Fuentes. Analog quantum simulation of gravitational waves in a Bose-Einstein condensate. *EPJ Quantum Technology*, 2(1):1–9, 2015.

[24] Robert Bücker. *Twin-atom beam generation in a one-dimensional Bose gas*. na, 2013.

[25] Robert Bücker, Tarik Berrada, Sandrine Van Frank, Jean-François Schaff, Thorsten Schumm, Jörg Schmiedmayer, Georg Jäger, Julian Grond, and Ulrich Hohenester. Vibrational state inversion of a Bose-Einstein condensate: optimal control and state tomography. *Journal of Physics B: Atomic, Molecular and Optical Physics*, 46(10):104012, 2013.

[26] Jeremie Caillat, Jürgen Zanghellini, Martin Kitzler, Othmar Koch, Wolfgang Kreuzer, and Armin Scrinzi. Correlated multielectron systems in strong laser fields: A multiconfiguration time-dependent hartree-fock approach. *Physical Review A*, 71(1):012712, 2005.

[27] LS Cederbaum and AI Streltsov. Best mean-field for condensates. *Physics Letters A*, 318(6):564–569, 2003.

[28] D. M. Ceperley. Path integrals in the theory of condensed helium. *Rev. Mod. Phys.*, 67:279–355, Apr 1995.

[29] Steven Chu. Nobel lecture: The manipulation of neutral particles. *Reviews of Modern Physics*, 70(3):685, 1998.

[30] Claude N. Cohen-Tannoudji. Nobel lecture: Manipulating atoms with photons. *Rev. Mod. Phys.*, 70:707–719, Jul 1998.

[31] Albert John Coleman and Vyacheslav I Yukalov. *Reduced density matrices: CoulsonÕs challenge*, volume 72. Springer Science & Business Media, 2000.

[32] CMS collaboration et al. Evidence for the direct decay of the 125 gev higgs boson to fermions. *Nature Physics*, 10(8):557–560, 2014.

[33] Bose-Einstein Condensation. A. griffin, dw snoke, and s. stringari. *Cambridge University Press*, 2:281, 1995.

[34] E. A. Cornell and C. E. Wieman. Nobel lecture: Bose-Einstein condensation in a dilute gas, the first 70 years and some recent experiments. *Rev. Mod. Phys.*, 74:875–893, Aug 2002.

[35] Ph Courteille, RS Freeland, DJ Heinzen, FA Van Abeelen, and BJ Verhaar. Observation of a feshbach resonance in cold atom scattering. *Physical Review Letters*, 81(1):69, 1998.

[36] Franco Dalfovo, Stefano Giorgini, Lev P Pitaevskii, and Sandro Stringari. Theory of Bose-Einstein condensation in trapped gases. *Reviews of Modern Physics*, 71(3):463, 1999.

[37] Kendall B Davis, M-O Mewes, Michael R Andrews, NJ Van Druten, DS Durfee, DM Kurn, and Wolfgang Ketterle. Bose-Einstein condensation in a gas of sodium atoms. *Physical Review Letters*, 75(22):3969, 1995.

[38] A Einstein. Zur quantentheorie des einatomigen idealen gases, sitzungsber. k. *Preuss. Akad. Wiss*, 261(3):70, 1924.

[39] A Einstein. Quantentheorie des idealen einatomigen gases. *Sitzungsber. Preuss. Akad. Wiss*, 3:18, 1925.

[40] Albert Einstein. Über gravitationswellen. *Sitzungsberichte der Königlich Preußischen Akademie der Wissenschaften (Berlin), Seite 154-167.*, 1918.

[41] J Esteve, C Gross, A Weller, S Giovanazzi, and MK Oberthaler. Squeezing and entanglement in a Bose-Einstein condensate. *Nature*, 455(7217):1216–1219, 2008.

[42] Schwabl F. *Statistical Mechanics*. Springer, 2 edition, 2006.

[43] Alexander L Fetter. Rotating trapped Bose-Einstein condensates. *Reviews of Modern Physics*, 81(2):647, 2009.

[44] Markus Fierz. über die relativistische theorie kräftefreier teilchen mit beliebigem spin. *Helvetica Physica Acta*, 12(1), 1939.

[45] Matthew PA Fisher, Peter B Weichman, G Grinstein, and Daniel S Fisher. Boson localization and the superfluid-insulator transition. *Physical Review B*, 40(1):546, 1989.

[46] Ron Folman, Peter Krüger, Donatella Cassettari, Björn Hessmo, Thomas Maier, and Jörg Schmiedmayer. Controlling cold atoms using nanofabricated surfaces: atom chips. *Physical Review Letters*, 84(20):4749, 2000.

[47] Ron Folman, Peter Krüger, Jörg Schmiedmayer, Johannes Denschlag, and Carsten Henkel. Microscopic atom optics: From wires to an atom chip. *Advances in Atomic Molecular and Optical Physics*, 48:263–356, 2002.

[48] Ron Folman, Peter Kruger, Jörg Schmiedmayer, Johannes Denschlag, and Carsten Henkel. Microscopic atom optics: from wires to an atom chip. *arXiv preprint arXiv:0805.2613*, 2008.

[49] József Fortágh and Claus Zimmermann. Magnetic microtraps for ultracold atoms. *Reviews of Modern Physics*, 79(1):235, 2007.

[50] Stefano Giorgini, Lev P Pitaevskii, and Sandro Stringari. Theory of ultracold atomic fermi gases. *Reviews of Modern Physics*, 80(4):1215, 2008.

[51] Vittorio Giovannetti, Seth Lloyd, and Lorenzo Maccone. Quantum-enhanced measurements: beating the standard quantum limit. *Science*, 306(5700):1330–1336, 2004.

[52] A Görlitz, JM Vogels, AE Leanhardt, C Raman, TL Gustavson, JR Abo-Shaeer, AP Chikkatur, S Gupta, S Inouye, T Rosenband, et al. Realization of Bose-Einstein condensates in lower dimensions. *Physical Review Letters*, 87(13):130402, 2001.

[53] Allan Griffin, David W Snoke, and Sandro Stringari. *Bose-Einstein Condensation*. Cambridge University Press, 1996.

[54] Julian Grond. Optimal quantum control of trapped Bose-Einstein condensates, 2010.

[55] Julian Grond, Ulrich Hohenester, Igor Mazets, and Jörg Schmiedmayer. Atom interferometry with trapped bose–einstein condensates: impact of atom-atom interactions. *New Journal of Physics*, 12(6):065036, 2010.

[56] Julian Grond, Ulrich Hohenester, Jörg Schmiedmayer, and Augusto Smerzi. Mach-zehnder interferometry with interacting trapped Bose-Einstein condensates. *Physical Review A*, 84(2):023619, 2011.

[57] Julian Grond, Jörg Schmiedmayer, and Ulrich Hohenester. Optimizing number squeezing when splitting a mesoscopic condensate. *Physical Review A*, 79(2):021603, 2009.

[58] Julian Grond, Jörg Schmiedmayer, and Ulrich Hohenester. Shaking the condensates: Optimal number squeezing in the dynamic splitting of a Bose-Einstein condensate. *Physica E: Low-dimensional Systems and Nanostructures*, 42(3):432–435, 2010.

[59] Julian Grond, Gregory von Winckel, Jörg Schmiedmayer, and Ulrich Hohenester. Optimal control of number squeezing in trapped Bose-Einstein condensates. *Physical Review A*, 80(5):053625, 2009.

[60] Christian Gross, Tilman Zibold, Eike Nicklas, Jerome Esteve, and Markus K Oberthaler. Nonlinear atom interferometer surpasses classical precision limit. *Nature*, 464(7292):1165–1169, 2010.

[61] EP Gross. Nuovo cimento 20 454 pitaevskii lp 1961. *Zh. Eksp. Teor. Fiz*, 40(646):1961, 1961.

[62] S Groth, P Krüger, S Wildermuth, R Folman, T Fernholz, J Schmiedmayer, D Mahalu, and I Bar-Joseph. Atom chips: Fabrication and thermal properties. *Applied Physics Letters*, 85(14):2980–2982, 2004.

[63] Paul Hamilton, Matt Jaffe, Philipp Haslinger, Quinn Simmons, Holger Müller, and Justin Khoury. Atom-interferometry constraints on dark energy. *Science*, 349(6250):849–851, 2015.

[64] Audrey Dell Hammerich, Ronnie Kosloff, and Mark A Ratner. Quantum mechanical reactive scattering by a multiconfigurational time-dependent self-consistent field (mctdscf) approach. *Chemical Physics Letters*, 171(1):97–108, 1990.

[65] W Hänsel, J Reichel, P Hommelhoff, and TW Hänsch. Trapped-atom interferometer in a magnetic microtrap. *Physical Review A*, 64(6):063607, 2001.

[66] Wolfgang Hänsel, Peter Hommelhoff, TW Hänsch, and Jakob Reichel. Bose-Einstein condensation on a microelectronic chip. *Nature*, 413(6855):498–501, 2001.

[67] Parameswaran Hariharan. *Basics of interferometry*. Academic Press, 2010.

[68] Lene Vestergaard Hau, BD Busch, Chien Liu, Zachary Dutton, Michael M Burns, and Jene A Golovchenko. Near-resonant spatial images of confined Bose-Einstein condensates in a 4-dee magnetic bottle. *Physical Review A*, 58(1):R54, 1998.

[69] S Hofferberth, I Lesanovsky, B Fischer, J Verdu, and J Schmiedmayer. Radiofrequency-dressed-state potentials for neutral atoms. *Nature Physics*, 2(10):710–716, 2006.

[70] Ulrich Hohenester. OctbecÑa matlab toolbox for optimal quantum control of Bose-Einstein condensates. *Computer Physics Communications*, 185(1):194–216, 2014.

[71] K Huang. Statistical mechanics (wiley, new york, 1987). *JL Lin and JP Wolfe, Phys. Rev. Lett.*, 31:71–1222, 1993.

[72] F Huarte-Larrañaga and U Manthe. Multidimensional quantum dynamics: Mctdh theory and applications, 2009.

[73] S Inouye, MR Andrews, J Stenger, H-J Miesner, DM Stamper-Kurn, and W Ketterle. Observation of feshbach resonances in a Bose-Einstein condensate. *Nature*, 392(6672):151–154, 1998.

[74] Georg Jäger. Optimal quantum control of Bose-Einstein condensates, 2015.

[75] Georg Jäger, Tarik Berrada, Jörg Schmiedmayer, Thorsten Schumm, and Ulrich Hohenester. Parametric-squeezing amplification of Bose-Einstein condensates. *Physical Review A*, 92(5):053632, 2015.

[76] Dieter Jaksch, Ch Bruder, Juan Ignacio Cirac, Crispin W Gardiner, and Peter Zoller. Cold bosonic atoms in optical lattices. *Physical Review Letters*, 81(15):3108, 1998.

[77] Dieter Jaksch and Peter Zoller. The cold atom hubbard toolbox. *Annals of Physics*, 315(1):52–79, 2005.

[78] Juha Javanainen and Misha Yu. Ivanov. Splitting a trap containing a Bose-Einstein condensate: Atom number fluctuations. *Phys. Rev. A*, 60:2351–2359, Sep 1999.

[79] GR Jin and CK Law. Relationship between spin squeezing and single-particle coherence in two-component Bose-Einstein condensates with josephson coupling. *Physical Review A*, 78(6):063620, 2008.

[80] G-B Jo, Y Shin, S Will, TA Pasquini, M Saba, W Ketterle, DE Pritchard, M Vengalattore, and M Prentiss. Long phase coherence time and number squeezing of two Bose-Einstein condensates on an atom chip. *Physical Review Letters*, 98(3):030407, 2007.

[81] Joshua Jortner and Alberte Pullman. *Large Finite Systems: Proceedings of the Twentieth Jerusalem Symposium on Quantum Chemistry and Biochemistry Held in Jerusalem, Israel, May 11–14, 1987*, volume 20. Springer Science & Business Media, 2012.

[82] Tsuyoshi Kato and Hirohiko Kono. Time-dependent multiconfiguration theory for electronic dynamics of molecules in an intense laser field. *Chemical Physics Letters*, 392(4):533–540, 2004.

[83] J. James Kelly. Ideal quantum gases - from statistical physics using mathematica, 2002.

[84] Wolfgang Ketterle. Experimental studies of Bose-Einstein condensation. *Phys. Today*, 52(12):30–35, 1999.

[85] Wolfgang Ketterle. Nobel lecture: When atoms behave as waves: Bose-Einstein condensation and the atom laser. *Reviews of Modern Physics*, 74(4):1131, 2002.

[86] Markus Kitzler, Jürgen Zanghellini, Ch Jungreuthmayer, M Smits, Armin Scrinzi, and Thomas Brabec. Ionization dynamics of extended multielectron systems. *Physical Review A*, 70(4):041401, 2004.

[87] Peter Kramer and Marcos Saraceno. Geometry of the time-dependent variational principle in quantum mechanics. In *Geometry of the Time-Dependent Variational Principle in Quantum Mechanics*, volume 140, 1981.

[88] Kenneth C Kulander. *Time-dependent methods for quantum dynamics*, volume 63. North Holland, 1991.

[89] Anthony J Leggett. Bose-Einstein condensation in the alkali gases: Some fundamental concepts. *Reviews of Modern Physics*, 73(2):307, 2001.

[90] Anthony J. Leggett. Bose-Einstein condensation in the alkali gases: Some fundamental concepts. *Rev. Mod. Phys.*, 73:307–356, Apr 2001.

[91] Anthony J Leggett and Fernando Sols. On the concept of spontaneously broken gauge symmetry in condensed matter physics. *Foundations of physics*, 21(3):353–364, 1991.

[92] I Lesanovsky, S Hofferberth, J Schmiedmayer, and Peter Schmelcher. Manipulation of ultracold atoms in dressed adiabatic radio-frequency potentials. *Physical Review A*, 74(3):033619, 2006.

[93] I Lesanovsky, T Schumm, S Hofferberth, L Mauritz Andersson, P Krüger, and J Schmiedmayer. Adiabatic radio-frequency potentials for the coherent manipulation of matter waves. *Physical Review A*, 73(3):033619, 2006.

[94] H. A. M. Leymann, A. Foerster, and J. Wiersig. Expectation value based equation-of-motion approach for open quantum systems: A general formalism. *Phys. Rev. B*, 89:085308, Feb 2014.

[95] Elliott H Lieb and Werner Liniger. Exact analysis of an interacting bose gas. i. the general solution and the ground state. *Physical Review*, 130(4):1605, 1963.

[96] Elliott H Lieb, Robert Seiringer, Jan Philip Solovej, and Jakob Yngvason. *The mathematics of the Bose gas and its condensation*, volume 34. Springer Science & Business Media, 2005.

[97] Elliott H Lieb, Robert Seiringer, and Jakob Yngvason. One-dimensional bosons in three-dimensional traps. In *The Stability of Matter: From Atoms to Stars*, pages 909–912. Springer, 2003.

[98] Axel UJ Lode, Alexej I Streltsov, Ofir E Alon, Hans-Dieter Meyer, and Lorenz S Cederbaum. Exact decay and tunnelling dynamics of interacting few-boson systems. *Journal of Physics B: Atomic, Molecular and Optical Physics*, 42(4):044018, 2009.

[99] F London. Nature. *London*, 141:643, 1938.

[100] Fritz London. On the Bose-Einstein condensation. *Physical Review*, 54(11):947, 1938.

[101] L Mach. Ueber einen interferenzrefraktor. *Zeitschrift für Instrumentenkunde*, 12:89–93, 1892.

[102] Nancy Makri and William H Miller. Time-dependent self-consistent field (td-scf) approximation for a reaction coordinate coupled to a harmonic bath: Single and multiple configuration treatments. *The Journal of Chemical Physics*, 87(10):5781–5787, 1987.

[103] Uwe Manthe, H-D Meyer, and Lorenz S Cederbaum. Wave-packet dynamics within the multiconfiguration hartree framework: General aspects and application to nocl. *The Journal of chemical physics*, 97(5):3199–3213, 1992.

[104] Christian Matthies, Sascha Zöllner, Hans-Dieter Meyer, and Peter Schmelcher. Quantum dynamics of two bosons in an anharmonic trap: Collective versus internal excitations. *Physical Review A*, 76(2):023602, 2007.

[105] C. Menotti, J. R. Anglin, J. I. Cirac, and P. Zoller. Dynamic splitting of a Bose-Einstein condensate. *Phys. Rev. A*, 63:023601, Jan 2001.

[106] H.-D. Meyer, U. Manthe, and L.S. Cederbaum. The multi-configurational time-dependent hartree approach. *Chemical Physics Letters*, 165(1):73 – 78, 1990.

[107] H-D Meyer, Uwe Manthe, and Lorenz S Cederbaum. The multi-configurational time-dependent hartree approach. *Chemical Physics Letters*, 165(1):73–78, 1990.

[108] Hans-Dieter Meyer, Fabien Gatti, and Graham A. Worth. *The Road to MCTDH*, pages 9–15. Wiley-VCH Verlag GmbH & Co. KGaA, 2009.

[109] G. J. Milburn, J. Corney, E. M. Wright, and D. F. Walls. Quantum dynamics of an atomic Bose-Einstein condensate in a double-well potential. *Phys. Rev. A*, 55:4318–4324, Jun 1997.

[110] GJ Milburn, J Corney, EM Wright, and DF Walls. Quantum dynamics of an atomic Bose-Einstein condensate in a double-well potential. *Physical Review A*, 55(6):4318, 1997.

[111] C. Monroe, E. Cornell, and C. Wieman. Proceedings of the international school of physics Òenrico fermiÓ, course cvxiii, laser manipulation of atoms and ions, 1992.

[112] C. Monroe, W. Swann, H. Robinson, and C. Wieman. Very cold trapped atoms in a vapor cell. *Phys. Rev. Lett.*, 65:1571–1574, Sep 1990.

[113] Oliver Morsch and Markus Oberthaler. Dynamics of Bose-Einstein condensates in optical lattices. *Reviews of Modern Physics*, 78(1):179, 2006.

[114] Erich J Mueller, Tin-Lun Ho, Masahito Ueda, and Gordon Baym. Fragmentation of Bose-Einstein condensates. *Physical Review A*, 74(3):033612, 2006.

[115] JL Gómez Muñoz and F Delgado. Quantum: A wolfram mathematica add-on for dirac bra-ket notation, non-commutative algebra, and simulation of quantum computing circuits. In *Journal of Physics: Conference Series*, volume 698, page 012019. IOP Publishing, 2016.

[116] Bogoliubov N N. On the theory of superfluidity. *J. Phys. USSR*, 11(23), 1947.

[117] M Nest, T Klamroth, and P Saalfrank. The multiconfiguration time-dependent hartree-fock method for quantum chemical calculations. *The Journal of Chemical Physics*, 122(12):124102, 2005.

[118] M Nest and H-D Meyer. Dissipative quantum dynamics of anharmonic oscillators with the multiconfiguration time-dependent hartree method. *The Journal of Chemical Physics*, 119(1):24–33, 2003.

[119] Mathias Nest. Quantum carpets and correlated dynamics of several fermions. *Physical Review A*, 73(2):023613, 2006.

[120] Ph Nozieres and D Saint James. Particle vs. pair condensation in attractive bose liquids. *Journal de Physique*, 43(7):1133–1148, 1982.

[121] The Royal Swedish Academy of Sciences. Information for the public, the nobel prize in physics 2001, 2001.

[122] Herwig Ott, József Fortagh, G Schlotterbeck, A Grossmann, and C Zimmermann. Bose-Einstein condensation in a surface microtrap. *Physical Review Letters*, 87(23):230401, 2001.

[123] W. Pauli. The connection between spin and statistics. *Phys. Rev.*, 58:716–722, Oct 1940.

[124] O Penrose and L Onsager. Phy. rev, 104, 576 (1956), cn yang. *Rev. Mod. Phys*, 34:694, 1962.

[125] Oliver Penrose and Lars Onsager. Bose-Einstein condensation and liquid helium. *Physical Review*, 104(3):576, 1956.

[126] Oliver Penrose and Lars Onsager. Bose-Einstein condensation and liquid helium. *Phys. Rev.*, 104:576–584, Nov 1956.

[127] Christopher J Pethick and Henrik Smith. *Bose-Einstein condensation in dilute gases*. Cambridge university press, 2002.

[128] DS Petrov, GV Shlyapnikov, and JTM Walraven. Regimes of quantum degeneracy in trapped 1d gases. *Physical Review Letters*, 85(18):3745, 2000.

[129] L Pezzé, LA Collins, A Smerzi, GP Berman, and AR Bishop. Sub-shot-noise phase sensitivity with a Bose-Einstein condensate mach-zehnder interferometer. *Physical Review A*, 72(4):043612, 2005.

[130] L. Pezzé, A. Smerzi, G. P. Berman, A. R. Bishop, and L. A. Collins. Nonlinear beam splitter in Bose-Einstein-condensate interferometers. *Phys. Rev. A*, 74:033610, Sep 2006.

[131] William D. Phillips. Nobel lecture: Laser cooling and trapping of neutral atoms. *Rev. Mod. Phys.*, 70:721–741, Jul 1998.

[132] L Pitaevskii and S Stringari. Thermal vs quantum decoherence in double well trapped Bose-Einstein condensates. *Physical Review Letters*, 87(18):180402, 2001.

[133] LP Pitaevskii. Vortex lines in an imperfect bose gas. *Sov. Phys. JETP*, 13(2):451–454, 1961.

[134] LP Pitaevskii and Zh Eksp. *Teor. Fiz*, 40:646, 1961.

[135] Uffe Vestergaard Poulsen. *Bose-Einstein Condensates: Excursions Beyond the Mean Field*. Department of Physics and Astronomy, University of Aarhus, 2002.

[136] David E. Pritchard. Cooling neutral atoms in a magnetic trap for precision spectroscopy. *Phys. Rev. Lett.*, 51:1336–1339, Oct 1983.

[137] Jakob Reichel and Joseph H Thywissen. Using magnetic chip traps to study tonks-girardeau quantum gases. In *Journal de Physique IV (Proceedings)*, volume 116, pages 265–274. EDP sciences, 2004.

[138] G Rosi, F Sorrentino, L Cacciapuoti, M Prevedelli, and GM Tino. Precision measurement of the newtonian gravitational constant using cold atoms. *arXiv preprint arXiv:1412.7954*, 2014.

[139] Kaspar Sakmann. Exact quantum dynamics of a bosonic josephson junction. In *Many-Body Schrödinger Dynamics of Bose-Einstein Condensates*, pages 65–80. Springer, 2011.

[140] Kaspar Sakmann. *Many-Body Schrödinger Dynamics of Bose-Einstein Condensates*. Springer Science & Business Media, 2011.

[141] Kaspar Sakmann, Alexej I Streltsov, Ofir E Alon, and Lorenz S Cederbaum. Reduced density matrices and coherence of trapped interacting bosons. *Physical Review A*, 78(2):023615, 2008.

[142] Kaspar Sakmann, Alexej I. Streltsov, Ofir E. Alon, and Lorenz S. Cederbaum. Reduced density matrices and coherence of trapped interacting bosons. *Phys. Rev. A*, 78:023615, Aug 2008.

[143] Kaspar Sakmann, Alexej I Streltsov, Ofir E Alon, and Lorenz S Cederbaum. Quantum dynamics of attractive versus repulsive bosonic josephson junctions: Bose-hubbard and full-hamiltonian results. *Physical Review A*, 82(1):013620, 2010.

[144] Fukashi Sasaki. Eigenvalues of fermion density matrices. *Physical Review*, 138(5B):B1338, 1965.

[145] Joerge Schmiedmayer. A wire trap for neutral atoms. *Applied Physics B*, 60(2-3):169–179, 1995.

[146] T Schumm, S Hofferberth, L Mauritz Andersson, S Wildermuth, S Groth, I Bar-Joseph, J Schmiedmayer, and P Krüger. Matter-wave interferometry in a double well on an atom chip. *Nature physics*, 1(1):57–62, 2005.

[147] F. Schwabl, R. Hilton, and A. Lahee. *Advanced Quantum Mechanics*. Springer Berlin Heidelberg, 2010.

[148] Julian Schwinger. The theory of quantized fields. i. *Phys. Rev.*, 82:914–927, Jun 1951.

[149] TR Sosnick, WM Snow, and PE Sokol. Deep-inelastic neutron scattering from liquid he 4. *Physical Review B*, 41(16):11185, 1990.

[150] RW Spekkens and JE Sipe. Spatial fragmentation of a Bose-Einstein condensate in a double-well potential. *Physical Review A*, 59(5):3868, 1999.

[151] Alexej I Streltsov, Ofir E Alon, and Lorenz S Cederbaum. General variational many-body theory with complete self-consistency for trapped bosonic systems. *Physical Review A*, 73(6):063626, 2006.

[152] Alexej I Streltsov, Ofir E Alon, and Lorenz S Cederbaum. Role of excited states in the splitting of a trapped interacting Bose-Einstein condensate by a time-dependent barrier. *Physical Review Letters*, 99(3):030402, 2007.

[153] Alexej I. Streltsov, Ofir E. Alon, and Lorenz S. Cederbaum. Role of excited states in the splitting of a trapped interacting Bose-Einstein condensate by a time-dependent barrier. *Phys. Rev. Lett.*, 99:030402, Jul 2007.

[154] Alexej I Streltsov, Ofir E Alon, and Lorenz S Cederbaum. Formation and dynamics of many-boson fragmented states in one-dimensional attractive ultracold gases. *Physical Review Letters*, 100(13):130401, 2008.

[155] Alexej I Streltsov, Ofir E Alon, and Lorenz S Cederbaum. Scattering of an attractive Bose-Einstein condensate from a barrier: Formation of quantum superposition states. *Physical Review A*, 80(4):043616, 2009.

[156] Alexej I Streltsov, Ofir E Alon, and Lorenz S Cederbaum. General mapping for bosonic and fermionic operators in fock space. *Physical Review A*, 81(2):022124, 2010.

[157] Alexej I Streltsov, Lorenz S Cederbaum, and Nimrod Moiseyev. Ground-state fragmentation of repulsive Bose-Einstein condensates in double-trap potentials. *Physical Review A*, 70(5):053607, 2004.

[158] Alexej I Streltsov, Kaspar Sakmann, Ofir E Alon, and Lorenz S Cederbaum. Accurate multi-boson long-time dynamics in triple-well periodic traps. *Physical Review A*, 83(4):043604, 2011.

[159] Joachim Ullrich and Viacheslav Shevelko. *Many-particle quantum dynamics in atomic and molecular fragmentation*, volume 35. Springer Science & Business Media, 2013.

[160] Henning Vahlbruch, Simon Chelkowski, Boris Hage, Alexander Franzen, Karsten Danzmann, and Roman Schnabel. Demonstration of a squeezed-light-enhanced power- and signal-recycled michelson interferometer. *Phys. Rev. Lett.*, 95:211102, Nov 2005.

[161] Sandrine van Frank, Antonio Negretti, Tarik Berrada, Robert Bücker, Simone Montangero, J-F Schaff, Thorsten Schumm, Tommaso Calarco, and Jörg Schmiedmayer. Interferometry with non-classical motional states of a Bose-Einstein condensate. *Nature Communications*, 5, 2014.

[162] Rob van Harrevelt and Uwe Manthe. Multidimensional time-dependent discrete variable representations in multiconfiguration hartree calculations. *The Journal of Chemical Physics*, 123(6):064106, 2005.

[163] R.K. Verma. *Wave Optics*. Discovery Publishing House Pvt. Limited, 2008.

[164] Ying-Ju Wang, Dana Z Anderson, Victor M Bright, Eric A Cornell, Quentin Diot, Tetsuo Kishimoto, Mara Prentiss, RA Saravanan, Stephen R Segal, and Saijun Wu. Atom michelson interferometer on a chip using a Bose-Einstein condensate. *Physical Review Letters*, 94(9):090405, 2005.

[165] JD Weinstein and KG Libbrecht. Microscopic magnetic traps for neutral atoms. *Physical Review A*, 52(5):4004, 1995.

[166] DJ Wineland, JJ Bollinger, WM Itano, and DJ Heinzen. Squeezed atomic states and projection noise in spectroscopy. *Physical Review A*, 50(1):67, 1994.

[167] GA Worth, H-D Meyer, and LS Cederbaum. Relaxation of a system with a conical intersection coupled to a bath: A benchmark 24-dimensional wave packet study treating the environment explicitly. *The Journal of Chemical Physics*, 109(9):3518–3529, 1998.

[168] Jürgen Zanghellini, Markus Kitzler, Christian Fabian, Thomas Brabec, and Armin Scrinzi. An mctdhf approach to multielectron dynamics in laser fields. *Laser Physics*, 13(8):1064–1068, 2003.

[169] L Zehnder. Ein neuer interferenzrefraktor. *Zeitschrift für Instrumentenkunde*, 11:275–285, 1891.

[170] Sascha Zöllner, Hans-Dieter Meyer, and Peter Schmelcher. Correlations in ultracold trapped few-boson systems: transition from condensation to fermionization. *Physical Review A*, 74(6):063611, 2006.

[171] Sascha Zöllner, Hans-Dieter Meyer, and Peter Schmelcher. Ultracold few-boson systems in a double-well trap. *Physical Review A*, 74(5):053612, 2006.

[172] Sascha Zöllner, Hans-Dieter Meyer, and Peter Schmelcher. Excitations of few-boson systems in one-dimensional harmonic and double wells. *Physical Review A*, 75(4):043608, 2007.

[173] Sascha Zöllner, Hans-Dieter Meyer, and Peter Schmelcher. Composite fermionization of one-dimensional bose-bose mixtures. *Physical Review A*, 78(1):013629, 2008.

[174] Sascha Zöllner, Hans-Dieter Meyer, and Peter Schmelcher. Few-boson dynamics in double wells: from single-atom to correlated pair tunneling. *Physical Review Letters*, 100(4):040401, 2008.

[175] Sascha Zöllner, Hans-Dieter Meyer, and Peter Schmelcher. Tunneling dynamics of a few bosons in a double well. *Physical Review A*, 78(1):013621, 2008.

List of Equations

1. Fermi-Dirac Distribution 9
2. Bose-Einstein Distribution 9
3. Occupancy Functions Limit 9
4. Bose-Einstein Distribution 16
5. Particle Number 16
6. Occupation Number Minimum 17
7. Particle Number in Continuous Approximation 17
8. Zeeman Hamiltonian 23
9. Static Magnetic Field 26
10. Time Dependent Field 26
11. Adiabatic Potentials along x 26
12. Heisenberg's Uncertainty Relation 33
13. Binomial State Uncertainties 34
14. Number Squeezing ξ_n 34
15. Phase Squeezing ξ_ϕ 35
16. Coherence Factor α 37
17. Spin Squeezing Factor ξ_S 37
18. Spin Squeezing Factor ξ_S and Phase Varriance $\Delta\phi$ for Binomial State . . 37

19. Two Parameter Optimization Method 39
20. Decomposition of the Field Operator into a *Left*- and *Right*- Mode 39
21. Two Mode Hamiltonian 2nd Quantized Form in LR-Basis 39
22. Tunnel Coupling 40
23. Nonlinear Interaction / Charging Energy 40
24. Pseudospin Operators 40
25. Hamiltonian with Pseudospin Operators 41
26. Model Hamiltonian with n and ϕ 41
27. Simplified Model Hamiltonian with n and ϕ 41
28. Hamiltonian of Harmonic Oscillator 42
29. Commutator of ϕ and n 42
30. N-fold product state of N two-level systems 44
31. Mean Value N-fold Product State 44
32. Variance N-fold Product State 45
33. Projection of Output-State on Input-State 45
34. Input-State and Output-State 46
35. Projection of Output-State on Input-State after Phase-Shift 46
36. Phase Sensitivity 46
37. Entangled State 46
38. Measurement Probability 47
39. Heisenberg Limited Measurement 48
40. Bosonic Commutation Relations 50
41. Orthonormality of Orbitals 50
42. Expansion of the Field Operator 51

43. Bosonic Commutation Relations . . . 51
44. Closure Relation . . . 51
45. Many-Body Schrödinger Equation . . . 52
46. Exact Hamiltonian . . . 52
47. Interaction Parameter of Contact Potential . . . 53
48. Exact Hamiltonian in 2nd Quantization . . . 53
49. Equivalent Exact Hamiltonian in 2nd Quantization . . . 53
50. Matrix Elements for Exact Hamiltonian in 2nd Quantization . . . 54
51. Langrangian . . . 55
52. Normalized Wave Function . . . 55
53. Principle of Least Action . . . 55
54. Action Functional . . . 56
55. Schrödinger Equation . . . 56
56. Permanents for N bosons in M orbitals . . . 57
57. Occupation Number Vector $\vec{n}$ . . . 57
58. Particle Number N . . . 57
59. Ansatz for Many-Body Bosonic Wave Function . . . 58
60. Finite Size Representations of the Field Operator $\hat{\Psi}_M$ . . . 58
61. Closure Relation for Finite Size Representations . . . 58
62. p-Particle Reduced Densities . . . 61
63. Diagonal of p-Particle Reduced Densities . . . 61
64. Bosonic Commutation Relations . . . 62
65. p-Particle Reduced Densities . . . 62
66. pth order RDM $\rho^{(p)}$ . . . 62

67. Restriction on Density Matrix Eigenvalues 63
68. Largest Eigenvalue of Density Matrix 63
69. 1-Particle Reduced Density 63
70. 1-Particle Reduced Density 64
71. 1-Particle Reduced Density 64
72. One-Body Density Matrix Elements 64
73. 2-Particle Reduced Density 64
74. 2-Particle Reduced Density 65
75. 2-Particle Reduced Density 65
76. Two-Body Density Matrix Elements 65
77. Largest Eigenvalue of 1st and 2nd order RDM 66
78. Condensed Bosons System Condition 67
79. Fully Condensed Bosons System Condition 67
80. Eigenvalue of 1st and 2nd order RDM for Max. Coherence 68
81. Fragmented Bosons System Condition 68
82. Depleted Condensate Condition 68
83. 1D Interaction Potential 69
84. Mean Density 69
85. 1D Homogeneous System Density 69
86. Lieb-Liniger Parameter 70
87. Classification Scheme of Trapped Interacting Bose-Gases 70
88. Exact Hamiltonian in 2nd Quantization 75
89. Field Operator Equation of Motion 75
90. Condensate - Depletion Decomposition 75

91. Time-Dependent Gross-Pitaevskii Equation 76
92. Time-Independent Gross-Pitaevskii Equation 76
93. Decomposition of the Field Operator into a *Left*- and *Right*- Mode 77
94. Two Mode Hamiltonian 2nd Quantized Form in LR-Basis 77
95. Tunnel Coupling 78
96. Nonlinear Interaction / Charging Energy 78
97. Hamiltonian $\kappa \gg \Omega$ 78
98. Hamiltonian $\Omega \gg \kappa$ 79
99. Gerade-Ungerade Basis 79
100. $\Omega \gg \kappa$ Groundstate 80
101. Pseudospin Operators 81
102. Hamiltonian with Pseudospin Operators 81
103. Phase Representation 82
104. Mean and Variance of $\hat{\phi}$ 82
105. Rotations of the State $|-N/2\rangle$ 82
106. Rotation Matrix 83
107. Probability Distribution for a Given State Vector $|\mathbf{C}\rangle$ 83
108. Prob. Distribution for Coherent State Vector $|\mathbf{C}\rangle$ with Zero Phase 83
109. MCTDHB Ansatz for the Field Operator 85
110. General Permanent of M One Particle Functions 86
111. General State 86
112. Action 87
113. Expectation Value of $\hat{H} - i\frac{\partial}{\partial t}$ 87
114. Time-Derivative $i\frac{\partial}{\partial t}$ as One-Body operator 88

115. Equations-of-Motion for the Time-Dependent Orbitals $\{\phi_j(\mathbf{r},t)\}$ 88
116. Time-Dependent *Local* Potentials $\hat{W}_{sl}(\mathbf{r},t)$ 88
117. Conditions for Orthogonality Constraints 89
118. Simplified EoM for the Time-Dependent Orbitals $\{\phi_j(\mathbf{r},t)\}$ 89
119. Expectation Value of $\hat{H} - i\frac{\partial}{\partial t}$ depending on $\{C_{\mathbf{n}}(t)\}$ 90
120. Expectation Value of $\hat{H} - i\frac{\partial}{\partial t}$ 90
121. Number Distribution 90
122. EoM for the Propagation of the Coefficients 90
123. Expectation Value of $\hat{H}$ 91
124. Variation of S with Respect to ϕ for $M = 1$ 91
125. Energy Functional 91
126. Many-Body Wave Function for Single Mode 92
127. Time Dependence of ϕ_g and ϕ_e 92
128. Coefficients for $M = 2$ 92
129. Projector 93
130. Number Distribution 93
131. Hamiltonian 93
132. Two-Particle Matrix Elements 93
133. Definition of CFs 96
134. Factorization of up to Three Operators 96
135. Implicit Definition of $\mathbf{F}^{-1}$ 97
136. Explicit Definition of $\mathbf{F}^{-1}$ 97
137. First Three 'Refactorized' CFs 97
138. Factorized EV of the Product of Three Operators 99

139. Truncation Operator CF 99
140. $\Delta_{\delta(2)}$ on $\mathbf{F}\langle b_1 b_2 b_3\rangle$ 99
141. Truncation Operator EV 100
142. Approximation of EV as a Sum of Products of Lower-Order EVs 100
143. $\Delta_{\delta(1)}\langle b_1 b_2\rangle$ 101
144. $\Delta_{\delta(1)}\langle b_1 b_2 b_3\rangle$ 101
145. $\Delta_{\delta(2)}\langle b_1 b_2 b_3\rangle$ 101
146. Approximation of CF as a Sum of Products of Lower-Order CFs 101
149. von Neumann-Lindblad Equation 103
150. Generalized Ehrenfest Equation of Motion 103
151. EV Hierarchy Without Truncation 104
153. Application of $\Delta_{\langle 2n\rangle}$ 104
154. EV Hierarchy Truncated by Neglecting EVs 105
155. EoM for CFs 106
156. CF Hierarchy Without Truncation 106
157. CF Hierarchy Truncated by Neglecting CFs 107
158. EV Hierarchy Truncated by Neglecting CFs 108
159. CF Hierarchy Truncated by Neglecting EVs 109
160. Approximation of 3PRDM with 3-Particle CF Equal Zero 113
161. Two Mode Hamiltonian 2nd Quantized Form in GE-Basis 117
162. Commutators of the 1- and 2-PRDM Elements with H 118
163. Ehrenfest Equation of Motion 118
164. EoM for EVs 119
165. Defintion of CFs ρ_{ij} and Δ_{ijkl} 122

166. EoM for CFs 123
167. Trace of the xPRDM 127
168. Trace of the 3PRDM 127
169. Explicit 3PRDM 128
170. 3PRDM Diagonal Elements Approximation 128
171. EoM for EVs 129
172. Pseudospin Operators 131
173. Hamiltonian with Pseudospin Operators 131
174. Ehrenfest Equation of Motion 131
175. EoM for EVs 132
176. Approximation for Pseudospin Operators 132
177. Single-Particle Bloch Vector 132
178. Second-Order Moments 133
179. Equations for the First- and Second-Order Moments 133

List of Figures

1.1. BEC formation 6

1.2. BEC size 7

1.3. BEC interference-pattern 8

1.4. Mean occupancy FD, BE, MB 10

1.5. Bose Einstein condensate 11

1.6. First BEC in Science 13

1.7. 1D BEC 15

2.1. Optical Mach-Zehnder interferometer 22

2.2. Magnetic trap 24

2.3. Atom chip 25

2.4. Atom chip side view 27

2.5. Single well potential to double well potential transformation 27

2.6. BEC on atom chip 28

2.7. B-field on atom chip 29

2.8. Lesanovsky-potential 30

2.9. Stages of a matter wave Mach-Zehnder interferometer 31

2.10. Stages of a matter wave TOF interferometer 32

2.11. Bloch-sphere 35

2.12. Squeezed-states on a Bloch-sphere 36

2.13. Dephasing on Bloch-sphere 38

2.14. Parametric Squeezing Amplification 43

4.1. Groundstates in two-mode model 80

4.2. Visualization on the Bloch-sphere 84

4.3. Sketch of MCTDHB(2) in a double well potential 94

5.1. Illustration of an EV hierarchy 105

5.2. Illustration of an CF hierarchy 107

5.3. Illustration of an EV hierarchy truncated by neglecting CFs 109

5.4. Illustration of an CF hierarchy truncated by neglecting EVs 110

6.1. Two-mode model density splitting 100ms 115

6.2. Two-mode model Bloch-plot splitting 100ms 115

6.3. Two-mode model 3PRDM approximation splitting 100ms 116

6.4. Two-mode model 1 particle EVs approximation splitting 100ms 120

6.5. Two-mode model 2 particle EVs approximation splitting 100ms 121

6.6. Two-mode model splitting 100ms approximations 1ms 125

6.7. Two-mode model splitting 100ms approximations 13ms 126

6.8. Two-mode model splitting 100ms approximations const. trace 130

6.9. Two-mode model 100ms Anglin-Vardi 134

6.10. Two-mode model splitting 100ms Anglin-Vardi 135

6.11. 4 Modes groundstate population 100ms with $\kappa = 0.01$ and $\lambda_{start} = 0.85$ for two particles 136

6.12. 4 Modes groundstate population 33ms with $\kappa = 0.01$ and $\lambda_{start} = 0.85$ for 100 particles 137

A.1. Two-mode model density splitting 30ms 140

A.2. Two-mode model Bloch-plot splitting 30ms 140

A.3. Two-mode model 3PRDM splitting 30ms 141

A.4. Two-mode model density splitting 10ms 142

A.5. Two-mode model Bloch-plot splitting 10ms 142

A.6. Two-mode model 3PRDM splitting 10ms 143

A.7. Two-mode model density splitting 3ms 144

A.8. Two-mode model Bloch-plot splitting 3ms 144

A.9. Two-mode model 3PRDM splitting 3ms 145

A.10.Two-mode model density splitting 1ms 146

A.11.Two-mode model Bloch-plot splitting 1ms 146

A.12.Two-mode model 3PRDM splitting 1ms 147